資料３

ミトコンドリア病診療マニュアル 2023

編集

日本ミトコンドリア学会

作成

ミトコンドリア病診療マニュアル編集委員会
村山　圭　千葉県こども病院代謝科
小坂　仁　自治医科大学小児科学
三牧 正和　帝京大学医学部小児科

診断と治療社

執筆者一覧

■編集　日本ミトコンドリア学会

古賀　靖敏　　日本ミトコンドリア学会理事長

■作成　ミトコンドリア病診療マニュアル編集委員会

委員長

村山　　圭　　千葉県こども病院代謝科

副委員長

小坂　　仁　　自治医科大学小児科学
三牧　正和　　帝京大学医学部小児科

委員（五十音順，敬称略）

秋山　奈々　　東京大学医学部附属病院ゲノム診療部
味原さや香　　埼玉医科大学病院小児科/ゲノム医療科
安藤　匡宏　　鹿児島大学大学院医歯学総合研究科脳神経内科・老年病学
井川　正道　　福井大学医学部地域健康学講座/遺伝診療部/脳神経内科
池田　善彦　　国立循環器病研究センター病理部病理診断科
石井亜紀子　　筑波大学医学医療系神経内科学
石川　　均　　北里大学医療衛生学部視覚機能療法
石田　秀和　　大阪大学大学院医学系研究科小児科学
泉　　岳　　北海道大学大学院医学研究院小児科学教室
市本　景子　　千葉県こども病院代謝科
伊藤　玲子　　国立成育医療研究センター総合診療部
今澤　俊之　　国立病院機構千葉東病院
岩﨑　直子　　東京女子医科大学附属八千代医療センター糖尿病・内分泌代謝内科
植松有里佳　　東北大学病院小児科
内野　俊平　　東京大学医学部附属病院小児科
海老原知博　　千葉県こども病院新生児科
大澤　　裕　　川崎医科大学神経内科学教室
大曽根義輝　　千葉大学医学部附属病院周産母子センター
大竹　　明　　埼玉医科大学ゲノム医療科/小児科
岡﨑　敦子　　順天堂大学大学院医学研究科難治性疾患診断・治療学
尾形真規子　　東京家政大学栄養学部管理栄養学科
岡本　裕嗣　　鹿児島大学医学部保健学科理学療法学専攻基礎理学療法学講座
小川えりか　　日本大学医学部小児科
小坂　　仁　　自治医科大学小児科学
梶　　俊策　　津山中央病院小児科
木村亜紀子　　兵庫医科大学眼科学講座
久保　　亨　　高知大学医学部老年病・循環器内科学講座
熊谷　秀規　　自治医科大学小児科学
倉信奈緒美　　鳥取大学医学部周産期・小児医学
小垣　滋豊　　大阪急性期・総合医療センター小児科・新生児科
後藤　雄一　　国立精神・神経医療研究センターメディカル・ゲノムセンター
齋藤　貴志　　国立精神・神経医療研究センター病院脳神経小児科

志村　優	千葉県こども病院代謝科
下澤　弘憲	自治医科大学小児科学
庄嶋　伸浩	東京大学医学部附属病院
末岡　浩	慶應義塾大学医学部臨床遺伝学センター
菅沼　正司	一般社団法人こいのぼり
鈴木　康夫	手稲渓仁会病院眼窩・神経眼科センター
須藤　章	楡の会こどもクリニック
砂田　芳秀	川崎医科大学神経内科学教室
髙嶋　博	鹿児島大学大学院医歯学総合研究科脳神経内科・老年病学
竹下　絵里	国立精神・神経医療研究センター病院脳神経小児科
武田　充人	北海道大学大学院医学研究院小児科学教室
田鹿　牧子	千葉県こども病院代謝科
谷川　健	公立八女総合病院病理診断科
中馬　秀樹	宮崎大学医学部眼科
鶴岡　智子	千葉県こども病院新生児科
長友　太郎	福岡赤十字病院小児科
中村　誠	神戸大学大学院医学研究科外科系講座眼科学分野
野津　寛大	神戸大学大学院医学研究科内科系講座小児科学分野
樋口雄二郎	鹿児島大学大学院医歯学総合研究科脳神経内科・老年病学
平野　大志	東京慈恵会医科大学小児科学講座
平松　有	鹿児島大学大学院医歯学総合研究科脳神経内科・老年病学
廣野　恵一	富山大学医学部小児科
福田　晃也	国立成育医療研究センター臓器移植センター
藤岡　正人	北里大学医学部分子遺伝学/耳鼻咽喉科
伏見　拓矢	千葉県こども病院代謝科
増田　正次	杏林大学医学部耳鼻咽喉科学教室
松永　綾子	聖マリアンナ医科大学小児科
松永　達雄	国立病院機構東京医療センター聴覚・平衡覚研究部/臨床遺伝センター
南　修司郎	国立病院機構東京医療センター耳鼻咽喉科
三牧　正和	帝京大学医学部小児科
宮内　彰彦	自治医科大学小児科学
村山　圭	千葉県こども病院代謝科
八ツ賀秀一	福岡大学医学部小児科
山内　敏正	東京大学医学部附属病院糖尿病・代謝内科
山上　明子	井上眼科病院
山澤　弘州	北海道大学大学院医学研究院小児科学教室
山野邉義晴	国立病院機構東京医療センター耳鼻咽喉科
湯地　美佳	鹿児島大学大学院医歯学総合研究科脳神経内科・老年病学
米田　誠	福井県立大学大学院健康生活科学研究科
和佐野浩一郎	東海大学医学部耳鼻咽喉科・頭頸部外科
和田　敬仁	京都大学大学院医学研究科ゲノム医療学講座

協力学会（五十音順）

日本周産期・新生児医学会
日本小児栄養消化器肝臓学会
日本小児循環器学会
日本小児神経学会
日本神経学会
日本神経眼科学会
日本新生児成育医学会
日本先天代謝異常学会
日本糖尿病学会

ミトコンドリア病診療マニュアル 2023 Contents

- カラー口絵 …… ii
- 発刊に寄せて …… xi
- 緒言 …… xii
- 執筆者一覧 …… xiv
- 略語一覧 …… xx

第1章 総 論

1 ミトコンドリア病の疾患概念 …… 2
2 ミトコンドリア病の臨床症状 …… 8
3 ミトコンドリア病の診断方法 …… 11
4 ミトコンドリア病の全般的な治療法 …… 15
5 治療可能な疾患 …… 23
6 てんかんの治療 …… 29
7 生殖補助医療 …… 32
8 ミトコンドリア病の栄養療法 …… 35
9 ミトコンドリア病の日常生活 …… 40
10 ミトコンドリア病の遺伝カウンセリング …… 42
11 ミトコンドリア病における全身麻酔と鎮静 …… 47
12 小児から成人への移行期医療の課題と対応 …… 49

第2章 各 論

A Leigh 脳症

CQ 1 Leigh 脳症とはどのような疾患ですか？ …… 54
CQ 2 Leigh 脳症の症状は？ …… 57
CQ 3 Leigh 脳症の診断の進め方は？ …… 59
CQ 4 Leigh 脳症の鑑別診断は？ …… 64
CQ 5 Leigh 脳症の一般的な治療法は？ …… 67
CQ 6 Leigh 脳症の特異的な治療法は？ …… 70
CQ 7 Leigh 脳症の予後は？ …… 73

B ミトコンドリア肝症

CQ 8 ミトコンドリア肝症とはどのような疾患ですか？ …… 75
CQ 9 ミトコンドリア肝症の頻度と予後は？ …… 80

CQ10 ミトコンドリア肝症の症状と疑う患者は？ ····· 84
CQ11 ミトコンドリア肝症の鑑別診断は？ ····· 86
CQ12 ミトコンドリア肝症の診断の進め方は？ ····· 88
CQ13 ミトコンドリア肝症の病理所見の特徴は？ ····· 90
CQ14 ミトコンドリア肝症の特異的な治療は？ ····· 93

C ミトコンドリア心筋症

CQ15 ミトコンドリア心筋症とはどのような疾患ですか？ ····· 96
CQ16 ミトコンドリア心筋症の症状は？ ····· 98
CQ17 ミトコンドリア心筋症の診断の進め方は？ ····· 99
CQ18 ミトコンドリア心筋症の遺伝子診断は？ ····· 106
CQ19 ミトコンドリア心筋症と鑑別すべき疾患は？ ····· 112
CQ20 ミトコンドリア心筋症に合併する不整脈とその治療は？ ····· 115
CQ21 m.3243A＞G バリアントを有する成人心筋症の臨床像は？ ····· 119
CQ22 ミトコンドリア心筋症の治療は？ ····· 120

D 新生児ミトコンドリア病

CQ23 新生児ミトコンドリア病とはどのような疾患ですか？ ····· 122
CQ24 新生児ミトコンドリア病の発症時期，初発症状は？ ····· 125
CQ25 新生児ミトコンドリア病の原因遺伝子は？ ····· 127
CQ26 どのようなときに新生児ミトコンドリア病を疑うか？ ····· 129
CQ27 新生児ミトコンドリア病を疑った場合の診断の進め方は？ ····· 132
CQ28 新生児ミトコンドリア病を疑った場合の治療は？ ····· 135

E MELAS

CQ29 MELAS とはどのような疾患ですか？ ····· 138
CQ30 MELAS の疫学は？ ····· 139
CQ31 MELAS の中枢神経症状は？ ····· 140
CQ32 MELAS の中枢神経外の症状は？ ····· 143
CQ33 MELAS の診断の進め方は？ ····· 145
CQ34 MELAS の遺伝学的検査とその注意点は？ ····· 149
CQ35 MELAS の特異的な治療は？ ····· 152
CQ36 MELAS 患者への生活，学校，就労への指導の仕方は？ ····· 155
CQ37 MELAS の予後は？ ····· 157

F MERRF

CQ38 MERRF とはどのような疾患ですか？ ····· 158
CQ39 MERRF でみられやすい症状や所見は？ ····· 160
CQ40 MERRF の診断の進め方は？ ····· 163
CQ41 MERRF の遺伝学的な特徴は？ ····· 166

CQ42 MERRF の治療および予後は？ …… 169
CQ43 MERRF でみられるてんかん発作の特徴と治療は？ …… 171

G CPEO/KSS

CQ44 CPEO/KSS とはどのような疾患ですか？ …… 172
CQ45 CPEO/KSS の遺伝形式と原因は？ …… 174
CQ46 CPEO/KSS の疫学は？ …… 177
CQ47-a CPEO/KSS の症状は？ …… 179
CQ47-b CPEO/KSS の眼症状・所見の特徴は？ …… 182
CQ48 CPEO/KSS にみられる心伝導障害，心合併症は？ …… 184
CQ49 CPEO を伴った特殊な病態は？ …… 186
CQ50 CPEO/KSS の遺伝子検査以外の検査は？ …… 188
CQ51 CPEO/KSS の鑑別診断は？ …… 190
CQ52-a CPEO/KSS の特異的な治療は？ …… 192
CQ52-b CPEO/KSS の眼合併症に対する治療は？ …… 194

H Leber 遺伝性視神経症（眼疾患）

CQ53 Leber 遺伝性視神経症とはどのような疾患ですか？ …… 195
CQ54 Leber 遺伝性視神経症の症状は？ …… 198
CQ55 Leber 遺伝性視神経症の診断の進め方は？ …… 201
CQ56 Leber 遺伝性視神経症で知られている遺伝子バリアントは？ …… 203
CQ57 Leber 遺伝性視神経症の特異的な治療法は？ …… 205

I ミトコンドリア腎症

CQ58 ミトコンドリア腎症とはどのような疾患ですか？ …… 208
CQ59 ミトコンドリア腎症の臨床像は？ …… 210
CQ60 どのようなときにミトコンドリア腎症を疑うか？ …… 214
CQ61 ミトコンドリア腎症の診断法は？ …… 219
CQ62 ミトコンドリア腎症の予後は？ …… 222
CQ63 ミトコンドリア腎症の治療は？ …… 223

J ミトコンドリア糖尿病

CQ64 ミトコンドリア糖尿病とはどのような疾患ですか？ …… 226
CQ65 ミトコンドリア糖尿病の症状は？ …… 229
CQ66 ミトコンドリア糖尿病の診断の進め方は？ …… 231
CQ67 ミトコンドリア糖尿病の治療は？ …… 234
CQ68 ミトコンドリア糖尿病の診療上，注意すべき症状は？ …… 237

K ミトコンドリアニューロパチー

CQ69 ミトコンドリアニューロパチーの頻度は？ …… 240
CQ70 ミトコンドリアニューロパチーの原因遺伝子と合併症は？ …… 242
CQ71 特殊なニューロパチー （1）MNGIE とは？ …… 247
CQ72 特殊なニューロパチー （2）NARP syndrome とは？ …… 249
CQ73 特殊なニューロパチー （3）SANDO とは？ …… 251
CQ74 CMT の原因となるミトコンドリア関連遺伝子異常は？ （1）*MFN2* …… 253
CQ75 CMT の原因となるミトコンドリア関連遺伝子異常は？ （2）その他の遺伝子 … 255

L ミトコンドリア難聴

CQ76 ミトコンドリア難聴とはどのような疾患ですか？ …… 258
CQ77 ミトコンドリア難聴の症状は？ …… 260
CQ78 どのような難聴に対してミトコンドリア関連遺伝子の検査を行うべきか？ …… 261
CQ79 ミトコンドリア病の病型別の難聴と全身症状の合併は？ …… 263
CQ80 ミトコンドリア難聴の遺伝子バリアントは？ …… 265
CQ81 ミトコンドリア難聴に人工内耳は有効か？ …… 267

巻末資料

A ミトコンドリア病の患者会・役立つ Web サイト …… 270
B ミトコンドリア病で受けることのできる補助制度・サービス …… 273

索 引 …… 277

ミトコンドリア病診療マニュアル 2023

ISBN978-4-7878-2570-4

2023 年 6 月 5 日　初版第 1 刷発行

※前書
「ミトコンドリア病診療マニュアル 2017」
2016 年 12 月 27 日　初版第 1 刷発行
2018 年 7 月 17 日　初版第 2 刷発行

編　　集　一般社団法人日本ミトコンドリア学会
作　　成　ミトコンドリア病診療マニュアル編集委員会
（委員長：村山　圭／副委員長：小坂　仁，三牧正和）
発 行 者　藤実正太
発 行 所　株式会社　診断と治療社
〒 100-0014　東京都千代田区永田町 2-14-2　山王グランドビル 4 階
TEL：03-3580-2750（編集）　03-3580-2770（営業）
FAX：03-3580-2776
E-mail：hen@shindan.co.jp（編集）
eigyobu@shindan.co.jp（営業）
URL：http://www.shindan.co.jp/
本文イラスト　小牧良次（イオジン）
印刷・製本　三報社印刷株式会社

ミトコンドリア病ハンドブック

ミトコンドリア病をもつ患者さんとそのご家族のために

第2版

国立精神・神経医療研究センター病院
ゲノム診療部 遺伝カウンセリング科

もくじ

はじめに

ミトコンドリアとミトコンドリア病

ミトコンドリア
ミトコンドリアの機能障害・検査法・診断名
ミトコンドリア病の診断基準（1）（2）

ミトコンドリア病の検査

ミトコンドリア病の検査
ミトコンドリア病のDNA（遺伝子）検査
核DNA・染色体・遺伝子・タンパク質
ミトコンドリアDNA・遺伝子・タンパク質
代表的なミトコンドリアDNAの変化
ホモプラスミーとヘテロプラスミー
ミトコンドリア病の病理検査
ミトコンドリア病の生化学検査

ミトコンドリア病の症状

ミトコンドリア病の主な症状
卒中様症状を伴うミトコンドリア病
ミオクローヌスを伴うミトコンドリア病
慢性進行性外眼筋麻痺症候群
Leigh脳症

ミトコンドリア病の治療

ミトコンドリア病の治療法（対症療法）（原因療法）

ミトコンドリア病の患者・家族のための社会資源

代表的な医療・福祉制度
情報サイト
患者登録制度

ミトコンドリア病の遺伝

ミトコンドリアDNAの遺伝＝母系（母性）遺伝
ミトコンドリアDNAの新しくおきた変化
核DNAの遺伝＝メンデル遺伝　顕性（優性）と潜性（劣性）
常染色体潜性遺伝（劣性遺伝）　常染色体顕性遺伝（優性遺伝）
X連鎖潜性遺伝（劣性遺伝）　X連鎖顕性遺伝（優性遺伝）
出生前診断・着床前診断

はじめに

このハンドブックは、ミトコンドリア病をもつ患者さんとそのご家族に、
病気への理解を深めるときの参考としていただくために作成しました。
各項目について、イラストと文章での説明があります。
イラストは、医療者から当事者の方へ説明するときの資料として、
文章は、当事者の方がご自身で読んで理解するときの補足説明として、
利用していただけるようになっています。
分かりにくいところがあれば、医療者へお尋ねください。
また、ミトコンドリア病の症状は多様ですので、
すべての患者さんには当てはまらない内容もたくさん書かれています。
病気とうまく付き合っていくためには、
それぞれの状況に合わせて対応することが大切ですので、
ご自身の病気については、担当の医療機関等でよくご相談ください。

ミトコンドリアとミトコンドリア病

ミトコンドリア

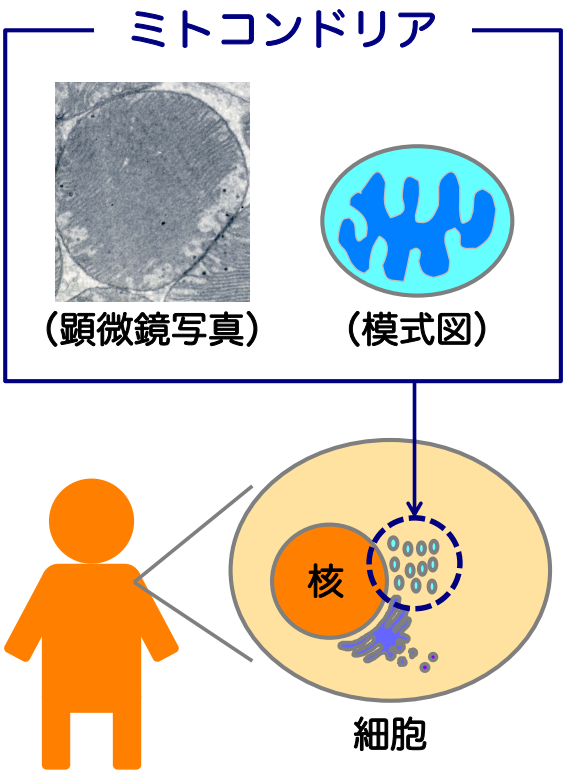

《細胞内での働き》

エネルギーの合成

活性酸素の発生

アポトーシス

カルシウムの貯蔵

感染の防御

ミトコンドリアの機能障害
→ ミトコンドリア病

私たちの体は、たくさんの細胞でできています。
その細胞の一つ一つの中にミトコンドリアは存在しています。
一つの細胞に数百個のミトコンドリアが入っていて、
細胞に必要なエネルギーを作り出しています。
そのため、ミトコンドリアに機能障害が生じると細胞の働きが悪くなり、
さまざまな症状が現れます。これがミトコンドリア病です。
体のどこのミトコンドリアに機能障害が生じるかによって症状は異なります。

また、ミトコンドリアは、活性酸素の発生、アポトーシス（細胞死）、
カルシウムの貯蔵、感染の防御などにも関わっていて、
ミトコンドリア病以外のさまざまな病気にも関与しています。

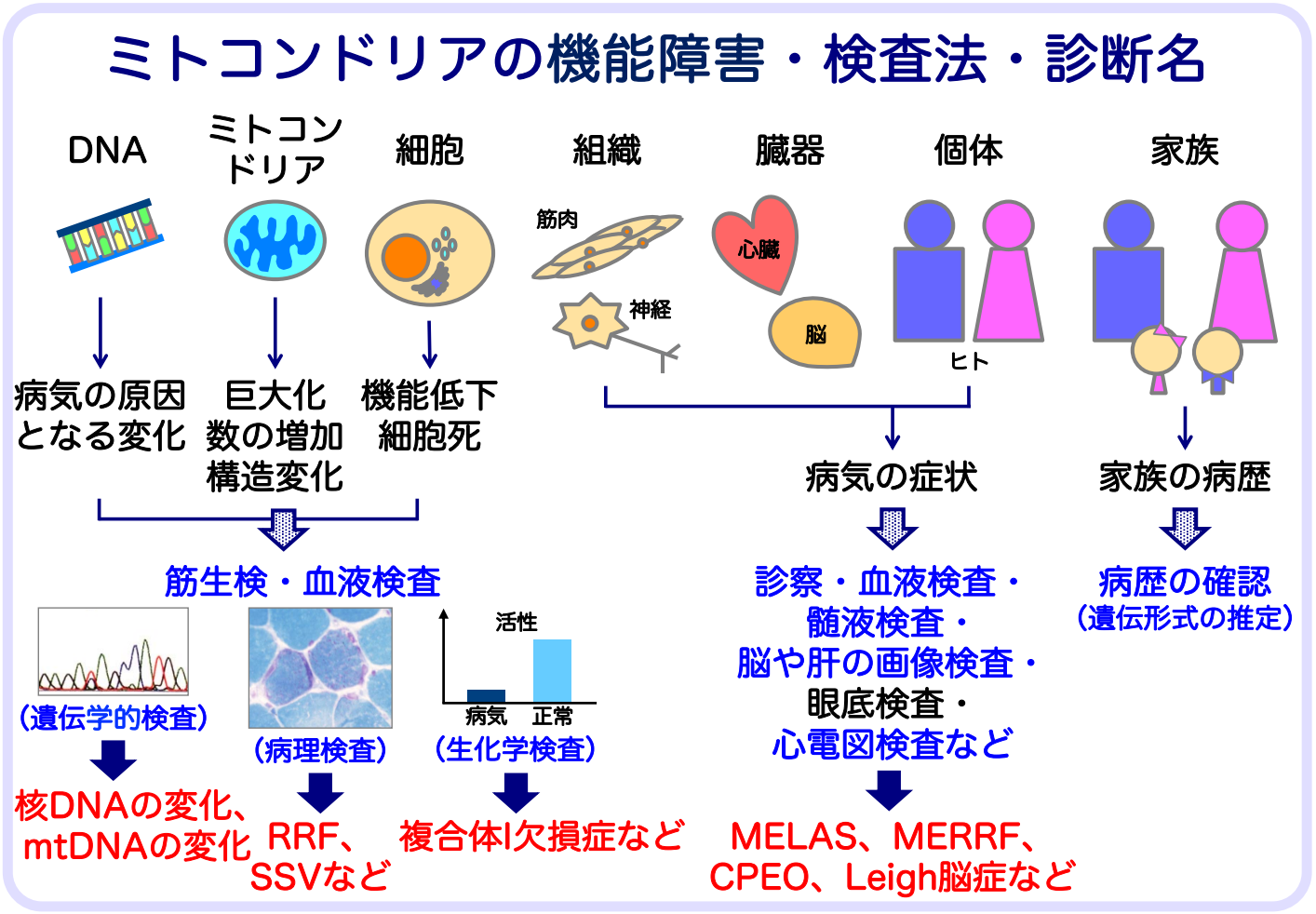

ミトコンドリアの機能障害を調べる検査には多くの種類があります。
それは、ミトコンドリアの機能障害がさまざまな形で現れるためです。
たとえば、設計図であるDNAには、
病気の原因となる変化（病的バリアント）が生じます。
DNAに病気の原因となる変化があるミトコンドリアは、
大きさや数、構造が変化し、そのミトコンドリアをもつ細胞は、
機能が低下したり、死んだりします。
そして私たちの体のさまざまな部分（臓器）に症状となって現れます。
DNAは先祖から代々受け継がれるものなので、
家族の中に同じような症状をもつ方がいる場合もあります。

指定難病医療費助成制度

ミトコンドリア病の診断基準（1）

（1）主症状

① 進行性の筋力低下、横紋筋融解症又は外眼筋麻痺を認める。
② 知的退行、記銘力障害、痙攣、精神症状、一過性麻痺、半盲、皮質盲、ミオクローヌス、ジストニア、小脳失調などの中枢神経症状のうち、1つ以上を認める。または手足のしびれなどの末梢神経障害を認める。
③ 心伝導障害、心筋症などの心症状、肺高血圧症などの呼吸器症状、糸球体硬化症、腎尿細管機能異常などの腎症状、強度の貧血などの血液症状、又は肝障害、黄疸、凝固能低下などの肝症状、体重増加不良、繰り返す嘔吐・下痢・便秘等の消化器症状を認める。
④ 低身長、甲状腺機能低下症などの内分泌症状や糖尿病を認める。
⑤ 強度視力低下、網膜色素変性などの眼症状、感音性難聴などの耳症状を認める。
⑥ 新生児期または乳児期に、発育異常、発達遅延を認める。

ミトコンドリア病は、平成27年（2015年）1月に、国の難病対策の
一つである指定難病医療費助成制度の対象に認められました。
この事業は、一定の条件を満たす病気を対象に、
その患者さんの医療費を助成し、原因の究明や治療法の開発などに向けた
調査研究を推進しようとする制度です。

指定難病としての「ミトコンドリア病」と診断されるためには
定められた診断基準を満たす必要があります。
ここに掲げた診断基準は、令和6年4月から施行される予定のものです。
具体的には、主症状として筋肉、中枢神経、心臓、肺、腎臓、血液、肝臓、
内分泌、膵臓、眼、耳のいずれかに症状があることが要件となります。
新生児期や乳児期には、あきらかな臓器の症状が現れていないこともあります。

いずれの場合も、次に示す「検査・画像所見」が明確に存在する時に
ミトコンドリア病の診断が付けられます。

指定難病医療費助成制度

ミトコンドリア病の診断基準（2）

（2）検査・画像所見

① ミトコンドリアDNAの質的、量的異常又はミトコンドリア関連分子をコードする核遺伝子変異を認める。（遺伝学的検査所見）

② 骨格筋生検や培養細胞又は症状のある臓器の細胞や組織でミトコンドリアの病理異常を認める。（病理検査所見）

③ ミトコンドリア関連酵素の活性低下、又はコエンザイムQ10などの中間代謝物の欠乏を認める。または、ミトコンドリアDNAの発現異常を認める。（生化学検査所見）

④ 安静臥床時の血清又は髄液の乳酸値が繰り返して高い、又は MRスペクトロスコピーで病変部に明らかな乳酸ピークを認める。

⑤ 脳CT/MRIにて大脳基底核、脳幹に両側対称性の病変等を認める。（脳画像所見）

⑥ 眼底検査にて、急性期においては蛍光漏出を伴わない視神経乳頭の発赤・腫脹、視神経乳頭近傍毛細血管蛇行、網膜神経線維腫大、視神経乳頭近傍の出血のうち１つ以上の所見を認めるか、慢性期（視力低下の発症から通常6か月以降）における視神経萎縮所見を両眼に認める。（眼底検査所見）

⑦ 腹部エコー、CT/MRI、あるいは肝組織所見にて、脂肪肝、あるいは肝硬変の所見を認める。（肝画像所見）

主症状と検査・画像所見の中で、満たす項目の種類と数により
Definite（確実）、Probable（ほぼ確実）、Possible（可能性あり）に分類される

本制度で医療費助成の対象になるのは、Definite か Probable と診断され、
さらに「重症度分類」に照らして病状の程度が一定程度以上の場合です。

初めて指定難病の申請をする際には、難病指定医による
「臨床調査個人票」と呼ばれる診断書の作成が必要となりますので、
主治医の先生にご相談ください。

また、18歳未満の患者さんの場合には、
小児慢性特定疾病医療費助成を受けられる場合があります。
申請する際には、小児慢性特定疾病指定医による
「医療意見書」と呼ばれる診断書の作成が必要となりますので、
主治医の先生にご相談ください。
なお、引き続き治療が必要と認められる場合には、有効期間終了前に
継続手続を行うことにより、20歳未満まで延長することができます。

ミトコンドリア病の検査

ミトコンドリア病の検査

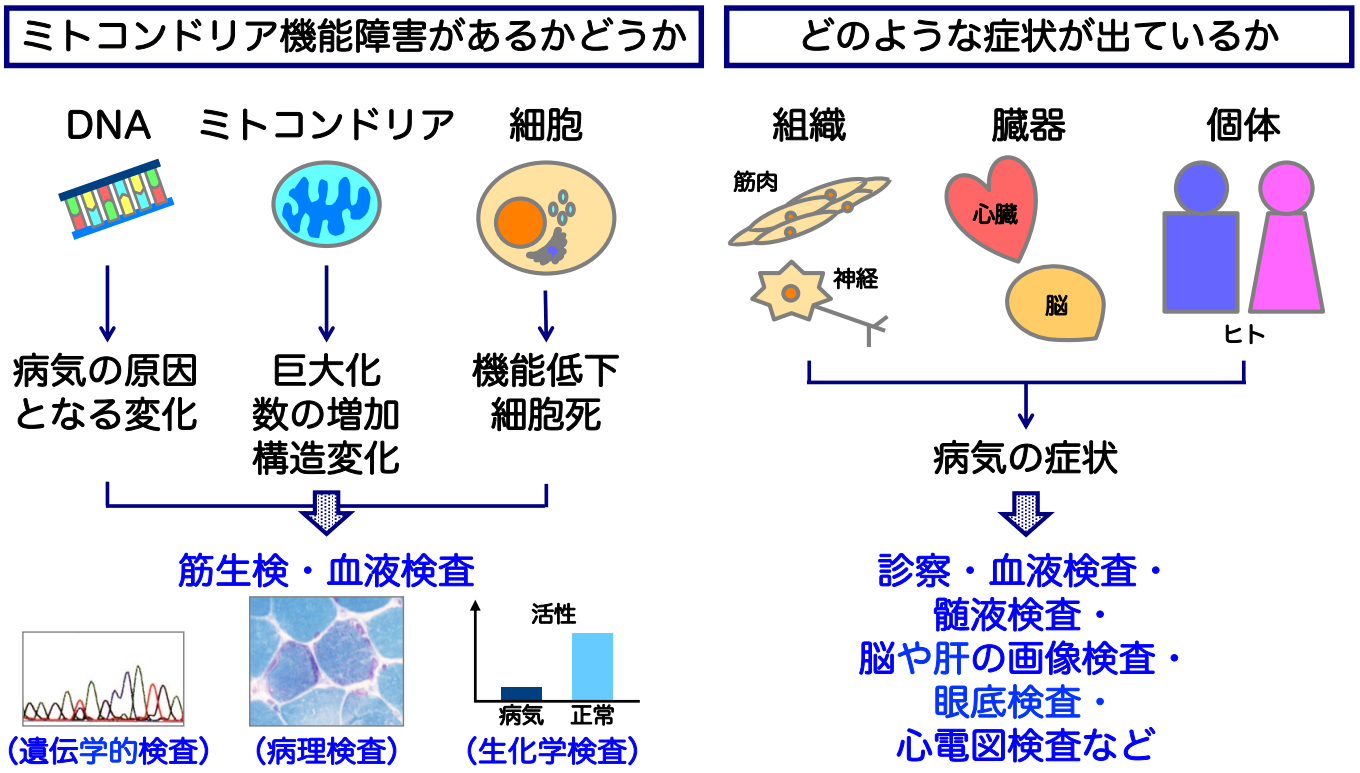

ミトコンドリア病の検査は、その目的によって大きく二つに分けられます。
一つは、どのような症状が出ているかを調べるための検査（右）です。
脳や肝の画像検査や心電図検査などを行い、
さまざまな臓器に異常があるかどうかを調べます。

もう一つは、ミトコンドリアの機能障害を調べるための検査（左）です。
筋生検や血液検査で採取した検体を用いて、
DNA（遺伝学的）検査、病理検査、生化学検査を実施します。
これによって、ミトコンドリアのDNA、形、働きを詳しく調べることができます。

ミトコンドリア病のDNA（遺伝学的）検査

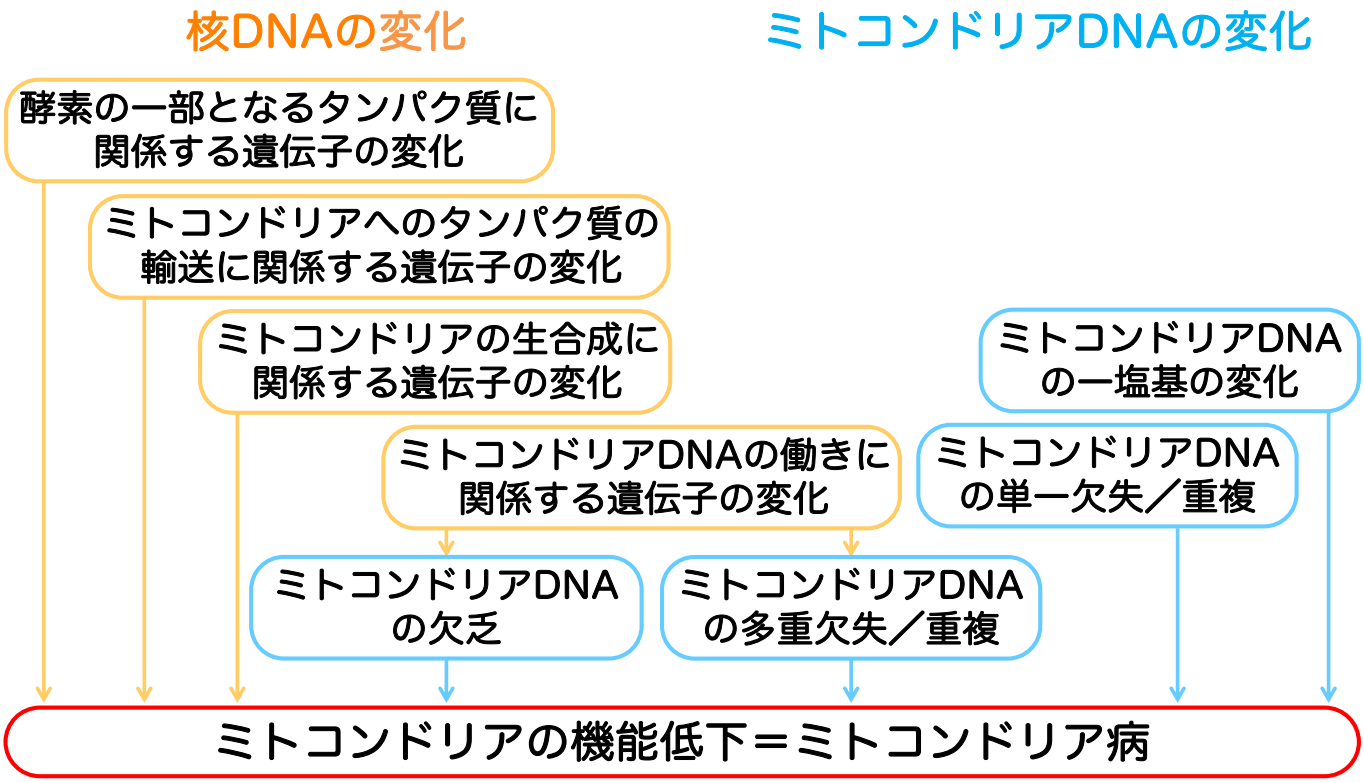

DNA（遺伝学的）検査は、筋生検や採血によって採取した細胞から
DNAを取り出して、特定の遺伝子に病気の原因となる変化があるかどう
かを調べます。
病気の原因となる変化が見つかれば、それが症状の原因であるということ
が分かります。
ミトコンドリア病の原因となる遺伝学的な変化は、
核DNAの場合とミトコンドリアDNAの場合があります。
どちらのDNAにどのような変化が生じているかによって、
その由来や次世代への遺伝の仕方が異なります。

核DNA・染色体・遺伝子・タンパク質

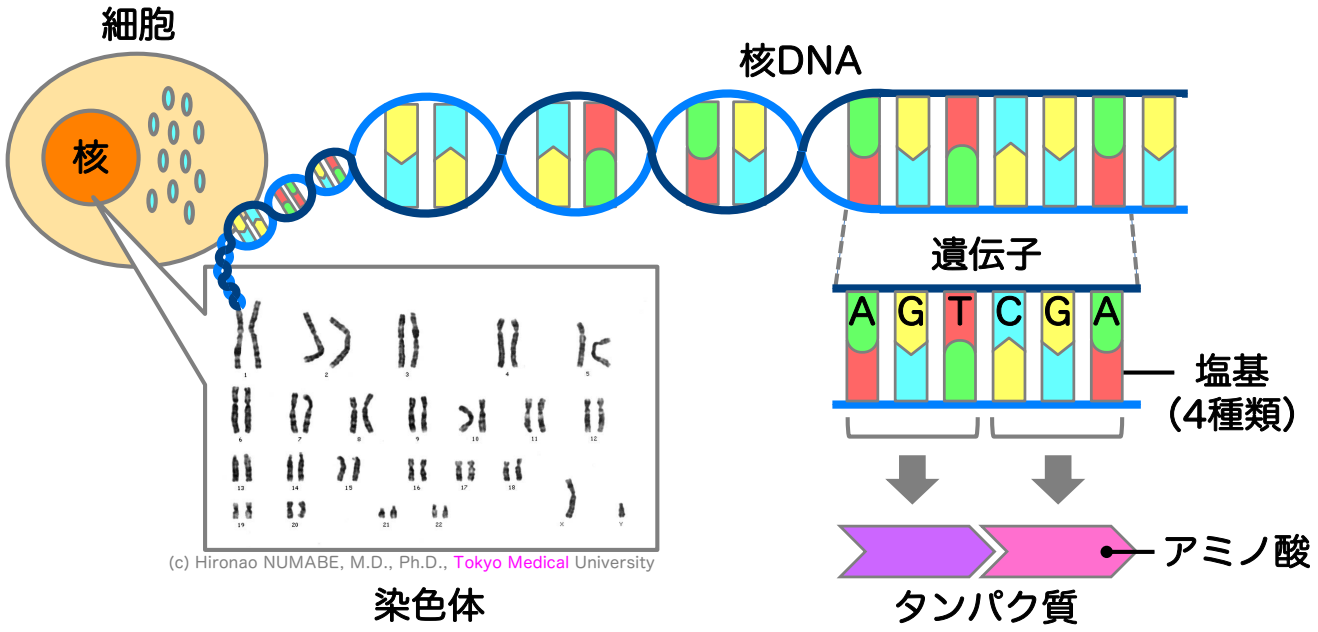

- ミトコンドリアに必要なタンパク質のうち、1500種類が核DNAの情報をもとに作られる
- 核DNAはミトコンドリアDNAの働きにも関与している

核DNAは、核という部分に入っているDNAで、
一般的には単に「DNA」と呼ばれることが多いようです。
核DNAは2本のひもが螺旋状に絡まったような構造をしていますが、
時期によって複数の棒のような状態で存在していて、染色体と呼ばれます。
DNAには、私たちの体を作ったり維持したりするのに必要な情報が
たくさんつまっていて、その一つ一つを遺伝子と呼んでいます。
塩基という4種類の物質（A・G・C・T）を暗号としてアミノ酸が作られ、
それが連なってタンパク質となります。
つまり遺伝子は私たちの体の設計図のようなものだと言えます。

ミトコンドリアに必要なタンパク質のうち、
約1500種類が核DNAの情報をもとに作られています。
核DNAはミトコンドリアDNAの働きにも関与しています。

ミトコンドリアDNA・遺伝子・タンパク質

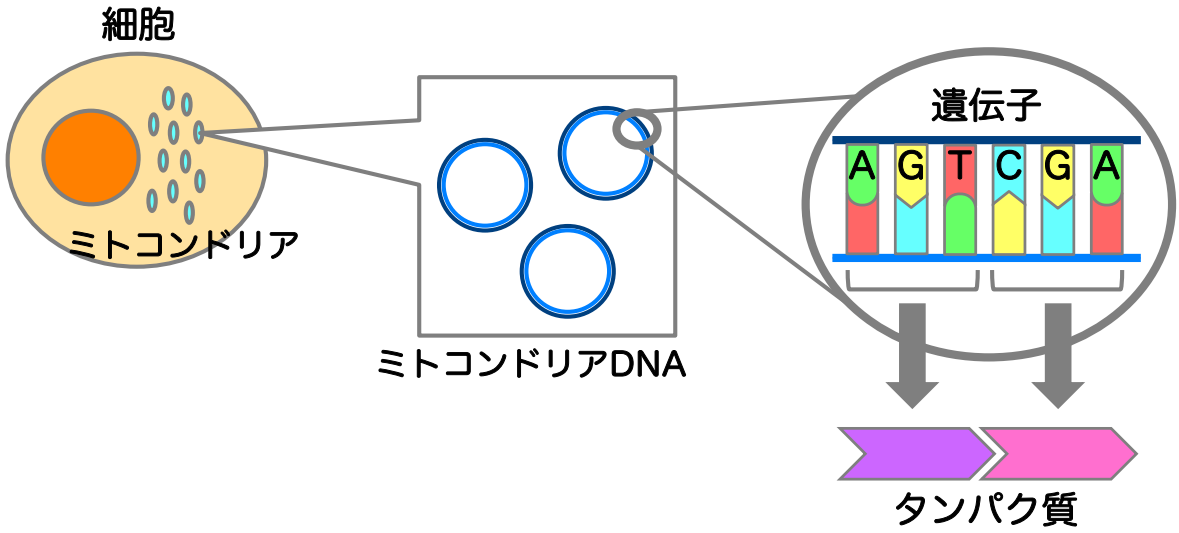

- 一つの細胞に数百～数千個のミトコンドリアDNAが入っている
- ミトコンドリアに必要なタンパク質のうち、13種類がミトコンドリアDNAの情報をもとに作られる
- ミトコンドリアDNAは核DNAの約10倍変化しやすい

ミトコンドリアDNAは、ミトコンドリアの中に入っているDNAです。
一つの細胞にはミトコンドリアが数百個存在していて、
それぞれにミトコンドリアDNAが複数個ずつ入っているため、
一つの細胞には数百～数千個のミトコンドリアDNAが入っています。
その構造は、2本のひもが輪になったような形をしています。

ミトコンドリアに必要なタンパク質のうち、
13種類がミトコンドリアDNAの情報をもとに作られます。
ミトコンドリアDNAは変化が生じやすいことが知られていて、
その頻度は核DNAの約10倍と言われています。

代表的なミトコンドリアDNAの変化

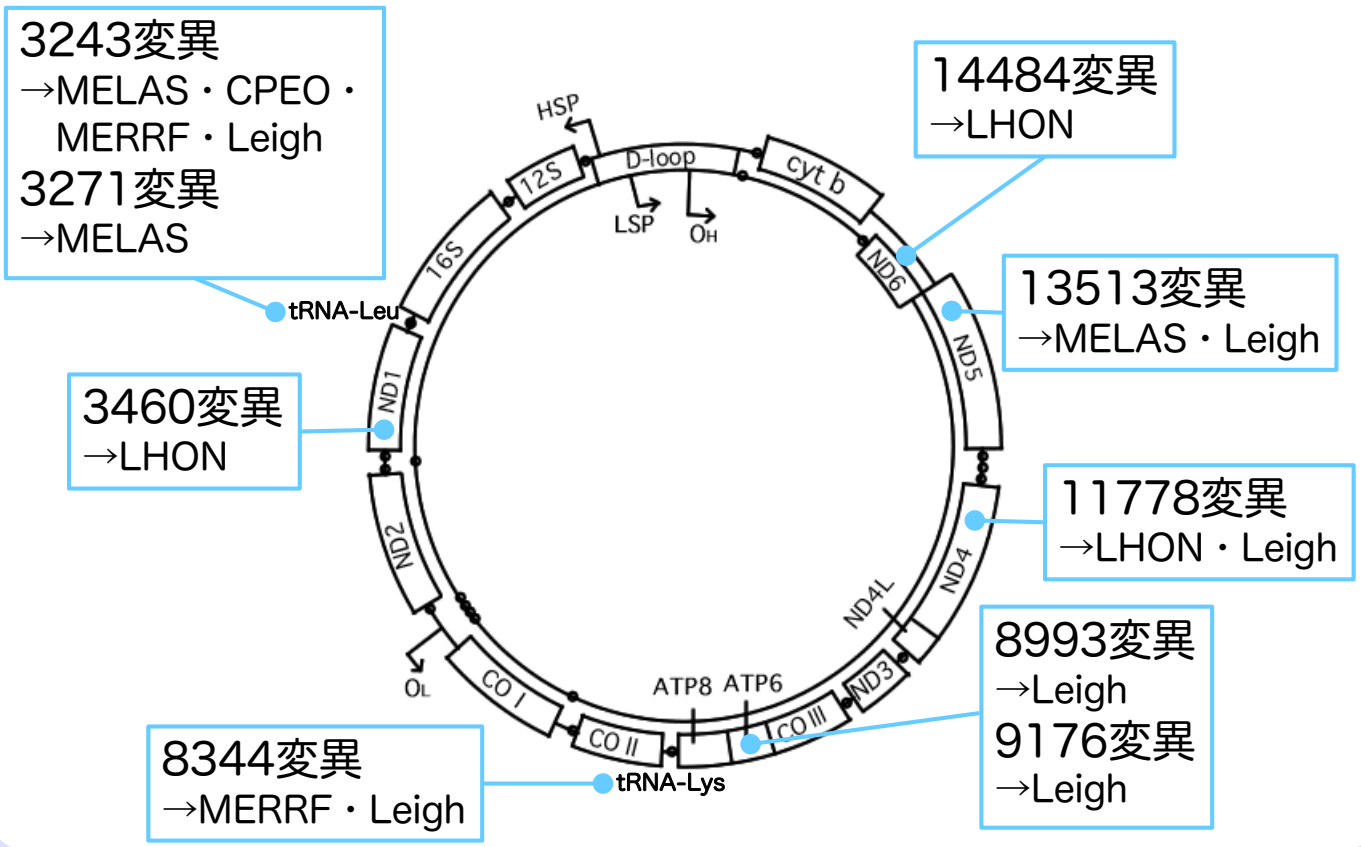

ミトコンドリア病の患者さんのミトコンドリアDNAを調べると、
さまざまな変化が見つかります。
そのうちいくつかは病気との関連が明らかになっています。
また、同じ変化によって異なる病気を発症したり、
同じ病気が異なる変化によって発症したりすることが
分かっています。

※病気の原因となる変化のことを「変異」と呼ぶため、上図では「変異」と記載しています。

ホモプラスミーとヘテロプラスミー

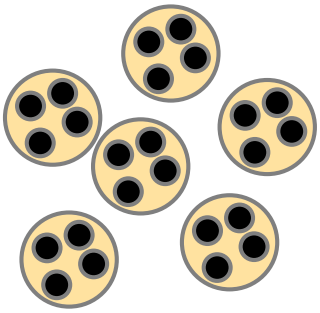

ホモプラスミー

● 変化あり
● 変化なし

細胞中のミトコンドリアDNAが
すべて同じ（病気の原因となる変化 または 正常）

ヘテロプラスミー

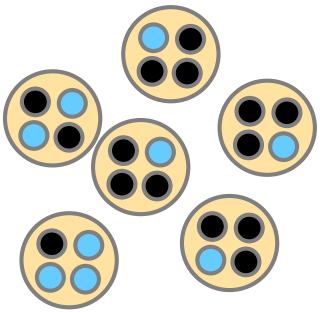

細胞中に正常なミトコンドリアDNAと
病気の原因となる変化をもつミトコンドリアDNAが
混在している
細胞や組織によって割合が異なる〈細胞／組織特異性〉
病気の原因となる変化をもつミトコンドリアDNAの割合が
一定以上になると機能が障害される
〈閾値（しきいち／いきち）効果〉
病気の原因となる変化をもつミトコンドリアDNAの割合は
細胞分裂のときに変化する

ミトコンドリアDNAの変化によって生じるミトコンドリア病の多くは、
正常なミトコンドリアDNAと病気の原因となる変化をもつミトコンドリア
DNAが混在している「ヘテロプラスミー」の状態で発症します。
この場合、
細胞や組織によって病気の原因となる変化をもつミトコンドリアDNAの
割合が異なること（細胞／組織特異性）、
病気の原因となる変化をもつミトコンドリアDNAの割合が一定以上になる
と機能が障害されること（閾値効果）が特徴として挙げられます。
また、病気の原因となる変化をもつミトコンドリアDNAの割合は、
細胞分裂のときに変化します。
つまり、一人の患者さんでも、体のどの部分にどのくらいの割合で
病気の原因となる変化をもつミトコンドリアDNAをもっているかによって
症状は異なり、さらにその割合は変化すると考えられています。
また、親から子へと伝わるときにも病気の原因となる変化をもつ
ミトコンドリアDNAの割合は変化します。

ミトコンドリア病の病理検査（左：光学／右：電子顕微鏡下の所見）

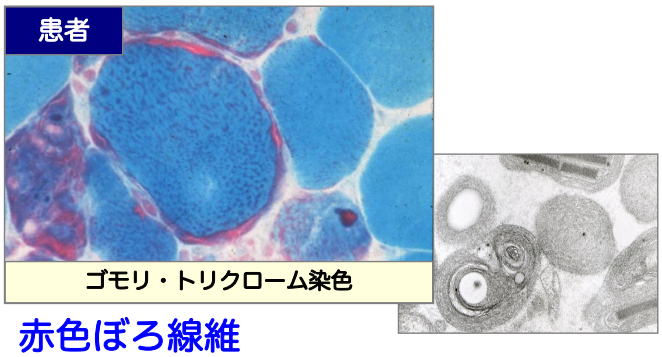

赤色ぼろ線維
Ragged Red Fiber; RRF

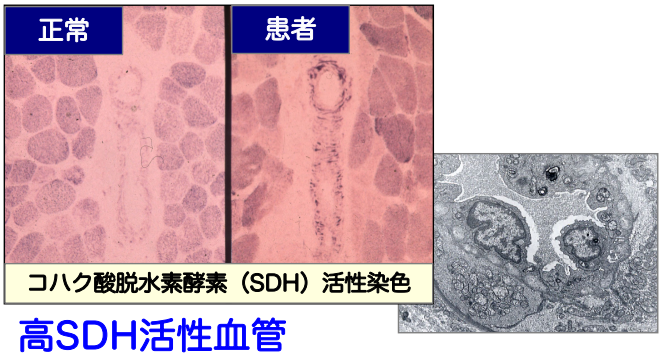

高SDH活性血管
Strongly SDH-reactive blood vessel; SSV

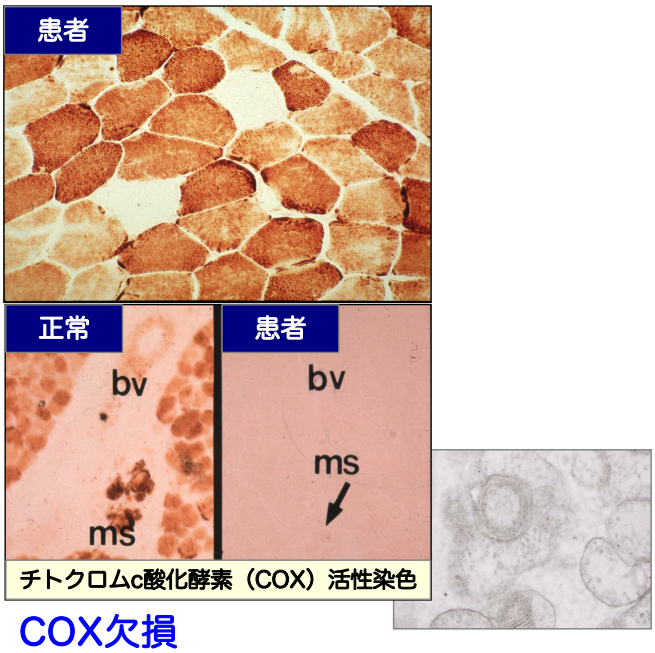

COX欠損
COX deficiency

病理検査は、筋生検などをおこなって細胞を採取し、
薬品（染色液や反応液）で処理した後、顕微鏡で細胞の特徴を観察します。
ミトコンドリア病の患者さんでは写真のような特徴的な所見が見られます。
これらの所見があればミトコンドリアや細胞に変化があるということが
分かります。

ミトコンドリア病の生化学検査

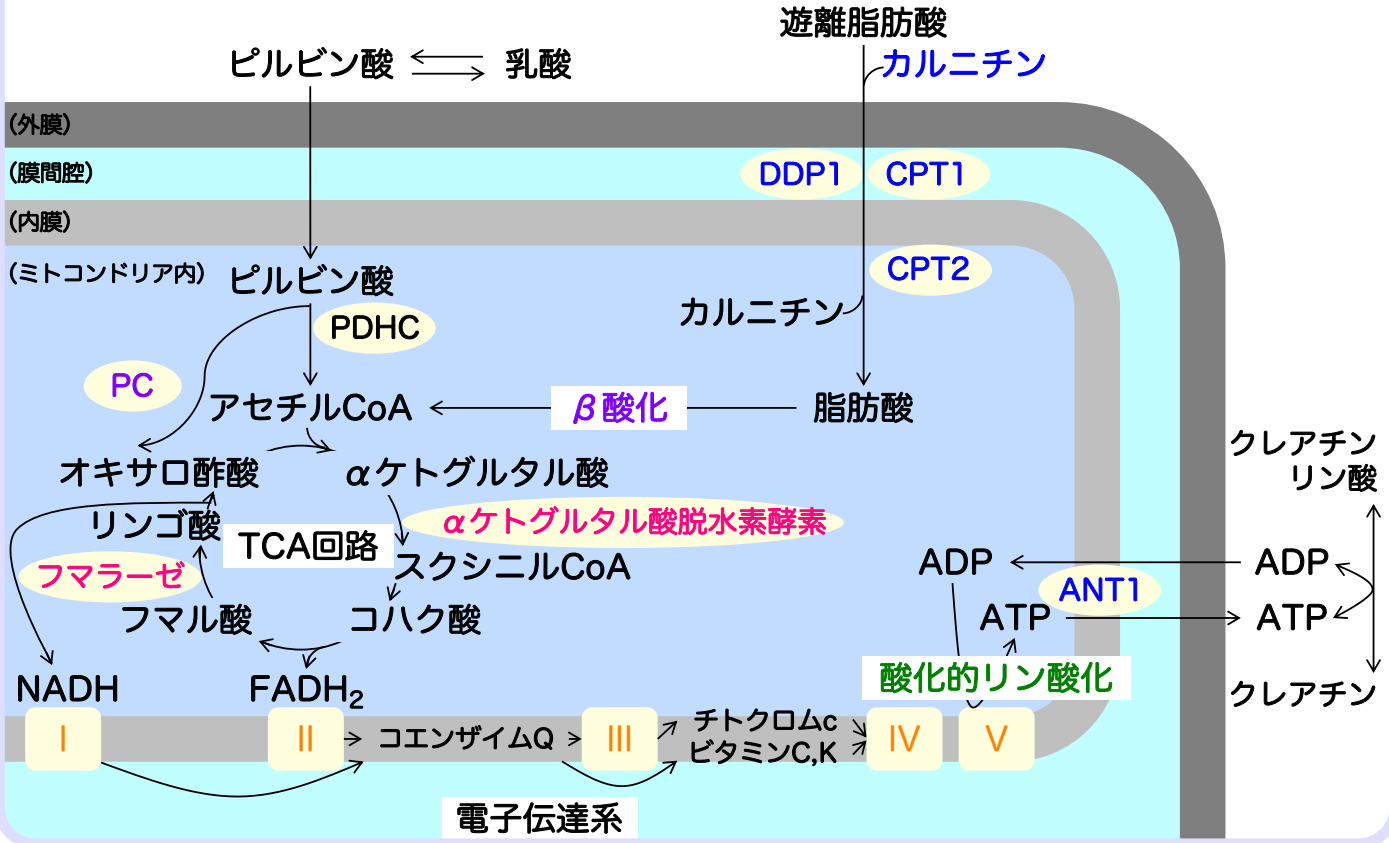

生化学検査では、筋肉や培養細胞を用いて、
ミトコンドリアの働きを調べます。
ミトコンドリアでは、私たちが摂取した栄養素が、
酵素と呼ばれるたんぱく質の働きによって順序よく分解されていきます。
その過程でエネルギーが合成されます。
このエネルギー合成に関わっている酵素や、
合成中に消費・産生される物質を測定することによって、
どの段階に機能障害があるのかを調べることができます。

ミトコンドリア病の症状

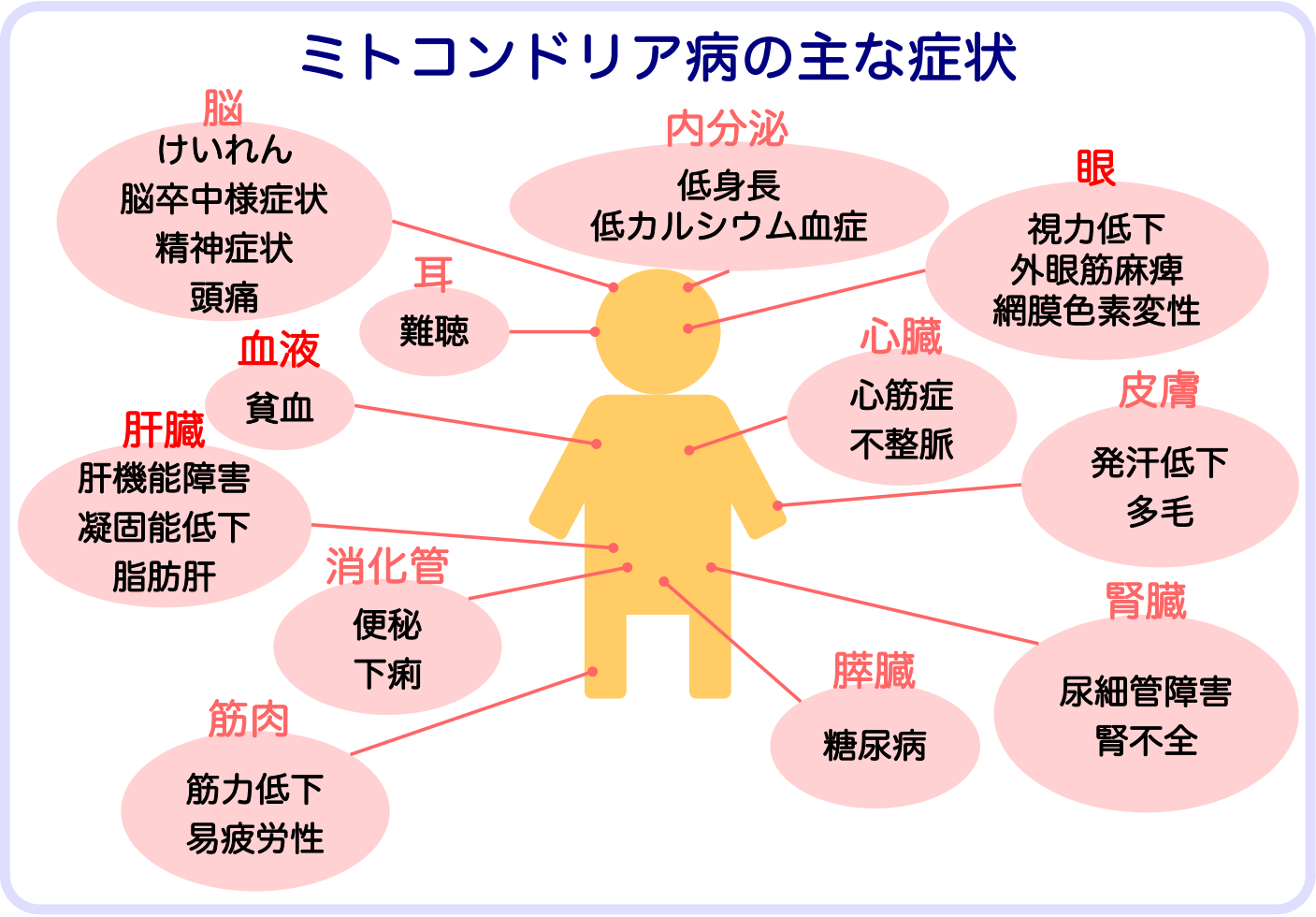

ミトコンドリアは体中の細胞に存在しているため、
ミトコンドリア病の症状は体のさまざまなところに現れます。
そのため、一人の患者さんがいくつもの症状をもっている場合には、
ミトコンドリア病が疑われることになります。
特にエネルギーを多く必要とする脳や筋肉などは症状が出やすいことが
知られていて、ミトコンドリア病は「ミトコンドリア脳症」
「ミトコンドリア脳筋症」と呼ばれることもあります。

症状によって、卒中様症状を伴うミトコンドリア病（MELAS）、
ミオクローヌスを伴うミトコンドリア病（MERRF）、
慢性進行性外眼筋麻痺症候群（CPEO）、Leigh脳症など、
さまざまな病気に分類されます。

卒中様症状を伴うミトコンドリア病

Mitochondrial encephalomyopathy with lactic acidosis and stroke-like episodes; MELAS（メラス）

〈主な症状〉

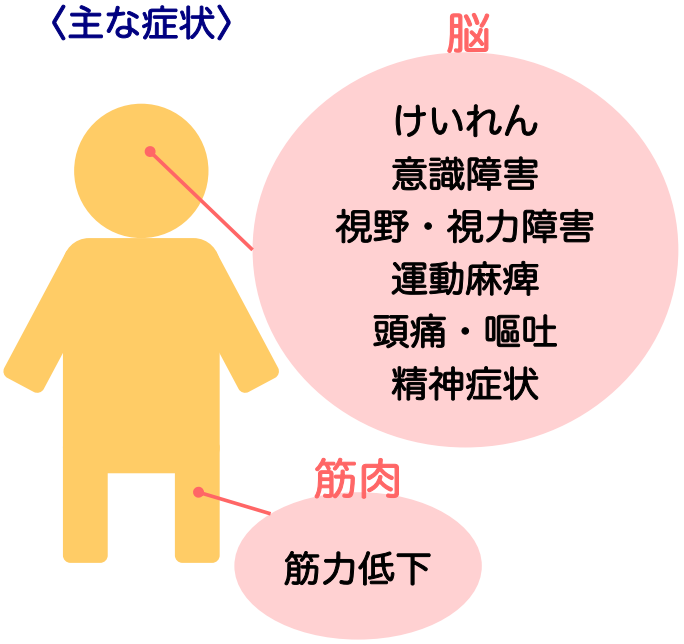

発症時期＝小児～成人

〈遺伝学的検査〉

mtDNAの一塩基の変化
＝母系遺伝、まれに新しくおきた変化
核DNAの変化
＝メンデル遺伝

〈病理〉

特徴的変化あり

〈生化学〉

髄液・血中乳酸値が中～高度に上昇
電子伝達系酵素複合体活性（I、IV、複数）が低下

〈画像〉

異常所見あり

卒中様症状を伴うミトコンドリア病（MELAS）には、
急激な意識障害や運動麻痺など脳卒中に似た症状が現れるという特徴があります。
心臓や膵臓、耳、内分泌器官などの臓器に症状がおこる場合もあります。
症状の種類や程度は患者さんごとに異なり、
一人の患者さんでも時間とともに変化することがあります。
多くの患者さんで、ミトコンドリアDNAの一塩基の変化が見つかるため、
通常は母系遺伝すると考えられますが、中には当てはまらない人もいます。
（遺伝については後のページに詳しい解説があります。）

ミオクローヌスを伴うミトコンドリア病

Myoclonic epilepsy with ragged-red fibers; MERRF (マーフ)

〈主な症状〉

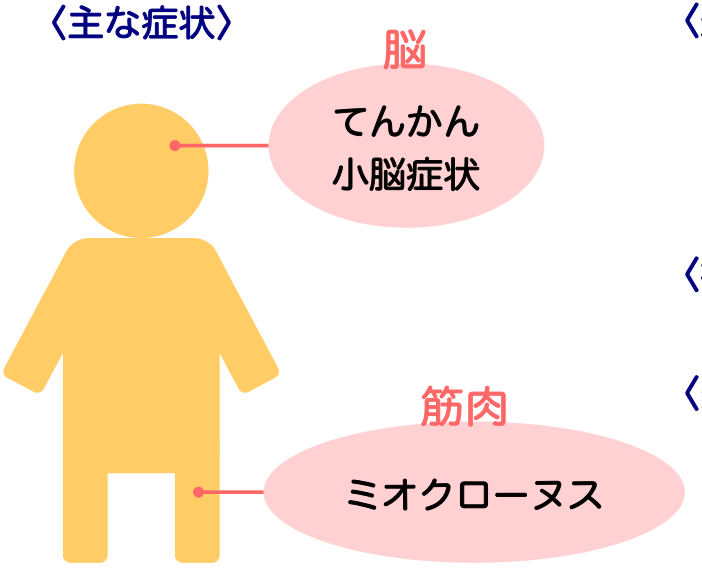

〈遺伝学的検査〉

mtDNAの一塩基の変化
＝母系遺伝、まれに新しくおきた変化
核DNAの変化
＝メンデル遺伝

〈病理〉

特徴的変化あり

〈生化学〉

血中乳酸値が中～高度に上昇

発症時期＝小児～成人

ミオクローヌスを伴うミトコンドリア病（MERRF）の症状は、
主に脳と筋肉に現れます。体がふらついたり（小脳症状）、
自分の意思とは関係なく筋肉が動いたりします（ミオクローヌス）。
まれに脳卒中のような症状がおこることもあります。
多くの患者さんで、ミトコンドリアDNAの一塩基の変化が見つかるため、
通常は母系遺伝すると考えられますが、中には当てはまらない人もいます。

慢性進行性外眼筋麻痺症候群

Chronic progressive external ophthalmoplegia;

CPEO（シーピーイーオー）

〈主な症状〉

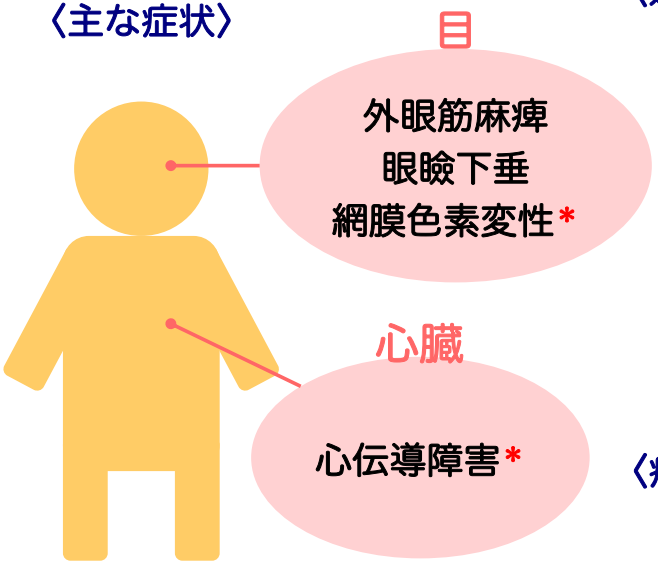

発症時期＝小児～成人

＊＝Kearns-Sayre（カーンズ・セイヤー）症候群

〈遺伝学的検査〉

mtDNA単一欠失
＝新しくおきた変化、まれに母系遺伝
mtDNAの一塩基の変化
＝母系遺伝、まれに新しくおきた変化
mtDNA重複
＝新しくおきた変化または母系遺伝
mtDNA多重欠失（核DNAの変化）
＝新しくおきた変化またはメンデル遺伝

〈病理〉

特徴的変化あり

〈生化学〉

血中乳酸値が軽度上昇

慢性進行性外眼筋麻痺症候群（CPEO）の主な症状は、
目の周りの筋肉が麻痺して眼球を動かせなくなることです。
これに網膜の変性と心臓の伝導障害を合併する場合、
Kearns-Sayre症候群と呼ばれます。
骨格筋、膵臓、腎臓、消化管などの臓器に症状が現れることもあります。
遺伝学的検査では、多くの場合、ミトコンドリアDNAの変化が
認められます。
変化の種類によって、由来や次世代への遺伝の仕方が異なります。

Leigh（リー）脳症

〈主な症状〉

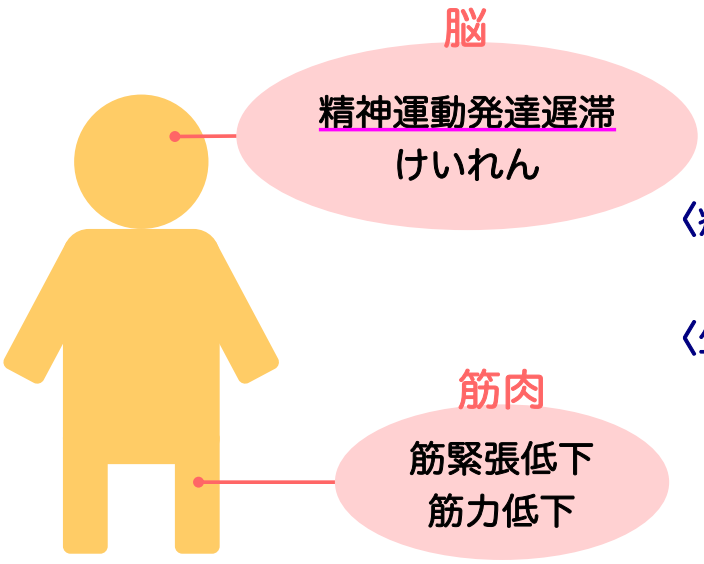

発症時期＝乳幼児～小児

〈遺伝学的検査〉
mtDNAの一塩基の変化
＝母系遺伝、まれに新しくおきた変化
核DNAの変化
＝メンデル遺伝

〈病理〉
特徴的変化なし

〈生化学〉
髄液・血中乳酸値が高度に上昇
電子伝達系酵素複合体活性（I、II、IV、V、複数）が低下
ATP合成が低下

〈画像〉
特徴的な所見あり

Leigh脳症では、脳と筋肉に主な症状が現れます。
通常は乳幼児期に発症し、精神運動発達の遅れや退行、けいれん、
筋緊張や筋力の低下といった症状が見られます。
ただし発症時期や進行の度合いは患者さんによってさまざまです。
原因は、ミトコンドリアDNAに変化がおきている場合と
核DNAに変化がおきている場合があります。
原因によって、由来や次世代への遺伝の仕方が異なります。

※退行：お座りや歩行、ことばなど、できていたことができなくなること

ミトコンドリア病の治療

ミトコンドリア病の治療法（対症療法）

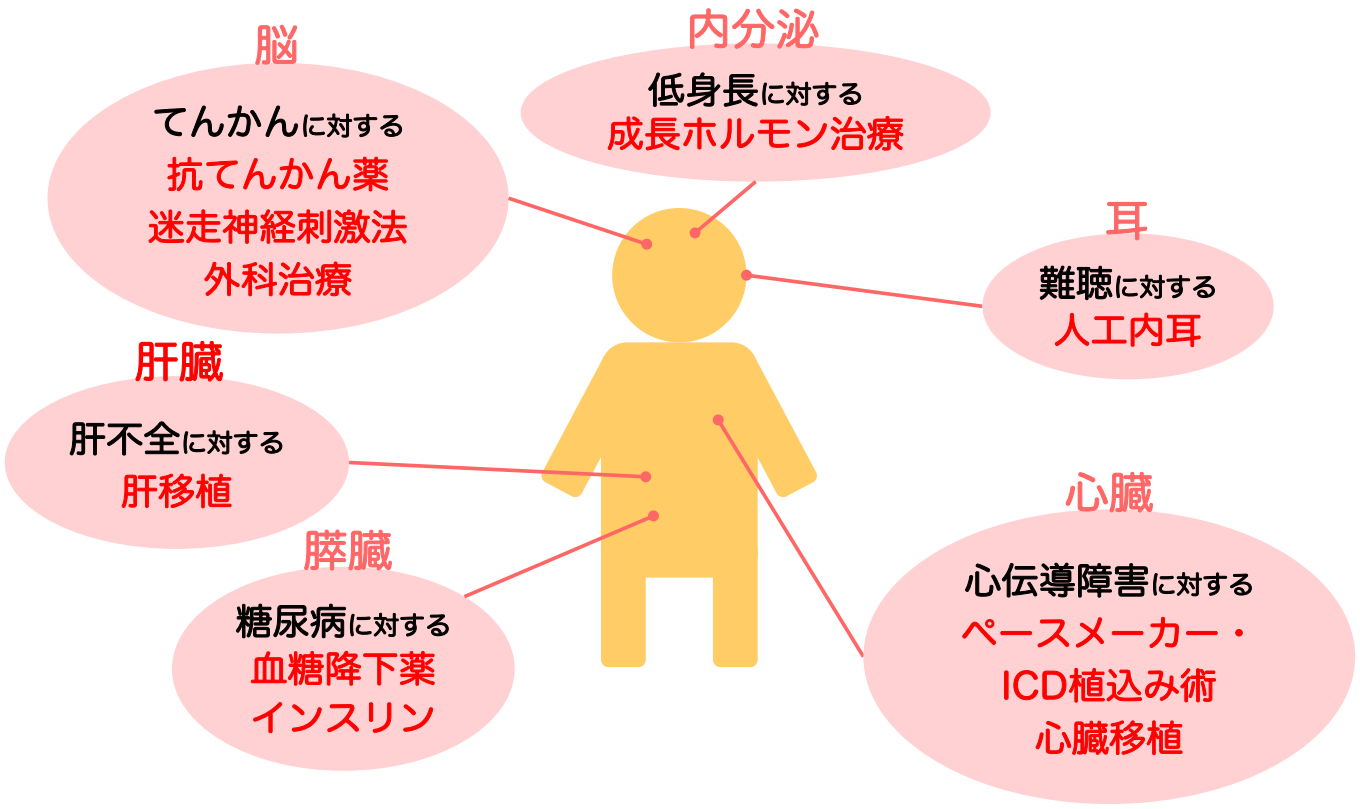

ミトコンドリア病の治療法は、大きく二つに分かれます。
一つは、現れている症状を和らげる対症療法です。

糖尿病、てんかん、低身長、肝不全など、
有効な治療法が確立されている症状に対しては、
その治療法が用いられます。
難聴や心伝導障害については、医療機器を利用することで、
低下した臓器の機能を補うことができます。

対症療法は、各臓器の専門医に診てもらうことが望ましいですので、
診療科の多い病院を中心として医療を受けることをお勧めします。

ミトコンドリア病の栄養療法

食事の注意点

・日常生活の活動度に応じた
カロリー量を計算する
・ビタミンを多く含む
バランスのよい食事をとる

〈呼吸鎖複合体Ⅰ欠損症〉

高脂質・低炭水化物栄養療法が
有効な場合がある

〈PDHC欠損症〉

ケトン食が有効な場合がある

〈小児難治性てんかん〉

登録外特殊ミルクの適応疾患

現在、ミトコンドリア病に対する栄養療法として確立されたものはありません。

さまざまな重症度があるため、日常生活の活動度に応じたカロリー量を計算し、
ビタミンを多く含んだバランスのよい食事をとることが推奨されます。
脱水や電解質異常、低血糖などには注意しましょう。

高脂質・低炭水化物栄養療法やケトン食、
特殊ミルクなどの栄養療法は医師の指導のもとに行われますので、
主治医の先生に指示を仰ぎましょう。

ミトコンドリア病の治療法（原因療法）

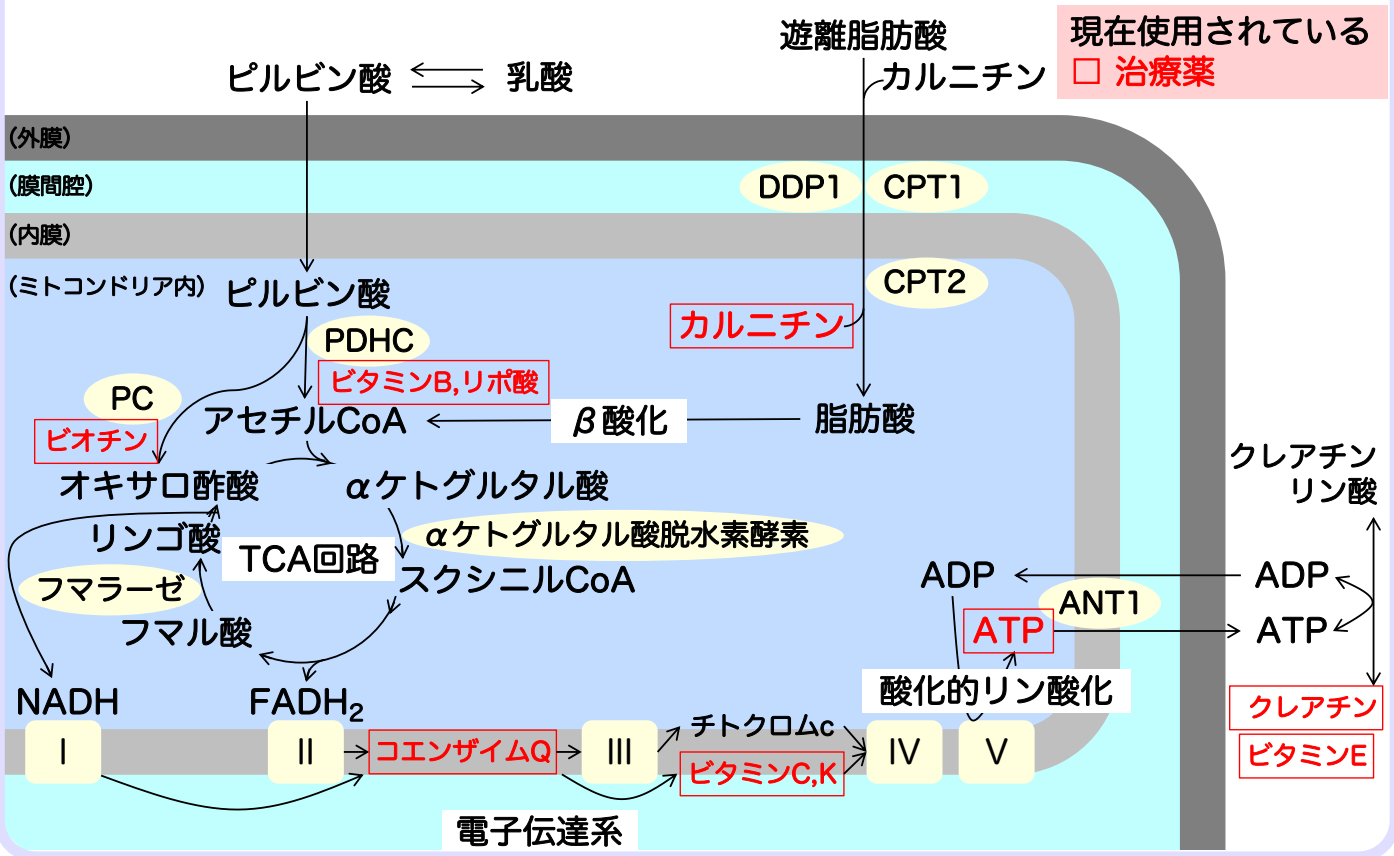

もう一つの治療法は、
病気の原因であるミトコンドリア機能の低下を改善させる原因療法です。
ミトコンドリアでの代謝に関わる物質やビタミンなども使用されていますが、
現時点では、有効性が証明されているものは限られます。
MELASという病気の患者さんに対しては、タウリンの内服により
脳卒中様発作を抑制する効果が認められ、保険薬として承認されています。

また、生活上の注意点としてミトコンドリア機能を低下させるような行動は
避けることが望ましいと考えられます。
飲酒、過食や飢餓は、ミトコンドリアに負担をかけます。
睡眠は十分とることが大切です。
感染をきっかけに症状が悪化することもありますので、注意しましょう。
栄養バランスのよい、ビタミンの多い食事と適度の運動、
生活リズムを整えることが、なにより重要です。

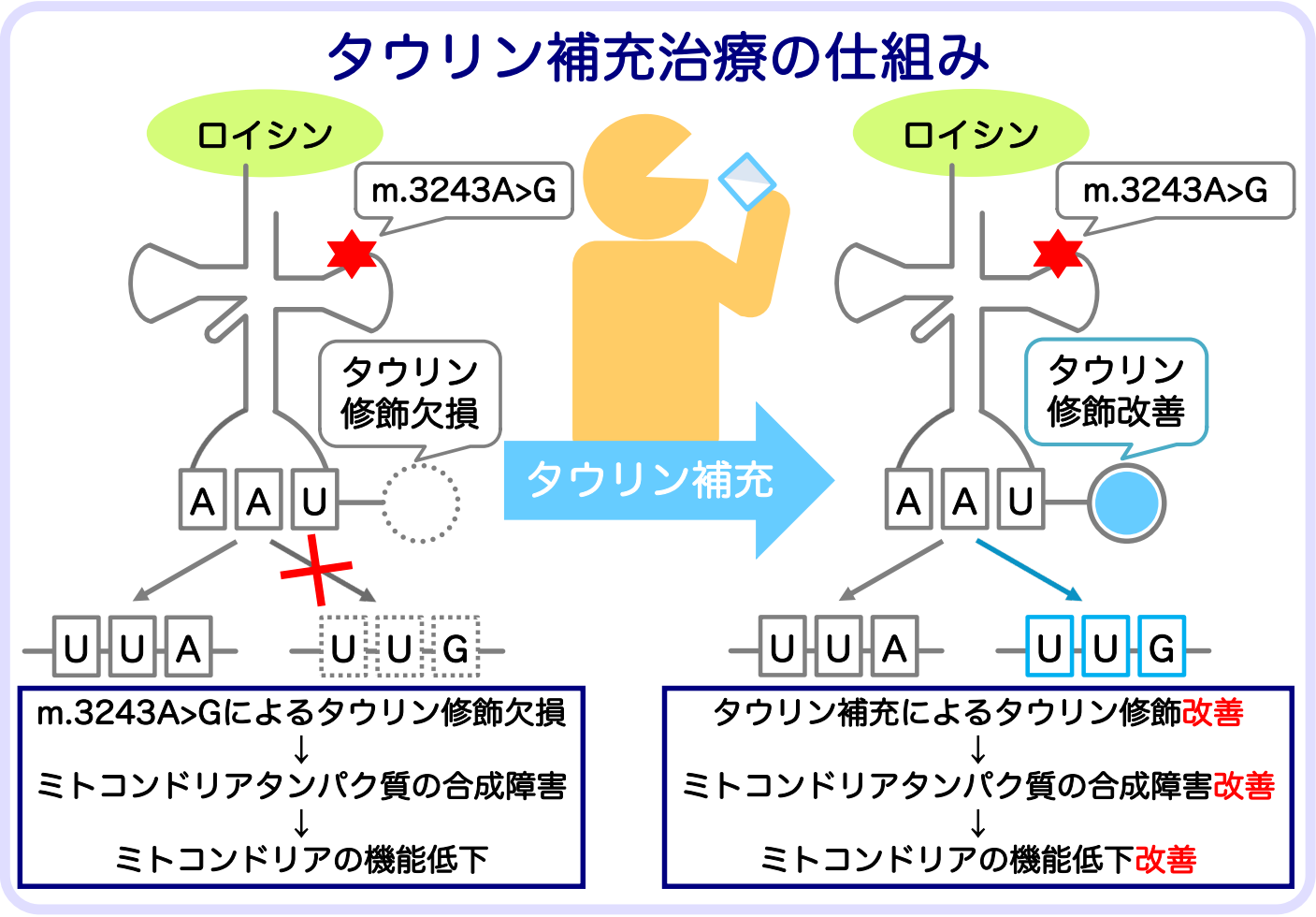

ミトコンドリアDNAのm.3243A>Gという変化をはじめ、
いくつかの一塩基の変化をもつMELASの患者さんは、
ミトコンドリア転移RNAのタウリン修飾が阻害されることが分かりました。
タウリン修飾が阻害されると、ミトコンドリア内のタンパク質が
合成されなくなり、病気が発症する一因と考えられています。

タウリン補充療法では、タウリンを大量に服用することで、
ミトコンドリア転移RNAのタウリン修飾欠損が改善し、
ミトコンドリア内のタンパク質合成と機能が改善すると考えられています。

ミトコンドリア病の
患者・家族のための社会資源

代表的な医療費助成制度

指定難病医療費助成制度

対象：
指定難病の診断基準を満たし「重症度分類」に照らして病状の程度が一定以上の人
（軽症者でも高額な医療※を継続することが必要な人は対象）※条件あり
内容：
医療費の助成

小児慢性特定疾病医療費助成制度

対象：
小児慢性特定疾病の認定基準を満たす症状をもつ18歳未満の子ども
（18歳到達後も引き続き治療が必要と認められる場合、20歳未満の人も対象）
内容：
医療費の助成

高額療養費制度

対象：
同一月（1日から月末まで）にかかった医療費の自己負担額が一定額を超えた人
内容：
医療費の払い戻し

ミトコンドリア病患者さんが利用を検討できる
代表的な医療費助成制度をご紹介します。

指定難病医療費助成制度、小児慢性特定疾病医療費助成制度は、
それぞれ指定の医療機関を受診し、
申請に必要な書類を指定医に記載してもらう必要があります。
病気の状態によって、助成制度の対象外となる人もいます。
詳しくは、主治医の先生や通院している病院の医療福祉相談室、
お住まいの市町村の担当窓口や保健所にご相談ください。

また、高額療養費制度の支給申請方法はご自身が加入されている
公的医療保険（健康保険組合・協会けんぽ・共済組合など）に
お問い合わせください。

代表的な福祉制度

障害福祉サービス

対象：
身体または知的障害のある人（児童含む）、精神障害のある人、難病患者等で一定の障害のある人
内容：
介護給付（居宅介護や重度訪問介護など）
訓練等給付（自立訓練や就労移行支援など）

介護保険

対象：
介護が必要と認定された一定年齢以上の人
内容：
ケアプランにもとづいた介護サービスの利用

身体障害者手帳

対象：
認定基準を満たす障害をもつ人
内容：
補装具の交付・税金の減免・交通費の割引など

障害年金

対象：
障害をもつ年金加入者
内容：
年金の給付

その他：特別障害者手当・障害児福祉手当など（所得制限あり）

ミトコンドリア病患者さんが利用を検討できる
代表的な福祉制度をご紹介します。
利用できる制度は、病気の状態やお住まいの地域などによって異なります。

自治体が独自に実施している制度もありますので、
詳しくは、お住まいの市区町村の担当窓口、保健所、
通院している病院の医療福祉相談室などでご相談ください。

制度をよく理解して有効に利用することで、
療養生活をより快適に過ごすことができるでしょう。

情報サイト

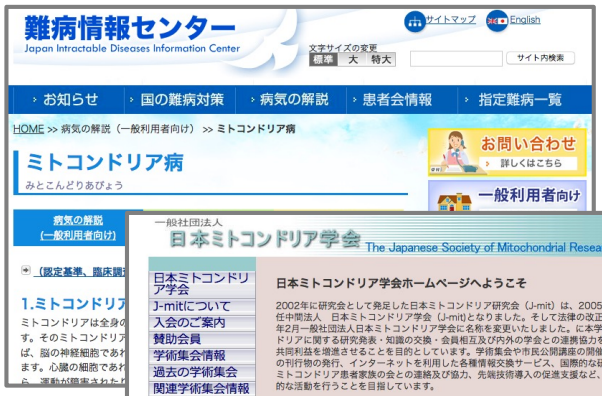

難病情報センター
病気の解説や研究班の活動など
http://www.nanbyou.or.jp/

日本ミトコンドリア学会
ドクター相談室や学術活動など
http://www.j-mit.org/

ミトコンドリア病
患者・家族の会
病気に関する情報共有など
http://mcm.sakura.ne.jp/wpnew/

インターネット上の情報源には、
国の「難病情報センター」や専門家による「ミトコンドリア学会」、
当事者による「ミトコンドリア病患者・家族の会」のページがあります。
ミトコンドリア病についてのさまざまな情報が公開されています。

ミトコンドリア病の患者登録制度

患者登録制度

Remudy（レムディ）

対象：
ミトコンドリア病患者さん

ホームページ：
http://www.remudy.jp/mitd/

J-MO Bank

対象：
新生児期・小児期発症の
ミトコンドリア病患者さん

ホームページ：http://mo-bank.com/

ミトコンドリア病患者さんを対象とした患者登録制度が始まっています。

患者登録制度は２つあり、どちらも治療研究および新薬開発の促進と、
円滑な臨床試験・治験実施などを目的としています。

登録を希望される患者さん、あるいはご家族が登録の手続きをする仕組みで
臨床情報の記入は主治医の先生に協力してもらう必要があります。

患者登録を検討される場合には、
それぞれの患者登録制度のホームページで登録方法をご確認ください。

ミトコンドリア病の遺伝

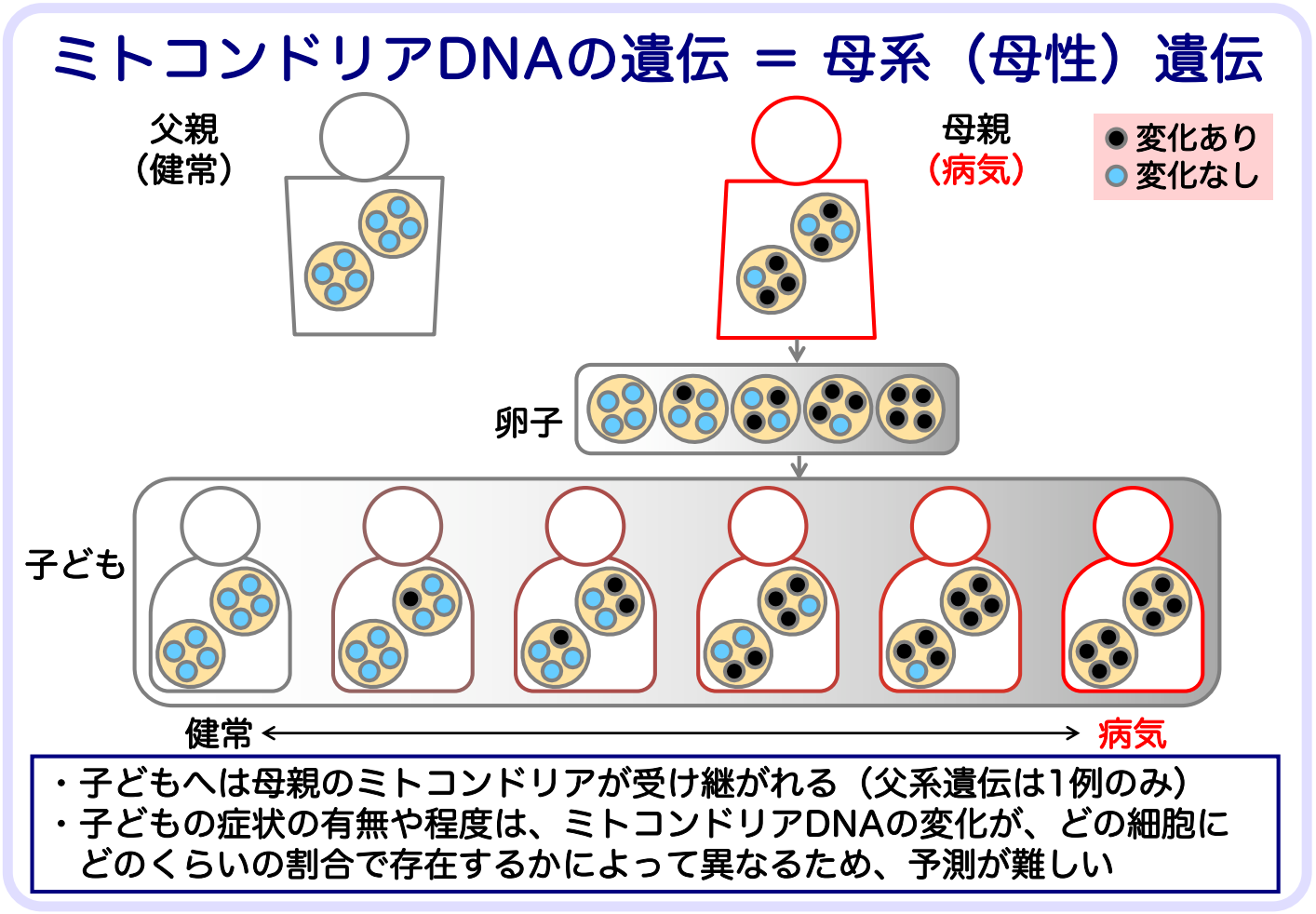

ミトコンドリア病の多くは、
ミトコンドリアDNAの変化が原因で発症します。
ミトコンドリアDNAは、母親から子どもに受け継がれます。
これを母系（母性）遺伝と呼びます。
父親のミトコンドリアは子どもへは通常受け継がれません。
（これまでに1例のみ報告されています。）
子どもの症状の有無や程度は、ミトコンドリアDNAの変化が、
どの細胞にどのくらいの割合で存在するかによって異なるため、
予測が難しいと考えられています。

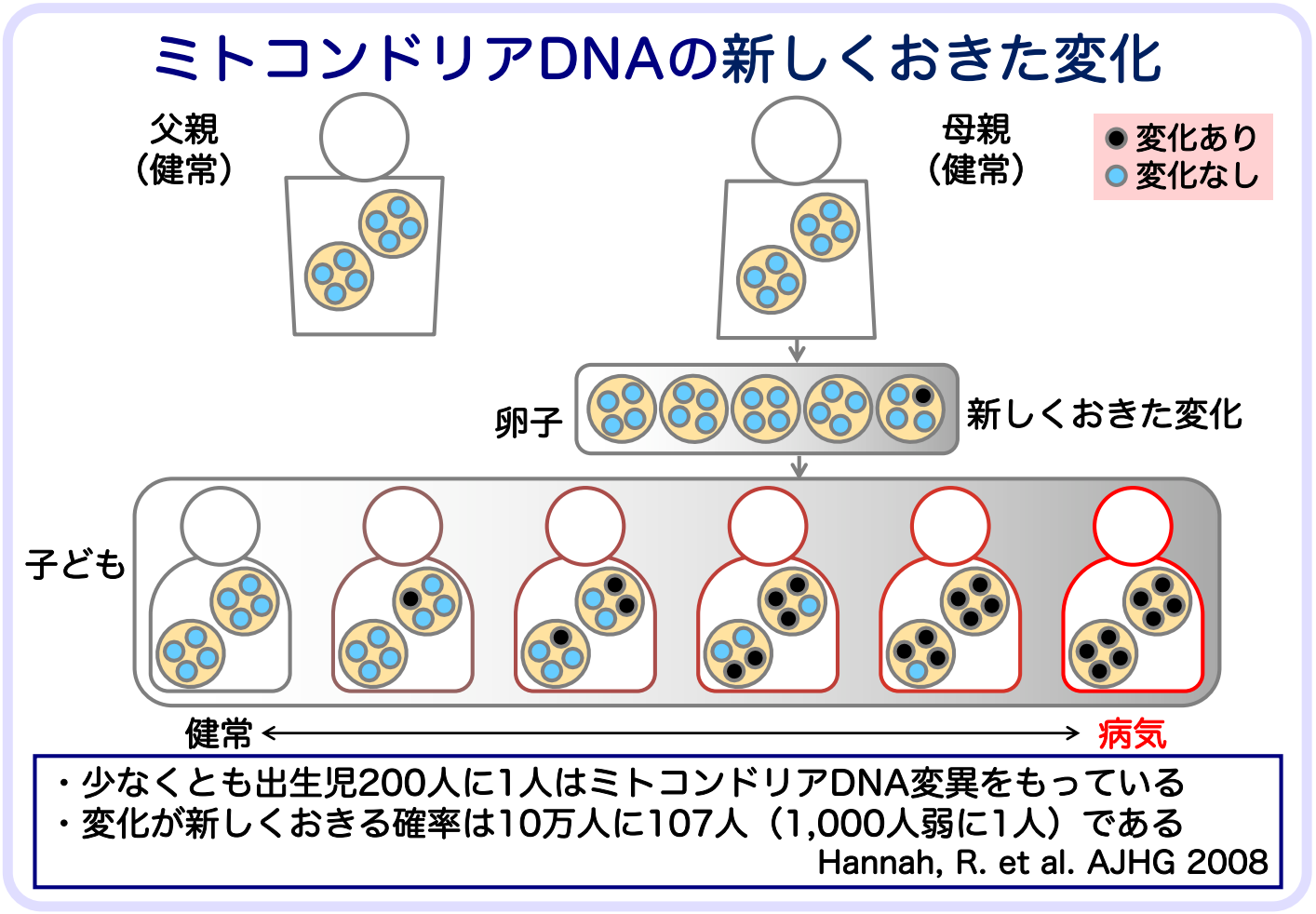

ミトコンドリアDNAの変化は、母親由来ではなく
新しくおきた変化である可能性もあります。
ある調査によると、少なくとも新生児200人に1人は
ミトコンドリアDNA変異をもっていることが分かっています。
変化が新しくおきる確率は、10万人に107人と計算されています。

核DNAの遺伝 ＝ メンデル遺伝

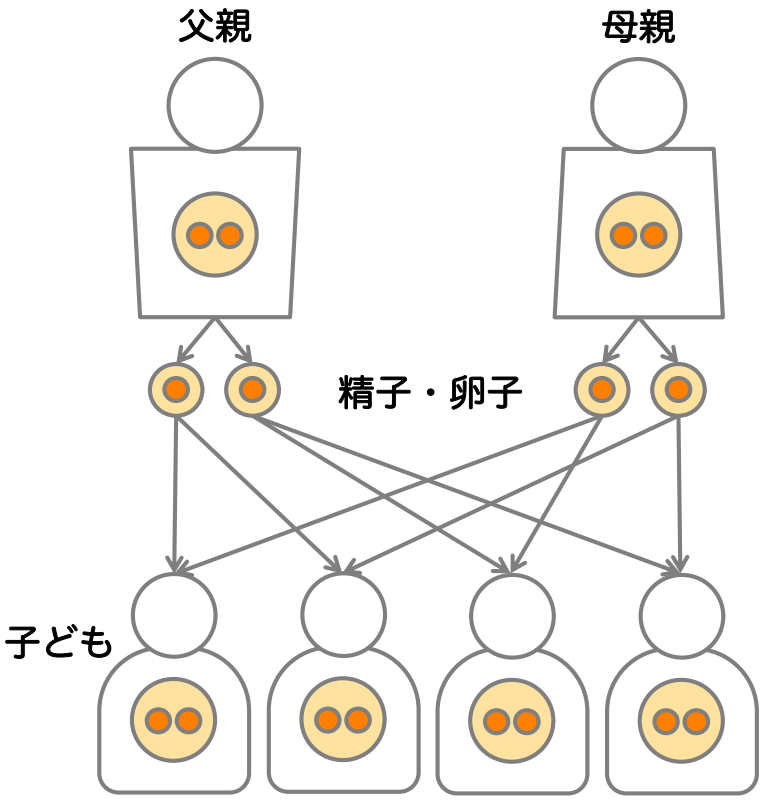

染色体写真（上：男性、下：女性）

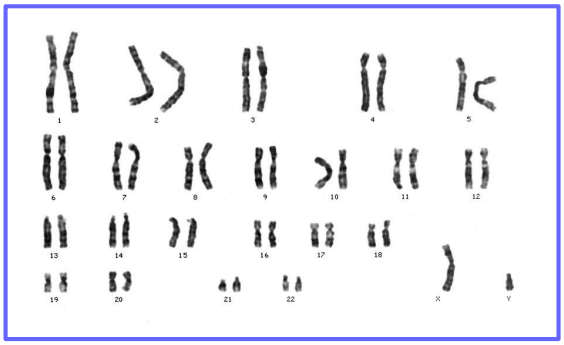

核DNAは、両親から子どもに受け継がれます。
私たちは両親から一つずつDNAを受け継ぎますので、
同じ種類の遺伝子を二つずつもっています。
そしてそれを子どもに伝えるときには、どちらか一つだけを渡します。
染色体も同じ種類のものが二つずつあります。
その中には、22番までの番号が振られた男女共通の染色体（常染色体）と
性別を決める染色体（性染色体）があります。
男性の場合はX染色体とY染色体を一つずつ、
女性の場合はX染色体を二つもっています。
性染色体に入っている遺伝子は男女間で数が異なるため、その遺伝子に
病気の原因となる変化が生じた場合には、
性別によって発症の仕方が異なります。

顕性（優性）と潜性（劣性）

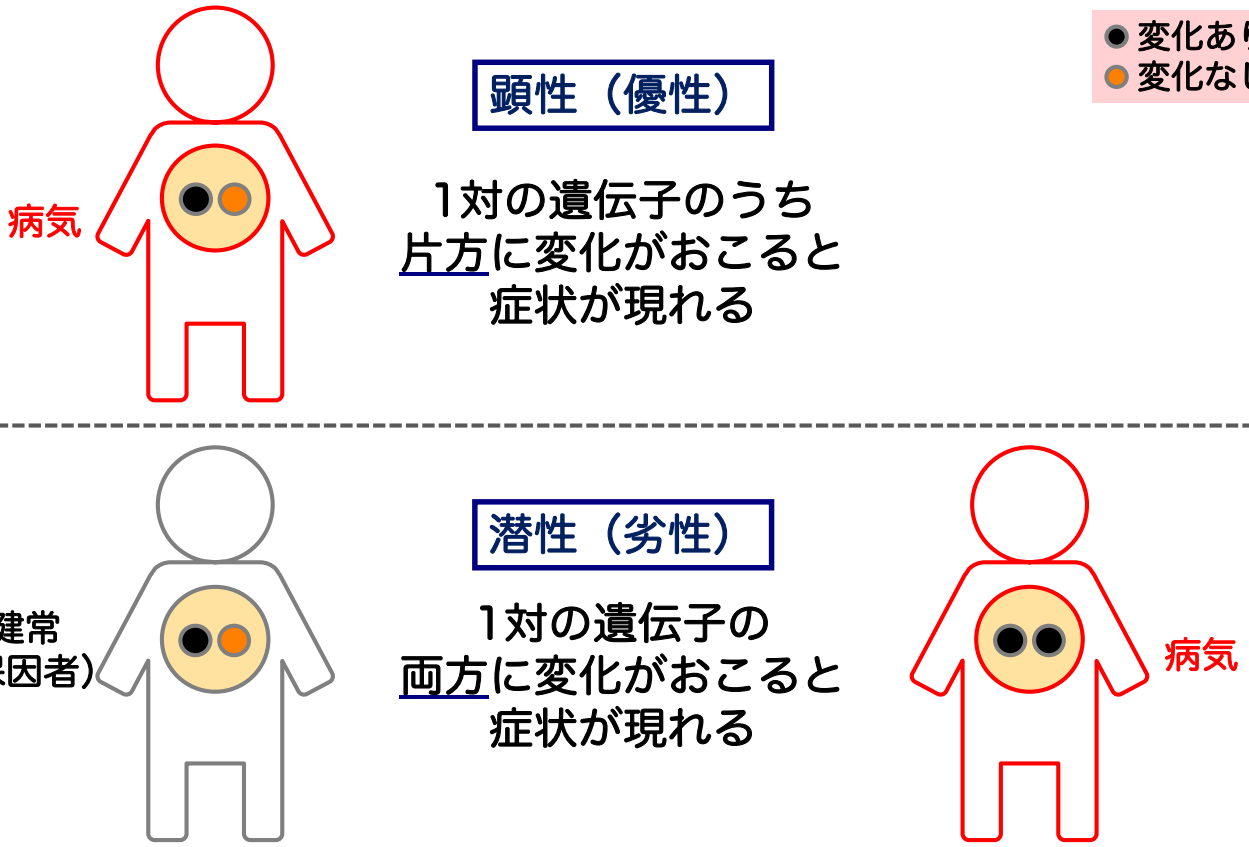

二つある遺伝子のうち、
片方に病気をおこす変化をもつと症状が現れる場合を顕性（優性）、
両方に病気をおこす変化をもつと初めて症状が現れる場合を潜性（劣性）と言います。
潜性（劣性）の場合に、片方の遺伝子に病気をおこす変化をもつ人を保因者と呼びます。
保因者は通常発症しませんが、
病気によっては何らかの症状が現れることもあります。
病気の原因となる遺伝子が入っているのが常染色体か性染色体か、
その遺伝子の変化が顕性（優性）か潜性（劣性）かによって、
次世代への遺伝の仕方が異なります。

常染色体潜性遺伝（劣性遺伝）

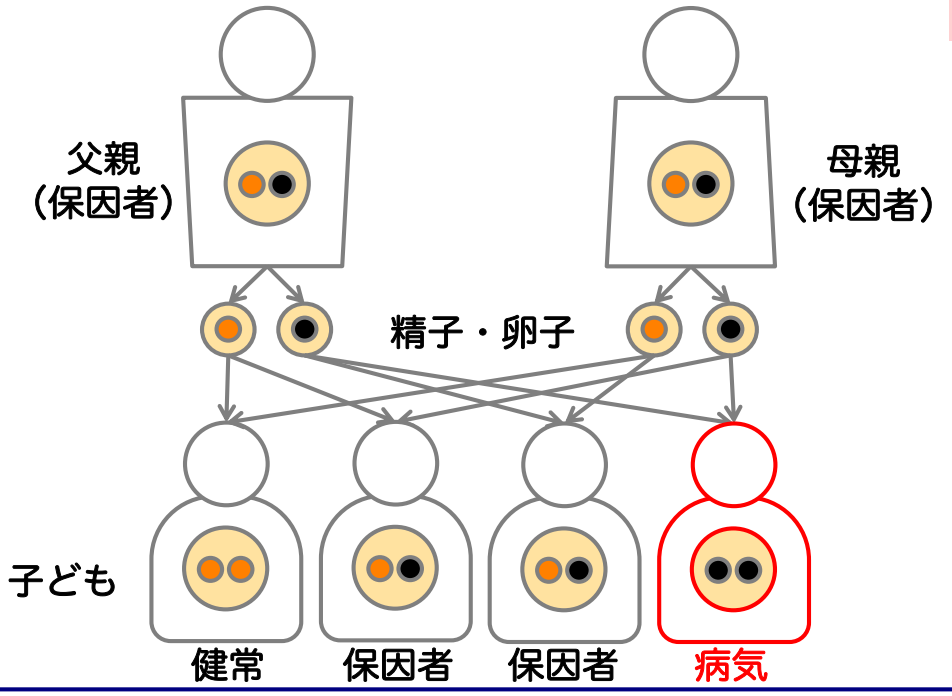

・両親とも保因者であると考えられる
・次の子が病気をもつ確率は1／4（25%）、保因者の確率は1／2（50%）

核DNAの変化が原因で起こるミトコンドリア病のほとんどは、
常染色体潜性遺伝（劣性遺伝）と呼ばれる形式で伝わります。
両親が一つずつもっている遺伝子の変化が、両方とも子どもに伝わる
ことで発症すると考えられます。つまり両親は保因者です。
したがって、次の子が病気をもつ確率は4分の1（25%）、
保因者となる確率は2分の1（50%）です。

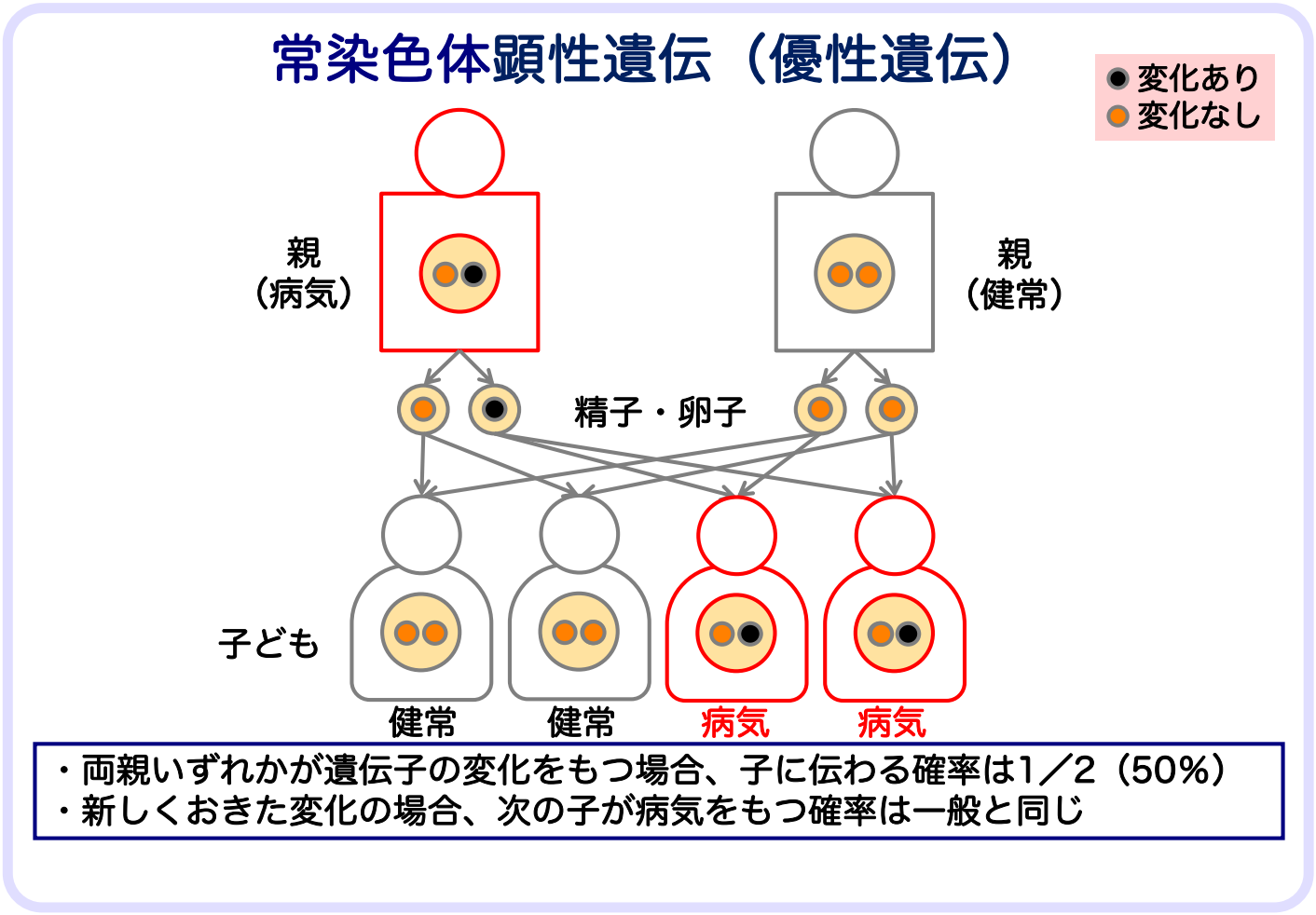

ミトコンドリア病のうち、常染色体顕性遺伝（優性遺伝）と呼ばれる形式で伝わる病気はまれで、CPEOの一部などに限られます。
この形式では、両親のいずれかが遺伝子の変化をもつ場合、
子どもには2分の1（50%）の確率でそれが伝わります。
両親が遺伝子の変化をもっておらず、
新しくおきた変化によって子どもが発症した場合には、
次の子が病気をもつ確率は一般の人と同じと考えられます。

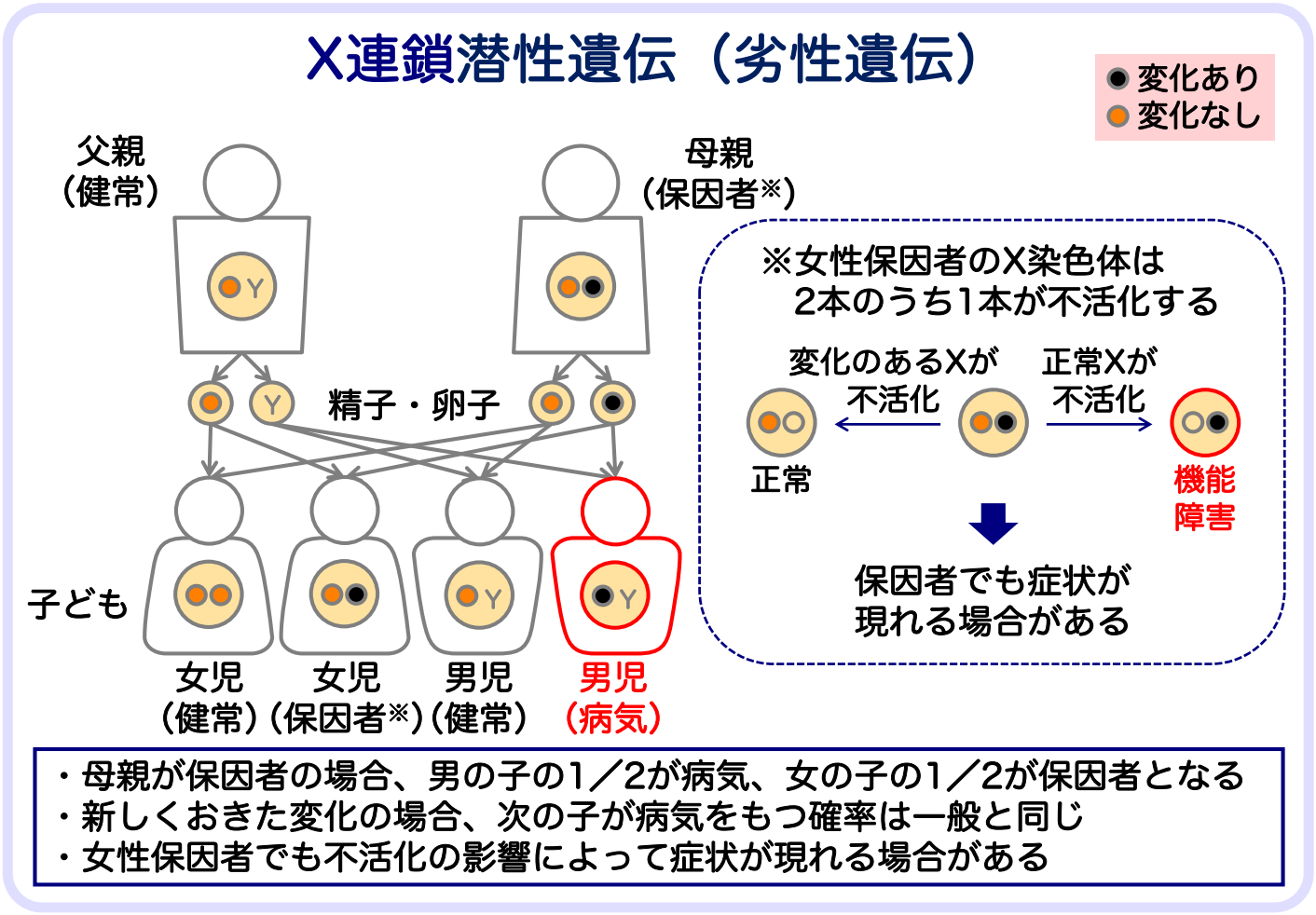

ミトコンドリア病のうち、
X連鎖潜性遺伝（劣性遺伝）と呼ばれる形式で伝わる病気は、
DDP 遺伝子の変化によって生じる難聴とジストニアなどに限られます。
男性のX染色体は1本なので、その中の遺伝子に変化がおこると発症します。
女性は2本あるため保因者となり、通常、症状は現れません。
ただし、2本のうち1本は不活化されていて働かないため、
どちらが不活化されるかによって、女性でも症状が現れる場合があります。
保因者である母親からは、X染色体2本のどちらかが子どもに伝わるため、
男の子の2分の1（50%）が病気、
女の子の2分の1（50%）が保因者となります。
病気の子がもっている変化が、
母親由来ではなく新しくおきた変化の場合、
次の子が病気をもつ確率は一般と同じと考えられます。

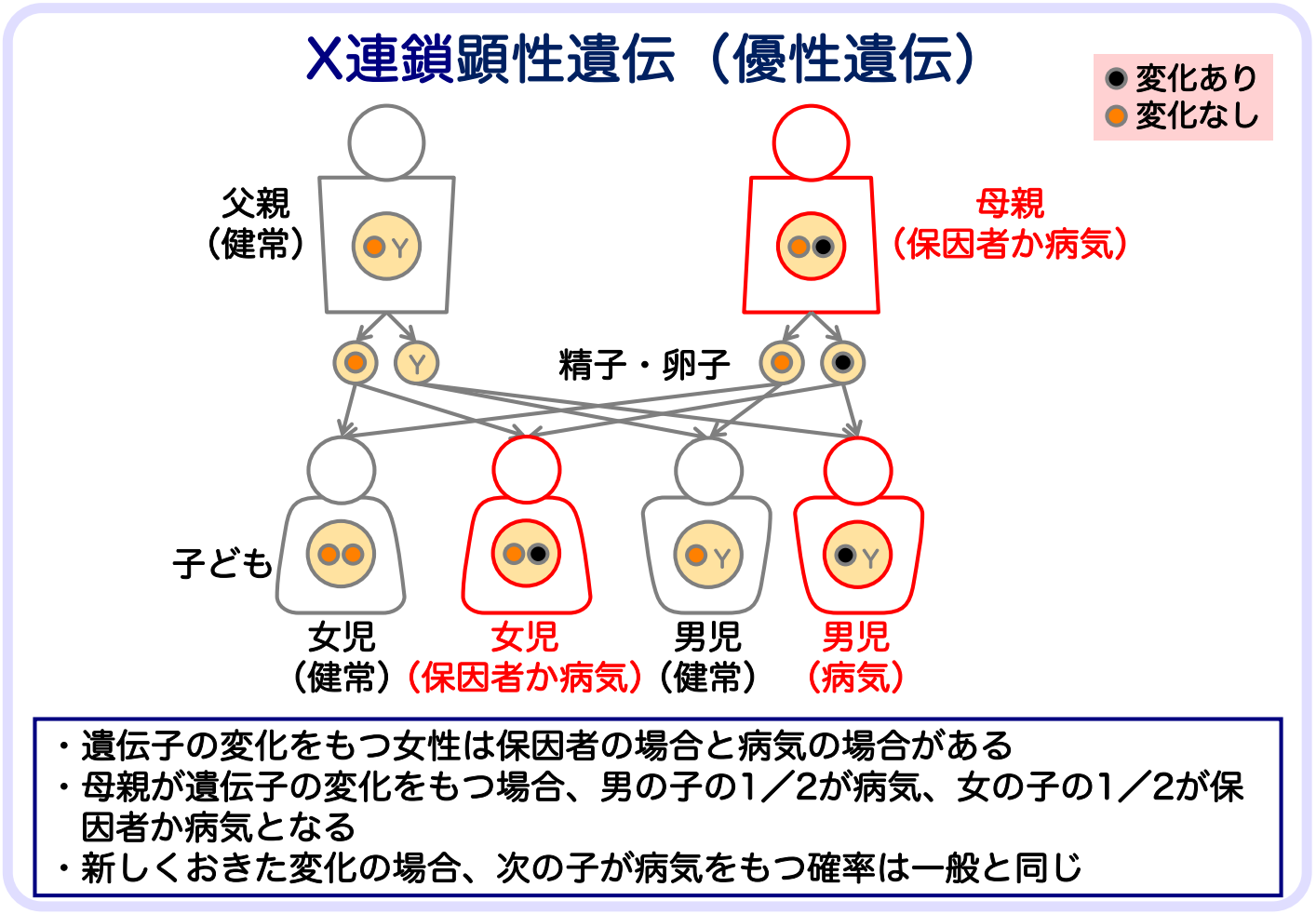

ミトコンドリア病のうち、
X連鎖顕性遺伝（優性遺伝）と呼ばれる形式で伝わる病気は、
PDHA1 遺伝子の変化によって生じるPDHC欠損症が知られています。

男性のX染色体は1本なので、その中の遺伝子に変化がおこると発症します。
女性は２本あるため症状の現れない保因者となる場合と、
病気になる場合があります。

遺伝子の変化をもつ母親からは、
X染色体2本のどちらかが子どもに伝わるため、
男の子の2分の1（50%）が病気、
女の子の2分の1（50%）が保因者か病気となります。
病気の子がもっている変化が、母親由来ではなく新しくおきた変化の場合、
次の子が病気をもつ確率は一般と同じと考えられます。

出生前診断・着床前診断

出生前診断	着床前診断
● 妊娠中に絨毛または羊水を採取して特定の遺伝子や染色体の異常の有無を調べる ● 流産の可能性あり	● 体外受精でできた受精卵を用いて特定の遺伝子や染色体の異常の有無を調べる ● 臨床研究のため申請が必要
● 胎児が重篤な病気をもつ可能性がある場合に限って実施する ● ヘテロプラスミーで発症する病気の場合は正確な診断ができないことがある ● 夫婦が希望していること、検査の意義について十分理解し、同意していることが条件となる ● 結果の解釈について事前に十分検討しておくことが重要 ● 胎児の病気を理由に妊娠を諦めてよいという法律はない	

子どもが遺伝子の変化をもっているかどうかを
生まれる前に調べる方法には、出生前診断と着床前診断があります。
出生前診断は、妊娠中に絨毛または羊水を採取して、
特定の遺伝子や染色体に変化があるかどうかを調べる技術です。
着床前診断は、体外受精でできた受精卵を用いて、
特定の遺伝子や染色体に変化があるかどうかを調べる技術です。
どちらも技術的な制約や倫理的な問題などがあるため、
それらを十分理解した上で実施するかどうかを考えることが重要です。

これらの診断について詳しく知りたい方は、
通っておられる病院の遺伝カウンセリングをご利用ください。

このハンドブックは
厚生労働科学研究費補助金難治性疾患政策研究事業
「ミトコンドリア病の調査研究」班（研究代表者：後藤雄一）初版
「ミトコンドリア病の診断水準やQOL向上を目指した調査研究」班
（研究代表者：三牧正和）第２版　の
分担研究（後藤雄一、佐藤有希子、杉本立夏）として作成されました。

初版　2012 年　5 月 24 日
第２版　2023 年 10月 31日

国立研究開発法人
国立精神・神経医療研究センター病院
ゲノム診療部　遺伝カウンセリング科
〒187-8551　東京都小平市小川東町4-1-1
電話：042-341-2711（内線：5824）

第8回ミトコンドリア病研究公開フォーラム

日時　2024年2月3日（土）12：30～16：30（予定）

Web開催。
ご家族そろって
ご参加ください！

ミトコンドリア病診療のこれから　2024

予定プログラム

＊ミトコンドリア病の臨床
- ・ミトコンドリア総論　…後藤　雄一先生（国立精神・神経医療研究センター）
- ・ミトコンドリア病の遺伝学的検査について　…八塚　由紀子先生（順天堂大学）

＊創薬
- ・変異ミトコンドリアDNAを標的とする薬剤開発　…高取　敦志先生（千葉県がんセンター）
- ・ミトコンドリア創薬　…菅沼　正司先生（ルカ・サイエンス株式会社）
- ・MA-5の治療開発について　…阿部　高明先生（東北大学）

＊患者会　…ASrid・MCMの会・みどりの会　より

＊ミトコンドリア雑感　…太田　成男先生（順天堂大学）

♪ミトコンドリア・ミニコンサート♪

参加費無料
要参加申込み

- ◆ 参加申し込み：y.konno.bn@juntendo.ac.jp にメールにてお申し込みください。
- ◆ 事前登録　：2024年1月29日まで
- ◆ 詳細は、JAMP-MITホームページ　http://jamp-mit.org/index.html
  J-MO Bankホームページ　http://mo-bank.com/　を参照ください。

主催：特定非営利活動法人　ミトコンドリア病医療推進機構 JAMP-MIT（理事長：高柳 正樹）
共催：日本医療研究開発機構(AMED)　難治性疾患実用化研究事業　ミトコンドリア病研究（研究者代表：村山　圭）
厚生労働省　難治性疾患政策研究事業　ミトコンドリア病研究(研究者代表：三牧　正和)
日本先天代謝学会　患者登録委員会　JaSMIn事務局（代表：小須賀　基通）

Molecular Genetics and Metabolism Reports 34 (2023) 100951

Contents lists available at ScienceDirect

Molecular Genetics and Metabolism Reports

journal homepage: www.elsevier.com/locate/ymgmr

Total and reduced/oxidized forms of coenzyme Q_{10} in fibroblasts of patients with mitochondrial disease

Chika Watanabe [a], Hitoshi Osaka [a,*], Miyuki Watanabe [a], Akihiko Miyauchi [a], Eriko F. Jimbo [a], Takeshi Tokuyama [b], Hideki Uosaki [b], Yoshihito Kishita [c,d], Yasushi Okazaki [c,e], Takanori Onuki [f], Tomohiro Ebihara [f], Kenichi Aizawa [g], Kei Murayama [f], Akira Ohtake [h], Takanori Yamagata [a]

[a] Department of Pediatrics, Jichi Medical University, Tochigi, Japan
[b] Division of Regenerative Medicine, Center for Molecular Medicine, Jichi Medical University, Tochigi, Japan
[c] Diagnostics and Therapeutic of Intractable Diseases, Intractable Disease Research Center, Graduate School of Medicine, Juntendo University, Tokyo, Japan
[d] Department of Life Science, Faculty of Science and Engineering, Kindai University, Osaka, Japan
[e] Laboratory for Comprehensive Genomic Analysis, RIKEN Center for Integrative Medical Sciences, Kanagawa, Japan
[f] Center for Medical Genetics and Department of Metabolism, Chiba Children's Hospital, Chiba, Japan
[g] Division of Clinical Pharmacology, Department of Pharmacology, Jichi Medical University, Tochigi, Japan
[h] Department of Clinical Genomics & Pediatrics, Faculty of Medicine, Saitama Medical University, Saitama, Japan

ARTICLE INFO

Keywords:
Mitochondrial disease
Primary coenzyme Q_{10} deficiency
Coenzyme Q_{10}
Reduced/total CoQ_{10}
Forward electron transport
Reverse electron transport

ABSTRACT

Coenzyme Q_{10} (CoQ_{10}) is involved in ATP production through electron transfer in the mitochondrial respiratory chain complex. CoQ_{10} receives electrons from respiratory chain complex I and II to become the reduced form, and then transfers electrons at complex III to become the oxidized form. The redox state of CoQ_{10} has been reported to be a marker of the mitochondrial metabolic state, but to our knowledge, no reports have focused on the individual quantification of reduced and oxidized CoQ_{10} or the ratio of reduced to total CoQ_{10} (reduced/total CoQ_{10}) in patients with mitochondrial diseases.

We measured reduced and oxidized CoQ_{10} in skin fibroblasts from 24 mitochondrial disease patients, including 5 primary CoQ_{10} deficiency patients and 10 respiratory chain complex deficiency patients, and determined the reduced/total CoQ_{10} ratio.

In primary CoQ_{10} deficiency patients, total CoQ_{10} levels were significantly decreased, however, the reduced/total CoQ_{10} ratio was not changed. On the other hand, in mitochondrial disease patients other than primary CoQ_{10} deficiency patients, total CoQ_{10} levels did not decrease. However, the reduced/total CoQ_{10} ratio in patients with respiratory chain complex IV and V deficiency was higher in comparison to those with respiratory chain complex I deficiency.

Measurement of CoQ_{10} in fibroblasts proved useful for the diagnosis of primary CoQ_{10} deficiency. In addition, the reduced/total CoQ_{10} ratio may reflect the metabolic status of mitochondrial disease.

1. Introduction

CoenzymeQ$_{10}$ (CoQ_{10}), also known as ubiquinone, is a lipophilic molecule composed of a redox-active benzoquinone head group and species-specific isoprenoid side chain (10 subunits in humans) [1,2]. CoQ_{10} takes three forms depending on the redox state of the benzoquinone ring; oxidized (CoQ_{10}, Ubiquinone), fully-reduced ($CoQ_{10}H_2$, Ubiquinol), and semi-reduced (CoQ^{+}_{10}, Semiubiquinone) forms [2]. It presents ubiquitously in all cellular membranes and cells [3]. The amount of CoQ_{10} and the proportion of reduced CoQ_{10} differ between organs and cells; CoQ_{10} is distributed in high amounts in the heart, kidneys, liver, and muscles, and the proportion of reduced CoQ_{10} is lower in the brain and lungs [3]. In cells, it is mostly localized in the mitochondria [3].

CoQ_{10} has multiple functions. One of the main roles of CoQ_{10} is as a component of the mitochondrial respiratory chain. As a mobile electron

* Corresponding author at: Department of Pediatrics, Jichi Medical University, 3311-1 Yakushiji, Shimotsuke-shi, Tochigi 329-0498, Japan.
E-mail address: hosaka@jichi.ac.jp (H. Osaka).

https://doi.org/10.1016/j.ymgmr.2022.100951
Received 25 October 2022; Received in revised form 22 December 2022; Accepted 22 December 2022
Available online 3 January 2023

carrier, CoQ_{10} accepts electrons from complex I and II and transfers them to complex III [2]. In the mitochondrial inner membrane, CoQ_{10} is proposed to exist as two independent pools: a CoQ_{NADH} pool in the super-complex (CI, CIII, CIV) involved in the oxidation of NADH; and a CoQ_{FADH} pool involved in the oxidation of CII and other enzymes that use CoQ as a cofactor [4]; CoQ_{NADH} receives electrons from NADH, and CoQ_{FADH} receives electrons from $FADH_2$ and other enzymes, such as glycerol phosphate dehydrogenase (GPDH), choline dehydrogenase (CHDH), sulphide:quinone oxidoreductase (SQOR), dihydroorote dehydrogenase (DHODH), and electron transfer flavoprotein dehydrogenase (ETFDH), and is reduced [5]. In respiratory chain complex III, electrons are transferred from reduced CoQ_{10} to cytochrome *c* in a process called the Q cycle. The Q cycle results in the oxidation of two molecules of reduced CoQ_{10}, the reduction of two molecules of cytochrome *c*, and the formation of one additional molecule of reduced CoQ_{10} [2]. This normal forward electron transfer results in the creation of an electrical gradient and a pH gradient (proton gradient) between the mitochondrial matrix and intermembrane space. The energy generated by this proton motive force enables complex V(ATP synthase) to synthesize ATP. On the other hand, reverse electron transfer (RET) of CoQ_{10} is also known to occur; in RET, electrons from reduced CoQ_{10} are returned to complex I, reducing NAD+ to NADH, and generating ROS [6] (Supplemental Fig. 1).

Another important role of CoQ_{10} is as an antioxidant. CoQ_{10} is the sole lipid-soluble antioxidant that is endogenously synthesized. Reduced CoQ_{10} inhibits both the initiation and the propagation of lipid peroxidation [7]. NADH-quinone oxidoreductase 1 and cytochrome *b*5 reductase, have been known to be the major oxidoreductases in the plasma membrane [8]. In addition, ferroptosis suppressor protein 1 (FSP1) was also found to be an important oxidoreductase. FSP1 reduces extra-mitochondrial CoQ_{10} and acts as a lipophilic radical-trapping antioxidant to suppress lipid peroxides, resulting in the inhibition of cell death, called ferroptosis [9,10]. Moreover, reduced CoQ_{10} also regenerates the other antioxidants—α-tocopherol and ascorbate—into an active reduced form [7]. CoQ_{10} is also involved in the β-oxidation of fatty acids [11], de novo pyrimidine biosynthesis [12], sulfide oxidation [13], an essential cofactor for uncoupling proteins (UCPs) [14], and modulation of the mitochondrial permeability transition pore [15]. Thus, the importance of the distinct state of CoQ_{10} is gaining growing attention [5].

Primary CoenzymeQ_{10} (CoQ_{10}) deficiency is an autosomal recessive mitochondrial disease caused by a decrease in CoQ_{10} due to mutations in genes involved in CoQ_{10} biosynthesis (*COQ* genes) [16]. To date, defects in at least 10 *COQ* genes (*COQ2, COQ4, COQ5, COQ6, COQ7, COQ8A, COQ8B, COQ9, PDSS1, PDSS2*) have been found to cause this disease [17]. Primary CoQ_{10} deficiency was first reported in 1989 as familial mitochondrial encephalomyopathy [18]. Currently, over 280 patients from 180 families have been reported [17]. Secondary CoQ_{10} deficiencies occur in a wider variety of pathologies, including mitochondrial disease [19,20]. Measuring the CoQ levels is known to be useful for diagnosing CoQ_{10} deficiency [21]. As described above, the ratio of reduction varies among organs and cells. As a result, in addition to the total amount of CoQ_{10}, evaluating the reduced/oxidized CoQ_{10} ratio may also be useful for further elucidating various pathophysiological states in cells.

Methods to measure CoQ_{10} in fibroblast and the reduced/oxidized state of CoQ_{10} have been reported [22,23]. However, to our knowledge, there are no reports on the measurement of the reduced/oxidized CoQ_{10} ratio in primary CoQ_{10} deficiency or mitochondrial diseases. Therefore, we decided to measure the total CoQ_{10} levels as well as the levels of reduced and oxidized CoQ_{10} in skin fibroblasts from patients affected by various mitochondrial diseases.

2. Material, methods, and patients

2.1. Subjects

We studied fibroblasts from 24 patients with mitochondrial disease, including primary CoQ_{10} deficiency (Table 1). The inclusion criterion for patients with primary CoQ_{10} deficiency was childhood onset with biallelic pathogenic variants in the *COQ* gene encoding proteins for the biosynthesis of CoQ_{10} [16]. Fibroblasts were obtained from patients at Kanagawa Children's Medical Center, Chiba Children's Medical Center, and Jichi Medical University under the approval of the Ethics Committee of Jichi Medical University. Written informed consent was obtained from the parents of each patient.

We obtained fibroblasts from five patients with primary CoQ_{10} deficiency. One patient carries biallelic *COQ2* variants with the c.[349G > C];[912 + 1G > del] (Case 1). Four patients had biallelic *COQ4* mutations: one with compound heterozygous biallelic variants c.[718C > T];[421C > T] (Case 2) [24], one with c.[431C > A];[718C > T] (Case 3) [25], and two with c.[190C > T];[479G > A] (Cases 4, 5).

Ten patients had disorders of mitochondrial respiratory chain subunits. Seven patients had mutations related to complex I: one with a c.[55C > T] mutation in *NDUFA1* (Case 6) [26], one with an m.10158 T>C mutation in *MT-ND3* (Case 7) [26], Three with an m.13513G > A mutation in *MT-ND5* (Case 8) [27], (Case 9), (Case 10) [28], one with a c.[811 T > G];[1766-2A > G] mutation in *ACAD9* (Case 11), and one with a c.[1150G > A];[1817 T > A] mutation in *ACAD9* (Case 12) [28]. NDUFA1, MT-ND3, and MT-ND5 are subunits of complex I, and ACAD9 is the assembly factor of complex I. Two patients had mutations related to complex IV: one with a c.[743C>A] mutation in *SURF1* (Case 13) [29], and one with a c.[367_368delAG]; [572delC] mutation in *SURF1* (Case 14) [25]. SURF1 is the assembly factor of complex IV. One patient had an m.8993 T > G mutation in *MT-ATP6* (Case 15) [25]. MT-ATP6 is a subunit of complex V.

Three patients had mitochondrial DNA (mtDNA) depletion syndrome: one with a c.[143-307_170del335];[143-307_170del335] mutation in *DGUOK* (Case 16) [30], one with a c.[451dupC];[308_310del] mutation (Case 17) [30] and one with a c.[148C > T];[149G > A] mutation in *MPV17* (Case 18) [30]. Both DGUOK and MPV17 are involved in the maintenance of mtDNA. One patient had Kearns-Sayre syndrome with a single mtDNA deletion (5513 bp del; m.8290–13,802) (Case 19). Two patients had MELAS: one with an m.3243 A > G mutation of tRNA-Leu (Case 20) [26] and one with an m.5541C > T, mutation of tRNA-Trp (Case 21) [26]. One patient had short-chain enoyl-CoA hydratase (ECHS1) deficiency with heterozygous mutations in maternal c.[832G > A] in *ECHS1* (Case 22) [31]. ECHS1 plays a role in valine and fatty acid catabolism in mitochondria. Two patients had c.[287A > G]; [287A > G] mutation in *BOLA3* (Cases 23) [28],(Case 24). BOLA3 is related to iron-sulfur cluster production and is involved in the assembly of the mitochondrial respiratory chain complex.

Five fibroblasts from healthy individuals were purchased: two fibroblasts from the PromoCell Company (#C-12300, GmbH, Heidelberg, Germany), two fibroblasts from Japanese Collection of Research Bioresources Cell Bank (#TIG-120, #HT-2020, Japan), and fibroblasts from Lonza Japan (#CC-2509, Tokyo, Japan). Another five fibroblasts from patients without mitochondrial disease were used as controls. Cells from passages 4–29 were used for assays.

2.2. Cell culture and growth conditions

The fibroblasts were maintained in 1.0 g/L low glucose Dulbecco's Modified Eagle's Medium (DMEM) (Life Technologies, Carlsbad, CA, USA) supplemented with 10% fetal bovine serum (FBS), 100 units/mL penicillin, and 100 μg/mL streptomycin. Cells were incubated at 37 °C under 5% CO_2.

Table 1
Fibroblast cell lines from patients with mitochondrial disease, including primary CoQ_{10} deficiency.

Case [ref]	diagnosis	DNA mutation	variants, heteroplasmy rate[a]	function
1	primary CoQ_{10} deficiency	*COQ2*	c.[349G > C];[912 + 1G > del]	CoQ_{10} biosynthesis
2 [24]	primary CoQ10 deficiency	*COQ4*	c.[718C > T];[421C > T]	CoQ_{10} biosynthesis
3 [25]	primary CoQ_{10} deficiency	*COQ4*	c.[431C > A];[718C > T]	CoQ_{10} biosynthesis
4	primary CoQ_{10} deficiency	*COQ4*	c.[190C > T];[479G > A]	CoQ_{10} biosynthesis
5	primary CoQ_{10} deficiency	*COQ4*	c.[190C > T];[479G > A]	CoQ_{10} biosynthesis
6 [26]	Leigh syndrome	*NDUFA1*	c.[55C > T], 100% (X-linked)	Respiratory chain subunits, complex I
7 [26]	Leigh syndrome	*MT-ND3*	m.10158 T>C, heteroplasmic (F; 90%)	Respiratory chain subunits, complex I
8 [27]	neonatal cardiomyopathy	*MT-ND5*	m.13513G > A, heteroplasmic (F; 78.87%)	Respiratory chain subunits, complex I
9	infantile mitochondrial disease	*MT-ND5*	m.13513G > A, heteroplasmic (B; 77%)	Respiratory chain subunits, complex I
10 [28]	Leigh syndrome	*MT-ND5*	m.13513G > A, heteroplasmic (F; 26%)	Respiratory chain subunits, complex I
11	mitochondrial cardiomyopathy	*ACAD9*	c.[811 T > G];[1766-2A > G]	Respiratory chain assembly factor, complex I
12 [28]	non-lethal infantile mitochondrial disease	*ACAD9*	c.[1150G > A];[1817 T > A]	Respiratory chain assembly factor, complex I
13 [29]	Leigh syndrome	*SURF1*	c.[743C>A], homoplasmy	Respiratory chain assembly factor, complex IV
14 [25]	Leigh syndrome	*SURF1*	c.[367_368delAG];[572delC]	Respiratory chain assembly factor, complex IV
15 [25]	Leigh syndrome	*MT-ATP6*	m.8993 T > G, homoplasmy	Respiratory chain subunits, complex V
16 [30]	mtDNA depletion syndrome	*DGUOK*	c.[143-307_170del335];[143-307_170del335]	Deoxynucleotide triphosphate synthesis
17 [30]	mtDNA depletion syndrome	*MPV17*	c.[451dupC];[308_310del]	mitochondrial protein synthesis
18 [30]	mtDNA depletion syndrome	*MPV17*	c.[148C > T];[149G > A]	mitochondrial protein synthesis
19	Kearns-Sayre syndrome		Single mtDNA deletion (5513 bp del; m.8290–13,802)	
20 [26]	MELAS	(tRNA-Leu)	m.3243 A > G, heteroplasmic (F; 21%)	Mitochondrial tRNA
21 [26]	MELAS	(tRNA-Trp)	m.5541C > T, heteroplasmic (F; 49%)	Mitochondrial tRNA
22 [31]	ECHS1 deficiency	*ECHS1*	c.[832G > A]	Metabolism of toxic compounds
23 [28]	cardiomyopathy	*BOLA3*	c.[287A > G];[287A > G]	Iron-sulfur protein assembly
24	cardiomyopathy	*BOLA3*	c.[287A > G];[287A > G]	Iron-sulfur protein assembly

[a] F; fibroblasts, B; blood

2.3. CoQ_{10} measurement in fibroblasts

2.3.1. CoQ extraction

The methods for the extraction CoQ_{10} were based on a previously reported method with slight modifications [32]. To extract CoQ_{10} from fibroblast in 60 mm dishes, cells were washed twice with PBS, and pellets were re-suspended in 500 μL of lysis buffer (0.25 mM Sucrose, 2 mM EDTA, 10 mM Tris, and 100 UI/mL heparin, pH 7.4.), and sonicated twice for 5 s. These homogenates were also used to citrate synthase and protein quantification. To measure CoQ_{10}, nine hundred microliters of ethanol containing internal standard CoQ_{10}-d9 (IsoSciences, Ambler, PA) and 20 μM *tert*-butyl hydroquinone (TBHQ) (FUJIFILM Wako, Osaka, Japan) was added to 100 μL of homogenates. TBHQ was added to prevent oxidation of reduced CoQ_{10}. The cell suspensions were vortexed and centrifuged at 15,700 ×*g* for 10 min (4 °C).

2.3.2. Reduction of ubiquinone

Reduced CoQ_{10} was required for use in the calibration curve measurement. However, since reduced CoQ_{10} is easily oxidized, reduced CoQ_{10} was prepared just before the analysis by reducing oxidized CoQ_{10} following a previously reported method with slight modification [33]. Briefly, 50 μL of CoQ_{10} was diluted in 1.95 mL hexane in a glass tube. Twenty milligrams of $NaBH_4$ was added and followed by the addition of 100 μL methanol, vortexed for 3 min, then placed in the dark for 5 min at room temperature. After reduction, 1 mL of water containing 100 μM EDTA was added to stop the reaction, vortexed for 1 min, and centrifuged 1500 ×*g* for 5 min at 4 °C. The upper layer containing reduced CoQ_{10} was transferred to a glass tube.

2.3.3. Liquid chromatography-tandem mass spectrometry (LC-MS/MS) analysis

The method for measuring reduced and oxidized CoQ_{10} was based on the previously reported method with slight modifications [23]. An LC-MS/MS analysis was performed on an LC-electrospray ionization-MS (LC-ESI-MS) with triple quadrupole (Nexera X2 and LCMS-8060, Shimadzu, Kyoto, Japan). A Kinetex C18 column (100 mm × 2.1 mm, 2.6 μm, Phenomenex) and a guard column filled with the same packing material were used. The column temperature was kept at 40 °C. The mobile phase was isocratic with 2 mM ammonium formate in methanol. The flow rate was 0.8 mL/min, the injection volume was 2 μL, and the run time was 6 min. The interface temperature was 300 °C, the desolvation line temperature was 250 °C, and the heat block temperature was 400 °C. The nebulizing gas flow was 3 L/min, the heating gas flow was 10 L/min, and the drying gas flow was 10 L/min. The samples were kept at 4 °C before injection by the autosampler. The MS/MS conditions for each target were optimized using the automated multiple reaction monitoring (MRM) optimization procedures in LabSolutions (Shimadzu). The MRM used for quantification was m/z 880.5 > 197.1 for oxidized CoQ_{10}, 882.4 > 197.0 for reduced CoQ_{10}, and 890.4 > 206.2 for CoQ_{10}-d9 (internal standard). Standards and samples were quantified using the LabSolutions software program to determine the peak area for oxidized CoQ_{10}, reduced CoQ_{10}, CoQ_{10}-d9, and the standard curves were used to determine the total amount of CoQ present in the samples.

Intra-assay coefficients of validation (CVs) and relative errors (REs), as measurements of precision and accuracy, respectively, were determined in five parallel analyses of the same cell. To evaluate inter-assay precision and accuracy, one cell line was independently evaluated on three different days. Precision was calculated as (standard deviation/mean concentration) × 100 (%), and accuracy was calculated as (quantitative value/theoretical value) × 100 (%). The intra-assay precision (CV) of reduced CoQ_{10} and oxidized CoQ_{10} was 0.58% and 1.39%, respectively. The intra-assay accuracy (RE) of reduced CoQ_{10} and oxidized CoQ_{10} was 4.20% and 2.50%, respectively. The inter-assay precision (CV) of reduced CoQ_{10} and oxidized CoQ_{10} was 1.27% and 1.84%, respectively. The intra-assay accuracy (RE) of reduced CoQ_{10} and oxidized CoQ_{10} was 10.54% and 1.18%, respectively (Supplemental Table 1, QC1).

2.3.4. Citrate synthase and protein quantification

Fibroblast CoQ_{10} levels were expressed as citrate synthase (CS) activity (measured CoQ_{10} values/CS units, nmol/CS units). CS activity was measured spectrophotometrically referring to the method described by Srere (1969), with 0.1 mM DTNB, 0.3 mM Acetyl-CoA, 0.5 mM Oxaloacetate, and 12–20 μg protein in 200 μL total incubation volume. CS units are determined as follows: CS Units (μmol/min/mL) = (ΔA_{412}/min x V (mL) × dil)/ 13.6 × L (cm) × V_{enz} (mL), V (mL); the reaction volume, dil; the dilution factor of the original sample, 13.6(mM^{-1} cm^{-1}); the extinction coefficient of TNB at 412 nm, L (cm); pathlength for

absorbance measurement (0.552 cm), V_{enz}(mL); the volume of the enzyme sample. Protein concentrations were quantified using Qubit™ Protein Assay Kits and a Qubit® 2.0 Fluorometer (Life Technologies, Carlsbad, CA, USA).

2.4. Statistical analyses

Statistical analyses were performed using the GraphPad Prism software program (version 9.01, GraphPad Software Inc., La Jolla, CA). Comparisons between samples were performed using a one-way ANOVA. The results are expressed as the mean (standard deviation). *P* values of <0.05 were considered to indicate statistical significance.

3. Results

3.1. Total CoQ_{10} levels were observed to decrease in all patients with primary CoQ_{10} deficiency

We showed the reduced, oxidized, and total (sum of reduced and oxidized) CoQ_{10} values corrected for the CS unit (nmol/CS unit) (Table 2). In addition, we also measured the CoQ_{10} values corrected for protein levels (nmol/g protein) (Supplemental Table 2). Six patients showed decreased the total CoQ_{10} values (<70% of the control): five with primary CoQ_{10} deficiency (Cases 1–5), and one with Kearns-Sayre syndrome (Case 19) (Table 2). The total CoQ_{10} levels were significantly decreased in primary CoQ_{10} deficiency than in controls (primary CoQ_{10} deficiency($n = 5$)1.00 ± 0.19 nmol / CS unit (mean ± SD), controls ($n = 10$)2.30 ± 0.24 nmol / CS unit, $p < 0.0001$) (Fig. 1). However, total CoQ_{10} levels were the same in mitochondrial disease other than primary CoQ_{10} deficiency as in controls (mitochondrial disease($n = 19$)2.23 ± 0.26 nmol / CS unit, $p = 0.93$).

Table 2
Reduced and oxidized CoQ_{10} values and total CoQ deficiency in fibroblasts.

Case	reduced CoQ_{10}		oxidized CoQ_{10}		total CoQ_{10} (nmol/CS unit)		% CoQ deficiency (%)
	mean	SD	mean	SD	mean	SD	
1	0.37	0.15	0.37	0.02	0.74	0.13	32
2	0.12	0.00	0.16	0.00	0.28	0.00	12
3	0.57	0.45	0.59	0.18	1.16	0.63	50
4	0.64	0.03	0.74	0.20	1.38	0.17	60
5	0.78	0.01	0.64	0.02	1.42	0.01	62
6	0.48	0.01	1.65	0.00	2.13	0.01	
7	1.03	0.04	1.00	0.32	2.03	0.29	
8	1.22	0.04	0.82	0.18	2.04	0.22	
9	1.40	0.54	0.96	0.03	2.36	0.51	
10	0.86	0.16	1.34	0.30	2.20	0.46	
11	1.02	0.08	2.17	0.53	3.19	0.44	
12	1.18	0.56	1.31	0.17	2.49	0.38	
13	1.33	0.03	0.57	0.02	1.90	0.00	
14	1.77	0.31	0.58	0.10	2.35	0.21	
15	1.54	0.09	0.71	0.00	2.25	0.09	
16	0.86	0.02	1.46	0.01	2.32	0.01	
17	1.37	0.40	1.28	0.14	2.65	0.25	
18	1.01	0.20	1.52	0.08	2.53	0.29	
19	0.57	0.01	0.72	0.02	1.29	0.02	56
20	1.41	0.40	0.51	0.11	1.92	0.51	
21	1.24	0.28	0.65	0.28	1.89	0.56	
22	1.19	0.11	0.87	0.23	2.06	0.34	
23	0.81	0.19	1.84	0.46	2.65	0.27	
24	0.92	0.01	1.23	0.00	2.15	0.01	
Reference (n = 10)	1.19	0.15	1.11	0.10	2.30	0.24	

% CoQ deficiency: <70% of control CoQ_{10} value.

3.2. The reduced/total CoQ_{10} ratio was unchanged in primary CoQ_{10} deficiency, but was higher in complex IV or V deficiency

We showed the ratio of reduced CoQ_{10} to total CoQ_{10} (reduced/total CoQ_{10}) of fibroblasts (Table 3). The ratio of reduced and oxidized CoQ_{10} to total CoQ_{10} in control fibroblasts was 52% and 48%, respectively (Table 3). In primary CoQ_{10} deficiency, the reduced/total CoQ_{10} ratio did not change compared to the control (reduced/total CoQ_{10} ratio of primary CoQ_{10} deficiency ($n = 5$) 49 ± 7% (mean ± SD), controls ($n = 10$) 52 ± 1%, $p = 0.92$) (Fig. 2). Regarding the cases with respiratory chain complex deficiency, there was no difference between control and complex I deficiency (reduced/total CoQ_{10} ratio of complex I deficiency ($n = 7$) 44 ± 7%, $p = 0.37$). However, the reduced/total CoQ_{10} ratio in complex IV or V deficiency was increased in comparison to the control (complex IV or V deficiency ($n = 3$) 71 ± 3%, $p = 0.022$). In addition, the reduced/total CoQ_{10} ratio in complex IV or V deficiency was higher in comparison to complex I deficiency and primary CoQ_{10} deficiency (complex IV or V deficiency vs. complex I deficiency: $p = 0.0021$, complex IV or V deficiency vs. primary CoQ_{10} deficiency: $p = 0.015$).

In individual cases, the reduced/total CoQ_{10} ratio decreased (<80% of the reduced/total CoQ_{10} ratio in the control) in six cases; three cases with complex I deficiency (Cases 6, 10, 11), two cases with mtDNA depletion syndrome (Cases 16, 18), one case with *BOLA3* mutation (Case 23)(Table 3). On the other hand, the reduced/total CoQ_{10} ratio increased (>120% of the reduced/total CoQ_{10} ratio in the control) in five cases; two cases with complex IV deficiency (Cases 13, 14), two cases with MELAS(Cases 20, 21), one case with complex V deficiency (Case 15) (Table 3).

4. Discussion

We showed here that the total CoQ_{10} values of fibroblasts were significantly lower in patients with primary CoQ_{10} deficiency. In this syndrome, early recognition and therapy can stop progression and improve the prognosis; however, established severe symptoms cannot be reversed [16,34]. Biochemical measurements of low CoQ_{10} levels in muscle biopsy have been utilized for the diagnosis of this syndrome

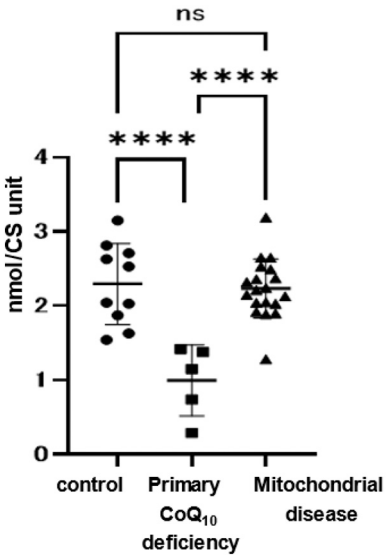

Fig. 1. Total CoQ_{10} values.
Total (sum of reduced and oxidized) CoQ_{10} values of mitochondrial patient fibroblasts. CoQ_{10} deficiency (CoQ_{10} levels <70% of control CoQ_{10}) was found in six cases. All cases of primary CoQ_{10} deficiency showed decreased CoQ_{10} levels. In mitochondrial disease, CoQ_{10} values were not decreased, with the exception of Case 19 (Kearns-Sayre syndrome). Data are expressed as **** $P <$ 0.0001, and n.s. indicates no significance.

Table 3
Ratio of reduced / total CoQ_{10}.

Case	reduced/total CoQ_{10} (%)		Reduced/total CoQ_{10} in cases versus reduced/total CoQ_{10} in controls (%)
	mean	SD	
1	50	11	96
2	43	1	83
3	49	14	95
4	47	8	90
5	55	1	106
6	23	0	44
7	51	9	97
8	60	4	115
9	59	10	114
10	39	1	75
11	32	7	61
12	47	15	91
13	70	1	135
14	75	7	145
15	68	1	131
16	37	1	71
17	52	10	100
18	40	3	77
19	44	0	85
20	74	1	142
21	66	5	127
22	58	4	111
23	30	10	59
24	43	0	83
Reference (n = 10)	52	1	

The reduced/total CoQ_{10} ratio decreased (< 80% of control value); cases 6, 10, 11, 16, 18, 23.
The reduced/total CoQ_{10} ratio increased (120% < of control value); cases 13, 14, 15, 20, 21.

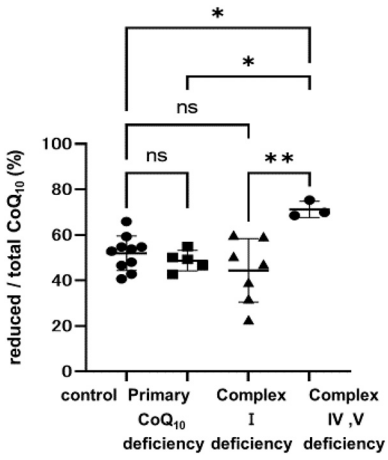

Fig. 2. Comparison of the reduced/total CoQ_{10} ratio.
Comparison of the reduced/total CoQ_{10} ratio in cases with primary CoQ_{10} deficiency, complex I deficiency, and complex IV or V deficiency. In primary CoQ_{10} deficiency, the reduced/total CoQ_{10} ratio was the same as that of the controls. In complex I deficiency, 3/7 cases showed a decreased (< 80% of control value) reduced/total CoQ_{10} ratio. In complex IV or V deficiency, 3/3 cases showed an increased (120% < of control value) reduced/total CoQ_{10} ratio. Data are expressed as $^{*}P < 0.05$, $^{**}P < 0.01$, and n.s. indicates no significance.

[16]. Moreover, the identification of biallelic pathogenic variants in the *COQ* genes, which encode proteins involved in coenzyme Q biosynthesis, enables a definitive diagnosis [16]. However, the invasiveness of muscle biopsy hampers this procedure and can delay the diagnosis. CoQ_{10} levels in fibroblasts were examined and implicated in their usefulness [21]. Our data with LC-MS/MS for the measurement of CoQ_{10} from fibroblasts also supported the usefulness for detecting CoQ_{10} deficiency [32,35]. The fibroblasts from Case 2 showed the lowest CoQ_{10} concentration and showed a very severe phenotype. A correlation between CoQ_{10} levels and phenotype has been suggested [24,36,37]. Therefore, the CoQ_{10} value from skin fibroblast may reflect the clinical severity.

In addition to primary CoQ_{10} deficiency, various mitochondrial diseases have also been reported to decrease CoQ_{10} in fibroblasts and muscle, particularly in mtDNA depletion syndrome [20,38]. However, in our analysis, three patients with mtDNA depletion, including *DGUOK* and *MPV17* mutations, showed no decrease in CoQ_{10} (Cases 16–18). Only one patient with large deletions of mtDNA showed markedly decreased CoQ_{10} (Case 19). Therefore, decreased CoQ_{10} was only a constant feature in primary CoQ_{10} deficiency syndrome in our analysis. Our results support the widely accepted idea that early CoQ_{10} therapy should is therefore indicated if decreased levels of CoQ_{10} are found in the fibroblasts of patients with suspected mitochondrial disease.

To our knowledge, this is the first report to describe the reduced/total CoQ_{10} ratios in patients with mitochondrial diseases, including primary CoQ_{10} deficiency. In primary CoQ_{10} deficiency, the reduced/total CoQ_{10} ratio did not change. On the other hand, the reduced/total CoQ_{10} ratio was decreased in 3/7 of cases of complex I deficiency and was increased in 3/3 of cases of complex IV or V deficiency. Primary CoQ_{10} deficiency is caused by impaired CoQ_{10} biosynthesis, which results in a decrease in the absolute value of CoQ_{10}; however, as expected, our data suggest that it does not affect the redox reaction in mitochondria. Since CoQ_{10} changes from the oxidized form to the reduced form by accepting electrons from complex I, complex II and other dehydrogenases, the reduced/total CoQ_{10} ratio is expected to decrease in complex I deficiency. However, only 3 out of 7 complex I patients in our cohort showed disturbed Q reduced/total ratios. In contrast, CoQ_{10} changes from the reduced form to the oxidized form in complex III, and the reduced/total CoQ_{10} ratio is expected to increase in complex III and later complex deficiencies (Supplemental Fig. 1, left panel). In fact, the reduced CoQ_{10} ratio was significantly decreased with complex I inhibitor, whereas the reduced CoQ_{10} ratio was increased with complex IV inhibitor [23]. Some (but not all) of our results support these observations. Among complex I deficiency patients, patients with isolated complex I deficiency tended to have a decreased reduced/total CoQ_{10} ratio (3/4 cases; Cases 6, 10, 11) (Supplemental Table 3). On the other hand, the reduced/total CoQ_{10} ratio was unchanged in a patient who also had a decreased complex III and IV enzyme activity (Case 8), in a patient without a decreased CI enzyme activity in fibroblasts (Case 12), and in a patient with a decreased CI enzyme activity in muscle (Case 7).

In recent years, it has been reported that the reduced/oxidized CoQ_{10} ratio may be a marker of mitochondrial metabolic status [39]. In situations where CoQ_{FADH} can be excessively reduced, RET is induced, and the production of reactive oxygen species (ROS) from complex I is stimulated, which causes complex I destruction [4,6]. On the other hand, oxidizing the CoQ pool by alternative oxidase (AOX) of *Ciona intestinalis* xenotopically expressed in mouse mitochondria induces forward electron transport (FET) from RET [40]. Our system of measuring the reduced/total CoQ_{10} ratio of skin fibroblasts provide the amount and redox states of CoQ_{10}.

As a limitation of our study, CoQ_{10} is mostly localized in the mitochondria in subcellular fractions but it has also been shown to localize in Golgi, lysosomes, and other organelles [3]. In this study, we measured the whole cell CoQ_{10} level without separating the mitochondrial and non-mitochondrial fractions. Moreover, we examined an only limited number of patients affected by only some mitochondrial diseases, which can be caused by >400 gene mutations [41].

In conclusion, we measured the reduced/total CoQ_{10} ratio in fibroblasts from a cohort of patients with mitochondrial disease for the first time. The reduced/total CoQ_{10} ratio tended to show no change in many of the cells that we measured. However, the reduced/total CoQ_{10} ratio was increased in complex IV or V deficiency, while the reduced/total CoQ_{10} ratio tended to decrease in some cases of complex I deficiency.

Supplementary data to this article can be found online at https://doi.org/10.1016/j.ymgmr.2022.100951.

Author contributions

CW, HO contributed to the conceptualization and performance of the statistical analysis of the data and wrote the manuscript; MW, AM, EFJ, TT, HU, OT, ET, and KA performed sampling and data acquisition; YK, YO performed genetic testing; KM, AO recruited patients, provided clinical information, collected samples; TY conducted supervision of the project. All authors read and approved the final manuscript.

Ethics

All procedures followed were by the ethical standards of the responsible committee on human experimentation and with the Helsinki Declaration of the World Medical Organization. This study was approved by the Ethics Committee of Jichi Medical University and written informed consent was obtained from all participants.

Funding

This work was supported in part by the Practical Research Project for Rare/Intractable Diseases from the Japan Agency for Medical Research and Development, AMED to H·O (JP21im0210625, JP21ek0109511), K. M (JP21ek0109468, JP19ek0109273) and Y·O (JP21kk0305015). Health and Labor Sciences Research Grant to H·O (JP21FC1015). The Acceleration Program for Intractable Diseases Research utilizing Disease-specific iPS cells to H·U (JP22bm0804018). JSPS KAKENHI to H. O. (JP20H03648).

CRediT authorship contribution statement

Chika Watanabe: Conceptualization, Writing – original draft. **Hitoshi Osaka:** Conceptualization, Writing – review & editing, Funding acquisition. **Miyuki Watanabe:** Investigation. **Akihiko Miyauchi:** Investigation. **Eriko F. Jimbo:** Investigation. **Takeshi Tokuyama:** Resources. **Hideki Uosaki:** Resources. **Yoshihito Kishita:** Resources. **Yasushi Okazaki:** Resources. **Takanori Onuki:** Resources. **Tomohiro Ebihara:** Resources. **Kenichi Aizawa:** Resources. **Kei Murayama:** Resources. **Akira Ohtake:** Resources. **Takanori Yamagata:** Supervision.

Declaration of Competing Interest

None.

Data availability

No data was used for the research described in the article.

Acknowledgments

We thank the patients and their families. We thank all the staff, especially Natsumi Oishi, Shiho Aoki, and Narumi Omika, in Jichi Children Medical Center Tochigi and Jichi Medical University Hospital.

References

[1] F.L. Crane, Y. Hatefi, R.L. Lester, C. Widmer, Isolation of a quinone from beef heart mitochondria, Biochim. Biophys. Acta 25 (1957) 220–221.
[2] Y. Wang, S. Hekimi, Understand. Ubiquinone, Trends Cell Biol. 26 (2016) 367–378.
[3] M. Turunen, J. Olsson, G. Dallner, Metabolism and function of coenzyme Q, Biochim. Biophys. Acta 1660 (2004) 171–199.
[4] E. Lapuente-Brun, R. Moreno-Loshuertos, R. Acín-Pérez, A. Latorre-Pellicer, C. Colás, E. Balsa, E. Perales-Clemente, P.M. Quirós, E. Calvo, M.A. Rodríguez-Hernández, P. Navas, R. Cruz, Á. Carracedo, C. López-Otín, A. Pérez-Martos, P. Fernández-Silva, E. Fernández-Vizarra, J.A. Enríquez, Supercomplex assembly determines electron flux in the mitochondrial electron transport chain, Science 340 (2013) 1567–1570.
[5] F. Pallotti, C. Bergamini, C. Lamperti, R. Fato, The roles of coenzyme Q in disease: direct and indirect involvement in cellular functions, Int. J. Mol. Sci. 23 (2021).
[6] F. Scialò, D.J. Fernández-Ayala, A. Sanz, Role of Mitochondrial Reverse Electron Transport in ROS Signaling: Potential Roles in Health and Disease, Front. Physiol. 8 (2017) 428.
[7] M. Bentinger, K. Brismar, G. Dallner, The antioxidant role of coenzyme, Q. Mitochondrion. 7 (Suppl) (2007) S41–S50.
[8] D.H. Hyun, Plasma membrane redox enzymes: new therapeutic targets for neurodegenerative diseases, Arch. Pharm. Res. 42 (2019) 436–445.
[9] K. Bersuker, J.M. Hendricks, Z. Li, L. Magtanong, B. Ford, P.H. Tang, M.A. Roberts, B. Tong, T.J. Maimone, R. Zoncu, M.C. Bassik, D.K. Nomura, S.J. Dixon, J. A. Olzmann, The CoQ oxidoreductase FSP1 acts parallel to GPX4 to inhibit ferroptosis, Nature 575 (2019) 688–692.
[10] S. Doll, F.P. Freitas, R. Shah, M. Aldrovandi, M.C. da Silva, I. Ingold, A.G. Grocin, T. N. Xavier da Silva, E. Panzilius, C.H. Scheel, A. Mourão, K. Buday, M. Sato, J. Wanninger, T. Vignane, V. Mohana, M. Rehberg, A. Flatley, A. Schepers, A. Kurz, D. White, M. Sauer, M. Sattler, E.W. Tate, W. Schmitz, A. Schulze, V. O'Donnell, B. Proneth, G.M. Popowicz, D.A. Pratt, J.P.F. Angeli, M. Conrad, FSP1 is a glutathione-independent ferroptosis suppressor, Nature 575 (2019) 693–698.
[11] S.K. Lee, J.O. Lee, J.H. Kim, N. Kim, G.Y. You, J.W. Moon, J. Sha, S.J. Kim, Y. W. Lee, H.J. Kang, S.H. Park, H.S. Kim, Coenzyme Q10 increases the fatty acid oxidation through AMPK-mediated PPARα induction in 3T3-L1 preadipocytes, Cell. Signal. 24 (2012) 2329–2336.
[12] D.R. Evans, H.I. Guy, Mammalian pyrimidine biosynthesis: fresh insights into an ancient pathway, J. Biol. Chem. 279 (2004) 33035–33038.
[13] P. González-García, A. Hidalgo-Gutiérrez, C. Mascaraque, E. Barriocanal-Casado, M. Bakkali, M. Ziosi, U.B. Abdihankyzy, S. Sánchez-Hernández, G. Escames, H. Prokisch, F. Martín, C.M. Quinzii, L.C. López, Coenzyme Q10 modulates sulfide metabolism and links the mitochondrial respiratory chain to pathways associated to one carbon metabolism, Hum. Mol. Genet. 29 (2020) 3296–3311.
[14] K.S. Echtay, E. Winkler, M. Klingenberg, Coenzyme Q is an obligatory cofactor for uncoupling protein function, Nature 408 (2000) 609–613.
[15] E. Fontaine, F. Ichas, P. Bernardi, A ubiquinone-binding site regulates the mitochondrial permeability transition pore, J. Biol. Chem. 273 (1998) 25734–25740.
[16] L. Salviati, E. Trevisson, M. Doimo, P. Navas, Primary coenzyme Q(10) deficiency, in: M.P. Adam, H.H. Ardinger, R.A. Pagon, S.E. Wallace, L.J.H. Bean, K. Stephens, A. Amemiya (Eds.), GeneReviews(®), University of Washington, Seattle Copyright © 1993–2020, University of Washington, Seattle. GeneReviews Is a Registered Trademark of the University of Washington, Seattle. All rights reserved., Seattle (WA), 1993.
[17] M. Alcázar-Fabra, F. Rodríguez-Sánchez, E. Trevisson, G. Brea-Calvo, Primary coenzyme Q deficiencies: a literature review and online platform of clinical features to uncover genotype-phenotype correlations, Free Radic. Biol. Med. 167 (2021) 141–180.
[18] S. Ogasahara, A.G. Engel, D. Frens, D. Mack, Muscle coenzyme Q deficiency in familial mitochondrial encephalomyopathy, Proc. Natl. Acad. Sci. U. S. A. 86 (1989) 2379–2382.
[19] M.A. Desbats, G. Lunardi, M. Doimo, E. Trevisson, L. Salviati, Genetic bases and clinical manifestations of coenzyme Q10 (CoQ 10) deficiency, J. Inherit. Metab. Dis. 38 (2015) 145–156.
[20] D. Yubero, R. Montero, M.A. Martín, J. Montoya, A. Ribes, M. Grazina, E. Trevisson, J.C. Rodriguez-Aguilera, I.P. Hargreaves, L. Salviati, P. Navas, R. Artuch, C. Jou, C. Jimenez-Mallebrera, A. Nascimento, B. Pérez-Dueñas, C. Ortez, F. Ramos, J. Colomer, M. O'Callaghan, M. Pineda, A. García-Cazorla, C. Espinós, A. Ruiz, A. Macaya, A. Marcé-Grau, J. Garcia-Villoria, A. Arias, S. Emperador, E. Ruiz-Pesini, E. Lopez-Gallardo, V. Neergheen, M. Simões, L. Diogo, A. Blázquez, A. González-Quintana, A. Delmiro, C. Domínguez-González, J. Arenas, M.T. García-Silva, E. Martín, P. Quijada, A. Hernández-Laín, M. Morán, E. Rivas Infante, R. Ávila Polo, C. Paradas Lópe, J. Bautista Lorite, E.M. Martínez Fernández, A.B. Cortés, A. Sánchez-Cuesta, M.V. Cascajo, M. Alcázar, G. Brea-Calvo, Secondary coenzyme Q10 deficiencies in oxidative phosphorylation (OXPHOS) and non-OXPHOS disorders, Mitochondrion 30 (2016) 51–58.
[21] R. Montero, J.A. Sánchez-Alcázar, P. Briones, A.R. Hernández, M.D. Cordero, E. Trevisson, L. Salviati, M. Pineda, A. García-Cazorla, P. Navas, R. Artuch, Analysis of coenzyme Q10 in muscle and fibroblasts for the diagnosis of CoQ10 deficiency syndromes, Clin. Biochem. 41 (2008) 697–700.
[22] P.H. Tang, M.V. Miles, Measurement of oxidized and reduced coenzyme Q in biological fluids, cells, and tissues: an HPLC-EC method, Methods Mol. Biol. 837 (2012) 149–168.
[23] N. Burger, A. Logan, T.A. Prime, A. Mottahedin, S.T. Caldwell, T. Krieg, R. C. Hartley, A.M. James, M.P. Murphy, A sensitive mass spectrometric assay for mitochondrial CoQ pool redox state in vivo, Free Radic. Biol. Med. 147 (2020) 37–47.
[24] G. Brea-Calvo, T.B. Haack, D. Karall, A. Ohtake, F. Invernizzi, R. Carrozzo, L. Kremer, S. Dusi, C. Fauth, S. Scholl-Bürgi, E. Graf, U. Ahting, N. Resta, N. Laforgia, D. Verrigni, Y. Okazaki, M. Kohda, D. Martinelli, P. Freisinger, T. M. Strom, T. Meitinger, C. Lamperti, A. Lacson, P. Navas, J.A. Mayr, E. Bertini, K. Murayama, M. Zeviani, H. Prokisch, D. Ghezzi, COQ4 mutations cause a broad spectrum of mitochondrial disorders associated with CoQ10 deficiency, Am. J. Hum. Genet. 96 (2015) 309–317.
[25] E. Ogawa, T. Fushimi, M. Ogawa-Tominaga, M. Shimura, M. Tajika, K. Ichimoto, A. Matsunaga, T. Tsuruoka, M. Ishige, T. Fuchigami, T. Yamazaki, Y. Kishita, M. Kohda, A. Imai-Okazaki, Y. Okazaki, I. Morioka, A. Ohtake, K. Murayama,

Mortality of Japanese patients with Leigh syndrome: effects of age at onset and genetic diagnosis, J. Inherit. Metab. Dis. 43 (2020) 819–826.
[26] A. Miyauchi, T. Kouga, E.F. Jimbo, T. Matsuhashi, T. Abe, T. Yamagata, H. Osaka, Apomorphine rescues reactive oxygen species-induced apoptosis of fibroblasts with mitochondrial disease, Mitochondrion 49 (2019) 111–120.
[27] H. Shimozawa, T. Sato, H. Osaka, A. Takeda, A. Miyauchi, N. Omika, Y. Yada, Y. Kono, K. Murayama, Y. Okazaki, Y. Kishita, T. Yamagata, A Case of Infantile Mitochondrial Cardiomyopathy Treated with a Combination of Low-Dose Propranolol and Cibenzoline for Left Ventricular Outflow Tract Stenosis, Int. Heart J. 63 (2022) 970–977.
[28] A. Imai-Okazaki, Y. Kishita, M. Kohda, Y. Mizuno, T. Fushimi, A. Matsunaga, Y. Yatsuka, T. Hirata, H. Harashima, A. Takeda, A. Nakaya, Y. Sakata, S. Kogaki, A. Ohtake, K. Murayama, Y. Okazaki, Cardiomyopathy in children with mitochondrial disease: prognosis and genetic background, Int. J. Cardiol. 279 (2019) 115–121.
[29] J. Tanigawa, K. Kaneko, M. Honda, H. Harashima, K. Murayama, T. Wada, K. Takano, M. Iai, S. Yamashita, H. Shimbo, N. Aida, A. Ohtake, H. Osaka, Two Japanese patients with Leigh syndrome caused by novel SURF1 mutations, Brain and Development 34 (2012) 861–865.
[30] M. Shimura, N. Kuranobu, M. Ogawa-Tominaga, N. Akiyama, Y. Sugiyama, T. Ebihara, T. Fushimi, K. Ichimoto, A. Matsunaga, T. Tsuruoka, Y. Kishita, S. Umetsu, A. Inui, T. Fujisawa, K. Tanikawa, R. Ito, A. Fukuda, J. Murakami, S. Kaji, M. Kasahara, K. Shiraki, A. Ohtake, Y. Okazaki, K. Murayama, Clinical and molecular basis of hepatocerebral mitochondrial DNA depletion syndrome in Japan: evaluation of outcomes after liver transplantation, Orphanet J. Rare Dis. 15 (2020) 169.
[31] M. Kuwajima, K. Kojima, H. Osaka, Y. Hamada, E. Jimbo, M. Watanabe, S. Aoki, I. Sato-Shirai, K. Ichimoto, T. Fushimi, K. Murayama, A. Ohtake, M. Kohda, Y. Kishita, Y. Yatsuka, S. Uchino, M. Mimaki, N. Miyake, N. Matsumoto, Y. Okazaki, T. Ogata, T. Yamagata, K. Muramatsu, Valine metabolites analysis in ECHS1 deficiency, Mol. Genet. Metab. Rep. 29 (2021), 100809.
[32] N. Buján, A. Arias, R. Montero, J. García-Villoria, W. Lissens, S. Seneca, C. Espinós, P. Navas, L. De Meirleir, R. Artuch, P. Briones, A. Ribes, Characterization of CoQ_{10} biosynthesis in fibroblasts of patients with primary and secondary CoQ_{10} deficiency, J. Inherit. Metab. Dis. 37 (2014) 53–62.
[33] R. Pandey, C.L. Riley, E.M. Mills, S. Tiziani, Highly sensitive and selective determination of redox states of coenzymes Q(9) and Q(10) in mice tissues: Application of orbitrap mass spectrometry, Anal. Chim. Acta 1011 (2018) 68–76.
[34] G. Montini, C. Malaventura, L. Salviati, Early coenzyme Q10 supplementation in primary coenzyme Q10 deficiency, N. Engl. J. Med. 358 (2008) 2849–2850.
[35] Y.T. Liu, J. Hersheson, V. Plagnol, K. Fawcett, K.E. Duberley, E. Preza, I. P. Hargreaves, A. Chalasani, M. Laurá, N.W. Wood, M.M. Reilly, H. Houlden, Autosomal-recessive cerebellar ataxia caused by a novel ADCK3 mutation that elongates the protein: clinical, genetic and biochemical characterisation, J. Neurol. Neurosurg. Psychiatry 85 (2014) 493–498.
[36] M.A. Desbats, V. Morbidoni, M. Silic-Benussi, M. Doimo, V. Ciminale, M. Cassina, S. Sacconi, M. Hirano, G. Basso, F. Pierrel, P. Navas, L. Salviati, E. Trevisson, The COQ2 genotype predicts the severity of coenzyme Q10 deficiency, Hum. Mol. Genet. 25 (2016) 4256–4265.
[37] A.K. Kwong, A.T. Chiu, M.H. Tsang, K.S. Lun, R.J.T. Rodenburg, J. Smeitink, B. H. Chung, C.W. Fung, A fatal case of COQ7-associated primary coenzyme Q(10) deficiency, JIMD Rep. 47 (2019) 23–29.
[38] R. Montero, M. Grazina, E. López-Gallardo, J. Montoya, P. Briones, A. Navarro-Sastre, J.M. Land, I.P. Hargreaves, R. Artuch, Coenzyme Q_{10} deficiency in mitochondrial DNA depletion syndromes, Mitochondrion 13 (2013) 337–341.
[39] A. Guarás, E. Perales-Clemente, E. Calvo, R. Acín-Pérez, M. Loureiro-Lopez, C. Pujol, I. Martínez-Carrascoso, E. Nuñez, F. García-Marqués, M.A. Rodríguez-Hernández, A. Cortés, F. Diaz, A. Pérez-Martos, C.T. Moraes, P. Fernández-Silva, A. Trifunovic, P. Navas, J. Vazquez, J.A. Enríquez, The CoQH2/CoQ Ratio Serves as a Sensor of Respiratory Chain Efficiency, Cell Rep. 15 (2016) 197–209.
[40] M. Szibor, T. Gainutdinov, E. Fernandez-Vizarra, E. Dufour, Z. Gizatullina, G. Debska-Vielhaber, J. Heidler, I. Wittig, C. Viscomi, F. Gellerich, A.L. Moore, Bioenergetic consequences from xenotopic expression of a tunicate AOX in mouse mitochondria: Switch from RET and ROS to FET, Biochim. Biophys. Acta Bioenerg. 1861 (2020), 148137.
[41] M. Gusic, H. Prokisch, Genetic basis of mitochondrial diseases, FEBS Lett. 595 (2021) 1132–1158.

Molecular Genetics and Metabolism Reports 35 (2023) 100963

Contents lists available at ScienceDirect

Molecular Genetics and Metabolism Reports

journal homepage: www.elsevier.com/locate/ymgmr

Case Report

Focal segmental glomerulosclerosis with a mutation in the *mitochondrially encoded NADH dehydrogenase 5* gene: A case report

Tsukasa Naganuma [a,1], Toshiyuki Imasawa [b,*,1], Ikuo Nukui [a], Masakiyo Wakasugi [a], Hiroshi Kitamura [c], Yukiko Yatsuka [d], Yoshihito Kishita [d,e], Yasushi Okazaki [d], Kei Murayama [f], Yoshimi Jinguji [a]

[a] Division of Nephrology, Department of Internal Medicine, Yamanashi Prefectural Central Hospital, 1-1-1 Fujimi, Kofu, Yamanashi 400-0027, Japan
[b] Department of Nephrology, National Hospital Organization Chiba-Higashi National Hospital, 673 Nitona-cho, Chuoh-ku, Chiba-city, Chiba 206-8712, Japan
[c] Department of Clinical Pathology, National Hospital Organization Chiba-Higashi National Hospital, 673 Nitona-cho, Chuoh-ku, Chiba-city, Chiba 206-8712, Japan
[d] Diagnostics and Therapeutics of Intractable Diseases, Intractable Disease Research Center, Graduate School of Medicine, Juntendo University, 2-1-1, Hongo, Bunkyo-ku, Tokyo 113-8421, Japan
[e] Department of Life Science, Faculty of Science and Engineering, Kindai University, 3-4-1 Kowakae, Higashiosaka, Osaka 577-8502, Japan
[f] Center for Medical Genetics, Department of Metabolism, Chiba Children's Hospital, 579-1, Heta-cho, Midori-ku, Chiba 266-0007, Japan

ARTICLE INFO

Keywords:
Focal segmental glomerulosclerosis
Mitochondrial nephropathy
NADH dehydrogenase 5
Podocyte
Case report

ABSTRACT

NADH dehydrogenase 5 (ND5) is one of 44 subunits composed of Complex I in mitochondrial respiratory chain. Therefore, a *mitochondrially encoded ND5* (*MT-ND5*) gene mutation causes mitochondrial oxidative phosphorylation (OXPHOS) disorder, resulting in the development of mitochondrial diseases. Focal segmental glomerulosclerosis (FSGS) which had podocytes filled with abnormal mitochondria is induced by mitochondrial diseases. An *MT-ND5* mutation also causes FSGS. We herein report a Japanese woman who was found to have proteinuria and renal dysfunction in an annual health check-up at 29 years old. Because her proteinuria and renal dysfunction were persistent, she had a kidney biopsy at 33 years of age. The renal histology showed FSGS with podocytes filled with abnormal mitochondria. The podocytes also had foot process effacement and cytoplasmic vacuolization. In addition, the renal pathological findings showed granular swollen epithelial cells (GSECs) in tubular cells, age-inappropriately disarranged and irregularly sized vascular smooth muscle cells (AiDIVs), and red-coloured podocytes (ReCPos) by acidic dye. A genetic analysis using peripheral mononuclear blood cells and urine sediment cells detected the m.13513 G > A variant in the *MT-ND5* gene. Therefore, this patient was diagnosed with FSGS due to an *MT-ND5* gene mutation. Although this is not the first case report to show that an *MT-ND5* gene mutation causes FSGS, this is the first to demonstrate podocyte injuries accompanied with accumulation of abnormal mitochondria in the cytoplasm.

1. Introduction

Mitochondrial diseases/disorders are rare and occur every 1 in 5000 births [1]. Mitochondria play a key role in the biosynthesis of adenosine triphosphate (ATP), the main energy source of cells, through oxidative phosphorylation (OXPHOS) using the mitochondrial respiratory chain (MRC) complex. Given that the genes related to the MRC complex are encoded in mitochondrial DNA (mtDNA) and nuclear DNA (nDNA), mitochondrial diseases can occur in cases of mtDNA or nDNA mutations [2,3]. As ATP is mandatory for all cells that require energy, the clinical phenotypes of mitochondrial diseases are versatile and are expressed as encephalopathy [4], myopathy [5], cardiomyopathy [6], hepatopathy

Abbreviations: ND5, NADH dehydrogenase 5; *MT-ND5*, mitochondrially encoded ND5; OXPHOS:, oxidative phosphorylation; MELAS, mitochondrial encephalomyopathy, lactic acidosis, and stroke-like episodes; FSGS, focal segmental glomerulosclerosis; GSECs, granular swollen epithelial cells; AiDIVs, age-inappropriately disarranged and irregularly sized vascular smooth muscle cells; ReCPos, red-coloured podocytes; ATP, adenosine triphosphate; MRC, mitochondrial respiratory chain; mtDNA, mitochondrial DNA; nDNA, nuclear DNA; Cr, creatinine; sCr, serum creatinine; eGFR, estimated glomerular filtration rate; COX IV, cytochrome *c* oxidase subunit 4.

* Corresponding author.
E-mail address: imasawa@nifty.com (T. Imasawa).
[1] These authors contributed equally.

https://doi.org/10.1016/j.ymgmr.2023.100963
Received 12 December 2022; Received in revised form 27 February 2023; Accepted 28 February 2023
Available online 9 March 2023

[7], deafness [8], and diabetes mellitus [9]. Mitochondrial nephropathy, which occurs because of a mitochondrial disorder in nephrons, has also been reported [10–12].

Focal segmental glomerulosclerosis (FSGS) is a histological term, rather than a specific disease category and diagnosed by the presence of sclerosis in parts of at least one glomerulus in the kidney biopsy specimen [13]. It can be classified into primary, secondary, genetic, and unknown forms of FSGS [14]. Among causative genes of mitochondrial nephropathy, m.3243A > G pathogenic variant in *MT-TL1* gene on mtDNA, which encodes mitochondrial transfer RNA leucine 1, is majority [12]. The m.3243A > G mutation leads to genetic cause of FSGS with accumulation of abnormal mitochondria in podocytes [11,15]. Because podocyte injury plays a key role in the pathogenesis of FSGS [16–18], impaired mitochondrial function in podocytes should induce FSGS [19–22].

The pathogenic variants in *mitochondrially encoded NADH dehydrogenase 5* (*MT-ND5*) gene cause mitochondrial diseases such as mitochondrial encephalomyopathy with lactic acidosis and stroke-like episodes (MELAS) [23–25]. ND5 is one of the 44 subunits of mitochondria respiratory complex I. The pathogenic variants in *MT-ND5* gene also cause FSGS [26–29]. However, in all cases with FSGS lesions presented in the past reports, abnormal mitochondria or their accumulation were not identified in podocytes. In another recent report of three cases with nephropathy due to *MT-ND5* gene mutation, one of the cases showed FSGS lesion. The authors of this report concluded that FSGS lesion of their case was secondary [28]. The pathogenesis of the secondary FSGS is considered to involve intraglomerular hypertension caused by hypertension or obesity, by adaptation to nephron loss due to progression of glomerulosclerosis or by a low nephron number due to low birth weight [30,31]. Therefore, it has not been evident whether genetic FSGS occurs with a pathogenic variant in *MT-ND5* gene. Here, we report the case with an *MT-ND5* mutation with apparent FSGS lesions. In this case, foot process effacement and cytoplasmic vacuolization in podocytes with accumulation of abnormal mitochondria were observed.

2. Case presentation

This case occurred in a Japanese woman born at 39 weeks of gestation with a birth weight of 3210 g. She had no remarkable medical history. Annual health check-ups showed no proteinuria on urinalysis until age 29. At 29 years of age, the annual health check-up revealed proteinuria (1+) for the first time using a urine dipstick and a high serum creatinine (sCr) level of 1.01 mg/dL. Her estimated glomerular filtration rate (eGFR) using the Japanese Eq. [32] was calculated to be 54.0 mL/min/1.73 m^2. At the same check-up, she was also found to have a slight hearing disturbance. Additionally, she had a headache once a week from 30 years of age and was diagnosed by a neurologist with migraine, uncontrolled with triptan. Her health check-up at 32 years of age again showed proteinuria (1+) and increased sCr (1.06 mg/dL). Hematuria has never been noted before. At 33 years of age, she was referred to the Yamanashi Prefectural Central Hospital by her primary doctor to examine the reason for her proteinuria and decreased eGFR. At the first visit, proteinuria (1.09 g/gCr), elevated sCr (1.28 mg/dL), and elevated uric acid (7.5 mg/dL) were detected. Febuxostat and sodium bicarbonate were prescribed for the treatment of hyperuricemia. Because of the continued presentation of proteinuria and decreased renal function, she was admitted for a kidney biopsy, at 6 months following the initial visit.

Upon admission, her blood pressure was 114/70 mmHg. Physical examination showed a height of 152 cm, body weight of 43.8 kg, and body mass index of 19.0. No crackles or murmurs were detected on chest auscultation. No abnormal neurological findings were observed. Neither skin lesions nor pitting oedema were detected. The laboratory data on admission are summarised in Table 1, which shows decreased eGFR and proteinuria. Hematuria was not observed. In the data we measured, there were no data to suggest the presence of tubular dysfunction such as Fanconi's syndrome or distal tubular acidosis. The long × short axis of the kidneys measured 101 × 38 mm on the left and 104 × 50 mm on the right, indicating no renal atrophy. The electrocardiogram test result was normal, and echocardiography revealed normal cardiac function. The standard pure-tone hearing test showed a right-ear value of 38.8 dB and a left-ear value of 40.0 dB. She was therefore diagnosed with sensorineural hearing loss by an otolaryngologist. No visual field defects were noted. Furthermore, because of hearing loss and headache symptoms, a brain magnetic resolution imaging (MRI) was also performed to examine for brain lesions, but no abnormal findings were found.

Her parents had died because of cancer (mother, breast cancer,

Table 1
Laboratory data on admission.

Blood cell count			Blood chemistry			Immunology			Urinalysis		
WBC	5400	/μL	TP	6.8	g/dL	CH50	54	U/mL	Gravity	1.01	
RBC	373	$\times 10^4$/μL	Alb	3.9	g/dL	C3	76.1	mg/dL	pH	7.0	
Hb	11.5	g/dL	AST	21	IU/L	C4	19.3	mg/dL	RBC	1–4	/HPF
Ht	35.1	%	ALT	11	IU/L	IgG	1340.3	mg/dL	WBC	<1	/HPF
MCV	94.1	fl	LDH	186	IU/L	IgA	225.7	mg/dL	Protein	2.04	g/gCr
MCHC	32.8	%	ALP	149	IU/L	IgM	180.1	mg/dL	Glucose	(−)	
Plt	25.7	$\times 10^4$/μL	Tbil	0.56	mg/dL	ANA	(−)		NAG	8.6	U/L
			BUN	21.8	mg/dL	M protein	(−)				
Coagulation			Cr	1.26	mg/dL	HBs Ag	(−)				
APTT	34.0	*sec*	eGFR	40.8	mL/min/1.73 m^2	HCV Ab	(−)				
PT	99.0	%	K	5.0	mEq/L						
INR	0.97	INR	P	3.1	mg/dL						
Fib	373.0	mg/dL	UA	5.4	mg/dL						
			Tcho	255	mg/dL						
			CRP	0.01	mg/dL						
			FBS	85	mg/dL						
			HbA1c	5.3	%						

Aberrant values are underlined.
WBC, white blood cells; RBC, red blood cells; Hb, haemoglobin; Hct, haematocrit; MCV, mean corpuscular volume; MCHC, mean corpuscular haemoglobin concentration; Plt, platelet; APTT, activated partial thromboplastin time; PT, prothrombin time; INR, international normalized ratio; Fib, fibrinogen; TP, total protein; Alb, albumin; AST, aspartate aminotransferase; ALT, alanine aminotransferase; LDH, lactate dehydrogenase; ALP, alkaline phosphatase; Tbil, total bilirubin; BUN, blood urea nitrogen; Cr, creatinine; eGFR, estimated glomerular filtration rate (by the Japanese equation); K, potassium; P, phosphate; UA, uric acid; Tcho, total cholesterol; CRP, C-reactive protein; FBS, fasting blood sugar; HbA1c, haemoglobin A1c (NGSP); CH50, 50% haemolytic complement activity; C3, complement 3; IgG, immunoglobulin G; ANA, antinuclear antibody; M protein, monoclonal protein; HBs Ag, hepatitis B surface antigen; HCV Ab, hepatitis C virus antibody; NAG, *N*-acetyl glucosaminidase; HPF, high power field.

father, colon cancer) without kidney disease or any hearing difficulty. Neither of her two older brothers had any abnormalities in kidney function, urine, or hearing. She had a 7-year-old daughter and a 5-year-old son. Her daughter's birth weight was 2840 g at 41 weeks and 2 days of gestation, and her son's birth weight was 2632 g at 39 weeks of gestation. Her daughter was born using suction delivery, whereas her son was born through normal delivery. None of her children had any urinary abnormalities or hearing difficulties, as examined during medical check-ups. However, the children sometimes complained of headaches that had not yet been diagnosed by any doctor.

A percutaneous kidney biopsy was performed under ultrasound guidance. Light microscopy photographs of renal biopsy specimens are shown in Fig. 1. Nine glomeruli were observed in the specimens. One glomerulus was globally sclerosed. Furthermore, segmental sclerosis was observed at the perihilar area in two glomeruli, compatible with the perihilar variant in the Columbia classification of FSGS (Fig. 1a) [13,30]. Interestingly, red-coloured podocytes (ReCPos), whose cytoplasm was dyed red, were observed using AZAN trichrome staining (Fig. 1a and b). Neither mesangial proliferation nor hypercellularity were detected. Interstitial fibrosis and tubular atrophy were observed in almost 30% of the interstitium. There were no abnormal findings such as thickening or lamellation of the tubular basement membrane. Characteristically, granular swollen epithelial cells (GSECs), reported to be specific to mitochondrial diseases [33,34], were markedly observed in the distal tubular cells using AZAN trichrome staining (Fig. 1c). Such GSECs were emphasised by staining with anti-cytochrome *c* oxidase subunit 4 (COX IV) antibody [mouse anti-COX IV antibody (20E8C12)] (ab14744; Abcam PLC., Cambridge, UK; Fig. 1d). COX IV staining is recognised as a loading control for mitochondria [34,35]. Furthermore, the sizes of the vascular smooth muscle cells in arterioles were irregular, and their arrangement was disorganized in a manner similar to that seen in older patients, despite the younger age (33 years) of the patient, without any medical history that may have caused arteriosclerosis (Fig. 1e). Such age-inappropriately disarranged and irregularly sized vascular smooth muscle cells (AiDIVs) were also noticeable in the interlobular arteries (Fig. 1f). Immunofluorescence analysis revealed IgM, C3 and C1q deposits in the glomeruli (Fig. 1g-i). IgG and IgA were negative in observed glomeruli. Electron microscopy analyses (Fig. 2a–e) also showed podocytes with increased mitochondria that had lost their normal cristae structure. Foot processes of such podocytes with accumulation of abnormal mitochondria were effaced (Fig. 2b and d). A vacuolization was also observed in the cytoplasm in the podocyte with mitochondrial accumulation (Fig. 2b). We also detected cells with increased abnormal mitochondria in the parietal epithelial cells of the Bowman's capsule (Fig. 2f). Although the glomerular basement membrane was partially thin at the part along with the podocytes with abnormal mitochondria, the membranes at other parts showed normal thickness (> 250 nm) without lamination or reticulation. Electron dense deposits were not observed in mesangium or glomerular basement membranes. These renal pathology findings strongly suggest genetic FSGS due to mitochondrial disease.

The serum lactate and pyruvate levels were slightly elevated at 21.0 mg/dL (normal: 3.0–17.0 mg/dL) and 1.34 mg/dL (normal: 0.30–0.94 mg/dL), respectively. The pathological finding of accumulation of abnormal mitochondria in glomerular epithelial cells and tubules, the presence of sensorineural hearing difficulty, and elevated blood lactate led us to perform a comprehensive genetic analysis of mitochondrial diseases.

After obtaining informed consent from the patient according to protocol and permission from our ethics committees, genomic DNA extracted from the patient's peripheral mononuclear blood cells and urine sediment cells was analysed by targeted resequencing coupled with next-generation sequencing, followed by Sanger sequencing. The DNA was subjected to fragmentation and library preparation using the Lotus DNA Library Prep Kit (#10001074; Integrated Device Technology, Inc., San Jose, CA, USA) according to the manufacturer's instructions. Target enrichment was performed with xGen Human mtDNA Research Panel (#1075705; Integrated Device Technology) targeting the whole mtDNA and with custom xGen® Predesigned Gene Capture Pools (Integrated Device Technology)/xGen Lockdown Probe pool (Integrated Device Technology) targeting the exons of 367 nuclear-encoded genes that cause mitochondrial diseases. The library was then sequenced on the Illumina MiSeq platform using the MiSeq Reagent Kit v2 (MS-102-2002; Illumina, Inc., San Diego, CA, USA). A pathogenic mtDNA variant of m.13513G > A was detected in both the patient's blood cells and urine sediment cells (Fig. 3). The Minor Variant Finder (MVF) software program (Thermo Fisher Scientific, Waltham, MA, USA) revealed that the heteroplasmy rates of the blood cells and urine sediment cells were 10.3% (forward: 11.6%/reverse: 9.0%) and 62.2% (forward: 63.7%/reverse: 60.7%), respectively. Therefore, we diagnosed her with renal dysfunction and proteinuria due to FSGS caused by an *MT-ND5* mutation.

3. Discussion and conclusions

MT-ND5 gene encodes NADH dehydrogenase 5 (ND5), which is a subunit of mitochondria respiratory complex I. Therefore, *MT-ND5* mutations cause mitochondrial diseases such as MELAS [23,36,37], Leigh syndrome [36–39], and Leber hereditary optic neuropathy [37]. Our case with the m.13513G > A variant in the *MT-ND5* gene showed FSGS lesions with injured podocytes that had accumulation of abnormal mitochondria in the cytoplasm. The m.13513G > A has already been confirmed as a pathogenic variant of the mitochondrial disease using MITOMAP, a human mitochondrial genome database (https://www.mitomap.org/MITOMAP).

Mitochondrial diseases cause genetic FSGS [11,12,15]. Its etiology is postulated to be caused by genetically disrupted mitochondrial function in podocytes [19,22]. As an indication of this, cases with FSGS due to m.3243A > G mutation had podocytes filled with mitochondria with abnormal cristae structure [10,11]. In the past, several cases of mitochondrial diseases due to *MT-ND5* mutations have been also reported to show FSGS lesions [26–29]. However, in these cases, pathological findings of podocyte injuries with accumulation of abnormal mitochondria were not confirmed, leaving the possibility of secondary FSGS caused by intraglomerular hypertension [14,28,30,31]. In contrast, our present case showed apparent FSGS lesions, and we detected increased abnormal mitochondria in the glomerular podocytes that also had pathological findings indicating their injuries such as foot process effacement and the cytoplasmic vacuolization. Our patient did not have hypertension, obesity, or a history of low birth weight. Furthermore, the diameters of all glomeruli observed under light microscopy in this patient were < 250 μm (mean ± SD; 149 ± −72 μm). Therefore, we deemed the etiology of FSGS, in this case, to be a disorder of the mitochondrial OXPHOS system due to an *MT-ND5* mutation and not due to 'secondary' by intraglomerular hypertension [14,30,31]. The pathological picture of tubulointerstitial nephropathy with GSECs was also observed in this case. This tubulointerstitial damage may be due to the *MT-ND5* mutation, as has been reported in the past [28].

In general, mitochondrial diseases induced by mtDNA mutations vary markedly based on differences in the rates of heteroplasmy by cell type or organ [40,41]. Therefore, while the reason for the differences between the present and the previous cases with the pathogenic variant in *MT-ND5* gene could not be completely ascertained, the heteroplasmy rate of mtDNA with the pathogenic variant in podocytes might have been higher in our case than that in the previous cases.

In this case, IgM, C3, and C1q were positive in glomeruli (Fig. 1g-i). Since neither hematuria, mesangial cell proliferation, nor electron dense deposits were observed, we considered that it was unlikely that IgM nephropathy or C1q nephropathy was complicated [42,43]. On the other hand, glomerular IgM and C3 deposits frequently accompany FSGS [44]. In addition, IgM and C3 were positive in glomeruli of two out of three cases report by Bakis et al., too [28]. Therefore, IgM and C3

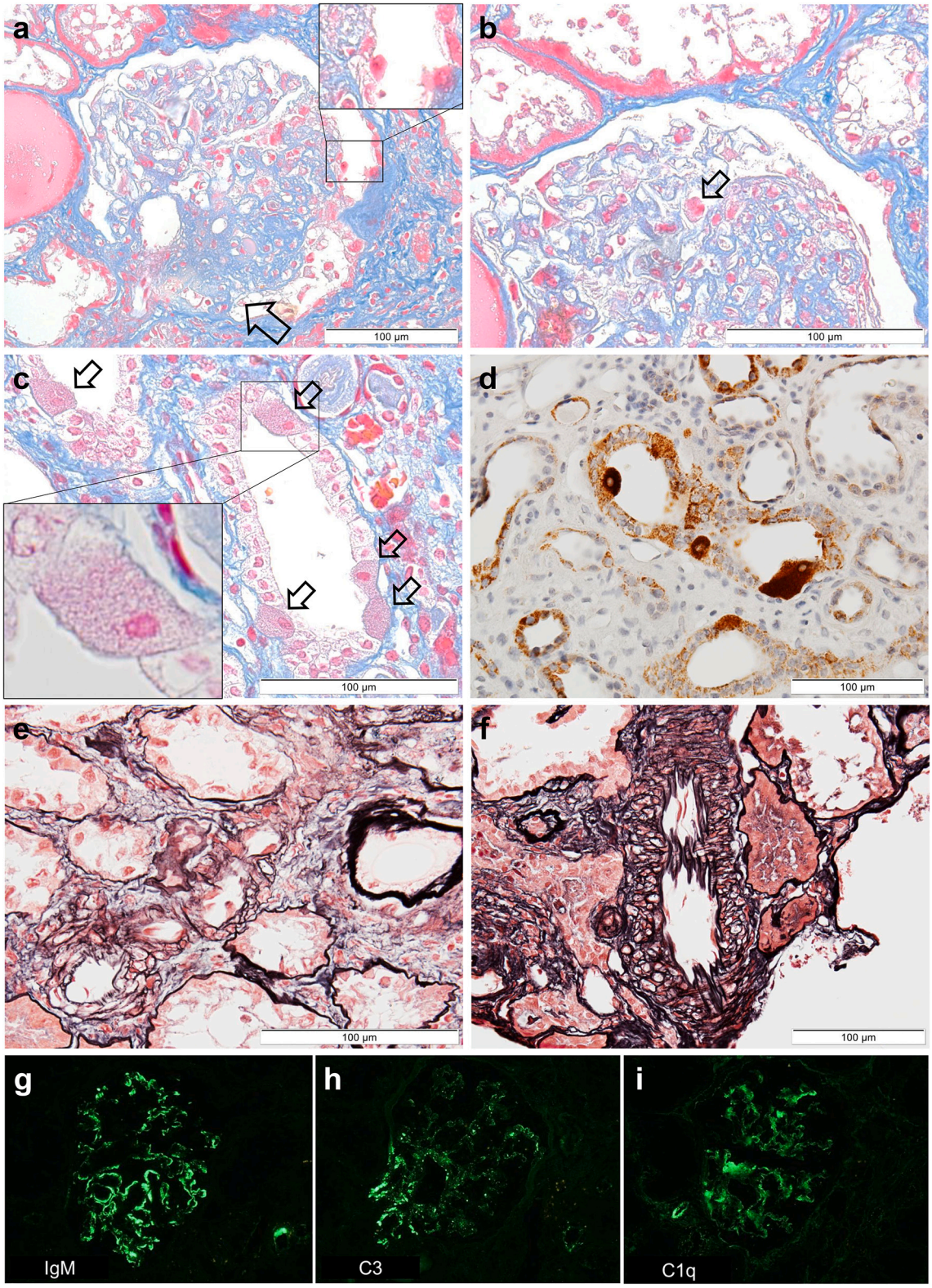

Fig. 1. Light microscopy and immunofluorescence findings (a): The segmental sclerosis lesion at the perihilar area is indicated by an arrow. A red-coloured podocyte (ReCPo) is surrounded by a square, magnified at the top right (AZAN stain). (b): The ReCPo is indicated by an arrow (AZAN stain). (c): GSECs in the distal tubules are indicated by arrows (AZAN stain). One GSEC is magnified at the lower left. (d): Staining of COX IV emphasizes tubular cells, including many mitochondria, which correspond to GSECs. (e): In the afferent arteriole that connects to the glomerulus of (a), the sizes of the vascular smooth muscle cells are irregular, and their arrangement is disorganized, similar to those seen in older patients (PAM-HE stain). (f): Age-inappropriately disarranged and irregularly sized vascular smooth muscle cells (AiDIVs) are observed in an interlobular artery (PAM-HE stain). (g): IgM deposits are detected in glomeruli. (h): IgG deposits are detected in glomeruli. (i): C1q deposits are detected in glomeruli.

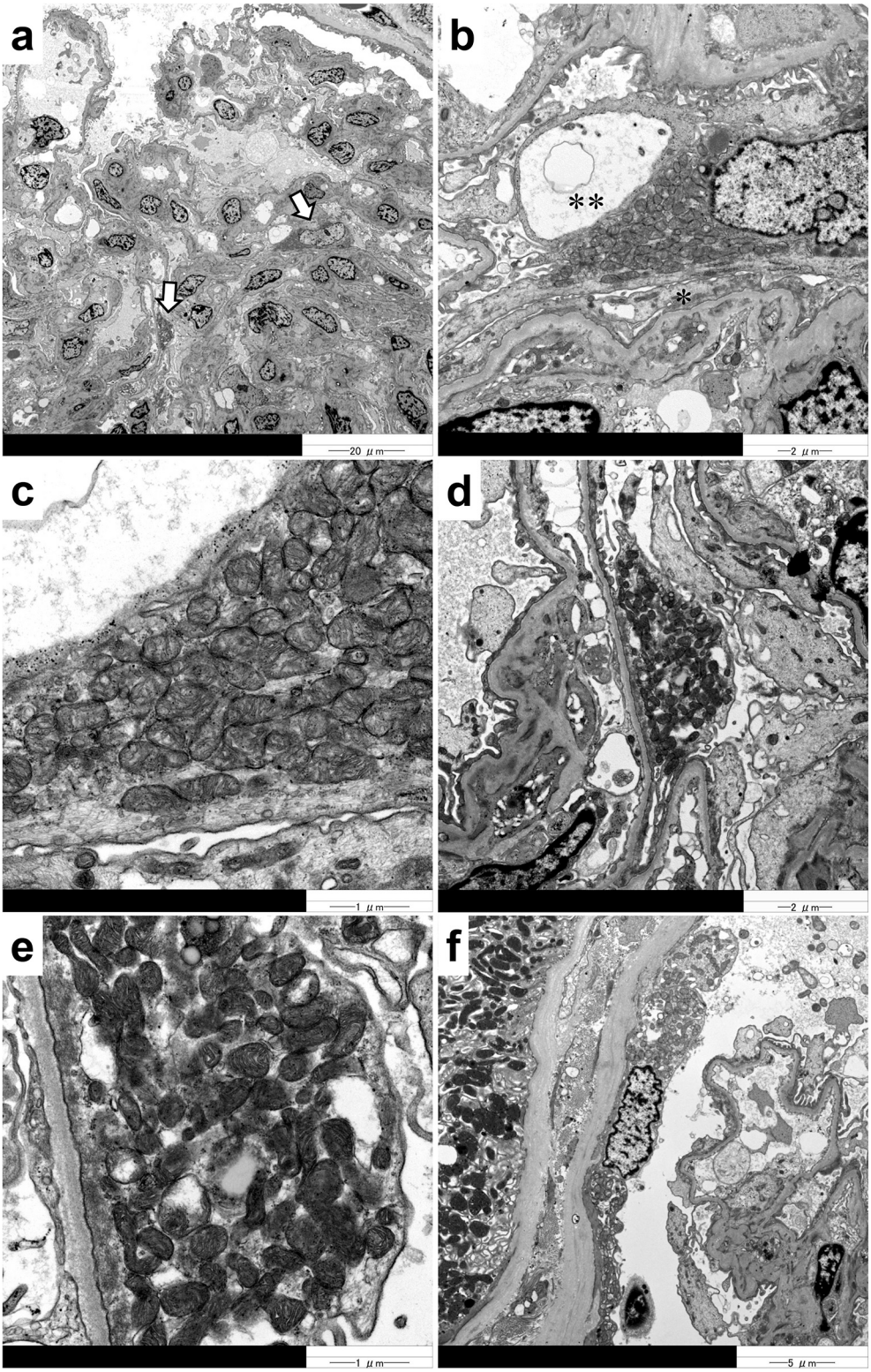

Fig. 2. Electron microscopy findings (a): Arrows indicate podocytes filled with increased mitochondria. (b): In a podocyte, abnormally high numbers of mitochondria are seen in the cytoplasm. Foot process effacement (*) and cytoplasmic vacuolization (**) are observed in this podocyte. (c): Magnification of (b) reveals that the increased mitochondria have lost their organized cristae structure. (d): A podocyte is filled with mitochondria. The foot process of this podocyte is effaced. (e): Magnification of (d) reveals that mitochondria with disorganized cristae increase. (f): The parietal epithelial cells in Bowman's capsule are also filled with abnormal mitochondria.

deposition may be related to a part of the pathogenesis of FSGS caused by *MT-ND5* mutation. Although the reason for C1q deposition in glomeruli is also not clear. Because C1q is reported to bind to mitochondria, it may be associated with the pathogenesis of FSGS by driving oxidative stress [45–47].

This case should be suggestive because it had several characteristic light-microscopical findings of mitochondrial nephropathy. In our case, GSECs with red-coloured cytoplasm were observed with AZAN trichrome staining. As mitochondria are dyed red by acidic dyes such as AZAN, red-coloured GSECs indicate that they abnormally include many mitochondria [33]. In addition, as COX IV is a subunit of complex IV, COX IV staining can be used to stain mitochondria [35] and may help confirm the presence of abnormally increased numbers of mitochondria [34,48]. Furthermore, age-inappropriately disarranged and irregularly sized vascular smooth muscle cells (AiDIVs) were observed in the arterioles and intralobular arteries in this case. Such findings have also been

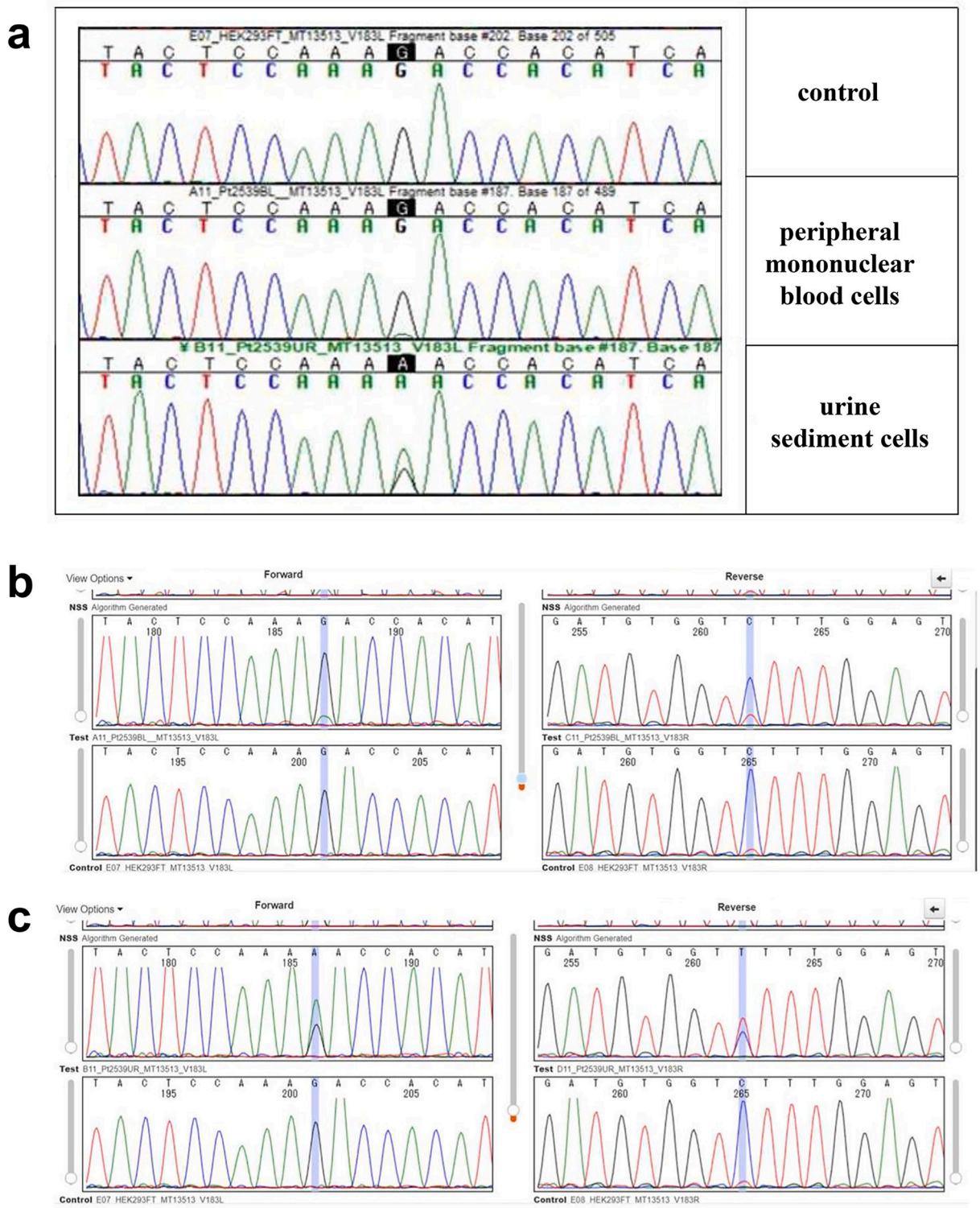

Fig. 3. Genetic analysis (a): The electropherogram from Sanger sequencing indicates that the patient has the m.13513 G > A variant in her peripheral mononuclear blood and urine sediment cells. (b): The rate of heteroplasmy calculated by the MVF software program is 10.3% (forward: 11.6%/reverse: 9.0%) in peripheral mononuclear blood cells (upper panel: patient, lower panel: control). (c): The rate of heteroplasmy is 62.2% (forward: 63.7%/reverse: 60.7%) in urine sediment cells (upper panel: patient, lower panel: control).

reported in other cases of mitochondrial nephropathy [12,34]. Interestingly, red-coloured podocytes (ReCPos) were detected using AZAN trichrome staining, as we recently reported in a case of mitochondrial nephropathy [49]. Like GSECs, ReCPos abnormally include many mitochondria in their cytoplasm [49]. In summary, in cases of FSGS or glomerulosclerosis with unknown aetiologies, the existence of GSECs, AiDIVs, and ReCPos should be carefully evaluated. COX IV staining may aid in the detection of abnormally increased mitochondrial counts.

We describe the weaknesses of our report. In this case, because mitochondrial disease was suspected based on the pathological findings of abnormal mitochondria, the presence of hearing loss, and high blood lactate levels, we comprehensively examined the genes associated with

mitochondrial diseases. Therefore, genetic FSGS due to other gene mutation [50] cannot be completely ruled out. In addition, because genetic testing was performed only on the patient but not on other family members, it could not be investigated whether they carried the heteroplasmic mitochondrial variant. The parents were already deceased and the two healthy brothers did not consent to genetic analysis. The two her children were still under 18 years old and the patient did not wish genetic test. Furthermore, measurement of MRC enzyme activity using kidney biopsy specimens is an effective for confirming mitochondrial dysfunction [51,52]. However, it could not be performed due to the paucity of kidney specimens for this analysis.

In conclusion, this is the first case report which indicates that the pathogenic variant an *MT-ND5* gene causes accumulation of abnormal mitochondria in podocytes, which leads to forming FSGS.

Ethics approval and consent to participate

The original study to perform a genetic analysis for mitochondrial diseases was approved by the Ethics Committee of Chiba Children's Hospital (2014-11-05). In addition, the analysis of this case was also approved by the Ethics Committee of Yamanashi Prefectural Central Hospital (2020–16). The patient provided informed consent and permission to participate in the study.

Consent for publication

Written informed consent was obtained from the patient for the publication of this case report and accompanying images. A copy of the written consent is available for review by the editor of this journal. All authors consented to the publication of the manuscript in *BMC Nephrology*.

Funding

This work was supported in part by the Practical Research Project for Rare/Intractable Diseases from the Japan Agency for Medical Research and Development, AMED (19ek0109273, 20ek0109468) (http://www.amed.go.jp/en/) to TI, YO, and KM.

Authors' contributions

TN drafted the manuscript. TI was involved in the coordination of the study and draft preparation. IN and MW provided clinical information. KH performed the pathological analysis. YY and YK performed molecular genetic studies. YO performed sequence alignment and data curation. KM was involved in the coordination of the study and data curation. YJ was involved in the coordination of the study and clinical information. All authors read and approved the final manuscript.

Declaration of Competing Interest

The authors declare that they have no competing interests.

Data availability

Most of the clinical data used and analysed in this case report are presented in this manuscript. More detailed information is available from the corresponding author upon request.

Acknowledgements

We thank Minako Tominaga and Eri Gomi for their technical assistance. We would like to thank Editage (http://www.editage.com) for English language editing.

References

[1] D. Skladal, J. Halliday, D.R. Thorburn, Minimum birth prevalence of mitochondrial respiratory chain disorders in children, Brain. 126 (Pt 8) (2003) 1905–1912, https://doi.org/10.1093/brain/awg170.
[2] S. Dimauro, G. Davidzon, Mitochondrial DNA and disease, Ann. Med. 37 (3) (2005) 222–232, https://doi.org/10.1080/07853890510007368.
[3] D.M. Kirby, D.R. Thorburn, Approaches to finding the molecular basis of mitochondrial oxidative phosphorylation disorders, Twin Res. Hum. Genet. 11 (4) (2008) 395–411, https://doi.org/10.1375/twin.11.4.395.
[4] D. Leigh, Subacute necrotizing encephalomyelopathy in an infant, J. Neurol. Neurosurg. Psychiatry 14 (3) (1951) 216–221, https://doi.org/10.1136/jnnp.14.3.216.
[5] S. Yatsuga, N. Povalko, J. Nishioka, et al., MELAS: a nationwide prospective cohort study of 96 patients in Japan, Biochim. Biophys. Acta 1820 (5) (2012) 619–624, https://doi.org/10.1016/j.bbagen.2011.03.015.
[6] M.G. Bates, J.P. Bourke, C. Giordano, G. d'Amati, D.M. Turnbull, R.W. Taylor, Cardiac involvement in mitochondrial DNA disease: clinical spectrum, diagnosis, and management, Eur. Heart J. 33 (24) (2012) 3023–3033, https://doi.org/10.1093/eurheartj/ehs275.
[7] W.S. Lee, R.J. Sokol, Mitochondrial hepatopathies: advances in genetics and pathogenesis, Hepatology. 45 (6) (2007) 1555–1565, https://doi.org/10.1002/hep.21710.
[8] P.R. Olmos, G.R. Borzone, J.P. Olmos, et al., Mitochondrial diabetes and deafness: possible dysfunction of strial marginal cells of the inner ear, J. Otolaryngol. Head Neck Surg. 40 (2) (2011) 93–103.
[9] S. Suzuki, Diabetes mellitus with mitochondrial gene mutations in Japan, Ann. N. Y. Acad. Sci. 1011 (2004) 185–192, https://doi.org/10.1007/978-3-662-41088-2_19.
[10] P.S. Thorner, J.W. Balfe, L.E. Becker, R. Baumal, Abnormal mitochondria on a renal biopsy from a case of mitochondrial myopathy, Pediatr. Pathol. 4 (1–2) (1985) 25–35, https://doi.org/10.3109/15513818509025900.
[11] H. Mochizuki, K. Joh, H. Kawame, et al., Mitochondrial encephalomyopathies preceded by de-Toni-Debré-Fanconi syndrome or focal segmental glomerulosclerosis, Clin. Nephrol. 46 (5) (1996) 347–352.
[12] T. Imasawa, D. Hirano, K. Nozu, et al., Clinicopathologic features of mitochondrial nephropathy, Kidney Int. Rep. 7 (3) (2022) 580–590, https://doi.org/10.1016/j.ekir.2021.12.028.
[13] V.D. D'Agati, A.B. Fogo, J.A. Bruijn, J.C. Jennette, Pathologic classification of focal segmental glomerulosclerosis: a working proposal, Am. J. Kidney Dis. 43 (2) (2004) 368–382, https://doi.org/10.1053/j.ajkd.2003.10.024.
[14] K. Sun, Q. Xie, C.M. Hao, Mechanisms of scarring in focal segmental glomerulosclerosis, Kidney Dis. (Basel) 7 (5) (2021 Sep) 350–358, https://doi.org/10.1159/000517108.
[15] O. Hotta, C.N. Inoue, S. Miyabayashi, T. Furuta, A. Takeuchi, Y. Taguma, Clinical and pathologic features of focal segmental glomerulosclerosis with mitochondrial tRNALeu(UUR) gene mutation, Kidney Int. 59 (4) (2001) 1236–1243, https://doi.org/10.1046/j.1523-1755.2001.0590041236.x.
[16] W. Kriz, N. Gretz, K.V. Lemley, Progression of glomerular diseases: is the podocyte the culprit? Kidney Int. 54 (3) (1998) 687–697, https://doi.org/10.1046/j.1523-1755.1998.00044.x.
[17] M. Nagata, Podocyte injury and its consequences, Kidney Int. 89 (6) (2016) 1221–1230, https://doi.org/10.1016/j.kint.2016.01.012.
[18] V.D. D'Agati, Pathobiology of focal segmental glomerulosclerosis: new developments, Curr. Opin. Nephrol. Hypertens. 21 (3) (2012 May) 243–250, https://doi.org/10.1097/MNH.0b013e32835200df.
[19] J. Müller-Deile, M. Schiffer, The podocyte power-plant disaster and its contribution to glomerulopathy, Front. Endocrinol. (Lausanne) 5 (2014 Dec 15) 209, https://doi.org/10.3389/fendo.2014.00209.
[20] S. Güçer, B. Talim, E. Aşan, et al., Focal segmental glomerulosclerosis associated with mitochondrial cytopathy: report of two cases with special emphasis on podocytes, Pediatr. Dev. Pathol. 8 (6) (2005 Nov-Dec), https://doi.org/10.1007/s10024-005-0058-z, 710-7.
[21] M. Hagiwara, K. Yamagata, R.A. Capaldi, A. Koyama, Mitochondrial dysfunction in focal segmental glomerulosclerosis of puromycin aminonucleoside nephrosis, Kidney Int. 69 (7) (2006 Apr) 1146–1152, https://doi.org/10.1038/sj.ki.5000207.
[22] T. Imasawa, R. Rossignol, Podocyte energy metabolism and glomerular diseases, Int. J. Biochem. Cell Biol. 45 (9) (2013 Sep) 2109–2118, https://doi.org/10.1016/j.biocel.2013.06.013.
[23] F.M. Santorelli, K. Tanji, R. Kulikova, et al., Identification of a novel mutation in the mtDNA ND5 gene associated with MELAS, Biochem. Biophys. Res. Commun. 238 (2) (1997) 326–328, https://doi.org/10.1006/bbrc.1997.7167.
[24] M. McKenzie, D. Liolitsa, N. Akinshina, et al., Mitochondrial ND5 gene variation associated with encephalomyopathy and mitochondrial ATP consumption, J. Biol. Chem. 282 (51) (2007 Dec 21) 36845–36852, https://doi.org/10.1074/jbc.M704158200.
[25] S. Shanske, J. Coku, J. Lu, et al., The G13513A mutation in the ND5 gene of mitochondrial DNA as a common cause of MELAS or Leigh syndrome: evidence from 12 cases, Arch. Neurol. 65 (3) (2008 Mar) 368–372, https://doi.org/10.1001/archneurol.2007.67.
[26] A. Motoda, T. Kurashige, T. Sugiura, et al., A case of MELAS with G13513A mutation presenting with chronic kidney disease long before stroke-like episodes, Rinsho Shinkeigaku 53 (6) (2013), https://doi.org/10.5692/clinicalneurol.53.446, 446-51. Japanese.

[27] P.S. Ng, M.V. Pinto, J.L. Neff, et al., Mitochondrial cerebellar ataxia, renal failure, neuropathy, and encephalopathy (MCARNE), Neurol. Genet. 5 (2) (2019 Mar 6), e314, https://doi.org/10.1212/NXG.0000000000000314.
[28] H. Bakis, A. Trimouille, A. Vermorel, et al., Adult onset tubulo-interstitial nephropathy in MT-ND5-related phenotypes, Clin. Genet. 97 (4) (2020) 628–633, https://doi.org/10.1111/cge.13670.
[29] V. Barone, C. La Morgia, L. Caporali, et al., Case report: optic atrophy and nephropathy with m.13513G>a/MT-ND5 mtDNA pathogenic variant, Front. Genet. 13 (2022 Jun 3), 887696, https://doi.org/10.3389/fgene.2022.887696.
[30] A. Tsuchimoto, Y. Matsukuma, K. Ueki, et al., Utility of Columbia classification in focal segmental glomerulosclerosis: renal prognosis and treatment response among the pathological variants, Nephrol. Dial. Transplant. 35 (7) (2020) 1219–1227, https://doi.org/10.1093/ndt/gfy374.
[31] A. Shabaka, A. Tato Ribera, G. Fernández-Juárez, Focal segmental glomerulosclerosis: state-of-the-art and clinical perspective, Nephron. 144 (9) (2020) 413–427, https://doi.org/10.1159/000508099.
[32] S. Matsuo, E. Imai, M. Horio, et al., Revised equations for estimated GFR from serum creatinine in Japan, Am. J. Kidney Dis. 53 (6) (2009) 982–992, https://doi.org/10.1053/j.ajkd.2008.12.034.
[33] A. Kobayashi, Y. Goto, M. Nagata, Y. Yamaguchi, Granular swollen epithelial cells: a histologic and diagnostic marker for mitochondrial nephropathy, Am. J. Surg. Pathol. 34 (2) (2010) 262–270, https://doi.org/10.1097/PAS.0b013e3181cb4ed3.
[34] T. Imasawa, M. Tanaka, Y. Yamaguchi, T. Nakazato, H. Kitamura, M. Nishimura, 7501 T>a mitochondrial DNA variant in a patient with glomerulosclerosis, Ren. Fail. 36 (9) (2014) 1461–1465, https://doi.org/10.3109/0886022X.2014.945181.
[35] D.J. Mahad, I. Ziabreva, G. Campbell, et al., Mitochondrial changes within axons in multiple sclerosis, Brain. 132 (Pt 5) (2009) 1161–1174, https://doi.org/10.1093/brain/awp046.
[36] T. Pulkes, L. Eunson, V. Patterson, et al., The mitochondrial DNA G13513A transition in ND5 is associated with a LHON/MELAS overlap syndrome and may be a frequent cause of MELAS [published correction appears in Ann Neurol 2000 Jun; 47(6):841], Ann. Neurol. 46 (6) (1999) 916–919, https://doi.org/10.1002/1531-8249(199912)46:6<916::aid-ana16>3.0.co;2-r.
[37] M. Chol, S. Lebon, P. Bénit, et al., The mitochondrial DNA G13513A MELAS mutation in the NADH dehydrogenase 5 gene is a frequent cause of Leigh-like syndrome with isolated complex I deficiency, J. Med. Genet. 40 (3) (2003) 188–191, https://doi.org/10.1136/jmg.40.3.188.
[38] V. Carelli, C. La Morgia, M.L. Valentino, P. Barboni, F.N. Ross-Cisneros, A. A. Sadun, Retinal ganglion cell neurodegeneration in mitochondrial inherited disorders, Biochim. Biophys. Acta 1787 (5) (2009) 518–528, https://doi.org/10.1016/j.bbabio.2009.02.024.
[39] E. Ogawa, T. Fushimi, M. Ogawa-Tominaga, et al., Mortality of Japanese patients with Leigh syndrome: effects of age at onset and genetic diagnosis, J. Inherit. Metab. Dis. 43 (4) (2020) 819–826, https://doi.org/10.1002/jimd.12218.
[40] J. van den Ameele, A.Y.Z. Li, H. Ma, P.F. Chinnery, Mitochondrial heteroplasmy beyond the oocyte bottleneck, Semin. Cell Dev. Biol. 97 (2020) 156–166, https://doi.org/10.1016/j.semcdb.2019.10.001.
[41] X. Geng, Y. Zhang, J. Yan, et al., Mitochondrial DNA mutation m.3243A>G is associated with altered mitochondrial function in peripheral blood mononuclear cells, with heteroplasmy levels and with clinical phenotypes, Diabet. Med. 36 (6) (2019) 776–783, https://doi.org/10.1111/dme.13874.
[42] A. Tejani, A.D. Nicastri, Mesangial IgM nephropathy, Nephron. 35 (1) (1983) 1–5, https://doi.org/10.1159/000183035.
[43] J.C. Jennette, C.G. Hipp, C1q nephropathy: a distinct pathologic entity usually causing nephrotic syndrome, Am. J. Kidney Dis. 6 (2) (1985 Aug) 103–110, https://doi.org/10.1016/s0272-6386(85)80150-5.
[44] D. Strassheim, B. Renner, S. Panzer, et al., IgM contributes to glomerular injury in FSGS, J. Am. Soc. Nephrol. 24 (3) (2013 Feb) 393–406, https://doi.org/10.1681/ASN.2012020187.
[45] S.B. Storrs, W.P. Kolb, R.N. Pinckard, M.S. Olson, Characterization of the binding of purified human C1q to heart mitochondrial membranes, J. Biol. Chem. 256 (21) (1981 Nov 10), 10924–9.
[46] A. Comis, S.B. Easterbrook-Smith, C1q binding to mitochondria: a possible artefact? FEBS Lett. 185 (1) (1985 Jun 3) 105–108, https://doi.org/10.1016/0014-5793(85)80749-3.
[47] V.S. Ten, J. Yao, V. Ratner, et al., Complement component c1q mediates mitochondria-driven oxidative stress in neonatal hypoxic-ischemic brain injury, J. Neurosci. 30 (6) (2010 Feb 10) 2077–2087, https://doi.org/10.1523/JNEUROSCI.5249-09.2010.
[48] T. Imasawa, M. Tanaka, N. Maruyama, et al., Pathological similarities between low birth weight-related nephropathy and nephropathy associated with mitochondrial cytopathy, Diagn. Pathol. 9 (2014) 181. Published 2014 Sep 30, https://doi.org/10.1186/s13000-014-0181-0.
[49] Y. Maeoka, T. Doi, M. Aizawa, et al., A case report of adult-onset COQ8B nephropathy presenting focal segmental glomerulosclerosis with granular swollen podocytes, BMC Nephrol. 21 (1) (2020) 376. Published 2020 Aug 28, https://doi.org/10.1186/s12882-020-02040-z.
[50] E.J. Brown, M.R. Pollak, M. Barua, Genetic testing for nephrotic syndrome and FSGS in the era of next-generation sequencing, Kidney Int. 85 (5) (2014 May) 1030–1038, https://doi.org/10.1038/ki.2014.48.
[51] M. Rudnicki, J.A. Mayr, J. Zschocke, et al., MELAS syndrome and kidney disease without Fanconi syndrome or proteinuria: a case report, Am. J. Kidney Dis. 68 (6) (2016) 949–953, https://doi.org/10.1053/j.ajkd.2016.06.027.
[52] A. Ghose, C.M. Taylor, A.J. Howie, A. Chalasani, I. Hargreaves, D.V. Milford, Measurement of respiratory chain enzyme activity in human renal biopsy specimens, J. Clin. Med. 6 (9) (2017 Sep 19) 90, https://doi.org/10.3390/jcm6090090.

Original research

Strategic validation of variants of uncertain significance in *ECHS1* genetic testing

Yoshihito Kishita ,[1,2] Ayumu Sugiura ,[2] Takanori Onuki,[3] Tomohiro Ebihara ,[4] Tetsuro Matsuhashi,[3] Masaru Shimura ,[3] Takuya Fushimi,[3] Noriko Ichino ,[2] Yoshie Nagatakidani,[1] Hitomi Nishihata,[1] Kazuhiro R Nitta,[2] Yukiko Yatsuka ,[2] Atsuko Imai-Okazaki,[2] Yibo Wu,[5,6] Hitoshi Osaka,[7] Akira Ohtake ,[8,9] Kei Murayama ,[3,10] Yasushi Okazaki [2,11]

► Additional supplemental material is published online only. To view, please visit the journal online (http://dx.doi.org/10.1136/jmg-2022-109027).

For numbered affiliations see end of article.

Correspondence to
Dr Yasushi Okazaki, Diagnostics and Therapeutics of Intractable Diseases, Intractable Disease Research Center, Juntendo University, Graduate School of Medicine, Bunkyo-ku, Tokyo, Japan;
ya-okazaki@juntendo.ac.jp

YK and AS are joint first authors.

Received 1 November 2022
Accepted 3 April 2023
Published Online First 13 April 2023

To cite: Kishita Y, Sugiura A, Onuki T, *et al*. *J Med Genet* 2023;**60**:1006–1015.

ABSTRACT

Background Enoyl-CoA hydratase short-chain 1 (ECHS1) is an enzyme involved in the metabolism of branched chain amino acids and fatty acids. Mutations in the *ECHS1* gene lead to mitochondrial short-chain enoyl-CoA hydratase 1 deficiency, resulting in the accumulation of intermediates of valine. This is one of the most common causative genes in mitochondrial diseases. While genetic analysis studies have diagnosed numerous cases with *ECHS1* variants, the increasing number of variants of uncertain significance (VUS) in genetic diagnosis is a major problem.

Methods Here, we constructed an assay system to verify VUS function for *ECHS1* gene. A high-throughput assay using *ECHS1* knockout cells was performed to index these phenotypes by expressing cDNAs containing VUS. In parallel with the VUS validation system, a genetic analysis of samples from patients with mitochondrial disease was performed. The effect on gene expression in cases was verified by RNA-seq and proteome analysis.

Results The functional validation of VUS identified novel variants causing loss of *ECHS1* function. The VUS validation system also revealed the effect of the VUS in the compound heterozygous state and provided a new methodology for variant interpretation. Moreover, we performed multiomics analysis and identified a synonymous substitution p.P163= that results in splicing abnormality. The multiomics analysis complemented the diagnosis of some cases that could not be diagnosed by the VUS validation system.

Conclusions In summary, this study uncovered new *ECHS1* cases based on VUS validation and omics analysis; these analyses are applicable to the functional evaluation of other genes associated with mitochondrial disease.

WHAT IS ALREADY KNOWN ON THIS TOPIC

⇒ Mitochondrial short-chain enoyl-CoA hydratase 1 deficiency is caused by variants in *ECHS1* gene.
⇒ *ECHS1* is the most frequent causative gene of mitochondrial diseases in Japan.

WHAT THIS STUDY ADDS

⇒ High-throughput and efficient assay system was constructed to validate the variants of uncertain significance (VUS) in *ECHS1* and 15 variants were evaluated.
⇒ Combination of multiomics analysis and VUS assay led to the diagnosis of five new cases.

HOW THIS STUDY MIGHT AFFECT RESEARCH, PRACTICE OR POLICY

⇒ Our methodology accelerates VUS evaluation, resulting in increased diagnostic rates and speed of diagnosis.

INTRODUCTION

ECHS1 encodes short-chain enoyl-CoA hydratase 1 (SCEH), which is responsible for the degradation of branched chain amino acids and fatty acids.[1] Abnormalities in valine metabolism particularly impact the pathogenesis of SCEH deficiency (MIM #616277); accumulation of valine metabolites such as S-(2-carboxypropyl) cysteine (SCPC) and S-(2-carboxypropyl) cysteamine derived from methacrylyl-CoA, and S-(2-carboxyethyl) cysteine (SCEC), S-(2-carboxyethyl) cysteamine and 2-methyl-2,3-dihydroxybutyric acid, derived from acryloyl-CoA, is often observed.[2] Pathogenic variants in *ECHS1* mainly cause Leigh encephalopathy presenting elevated plasma lactate and brain MRI abnormalities.[3–7] In addition, mitochondrial respiratory chain complex abnormalities have also been reported to cause mitochondrial dysfunction in cases with *ECHS1* pathogenic variants.[5–7] Many Japanese cases with *ECHS1* pathogenic variants have also been reported.[4 5 7–10] Numerous *ECHS1* variants have been reported all over the world and pathogenic variants are located throughout the *ECHS1* gene. A variant frequently reported in Asians is c.176A>G (NM_004092.4): Asn59Ser (NP_004083.3). The expansion in the clinic of genetic testing has resulted in the rapid accumulation of variants of uncertain significance (VUS). That is no exception in mitochondrial diseases, and the VUS number in *ECHS1* is increasing. On the other hand, recent studies have also shown that a valine-restricted diet is effective for cases with *ECHS1* pathogenic variants.[11 12] Quick diagnosis is important for early treatment of SCEH deficiency.

Recently, various approaches have been tried to solve VUS. Functional analysis using cultured cells and model organisms is a powerful validation

method, providing strong evidence of pathogenicity according to the American College of Medical Genetics and Genomics guidelines.[13] Especially, high-throughput assays combining CRISPR/Cas9 and genome-sequencing technologies are being used for VUS verification in cancer-causing genes.[14 15] Although VUS have been validated for *IVD*, *ACADVL* and *ACAD9*, all causative genes of inborn errors of metabolism,[16–18] there is little research on VUS verification in rare diseases.

In this study, we focused on VUS in *ECHS1*, common in many cases of mitochondrial diseases.[8 9 19] In Japan, Tohoku Medical Megabank Organization (ToMMo) has a genome project for healthy subjects.[20 21] In recessive diseases, the causative variant is often present at a certain frequency within a given race. Therefore, in addition to the VUS found in our previous studies of patients with mitochondrial diseases, we conducted VUS validation of rare variants registered in the Japanese Multi-Omics Reference Panel (jMorp) operated by ToMMo.

Here, we constructed an assay system with ATP measurement using cells deficient in the *ECHS1* gene for systematic VUS verification and validation of heterozygotic variants. Furthermore, we found a novel *ECHS1* variant by multiomics analysis. Coincidentally, the uncharacterised variants were verified by the assay system as being caused by *ECHS1*.

MATERIALS AND METHODS

Cell culture and knockout cell generation

Cells were cultured at 37°C and 5% CO_2 in Dulbecco's modified Eagle's medium (with 4.5 g/L glucose; Nacalai Tesque, Kyoto, Japan) supplemented with 10% fetal bovine serum and 1% penicillin-streptomycin.

Single guide RNAs (sgRNAs) were designed using CRISPRdirect software.[22] The target sequence was as follows: 5′-GGGCCTTGGGGCGGTTCAGT-3′. gRNA oligonucleotides were inserted into a pSpCas9(BB)−2A-Puro (PX459) V2.0 (Addgene 62988) plasmid as previously described.[23] HEK293FT cells were transfected with PX459 including *ECHS1* targeted sgRNA. Cells were selected using 2 µg/mL puromycin and single cells were isolated. Genomic DNA was extracted from isolated cells, and sgRNA target sites were amplified using KOD FX Neo (Toyobo). Primer sequences are as follows: 5′-CCCATGACCGTCTTCACTCG-3′ and 5′-ACATCCCTTC-CCCCACTCTC-3′. PCR products were purified and directly sequenced.

ATP assay

HEK293FT wild-type (WT) or *ECHS1* knockout (KO) cells were seeded in a collagen-coated 96-well plate (354650, Corning, Arizona, USA) at 1×10^4 cells/well with growth medium containing 25 mM glucose. For VUS validation, *ECHS1* KO cells were transfected with 20 ng of expression vectors encoding WT or *ECHS1* variants. One day after plating or transfection, the medium was replaced with 25 mM glucose or 10 mM galactose medium supplemented with dialysed 10% fetal bovine serum (04-011-1A, Biological industries, KibbutzBeit-Haemek, Israel) and L-valine (13046-62, Nacalai Tesque, Kyoto, Japan). Four days after culture in galactose or glucose medium, the ATP content was measured using the CellTiter-Glo Luminescent Cell Viability Assay kit (Promega) with a VICTOR Nivo multimode microplate reader (PerkinElmer, Massachusetts, USA).

RNA-seq

RNA was purified from fibroblasts by the Maxwell RSC simplyRNA Cells Kit and a Maxwell RSC Instrument (Promega). After quality check by Agilent 2100 and Qubit 2.0, the mRNA was enriched using oligo(dT) beads and rRNA was removed using the Ribo-Zero kit. The mRNA was fragmented randomly by adding fragmentation buffer; then, cDNA was synthesised by using the mRNA template and random hexamer primers, followed by addition of a custom second-strand synthesis buffer (Illumina), dNTPs, RNase H and DNA polymerase I to initiate second-strand synthesis. Second, after a terminal repair, a ligation and sequencing adaptor ligation, the double-stranded cDNA library was completed through size selection and PCR enrichment. Sequencing was performed using 150 bp paired-end reads on a NovaSeq6000 (Illumina). Fastq files were aligned to the GRCh38/hg38 genome by STAR. Gene read counts were quantified by STAR quantMode GeneCounts function. The aligned BAM files were loaded into the Integrated Genomics Viewer and visualised using a Sashimi plot for mRNA splicing analysis.

Proteome

Samples from fibroblasts were prepared as described previously.[24] The samples were measured in both data-dependent and data-independent modes performed on the Q-Exactive Plus mass spectrometer (Thermo Fisher Scientific) as previously described.[24] Finally, 5979 proteins were detected in 16 samples including 2 healthy controls and 14 patients with mitochondrial disease. Then, outlier protein expression analysis was performed using OUTRIDER.[25]

Western blotting analysis

Sodium dodecyl sulfate polyacrylamide gel electrophoresis (SDS-PAGE) and western blot were performed as previously described.[19] Five days after transfection, cells were directly harvested by 1x SDS sample buffer (62.5 mM Tris-HCl pH6.8, 2% SDS, 5% sucrose) containing protease inhibitor cocktail (Nacalai Tesque). After sonication, 2-mercaptoethanol was added to the samples to a final concentration of 5%. Prepared samples were denatured for 5 min at 95°C and separated by SDS-PAGE on the 5%–20% gradient polyacrylamide gel (2331730, ATTO, Tokyo, Japan). Proteins were transferred to polyvinylidenefluoride (PVDF) membrane and subjected to western blotting (WB). Each antibody was obtained as follows: ECHS1 (11 305-1-AP, Proteintech, Illinois, USA), GAPDH (G9545, Sigma-Aldrich), beta-actin (A5441, Sigma-Aldrich).

Statistics

Data are expressed as mean±SEM. The statistical significance of differences was determined by one-way analysis of variance (ANOVA) followed by Dunnett's test using Prism V.9 (GraphPad Software, California, USA).

RESULTS

Cases with *ECHS1* variants

In previous genomic studies on patients with mitochondrial disease including suspected cases (1221 cases), direct Sanger sequencing (4 cases), gene panel sequencing (857 cases) and whole exome sequencing (603 cases (243 cases of panel sequencing have been performed)) led to the discovery of 8 variants in 15 *ECHS1* cases (figure 1A). In Japanese people, the most frequently identified variant was c.176A>G(p.Asn59Ser), followed by c.5C>T(p.Ala2Val)[6 7 9] (figure 1A,B). These variants are common in other Asian cases; the allele frequencies of c.176A>G(p.Asn59Ser) and c.5C>T(p.Ala2Val) are 0.0005769 and 0.0001927 in the gnomAD v3.1.2 East Asian, respectively. Several of these cases also had VUS in ClinVar (as of 20220715,

A

Patient ID	DNA (NM_004092.4)	Protein(NP_004083.3)
0207	c.5C>T	p.Ala2Val
0207	c.176A>G	p.Asn59Ser
0255	c.176A>G	p.Asn59Ser
0255	c.413C>T	p.Ala138Val
0346ES	c.176A>G	p.Asn59Ser
0346ES	c.476A>G	p.Gln159Arg
0346YS	c.176A>G	p.Asn59Ser
0346YS	c.476A>G	p.Gln159Arg
0376	c.98T>C	p.Phe33Ser
0376	c.176A>G	p.Asn59Ser
0536	c.1A>G	p.Met1?
0536	c.5C>T	p.Ala2Val
0775	c.5C>T	p.Ala2Val
0775	c.88+2T>C	

Patient ID	DNA (NM_004092.4)	Protein(NP_004083.3)
1038ES	c.5C>T	p.Ala2Val
1038ES	c.176A>G	p.Asn59Ser
1038YS	c.5C>T	p.Ala2Val
1038YS	c.176A>G	p.Asn59Ser
1135ES	c.5C>T	p.Ala2Val
1135ES	c.176A>G	p.Asn59Ser
1135YS	c.5C>T	p.Ala2Val
1135YS	c.176A>G	p.Asn59Ser
1553	c.5C>T	p.Ala2Val
1553	c.176A>G	p.Asn59Ser
2521	c.23T>C	p.Leu8Pro
2521	c.176A>G	p.Asn59Ser
2637	c.5C>T	p.Ala2Val
2637	c.176A>G	p.Asn59Ser
2816	c.23T>C	p.Leu8Pro
2816	c.176A>G	p.Asn59Ser

B

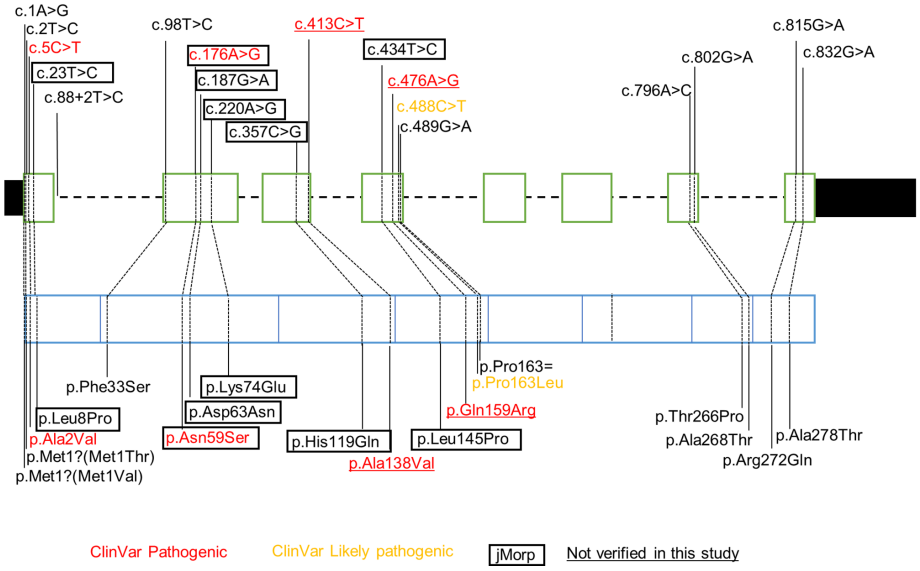

Figure 1 Summary of *ECHS1* variants. (A) *ECHS1* variants identified from genomic analysis. (B) Gene structure (top) and corresponding amino acids (bottom) of *ECHS1*. Variants registered as pathogenic (red) and likely pathogenic (yellow) in ClinVar and jMorp (square) are shown. The two underlined variants were identified from our genomic analysis study; no experimental variants of uncertain significance verification was performed. ECHS1, enoyl-CoA hydratase short-chain 1; jMorp, Japanese Multi-Omics Reference Panel.

and the same afterhere), such as c.1A>G(p.Met1Val) and c.23T>C(p.Leu8Pro).[8 26] In addition, we selected rare variants (minor allele frequency <0.005 in gnomAD) without taking into account zygosity. We also found heterozygous variants in *ECHS1* with conflicting interpretations of pathogenicity (c.796A>C:p.Thr266Pro and c.832G>A:p.Ala278Thr), VUS (c.815G>A:p.Arg272Gln) or unreported (c.802G>A:p.Ala268Thr). All these variants are rare and may be disease-causing, but no experimental verification of the variants has been performed so far. Variants with low allele frequency have been identified, and a number of them have been designated as VUS. Accurate and quick interpretation of these variants is essential for improved diagnosis.

VUS validation in *ECHS1*

To perform VUS validation of *ECHS1*, we first generated cells deficient in the *ECHS1* gene by targeting *ECHS1* using the CRISPR/Cas9 system in HEK293FT cells. The *ECHS1* KO cell line had an in-frame deletion of 18 bases in exon 2 of the *ECHS1* gene (figure 2A). This in-frame deletion resulted in loss of ECHS1 mRNA and protein, as confirmed by qRT-PCR and WB (figure 2B). We also confirmed abnormalities in the mitochondrial function in *ECHS1* KO cells. In galactose medium, ATP production is largely dependent on mitochondrial respiration.[27] Accordingly, we measured ATP levels of WT and *ECHS1* KO cells after incubation in glucose and galactose media. The ratio of ATP levels under galactose and glucose conditions was stable, and no significant difference was observed between *ECHS1* KO and WT cells under these conditions (figure 2C). The cellular toxicity of ECHS1 deficiency is due to the accumulation of intermediates in valine metabolism. That explains why a valine-restricted diet is recommended to patients harbouring *ECHS1* pathogenic variants.[12] Consistently, valine addition to the galactose medium led to further reduced ATP levels in *ECHS1* KO cells, in a dose-dependent manner (figure 2D,E). These results suggest that the abnormal mitochondrial function in *ECHS1* KO cells results from the abnormal valine metabolism, as shown in human patients, making it a suitable model to validate VUS of *ECHS1*. Accordingly, we performed a functional verification of VUS using *ECHS1* KO cells expressing VUS under additional valine supplementation.

First, 15 variants identified from previous genomic studies and jMorp were selected for functional validation. Six rare

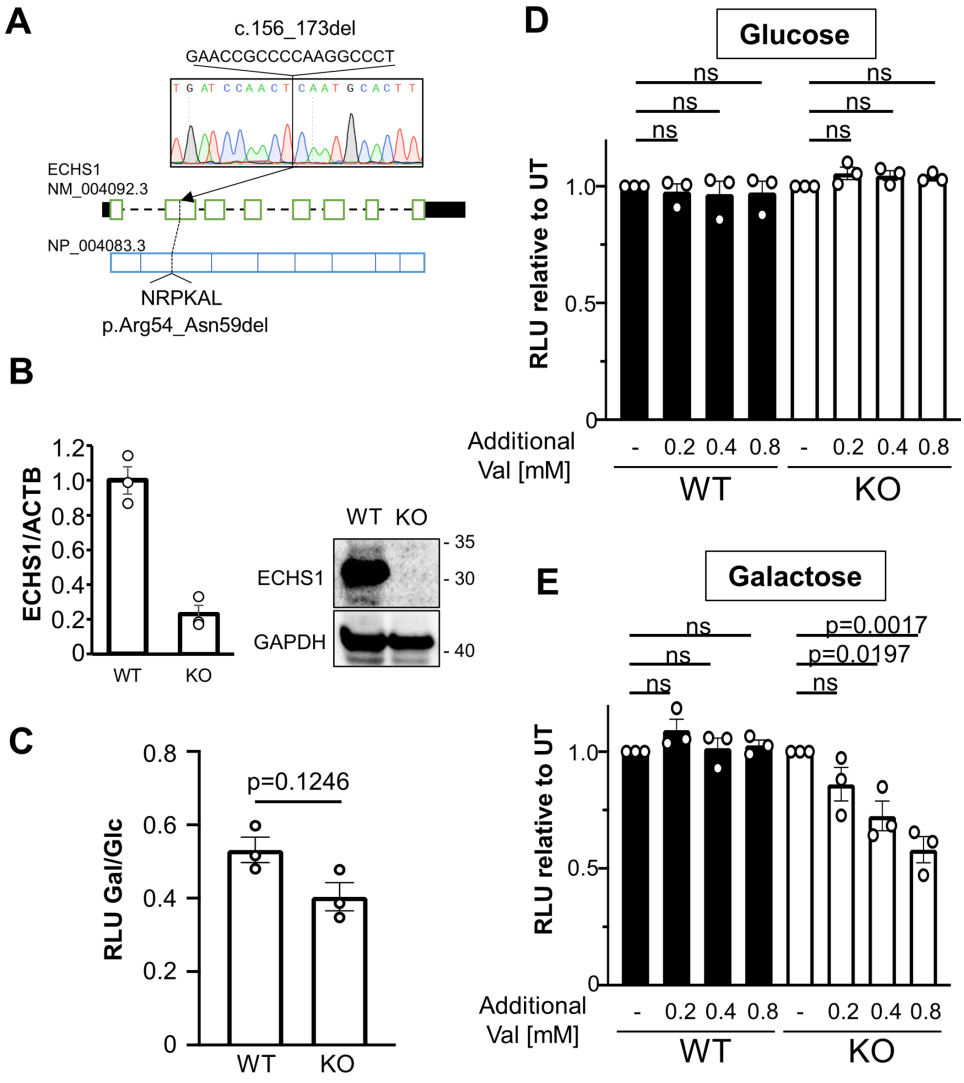

Figure 2 Characterisation of *ECHS1* KO cells. (A) Genomic analysis of *ECHS1* KO cells by Sanger sequencing. (B) *EHCS1* expression levels in WT and *ECHS1* KO HEK293FT cells were quantified by qRT-PCR (left). Whole cell extracts from WT and *ECHS1* KO HEK293FT cells analysed by immunoblotting using the indicated antibodies. Single and double asterisks indicate uncleaved and cleaved forms, respectively (right). (C) ATP assay of WT and *ECHS1* KO HEK293FT cells cultured in glucose or galactose medium. The graph shows the ATP level in galactose medium divided by galactose. (D, E) ATP assay of WT and *ECHS1* KO HEK293FT cells treated with the indicated L-valine concentrations under glucose (D) and galactose (E) medium. Bar graphs represent the average ATP level in each condition from three biological independent experiments. Error bars: ±SEM. Statistical analysis was performed using analysis of variance followed by Dunnett's test. KO, knockout; RLU, relative luciferase unit; WT, wild-type.

variants out of the 15 variants were registered in jMorp (4.7KJPN released on 20190902; figure 1B, online supplemental table 1). The c.23T>C(p.Leu8Pro) and c.176A>G(p.Asn59Ser) variants were found in our patients as well as registered in jMorp (4.7KJPN). Other four variants were not identified in our genome analysis of patients with mitochondrial disease. ECHS1 is a mitochondria-localised protein with a mitochondrial targeting sequence (MTS) at the N-terminal 1–22 amino acid residues. Four variants were located at the translation initiation site and the MTS. c.176A>G(p.Asn59Ser) and c.5C>T(p.Ala2Val), two of the most frequent variants, were selected as positive controls for pathogenic variants. We compared *ECHS1* KO cells transfected with an empty vector and *ECHS1* WT cDNA to *ECHS1* KO cells transfected with an *ECHS1* gene including VUS.

Exogenously expressed ECHS1 shows uncleaved and cleaved forms (figure 3A, single and double asterisks, respectively). Some variants were superiorly expressed in an uncleaved form. Further, we found a significant decrease in the expression level for vectors expressing variants located in the MTS and enoyl-CoA hydratase conserved site (131–151 residues) including at leucine 145 (figure 3A).

Next, we examined VUS functions in the mitochondria. *ECHS1* WT expression restored ATP levels in *ECHS1* KO cells (figure 3B). The ATP levels of KO cells transfected with each variant were compared with that of KO cells transfected with empty vector or *ECHS1* WT expression vector; changes in ATP levels were evaluated by one-way ANOVA followed by Dunnett's test (figure 3C). In addition to p.Ala2Val(c.5C>T) and p.Asn59Ser(c.176A>G), reported as pathogenic variants, p.Met1Val(c.1A>G) and p.Met1Thr(c.2T>C) altered start codons, and p.Leu145Pro(c.434T>C) failed to restore ATP levels probably due to significantly reduced protein expression. p.Leu8Pro(c.23T>C) showed a significant reduction in the lower band considered to correspond to mature ECHS1, but partially restored ATP levels in KO cells. p.His119Gln(c.357C>G),

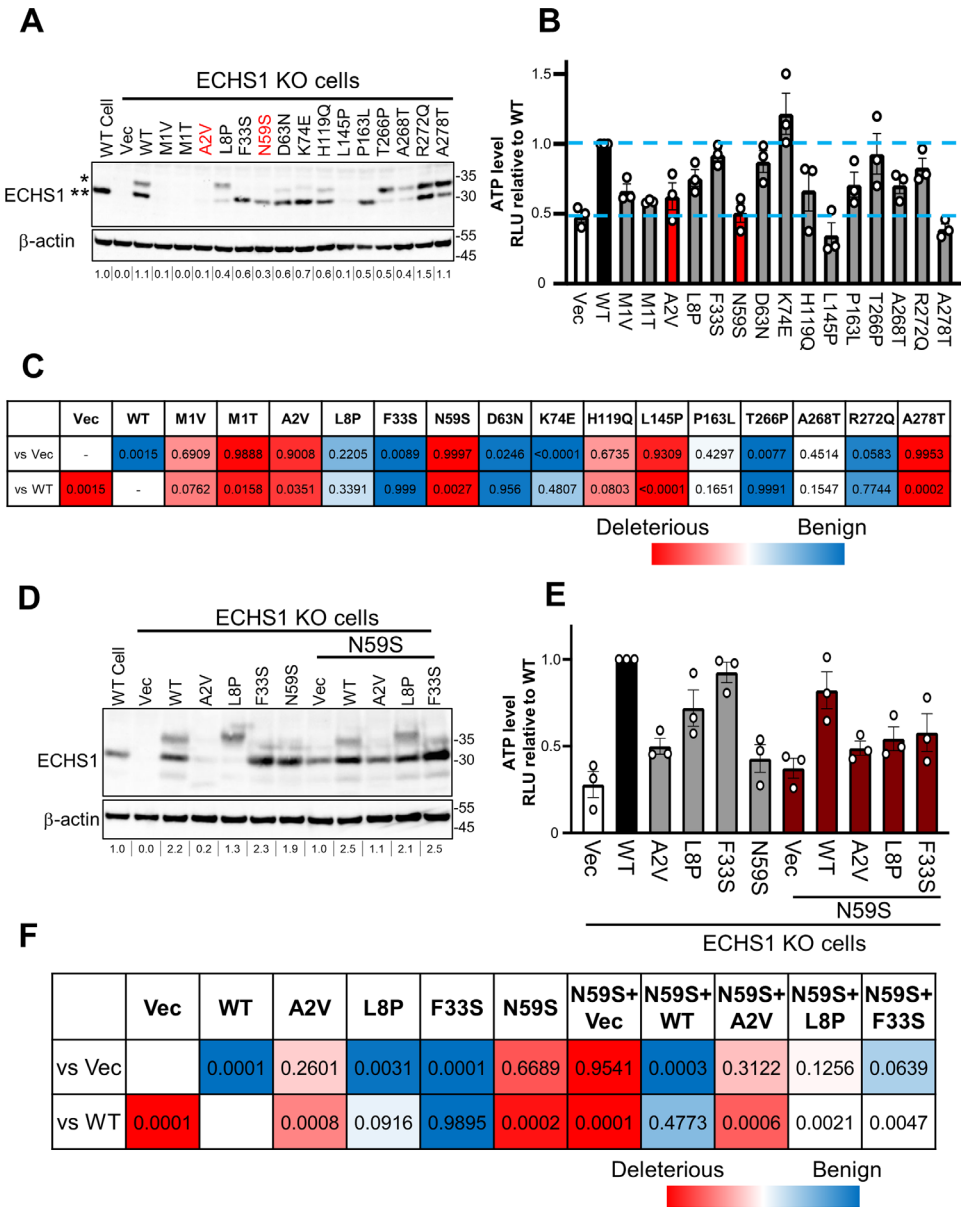

Figure 3 Validation of *ECHS1* VUS. WT and *ECHS1* KO HEK293FT cells transfected with the indicated expression vectors subjected to immunoblotting analysis (A) and ATP assay (B). (A) Whole cell extracts were analysed by immunoblotting using the indicated antibodies. Single and double asterisks indicate uncleaved and cleaved forms, respectively. Quantification analysis of ECHS1/ β-actin relative to WT cell is shown below blotting for β-actin. (B) ATP assay 4 days after treatment with L-valine (0.8 mM). Bar graphs represent the average ATP level in each condition from three biological independent experiments. Error bars: ±SEM. Red bars: pathogenic variants. Grey bars: VUS. (C) Statistical analysis of (B) using ANOVA followed by Dunnett's test. The colour scale shows the p value compared with vector (vs Vec, statistically different red to blue) and WT *ECHS1* (vs WT, statistically different blue to red). (D) Whole cell extracts from WT and *ECHS1* KO HEK293FT cells transfected with the indicated expression vectors analysed by immunoblotting using the indicated antibodies. Quantification analysis of ECHS1/ β-actin relative to WT cell is shown below blotting for β-actin. (E) ATP assay of *ECHS1* KO HEK293FT cells expressing the indicated expression vectors treated with additional L-valine (0.8 mM) for 4 days. Bar graphs represent the average ATP level in each condition from three biological independent experiments. Error bars: SEM. (F) Statistical analysis of (B) using ANOVA followed by Dunnett's test. The colour scale shows the p value compared with vector (vs Vec, statistically different red to blue) and WT *ECHS1* (vs WT, statistically different blue to red). ANOVA, analysis of variance; KO, knockout; RLU, relative luciferase unit; VUS, variants of uncertain significance; WT, wild-type.

p.Pro163Leu(c.488C>T), p.Ala268Thr(c.802G>A) and p.Ala278Thr(c.832G>A) variants had higher expression levels but failed to fully improve ATP levels equivalent to WT, suggesting that these variants were deleterious.

Although p.Leu8Pro(c.23T>C) and p.Phe33Ser(c.98T>C) were reported as pathogenic variants,[19 26] ATP assays demonstrate a mild functional decline. Since p.Leu8Pro(c.23T>C) and p.Phe33Ser(c.98T>C) were identified as a compound heterozygote with p.Asn59Ser(c.176A>G), a non-functional variant (figure 3B), we hypothesised that p.Leu8Pro(c.23T>C) and p.Phe33Ser(c.98T>C) might be mild deleterious variants capable of restoring KO cells but not KO cells expressing highly deleterious variants. To test this hypothesis, we reproduced compound heterozygous genotypes by transfecting *ECHS1* KO cells with two different variants (figure 4A). The ATP assay demonstrated that WT restored KO cells on co-transfection with p.Asn59Ser(c.176A>G), whereas, as expected, all three variants did not show recovery (figure 3E,F). These results demonstrate

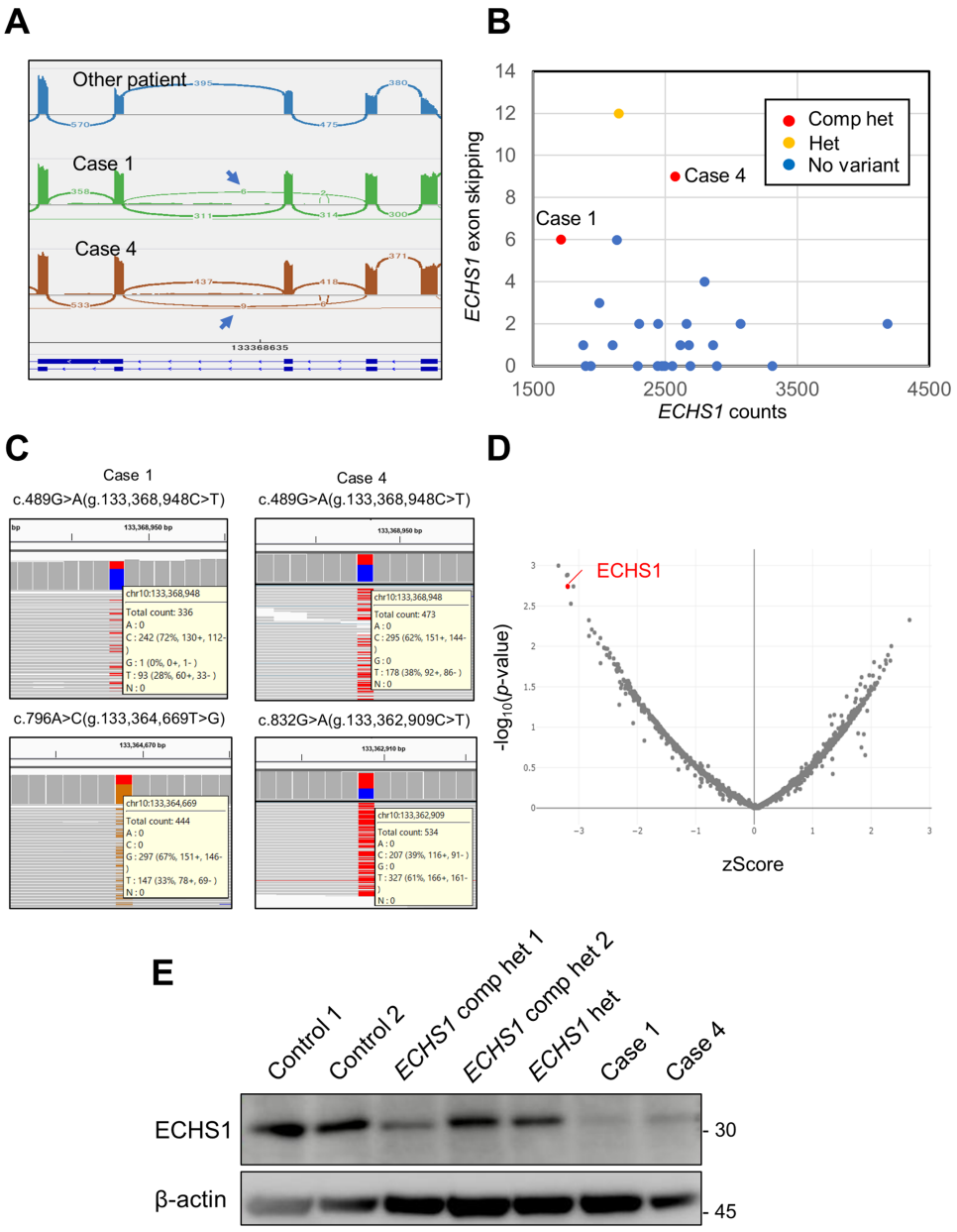

Figure 4 Abnormal splicing and allele-biased gene expression resulting aberrant protein expression. (A) RNA-seq data from two patients with c.489G>A (p.P163=) showing reads suggestive of splicing abnormalities in exons with c.489G>A. (B) Read counts of the *ECHS1* gene are plotted on the horizontal axis and the number of detected exon skipping is plotted on the vertical axis. Gene counts were calculated by STAR, and the number of exon skipping was extracted from the Sashimi plot data. (C) The ratio of c.489G>A and c.796A>C and c.832G>A variants on the IGV viewer. In two cases, the allele expression with c.489G>A was decreased. (D) OUTRIDER analysis illustrating protein expression in a volcano plot. ECHS1 was detected as a protein with a large decrease in expression. (E) Western blotting for ECHS1 in patients with *ECHS1* pathogenic variants and controls. Compared with previously reported ECHS1 cases, case 1 and case 4 showed significantly reduced ECHS1 expression. β-actin was detected as a loading control. ECHS1, enoyl-CoA hydratase short-chain 1.

that our system is potentially valuable to validate the pathogenic nature of the compound heterozygous state.

Validation of ECHS1 variants from omics analysis

Multiomics analysis is an effective and useful method in the search for causative genes. In this study, multiomics analysis was conducted together with VUS validation to improve the efficiency and speed of genetic diagnosis. Here, we identified ECHS1 decreases in two cases (case 1 and case 4) with multiomics analysis and found a common c.489G>A(p.Pro163=) variant. We further re-searched for cases with c.489G>A(p.Pro163=) from our previous genome analysis data and finally identified three cases (cases 2, 3 and 5). In case 1, c.796A>C(p.Thr266Pro) variant was identified; in case 2, c.802G>A(p.Ala268Thr) variant was identified; in cases 3 and 4, c.832G>A(p.Ala278Thr) variant was identified; in case 5, c.833C>T(p.Ala278Val) variant was identified (table 1, online supplemental figure 2). In addition, these cases also had c.489G>A(p.Pro163=) variant, identified in a Samoan family and a very frequent variant (0.01156) in gnomAD v3.1.2 East Asian populations, and suggested to exhibit splicing abnormalities.[28] In the present study, RNA-seq analysis was performed on case 1 and case 4. Then, we identified

Table 1 Patient summary of cases with *ECHS1* variants

Case ID	Sex	Age range at onset (years)	Symptoms	Complex deficiency	OCR	Var 1	Var 2
1	Female	<1	Poor suckling, metabolic acidosis	CIV deficiency (Fb)	Down (Fb)	c.796A>C (p.Thr266Pro)	c.489G>A (p.Pro163=)
2	Male	>3–5	Gait disorder, nystagmus, mental retardation, MRI abnormality	Normal (Fb)	N.T.	c.802G>A (p.Ala268Thr)	c.489G>A (p.Pro163=)
3	Male	1–3	Listlessness, mental retardation, regression after exanthema subitum, MRI abnormalities, deafness, fatigue, hypotonia	Normal (Fb)	Down (Fb)	c.832G>A (p.Ala278Thr)	c.489G>A (p.Pro163=)
4	Male	<1	Developmental delay, convulsion, MRI abnormalities, regression	Normal (Fb)	Down (Fb)	c.832G>A (p.Ala278Thr)	c.489G>A (p.Pro163=)
5	Male	<1	Leigh syndrome, increase of 2-methyl-2,3-dihydroxybutyric acid	Normal (Fb)	Down (Fb)	c.833C>T (p.Ala278Val)	c.489G>A (p.Pro163=)

Complex enzyme activity was defined by <40% decrease. For OCR, a value <71.6% was used as a diagnostic criterion.
CIV, mitochondrial respiratory chain complex IV; Fb, fibroblast; OCR, oxygen consumption rates.

sequence reads showing exon skipping as a consequence of the c.489G>A(p.Pro163=) variant (figure 4A). To examine whether exon skipping actually increased in cases with c.489G>A(p.Pro163=), we plotted RNA-seq counts of the *ECHS1* gene and the number of detected reads showing exon skipping (figure 4B). We analysed 26 RNA-seq data, including case 1 and case 4, as well as one case with heterozygous c.489G>A(p.Pro163=); exon skipping increased in these samples. We also found that exon skipping is detectable in case 1 and case 4 fibroblasts and that blocking nonsense-mediated mRNA decay using puromycin and cycloheximide significantly increased its levels by RNA-seq and qRT-PCR analysis (online supplemental figure 3). In addition, after counting the allele numbers at the c.796A>C(p.Thr266Pro) and c.832G>A(p.Ala278Thr) variant positions showed a bias in allele expression (figure 4C). This indicates that the significantly reduced expression of alleles with c.489G>A(p.Pro163=) in case 1 and case 4 fibroblasts. Proteome analysis in case 1 fibroblasts confirmed a significant decrease in ECHS1 expression (figure 4D). Furthermore, previous studies experimentally demonstrated that case 4 leads to decreased ECHS1 expression and enzymatic activity, as well as accumulation of intermediate products of valine metabolism.[29] WB analysis further confirmed a marked decrease in protein expression in case 1 and case 4 fibroblasts (figure 4E). We here concluded that synonymous and non-synonymous substitution combinations are disease-causing in these cases.

DISCUSSION

ECHS1 is one of the most frequent genes found in patients with mitochondrial diseases. In addition to our genetic study,[7–9] *ECHS1* has been reported as a frequent cause of mitochondrial disease in genetic studies of Leigh encephalopathy in Asian countries such as China[30] and Korea.[31] The length of the coding region is 873 bp. About 250 variants have been reported in ClinVar, of which about 40 are pathogenic/likely pathogenic and nearly 80 have been registered as VUS or with conflicting interpretations of pathogenicity. However, the molecular mechanism by which *ECHS1* variants cause disease is poorly understood. In this study, we established a system to functionally validate *ECHS1* variants, finding some potential pathogenic variants.

Resolving VUS is a major challenge in various diseases, because VUS continue to accumulate under circumstances where genome analysis is becoming more common. Genome sequence projects in healthy individuals have revealed allele frequencies in various races. The accumulation of genome analysis information is expected to lead to the discovery of novel pathogenic variants, since rare variants also found in healthy individuals can be pathogenic. Against this background, it may be possible to make a proactive evaluation of variants not yet associated with the disease. Based on the above, we could identify novel pathogenic variants in this study. Furthermore, the combination of RNA-seq, proteomics and conventional genomic analysis enabled a reliable diagnosis.

ECHS1 is a nuclear-encoded protein transported into the mitochondria by the MTS.[32] MTS locates at the N-terminus and is cleaved in the mitochondria by mitochondrial proteases.[33] There are three points involved in pathogenicity: (1) expression level, (2) location and (3) function. As reported that ECHS1 is degraded through ubiquitin-proteasome pathway in cancer cells,[34] inhibition of proteasome degradation by MG132 leads to subtle increase in the protein level of all ECHS1 variants tested in this study (online supplemental figure 1C). As shown in figure 3A, p.Met1Val (c.1A>G), p.Met1Thr(c.2T>C) and p.Ala2Val(c.5C>T) were weakly expressed. Consistently, these variants failed to restore ATP decrease in *ECHS1* KO cells. The p.Leu8Pro(c.23T>C) variant was detected superiorly in the uncleaved form (figure 3A), suggesting mistargeting to the mitochondria. p.Leu145Pro(c.434T>C) variant showed a weak signal at the estimated molecular weight (figure 3A) and was detected at thee high molecular weight (higher than 70 kDa; online supplemental figure 1C). ECHS1 is known to form a dimer of 2 trimers,[35 36] but p.Leu145Pro(c.434T>C) failed to restore KO cells, suggesting that these high molecular weight forms are abnormal oligomerisation or aggregation. As with p.Asn59Ser(c.176A>G), p.Leu145Pro(c.434T>C) is likely to be a functionally disrupted variant. Interestingly, c.434T>C(p.Leu145Pro) is a variant reported only in jMorp and not previously identified in patients with the disease. The variant registered in jMorp has not been reported as a cause of SCEH deficiency at this time, but it is expected to be found in Japanese cases with this variant in the future. We propose that those who identify variants in *ECHS1* by the genetic test will refer to our variant evaluation study as evidence and that this will lead to a solution to the cause of the disease in the future.

p.Leu8Pro(c.23T>C) and p.Phe33Ser(c.98T>C), considered 'Likely benign' variants from VUS validation experiments (figure 3B,C), were validated by coexpressing with the p.Asn59Ser(c.176A>G) variant (figure 3E,F). By validating

the assumption of compound heterozygosity in combination with a pathogenic variant, we could obtain data accurately reflecting the functional evaluation of hypomorphic variants. The assay was effective for variants in the borders, for which very subtle validation results were obtained. Despite its higher experimental complexity, the assay can be performed while maintaining the conventional throughput, and the validation targets can be expanded. In our reported *ECHS1* mutant cases, the most common combinations are c.176A>G(p.Asn59Ser) and c.5C>T(p.Ala2Val). Since c.176A>G(p.Asn59Ser) has a higher allele frequency than c.5C>T(p.Ala2Val), homozygous cases for c.176A>G(p.Asn59Ser) should be more frequent, but no patients homozygous for c.176A>G(p.Asn59Ser) have been found. This suggests that c.176A>G(p.Asn59Ser) may be so harmful that in homozygosity it may result in severe developmental abnormalities in the prenatal period. The high number of c.176A>G(p.Asn59Ser) and c.5C>T(p.Ala2Val) combinations may be due to c.5C>T(p.Ala2Val) having a smaller functional loss than p.Asn59Ser(c.176A>G), as shown experimentally in this study. c.176A>G(p.Asn59Ser) is only viable in a compound heterozygous state with less deleterious variants. The combination with milder variants such as p.Leu8Pro(c.23T>C) and p.Phe33Ser(c.98T>C), verified in this study, might allow normal development until birth. In other words, this combined assay could first accurately indicate functional abnormalities for variants with intermediate abnormality between normal and completely defective, being a very effective and essential method for variant evaluation.

Mostly, in silico predictions and experimental validation of most variants are comparable. On the other hand, in silico predictions for some variants differ from our validation experiments; therefore, validation experiments are important for such variants. For example, p.Ala2Val(c.5C>T) reported as pathogenic, was not highly damaging on in silico predictions (online supplemental table 1). However, the validation results suggest that although the experimental data indicate an effect on protein gene expression itself, the functional effect may not be significant. A similar trend was observed for p.Leu8Pro(c.23T>C), expected to have a significant effect on protein localisation but relatively little effect on protein function. p.His119Gln(c.357C>G) was also rated mostly tolerant or benign in silico, but experimental validation suggested that the variant negatively affects gene function. The major achievement of this study is providing quantitative experimental validation data for each variant on the same functional platform. We are expanding the validation of other genes; in particular, VUS validation of genes involved in respiratory chain complex I confirmed this to be a reproducible and efficient analysis.

In this validation, we focused on variants specific to Japanese and Asian populations. Naturally, this should be further expanded to include variants from other ethnicities. Our assay system is based on a very simple method and can easily be expanded to other VUS, by including gnomAD and ClinVar variants. In the present study, VUS was verified for jMorp (4.7KJPN) variants, but since then, the jMorp data have been updated and the number of registrations has increased. While planning our validation experiment, the variant data of 4.7KJPN were registered, from which we extracted variants with very low allele frequencies (online supplemental table 2). However, there are now 38KJPN, with 20 more registrations from our validated variants. The data are being updated at an accelerated pace, with 14KJPN in 2021 and 38KJPN in 2022. Given the constant updates to the database, it is important to verify these variants in the future.

ECHS1 protein loss is considered to have a threshold of 30%–40% for disease.[28] This is shown by the analysis with c.489G>A(p.Pro163=) and c.832G>A(p.Ala278Thr) from the study of Simon *et al*. Those homozygous for c.489G>A (p.Pro163=) did not develop the disease, despite showing a protein expression decrease around 40%. On the other hand, the combination of p.Pro163=(c.489G>A) and p.Ala278Thr(c.832G>A) showed <30% protein expression and developed the disease. p.Ala278Thr(c.489G>A) is considered highly damaging in the previous study, as it was found to be deleterious in the VUS validation experiment. Although p.Ala278Val(c.833C>T) has not been validated, we think it likely to be as deleterious as p.Ala278Thr(c.832G>A) since many scores in silico also indicated damaging effects. For p.Thr266Pro(c.796A>C), no significant decrease in ATP levels was observed in VUS validation. However, abnormalities at the protein level were evident from the proteome and immunoblotting. VUS expression experiments with the p.Thr266Pro(c.796A>C) variant also showed reduced ECHS1 expression (figure 3A). Considering these results, p.Thr266Pro(c.796A>C) might have less functional loss and more impact on protein expression. In addition, the forced expression system showed a protein decrease not expected to significantly reduce ATP levels. In protein expression validation (online supplemental figure 1), the amount of mature ECHS1 synthesised from p.Thr266Pro(c.796A>C) was lower than that of immature ECHS1, suggesting that this variant has a significant effect on protein expression and maturation. For p.Ala268Thr(c.802G>A), a mild decrease in ATP levels was observed. Since the value of p.Ala268Thr(c.802G>A) was similar to that of p.Pro163Leu(c.488C>T), reported as likely pathogenic in ClinVar, p.Ala268Thr(c.802G>A) was considered to have an effect on protein function. Case 2 with the c.802G>A(p.Ala268Thr) variant had later onset and milder symptoms than other ECHS1 cases, suggesting that the variant itself has a milder effect. c.489G>A(p.Pro163=), despite its high allele frequency (0.01156 in gnomAD v3.1.2 East Asian, 0.00789 in the jMorp (38KJPN)), is a possible causative variant; its combination with other pathogenic variants leads to disease development. We found five cases with c.489G>A(p.Pro163=) and another rare variant in this study. There have been very few reports of such a high frequency variant in studies of mitochondrial diseases; this variant might be responsible for the increased frequency of cases with *ECHS1* pathogenic variants. However, variants without amino acid substitutions have been overlooked as benign in previous genetic diagnoses. Given the high potential number of patients with c.489G>A(p.Pro163=), it is expected that the number of cases with c.489G>A(p.Pro163=) will further increase because of our findings.

Our VUS verification system has some limitations. Even pathogenic variants may be missed in this experimental system. In fact, p.Pro163Leu(c.488C>T), registered as likely pathogenic in ClinVar, showed a mild score. Thus, variants with intermediate ratings could be pathogenic. In such cases, it would be necessary to validate them using an assay system that assumes compound heterozygosity. Moreover, since this is a forced expression system, variants that cause protein stability or splicing abnormalities may be missed. To extract these variants, other assay systems and functional experiments using patient specimens are required.

Author affiliations
[1]Department of Life Science, Faculty of Science and Engineering, Kindai University, Higashiosaka, Osaka, Japan
[2]Diagnostics and Therapeutics of Intractable Diseases, Intractable Disease Research Center, Juntendo University, Graduate School of Medicine, Bunkyo-ku, Tokyo, Japan
[3]Department of Metabolism, Chiba Children's Hospital, Midori-ku, Chiba, Japan
[4]Department of Neonatology, Chiba Children's Hospital, Midori-ku, Chiba, Japan
[5]Chemical Biology Mass Spectrometry Platform (CHEMBIOMS), Faculty of Sciences, University of Geneva, Geneve, Switzerland
[6]YCI Laboratory for Next-Generation Proteomics, RIKEN Center of Integrative Medical Sciences, Yokohama, Kanagawa, Japan
[7]Department of Pediatrics, Jichi Medical University, Shimotsuke, Tochigi, Japan
[8]Department of Pediatrics & Clinical Genomics, Faculty of Medicine, Saitama Medical University, Moroyama, Saitama, Japan
[9]Center for Intractable Diseases, Saitama Medical University Hospital, Moroyama, Saitama, Japan
[10]Center for Medical Genetics, Chiba Children's Hospital, Midori-ku, Chiba, Japan
[11]Laboratory for Comprehensive Genomic Analysis, RIKEN Center for Integrative Medical Sciences, Yokohama, Kanagawa, Japan

Acknowledgements We thank the family for their participation in the research presented here and the Laboratory of Molecular and Biochemical Research, Biomedical Research Core Facilities, Juntendo University Graduate School of Medicine, and Kasumi Kanai for technical assistance.

Contributors YK, AS and YO wrote the manuscript. YK, AS, TK, TE, TM, MS, NI, YN, HN, YY and YW performed the experiments. YK, AS, TK, TE, TM, MS, NI, YN, HN, YY, AI-O, YW and YO analysed the data. TK, TE, TM, MS, TF, HO, AO and KM acquired clinical information. YK, AS, TF, KRN and AI-O did bioinformatics and statistical analysis. YK, AS and AO supervised the study. All authors discussed the results and commented on the manuscript. YO is responsible for the overall content as the guarantor.

Funding This work was supported by a grant for the Practical Research Project for Rare/Intractable Diseases from AMED to HO, KM, YO and AO (Fund ID: JP21im0210625, JP21ek0109511, JP22ek0109485, JP22ek0109468, JP19ek0109273), Program for Promoting Platform of Genomics based Drug Discovery to YO (Fund ID: JP22kk0305015), the Research Center Network for Realization of Regenerative Medicine (The Acceleration Program for Intractable Diseases Research utilizing Disease-specific iPS cells, JP21bm0804018), and JSPS KAKENHI JP19H03624 to YO and JP20H03648 to HO.

Competing interests None declared.

Patient consent for publication Not applicable.

Ethics approval The studies were approved by the regional Institutional Review Board (Saitama Medical University) and Research Ethics Committee (Juntendo University, Chiba Children's Hospital, Kindai University, Jichi Medical University and RIKEN). The lead institution for the review is Saitama Medical University, with an approval number of 2021-094. Participants gave informed consent to participate in the study before taking part.

Provenance and peer review Not commissioned; externally peer reviewed.

Data availability statement Data are available upon reasonable request. Raw data are available from the corresponding author on reasonable request. ECHS1 knockout cells can also be distributed. Some genomic information that could be used to identify individuals cannot be shared due to ethical restrictions.

ORCID iDs
Yoshihito Kishita http://orcid.org/0000-0003-4978-1680
Ayumu Sugiura http://orcid.org/0000-0002-4776-1478
Tomohiro Ebihara http://orcid.org/0000-0003-2296-5527
Masaru Shimura http://orcid.org/0000-0002-1998-7349
Noriko Ichino http://orcid.org/0000-0002-7009-8299
Yukiko Yatsuka http://orcid.org/0000-0003-3137-6919
Akira Ohtake http://orcid.org/0000-0003-1147-3113
Kei Murayama http://orcid.org/0000-0002-3923-8636
Yasushi Okazaki http://orcid.org/0000-0003-3241-5502

REFERENCES

1 Sharpe AJ, McKenzie M. Mitochondrial fatty acid oxidation disorders associated with short-chain enoyl-coa hydratase (ECHS1) deficiency. *Cells* 2018;7:46:1–13.:.
2 Peters H, Buck N, Wanders R, *et al*. ECHS1 mutations in leigh disease: A new inborn error of metabolism affecting valine metabolism. *Brain* 2014;137(Pt 11):2903–8.
3 Peters H, Ferdinandusse S, Ruiter JP, *et al*. Metabolite studies in hibch and echs1 defects: implications for screening. *Mol Genet Metab* 2015;115:S1096-7192(15)30027-5:168–73.:.
4 Yamada K, Aiba K, Kitaura Y, *et al*. Clinical, biochemical and metabolic characterisation of a mild form of human short-chain enoyl-coa hydratase deficiency: significance of increased n-acetyl-s-(2-carboxypropyl)cysteine excretion. *J Med Genet* 2015;52:691–8.
5 Sakai C, Yamaguchi S, Sasaki M, *et al*. ECHS1 mutations cause combined respiratory chain deficiency resulting in leigh syndrome. *Hum Mutat* 2015;36:232–9.
6 Tetreault M, Fahiminiya S, Antonicka H, *et al*. Whole-Exome sequencing identifies novel ECHS1 mutations in Leigh syndrome. *Hum Genet* 2015;134:981–91.
7 Haack TB, Jackson CB, Murayama K, *et al*. Deficiency of ECHS1 causes mitochondrial encephalopathy with cardiac involvement. *Ann Clin Transl Neurol* 2015;2:492–509.
8 Ogawa E, Shimura M, Fushimi T, *et al*. Clinical validity of biochemical and molecular analysis in diagnosing Leigh syndrome: a study of 106 Japanese patients. *J Inherit Metab Dis* 2017;40:685–93.
9 Ogawa E, Fushimi T, Ogawa-Tominaga M, *et al*. Mortality of Japanese patients with Leigh syndrome: effects of age at onset and genetic diagnosis. *J Inherit Metab Dis* 2020;43:819–26.
10 Illsinger S, Korenke GC, Boesch S, *et al*. Paroxysmal and non-paroxysmal dystonia in 3 patients with biallelic ECHS1 variants: expanding the neurological spectrum and therapeutic approaches. *Eur J Med Genet* 2020;63:104046.
11 Yang H, Yu D. Clinical, biochemical and metabolic characterization of patients with short-chain enoyl-CoA hydratase (ECHS1) deficiency: two case reports and the review of the literature. *BMC Pediatr* 2020;20:1–10.
12 Sato-Shirai I, Ogawa E, Arisaka A, *et al*. Valine-restricted diet for patients with echs1 deficiency: divergent clinical outcomes in two japanese siblings. *Brain Dev* 2021;43:308–13.
13 Richards S, Aziz N, Bale S, *et al*. Standards and guidelines for the interpretation of sequence variants: a joint consensus recommendation of the American College of medical genetics and genomics and the association for molecular pathology. *Genetics in Medicine* 2015;17:405–24.
14 Findlay GM, Daza RM, Martin B, *et al*. Accurate classification of BRCA1 variants with saturation genome editing. *Nature* 2018;562:217–22.
15 Kweon J, Jang A-H, Shin HR, *et al*. A CRISPR-based base-editing screen for the functional assessment of BRCA1 variants. *Oncogene* 2020;39:30–5.
16 D'Annibale OM, Koppes EA, Alodaib AN, *et al*. Characterization of variants of uncertain significance in isovaleryl-coa dehydrogenase identified through newborn screening: an approach for faster analysis. *Mol Genet Metab* 2021;134:29–36.
17 Xia C, Lou B, Fu Z, *et al*. Molecular mechanism of interactions between acad9 and binding partners in mitochondrial respiratory complex i assembly. *IScience* 2021;24:103153.
18 D'Annibale OM, Koppes EA, Sethuraman M, *et al*. Characterization of exonic variants of uncertain significance in very long-chain acyl-CoA dehydrogenase identified through newborn screening. *J Inherit Metab Dis* 2022;45:529–40.
19 Kohda M, Tokuzawa Y, Kishita Y, *et al*. A comprehensive genomic analysis reveals the genetic landscape of mitochondrial respiratory chain complex deficiencies. *PLoS Genet* 2016;12:e1005679.
20 Tadaka S, Katsuoka F, Ueki M, *et al*. 3.5kjpnv2: an allele frequency panel of 3552 japanese individuals including the x chromosome. *Hum Genome Var* 2019;6:28.
21 Tadaka S, Hishinuma E, Komaki S, *et al*. JMorp updates in 2020: large enhancement of multi-omics data resources on the general Japanese population. *Nucleic Acids Res* 2021;49:D536–44.
22 Naito Y, Hino K, Bono H, *et al*. CRISPRdirect: software for designing CRISPR/Cas guide RNA with reduced off-target sites. *Bioinformatics* 2015;31:1120–3.
23 Ran FA, Hsu PD, Wright J, *et al*. Genome engineering using the CRISPR-Cas9 system. *Nat Protoc* 2013;8:2281–308.
24 Borna NN, Kishita Y, Kohda M, *et al*. Mitochondrial ribosomal protein PTCD3 mutations cause oxidative phosphorylation defects with Leigh syndrome. *Neurogenetics* 2019;20:9–25.
25 Brechtmann F, Mertes C, Matusevičiūtė A, *et al*. OUTRIDER: a statistical method for detecting aberrantly expressed genes in rna sequencing data. *Am J Hum Genet* 2018;103:907–17.
26 Uchino S, Iida A, Sato A, *et al*. A novel compound heterozygous variant of *echs1* identified in A japanese patient with leigh syndrome. *Hum Genome Var* 2019;6:19.
27 Robinson BH, Petrova-Benedict R, Buncic JR, *et al*. Nonviability of cells with oxidative defects in galactose medium: a screening test for affected patient fibroblasts. *Biochemical Medicine and Metabolic Biology* 1992;48:122–6.
28 Simon MT, Eftekharian SS, Ferdinandusse S, *et al*. ECHS1 disease in two unrelated families of Samoan descent: common variant-rare disorder. *Am J Med Genet A* 2021;185:157–67.

29 Kuwajima M, Kojima K, Osaka H, *et al*. Valine metabolites analysis in ECHS1 deficiency. *Molecular Genetics and Metabolism Reports* 2021;29:100809.
30 Stenton SL, Zou Y, Cheng H, *et al*. Leigh syndrome: a study of 209 patients at the Beijing children's Hospital. *Ann Neurol* 2022;91:466–82.
31 Lee JS, Yoo T, Lee M, *et al*. Genetic heterogeneity in Leigh syndrome: highlighting treatable and novel genetic causes. *Clin Genet* 2020;97:586–94.
32 Burgin HJ, McKenzie M. Understanding the role of OXPHOS dysfunction in the pathogenesis of ECHS1 deficiency. *FEBS Lett* 2020;594:590–610.
33 Vaca Jacome AS, Rabilloud T, Schaeffer-Reiss C, *et al*. N-terminome analysis of the human mitochondrial proteome. *Proteomics* 2015;15:2519–24.
34 Zhang Y-K, Qu Y-Y, Lin Y, *et al*. Enoyl-Coa hydratase-1 regulates mTOR signaling and apoptosis by sensing nutrients. *Nat Commun* 2017;8:464.
35 Hass GM, Hill RL. The subunit structure of crotonase. *Journal of Biological Chemistry* 1969;244:6080–6.
36 Fong JC, Schulz H. Purification and properties of pig heart crotonase and the presence of short chain and long chain enoyl coenzyme A hydratases in pig and guinea pig tissues. *J Biol Chem* 1977;252:542–7.

BRIEF COMMUNICATION

Novel *ITPA* variants identified by whole genome sequencing and RNA sequencing

Nanako Omichi[1,13], Yoshihito Kishita[1,2,13], Mina Nakama[1,3,4], Hideo Sasai[3,4,5], Atsushi Terazawa[6], Emiko Kobayashi[7], Takuya Fushimi[8], Yohei Sugiyama[8], Keiko Ichimoto[8], Kazuhiro R. Nitta[2], Yukiko Yatsuka[2], Akira Ohtake[9,10], Kei Murayama[2,8,11] and Yasushi Okazaki[2,12]✉

Approximately 80% of rare diseases have a genetic cause, and an accurate genetic diagnosis is necessary for disease management, prognosis prediction, and genetic counseling. Whole-exome sequencing (WES) is a cost-effective approach for exploring the genetic cause, but several cases often remain undiagnosed. We combined whole genome sequencing (WGS) and RNA sequencing (RNA-seq) to identify the pathogenic variants in an unsolved case using WES. RNA-seq revealed aberrant exon 4 and exon 6 splicing of *ITPA*. WGS showed a previously unreported splicing donor variant, c.263+1G>A, and a novel heterozygous deletion, including exon 6. Detailed examination of the breakpoint indicated the deletion caused by recombination between Alu elements in different introns. The proband was found to have developmental and epileptic encephalopathies caused by variants in the *ITPA* gene. The combination of WGS and RNA-seq may be effective in diagnosing conditions in proband who could not be diagnosed using WES.

Journal of Human Genetics (2023) 68:649–652; https://doi.org/10.1038/s10038-023-01156-y

Identifying the differentiating disease based on symptoms and general examination is often difficult in rare intractable diseases. Comprehensive genetic testing is usually essential to make a definitive diagnosis of an incurable disease. In recent years, whole-exome sequencing (WES) and whole-genome sequencing (WGS) have aided in determining the molecular cause of rare and undiagnosed diseases. WES has enabled the diagnosis of conditions in ~35% of the patients [1]. However, the large majority of these patients have undiagnosed conditions. Variants in deep intronic/intergenic regions are usually undetectable because they are not covered by WES. On the contrary, WGS provides comprehensive information on the human genome, including deep intronic/intergenic regions. The technique has been reported to be appropriate for increasing the diagnostic rates of rare disorders [2, 3]. RNA-seq could detect aberrant expression [4], aberrant splicing, and mono-allelic expression, which makes it a powerful method for variant interpretation. We performed WGS and RNA-seq on a case that could not be diagnosed using WES, which revealed a novel splicing variant and a deletion of ~3.4 kb via recombination between two Alu elements in *ITPA*. Variants in *ITPA* are known to cause developmental epileptic encephalopathy 35 (MIM:616647). In addition to neurological symptoms, the family had recurrent episodes of dilated cardiomyopathy caused by *ITPA* deficiency.

The proband (II-3) was the third child of nonconsanguineous parents. She was born at the 39th gestational week via spontaneous vaginal delivery with a birth weight of 2565 g (−1.6 SD), a body length of 48.8 cm (−0.3 SD), and an occipitofrontal circumference of 32.5 cm (−0.6 SD). The Apgar score was 8/9. She had hypotonia, mild feeding difficulties, and refractory epilepsy at birth. At 11 months of age, the proband had not yet acquired a fixed neck. She is now 6 years old and has refractory epilepsy associated with severe developmental delay and requires percutaneous endoscopic gastronomy for nutritional support. Her symptoms are similar to those of dilated cardiomyopathy, with the left ventricular ejection fraction being ~45% that has been stabilized by β-blocker treatment. Her two elder brothers had a similar presentation. The eldest brother was born at 40 weeks of gestational age with a birth weight of 3392 g (0.7 SD). He exhibited myotonia, feeding difficulties, and poor weight gain. Febrile seizures began at 10 months of age, followed by refractory epilepsy at 14 months of age. The second brother was born at 39 weeks of gestational age with a birth weight of 2730 g (−1.1 SD). He was diagnosed with congenital hypotonia at birth and, then at 4 months of age, began having involuntary movements, seizures, and epileptic gaze deviations. Finally, her eldest brother and the second brother died of dilated cardiomyopathy at 5 and 3 years of age, respectively.

[1]Department of Life Science, Faculty of Science and Engineering, Kindai University, Osaka, Japan. [2]Diagnostics and Therapeutic of Intractable Diseases, Intractable Disease Research Center, Graduate School of Medicine, Juntendo University, Tokyo, Japan. [3]Clinical Genetics Center, Gifu University Hospital, Gifu, Japan. [4]Department of Pediatrics, Graduate School of Medicine, Gifu University, Gifu, Japan. [5]Department of Applied Genomics, Kazusa DNA Research Institute, Chiba, Japan. [6]Department of Pediatric Cardiology, Gifu Prefectural General Medical Center, Gifu, Japan. [7]Department of Pediatrics, Gifu Prefectural General Medical Center, Gifu, Japan. [8]Department of Metabolism, Chiba Children's Hospital, Chiba, Japan. [9]Department of Pediatrics and Clinical Genomics, Saitama Medical University, Moroyama, Saitama, Japan. [10]Center for Intractable Diseases, Saitama Medical University Hospital, Moroyama, Saitama, Japan. [11]Center for Medical Genetics, Chiba Children's Hospital, Chiba, Japan. [12]Laboratory for Comprehensive Genomic Analysis, RIKEN Center for Integrative Medical Sciences, Kanagawa, Japan. [13]These authors contributed equally: Nanako Omichi, Yoshihito Kishita.
✉email: ya-okazaki@juntendo.ac.jp

Received: 26 February 2023 Revised: 20 April 2023 Accepted: 21 April 2023
Published online: 29 May 2023

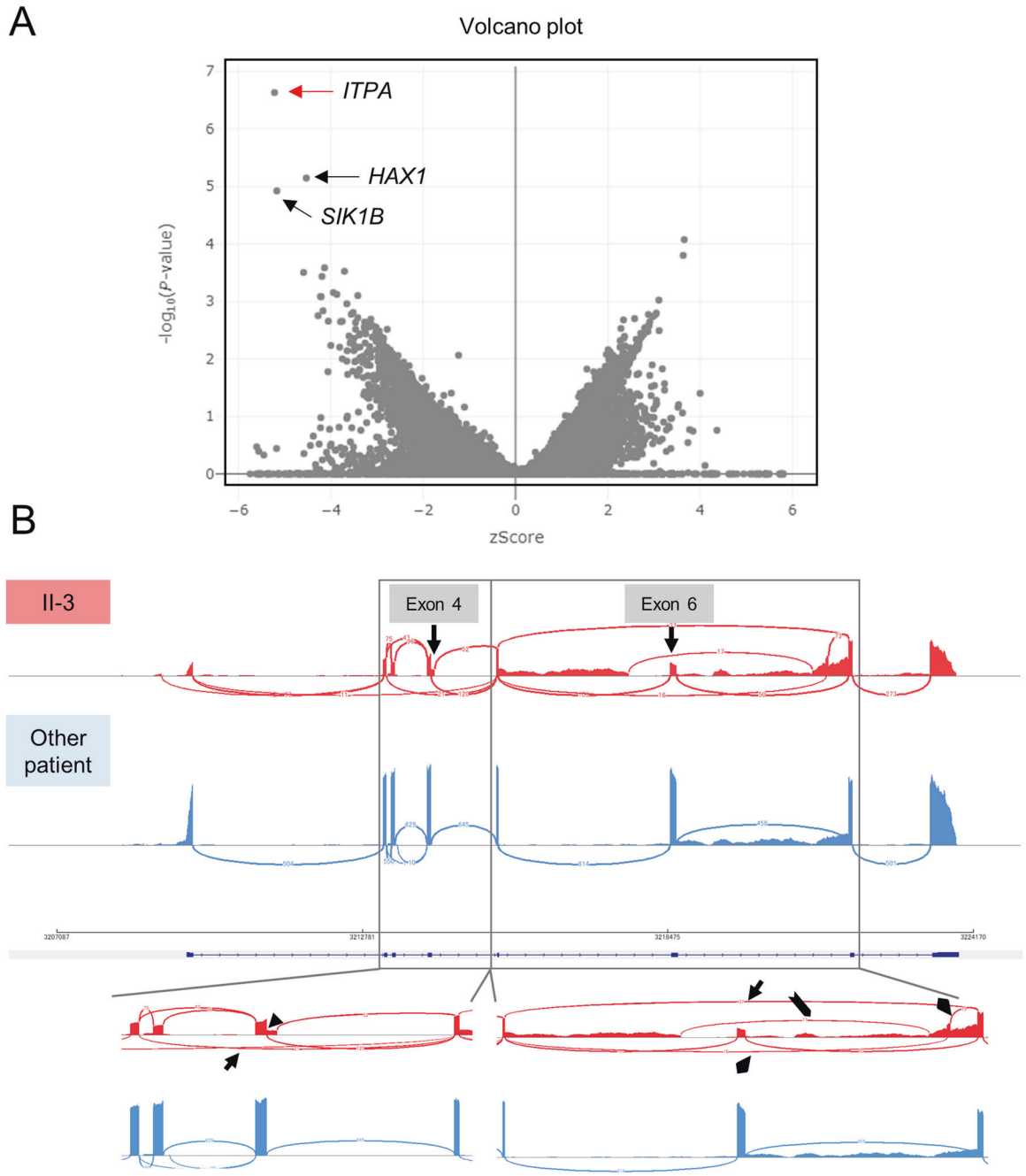

Fig. 1 Abnormal expression of *ITPA* revealed using RNA-seq. **A** Volcano plot at gene level from OUTRIDER analysis. RNA-seq is performed on 35 patients with suspected mitochondrial disease (undiagnosed cases) including the proband. The RNA-seq data of proband was compared with those of 34 cases. We used the patient population as a control and extracted outlier genes by using OUTRIDER software. *ITPA, HAX1* and *SIK1B* were genes that were significantly downregulated. **B** IGV Sashimi plot of RNA-seq data of II-3 and control at the whole *ITPA* gene (upper panel). At the bottom are zoomed-in views of exon 4 and exon 6. The arrows indicate exon skipping, and the arrowhead indicates exon extension. Diamond-shaped arrows indicate abnormal splicing events. The chevron arrow shows the location of the deletion

The disease-causing variants could not be determined by the trio-WES analysis. Initially, we performed RNA-seq using the proband's fibroblast cell (F1431). RNA-seq analysis using OUTRIDER software [4] revealed decreased expression of *ITPA* (Fig. 1A). We first found exon elongation on the 3' side of exon 4 (Fig. 1B), and exon skipping of exon 3 and 4 were detected as well (Fig. 1B and Supplementary Fig. 1). We observed a decrease in the read depth of exon 6 when compared with the other exons (Fig. 1B). In addition to exon 6 depth reduction, exon skipping and several abnormal splicing events were also detected (Fig. 1B). The Sashimi plot revealed skipping of exon 6 and other connections indicating abnormal splicing in the middle of introns (Fig. 1B and Supplementary Fig. 1). By performing reverse transcription-PCR in patient cells with suppressed nonsense-mediated mRNA decay, we found that these aberrant transcripts undergo degradation (Supplementary Fig. 2). A decrease in the expression of *HAX1* and *SIK1B* was also observed (Fig. 1A). The pathogenic heterozygous variant c.256C>T (p.Arg86Ter) in *HAX1* (NM_006118.4) was identified from WGS. *HAX1* has been reported to cause Neutropenia, severe congenital 3, autosomal recessive (MIM: 610738). The blood tests showed mild decrease in neutrophils (1585 cells/μl: neutropenia is defined as less than 1500 cells/μl) that might be caused by the heterozygous variant in *HAX1*. *SIK1B* encodes a putative serine/threonine-protein kinase

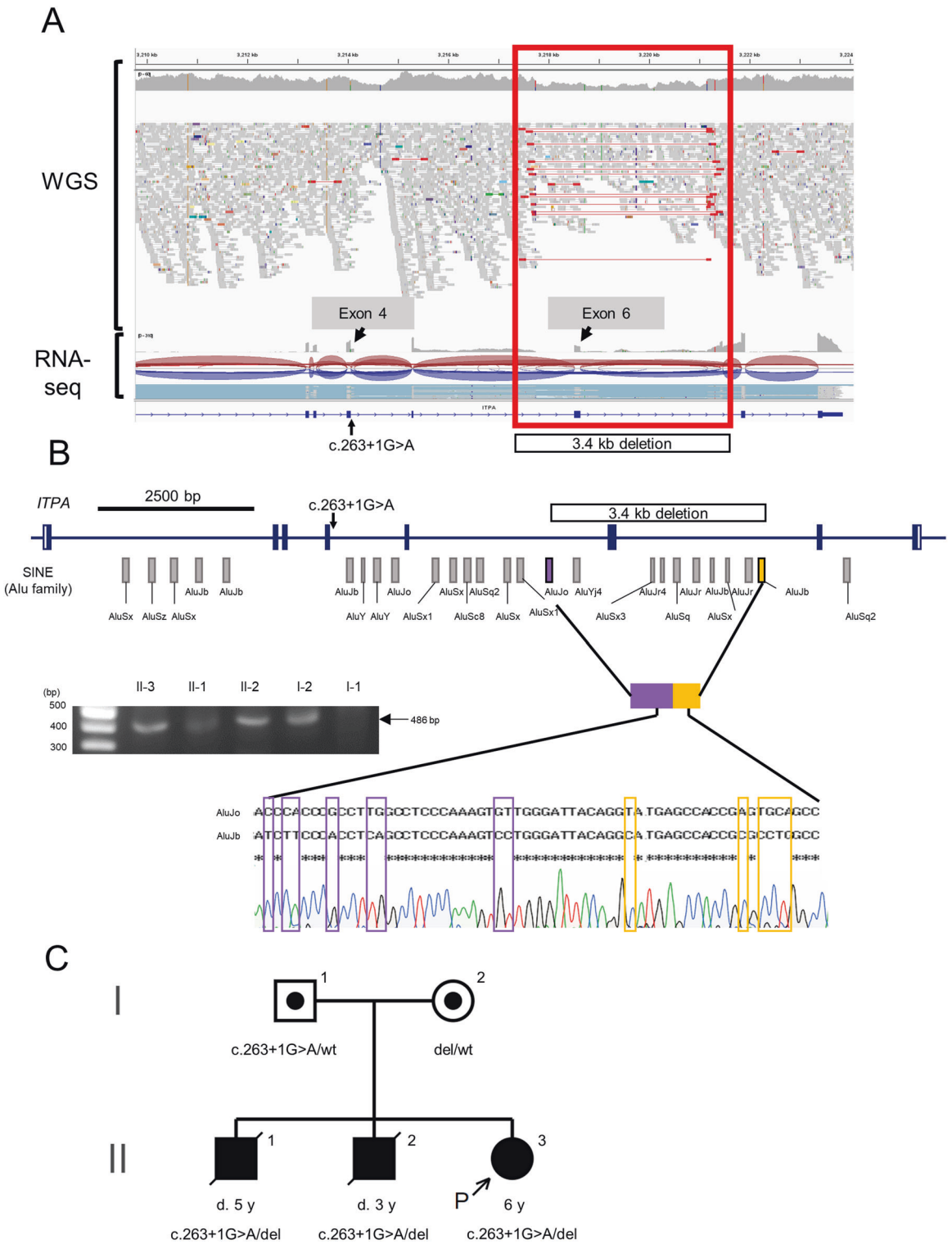

Fig. 2 Variants in *ITPA* revealed using WGS. **A** The deletion around exon 6 is indicated by IGV. Red indicates paired reads in distant regions. **B** The region surrounding exon 6 was amplified using PCR and sequenced using Sanger sequencing. The deletion was probably caused by recombination between AluJo (purple) in intron 5 and AluJb (orange) in intron 6. The Alu sequences were present in a mixed state, with purple derived from AluJo and orange from AluJb. **C** Pedigree of the family. Affected members are indicated with filled symbols. Individuals labeled with dots are carriers. The arrow indicates the index proband

protein, but its function is unknown. No variant in *SIK1B* has been detected by WGS. An association between *ITPA* deficiency and decreased expression of these genes has not been reported to date.

We performed WGS to search for deep intronic and intergenic variants. Analysis of structural variation (SV) and copy number variation (CNV) from the WGS data using Manta and Lumpy identified a heterozygous deletion of 3.4 kbp containing exon 6 (Fig. 2A, B). Furthermore, we found a heterozygous variant c.263+1G>A (NM_033453.4), in *ITPA*, which is likely to be involved in the extension of exon 4. The integrative genomics viewer (IGV)

screen snapshot showed a prominent decrease in depth around intron 5, exon 6, and intron 6. Read pairs showing deletions at the paired-end were also detected.

Trio Sanger sequencing confirmed that c.263+1G>A is of paternal origin (Fig. 2C). The PCR of a deletion region containing exon 6 revealed short fragments in DNA from the proband and the mother, which confirmed NC_000020.11: g.(3217736_3217747)_(3221159_3221170) del. The two elder brothers who died of dilated cardiomyopathy had the same genotype as the proband. To determine the detailed sequence of the breakpoint, PCR fragments were analyzed using Sanger sequencing, which revealed that the deletion was caused by homologous recombination between AluJo and AluJb (Fig. 2B).

We performed a multi-omics analysis for the proband whose condition could not be diagnosed using WES and finally identified compound heterozygous variants in *ITPA*. *ITPA* encodes inosine triphosphate pyrophosphohydrolase (ITPase) that hydrolyzes inosine triphosphate (ITP) and deoxyinosine triphosphate. Variants in *ITPA* cause developmental epileptic encephalopathy 35 (DEE35) [5] or Inosine triphosphatase deficiency [6]. DEE35 is a rare neurodegenerative disease characterized by developmental delay, microcephaly, feeding difficulties, early-onset intractable seizures, subsequent psychomotor retardation, and early childhood fatality [7]. In this family, siblings with *ITPA* mutations have died of dilated cardiomyopathy. Cardiac involvement has been noted in 28.6% of patients with *ITPA* deficiency, and dilated cardiomyopathy is the most common cause of cardiac involvement [7]. Furthermore, dilated cardiomyopathy has been reported in *ITPA* gene-disrupted mouse [8, 9]. Thus, in this proband and her brothers, dilated cardiomyopathy is thought to be caused by variants in *ITPA*. The other clinical features of the proband were consistent with those of DEE35.

Our analysis identified a novel Alu recombination-mediated deletion (ARMD). Deletions due to ARMD have been reported to account for 0.3% of human genetic disorders [10]. To the best of our knowledge, this is the first report of ARMD with DEE35. Such ARMDs are thought to have been missed by previous genetic testing because Alu is present in introns, which are difficult to cover with WES and panel sequencing. We must actively promote genetic testing methodologies to identify Alu-mediated recombination, such as ARMD. A recent study reported that capture-seq and long-read sequencing specifically examine recombination between Alu or L1 [11]. We believe that improving the accuracy of methods for detecting CNV and SV from WGS data and applying techniques to specifically detect transposable elements such as Alu, for the genetic testing of diseases are necessary to improve diagnostic accuracy. RNA-seq enables more effective identification of genes showing aberrant expression and abnormal splicing, which is handy when combined with WGS. In our previous studies, Alu-mediated deletions have been identified using RNA-seq and WGS [12, 13]. These methods should be considered for WES-negative cases to detect pathogenic variants missed by WES.

DATA AVAILABILITY

Raw data are available from the corresponding author upon reasonable request. Some genomic information that could be used to identify individuals cannot be shared due to ethical constraints.

REFERENCES

1. Clark MM, Stark Z, Farnaes L, Tan TY, White SM, Dimmock D, et al. Meta-analysis of the diagnostic and clinical utility of genome and exome sequencing and chromosomal microarray in children with suspected genetic diseases. npj Genom Med. 2018;3:1–10.
2. Kremer LS, Bader DM, Mertes C, Kopajtich R, Pichler G, Iuso A, et al. Genetic diagnosis of Mendelian disorders via RNA sequencing. Nat Commun. 2017;8:1–11.
3. Cummings BB, Marshall JL, Tukiainen T, Lek M, Donkervoort S, Foley AR, et al. Improving genetic diagnosis in Mendelian disease with transcriptome sequencing Genotype-Tissue Expression Consortium. Sci Transl Med. 2016;5209:1–12.
4. Brechtmann F, Mertes C, Matusevičiūtė A, Yépez VA, Avsec Ž, Herzog M, et al. OUTRIDER: a statistical method for detecting aberrantly expressed genes in RNA sequencing data. Am J Hum Genet. 2018;103:907–17.
5. Kevelam SH, Bierau J, Salvarinova R, Agrawal S, Honzik T, Visser D, et al. Recessive ITPA mutations cause an early infantile encephalopathy. Ann Neurol. 2015;78:649–58.
6. Sumi S, Marinaki AM, Arenas M, Fairbanks L, Shobowale-Bakre M, Rees DC, et al. Genetic basis of inosine triphosphate pyrophosphohydrolase deficiency. Hum Genet. 2002;111:360–7.
7. Scala M, Wortmann SB, Kaya N, Stellingwerff MD, Pistorio A, Glamuzina E, et al. Clinico-radiological features, molecular spectrum, and identification of prognostic factors in developmental and epileptic encephalopathy due to inosine triphosphate pyrophosphatase (ITPase) deficiency. Hum Mutat. 2022;43:403–19.
8. Handley MT, Reddy K, Wills J, Rosser E, Kamath A, Halachev M, et al. ITPase deficiency causes a martsolf-like syndrome with a lethal infantile dilated cardiomyopathy. PLoS Genet. 2019;15:1–23.
9. Behmanesh M, Sakumi K, Abolhassani N, Toyokuni S, Oka S, Ohnishi YN, et al. ITPase-deficient mice show growth retardation and die before weaning. Cell Death Differ. 2009;16:1315–22.
10. Kim S, Cho C-S, Han K, Lee J. Structural variation of Alu element and human disease. Genom Inf. 2016;14:70–7.
11. Pascarella G, Hon CC, Hashimoto K, Busch A, Luginbühl J, Parr C, et al. Recombination of repeat elements generates somatic complexity in human genomes. Cell. 2022;185:3025–3040.e6.
12. Kishita Y, Shimura M, Kohda M, Fushimi T, Nitta KR, Yatsuka Y, et al. Genome sequencing and RNA-seq analyses of mitochondrial complex I deficiency revealed Alu insertion-mediated deletion in NDUFV2. Hum Mutat. 2021;42:1422–8.
13. Yépez VA, Gusic M, Kopajtich R, Mertes C, Smith NH, Alston CL, et al. Clinical implementation of RNA sequencing for Mendelian disease diagnostics. Genome Med. 2022;14:1–26.

ACKNOWLEDGEMENTS

We thank the family for their participation in the study.

AUTHOR CONTRIBUTIONS

NO and YK wrote the manuscript. NO and YK performed the experiments. NO, YK, KRN, TF and YY analyzed the data. MN, HS, AT, EK, YS, KI and KM acquired clinical information. YK, AO, KM, and YO supervised the study. All authors discussed the results and commented on the manuscript.

FUNDING

This work was supported by a grant for the Practical Research Project for Rare/Intractable Diseases from AMED to KM, YO, and AO (Fund ID: JP21ek010946, 22ek0109485, JP22ek0109468, JP19ek0109273), Program for Promoting Platform of Genomics based Drug Discovery to YO (Fund ID: JP22kk0305015) and JSPS KAKENHI JP19H03624 to YO.

COMPETING INTERESTS

The authors declare no competing interests.

ETHICS APPROVAL AND CONSENT TO PARTICIPATE

The study was approved by the regional Ethics Committees of Juntendo University, Saitama Medical University, Chiba Children's Hospital, and Kindai University. Written informed consent was obtained from the parents. All methods were performed by relevant guidelines and regulations.

ADDITIONAL INFORMATION

Supplementary information The online version contains supplementary material available at https://doi.org/10.1038/s10038-023-01156-y.

Correspondence and requests for materials should be addressed to Yasushi Okazaki.

Reprints and permission information is available at http://www.nature.com/reprints

Publisher's note Springer Nature remains neutral with regard to jurisdictional claims in published maps and institutional affiliations.

Ⅰ．ミトコンドリア病

1. ミトコンドリア病の遺伝子診断と病態解析

杉山洋平，八塚由紀子，村山　圭，岡﨑康司

ミトコンドリア病はミトコンドリアDNAまたは核DNAの変化によって引き起こされるが，病因遺伝子は非常に多岐にわたる．遺伝子解析において，われわれはこれまでのミトコンドリア病遺伝子パネルシークエンスに加え，マルチオミクス解析を行うことで新規病因遺伝子を明らかにしてきている．令和４年度診療報酬改定でミトコンドリア病の一般的な遺伝学的検査は保険診療の対象となり，マルチオミクス解析などのより複雑な解析が今後重要性を増してくる．

はじめに

ミトコンドリア病は「ミトコンドリア機能およびエネルギー産生不全によってもたらされるさまざまな臨床的障害に対する総称」と現時点では定義できる．ミトコンドリアは細胞内小器官の一つであり，その主要な役割の1つは，ATPとしてエネルギーを生合成することである．そのATP生合成の場が呼吸鎖複合体※1であり，酸化的リン酸化反応によって行われる．これら呼吸鎖複合体酵素の働き，あるいは酸化的リン酸化反応が低下することによって，種々の臓器障害を引き起こす．ミトコンドリアは赤血球以外の細胞に分布するため，その機能異常はあらゆる臓器障害をもたらし，病型が多彩で診断に苦慮する場合も多い[1]．現在ミトコンドリア病の原因遺伝子と判明しているものは400以上にのぼる（**表1**）[2]．遺伝形式は母系遺伝を含めてすべての遺伝形式が存在し，小児では核DNAの遺伝（特に常染色体潜性）が多く，成人ではmtDNAの遺伝（母系遺伝）が多い．近年の診断技術の革新に伴い，ミトコンドリア病と確定診断できる症例が増えてきている．

[略語]
BN-PAGE：blue native polyacrylamide gel electrophoresis（ブルーネイティブポリアクリルアミドゲル電気泳動）
CI：confidence interval（信頼区間）
mtDNA：mitochondrial DNA（ミトコンドリアDNA/ミトコンドリアゲノム）
RNA-seq：RNA-sequence（RNAシークエンス）
TCA回路：tricarboxylic acid cycle（トリカルボン酸回路）
WES：whole exome sequence（全エクソームシークエンス）
WGS：whole genome sequence（全ゲノムシークエンス）

Genetic diagnosis and pathological analysis of mitochondrial diseases
Yohei Sugiyama[1] /Yukiko Yatsuka[2] /Kei Murayama[1] /Yasushi Okazaki[2] ：Center for Medical Genetics, Department of Metabolism, Chiba children's Hospital[1] /Diagnostics and Therapeutics of Intractable Diseases, Intractable Disease Research Center, Graduate School of Medicine, Juntendo University[2]（千葉県こども病院遺伝診療センター・代謝科[1] /順天堂大学難病の診断と治療研究センター・難治性疾患診断・治療学[2]）

表1　ミトコンドリア病の病因遺伝子

OXPHOS 関連遺伝子

OXPHOS サブユニット

CⅠ	CⅡ	CⅢ	CⅣ	CⅤ
MT-ND1	NDUFB3	SDHA	MT-CYB	MT-CO1	MT-ATP6
MT-ND2	NDUFB8	SDHB	CYC1	MT-CO2	MT-ATP8
MT-ND3	NDUFB9	SDHD	UQCRB	MT-CO3	ATP5F1A
MT-ND4	NDUFB10		UQCRC2	COX4I1	ATP5F1D
MT-ND4L	NDUFB11		UQCRQ	COX4I2	ATP5F1E
MT-ND5	NDUFS1			COX5A	
MT-ND6	NDUFS2			COX6A1	
NDUFA1	NDUFS3			COX6B1	
NDUFA2	NDUFS4			COX7B	
NDUFA6	NDUFS6			COX8A	
NDUFA8	NDUFS7			NDUFA4	
NDUFA9	NDUFS8				
NDUFA10	NDUFV1				
NDUFA11	NDUFV2				
NDUFA12					
NDUFA13					

電子担体

CoQ	Cyt. c
COQ2	CYCS
COQ4	HCCS
COQ5	
COQ6	
COQ7	
COQ8A	
COQ8B	
COQ9	
PDSS1	
PDSS2	

mtDNA ホメオスタシス

DNA2
MGME1
POLG
POLG2
RNASEH1
SSBP1
TFAM
TWNK
TOP3A

ヌクレオチドプール

ABAT
DGUOK
MPV17
RRM2B
SAMHD1

mt-tRNA 生合成 / アミノアシル化

MT-TA	GTPBP3	AARS2
MT-TC	MTFMT	CARS2
MT-TD	MTO1	DARS2
MT-TE	NSUN3	EARS2
MT-TF	PUS1	FARS2
MT-TG	QRSL1	GARS
MT-TH	TRIT1	GATB
MT-TI	TRMT5	GATC
MT-TK	TRMU	HARS2
MT-TL1	TRNT1	IARS2
MT-TL2		KARS
MT-TM		LARS2
MT-TN		MARS2
MT-TP		NARS2
MT-TQ		PARS2
MT-TR		RARS2
MT-TS1		SARS2
MT-TS2		TARS2
MT-TT		VARS2
MT-TV		WARS2
MT-TW		YARS2
MT-TY		

ミトリボソーム生合成

MT-RNR1
ERAL1
MRPL3
MRPL12
MRPL44
MRPS2
MRPS7
MRPS14
MRPS16
MRPS22
MRPS23
MRPS28
MRPS34
PTCD3

OXPHOS アセンブリ因子

CⅠ	CⅡ	CⅢ	CⅣ	CⅤ
ACAD9	SDHAF1	BCS1L	COA3	COX20	ATPAF2
FOXRED1		LYRM7	COA5	PET100	TMEM70
NDUFAF1		TTC19	COA6	PET117	
NDUFAF2		UQCC2	COA7	SCO1	
NDUFAF3		UQCC3	COX10	SCO2	
NDUFAF4			COX14	SURF1	
NDUFAF5			COX15		
NDUFAF6					
NDUFAF8					
NUBPL					
TIMMDC1					
TMEM126B					

mtRNA 発現 / プロセッシング

ELAC2
FASTKD2
HSD17B10
LRPPRC
MRM2
MTPAP
PNPT1
TRMT10C

翻訳

C12orf65
GFM1
GFM2
RMND1
TACO1
TSFM
TUFM

279　核遺伝子
36　ミトコンドリア遺伝子

二次的に OXPHOS に影響する遺伝子

Fe-S クラスター生合成	補酵素	品質管理	蛋白輸送 / プロセッシング	ミトコンドリア形態
ABCB7	COASY	AFG3L2	AGK	CHCHD10
BOLA3	FLAD1	CLPB	AIFM1	C19orf70
FDX1L	FDX1L	CLPP	DNAJC19	DNM1L
FDXR	LIPT1	HSPD1	GFER	GDAP1
FXN	LIPT2	LONP1	MIPEP	MFF
GLRX5	PANK2	SPG7	PIMD1	MFN2
IBA57	TPK1	YME1L1	PITRM1	MSTO1
ISCA1			PMPCA	NME3
ISCA2	脂質修飾 / ホメオスタシス		PMPCB	OPA1
ISCU	ATAD3A	PNPLA8	TIMM8A	OXA1L
LYRM4	CHKB	SERAC1	TIMM22	SACS
NFS1	PLA2G6	TAZ	TIMM50	SLC25A46
NFU1	PNPLA4		XPNPEP3	STAT2
代謝産物輸送	TCA サイクル	毒性化合物代謝		TRAK1
SLC19A2	ACO2	MDH2	D2HGDH	
SLC19A3	ALDH18A1	MECR	ECHS1	
SLC25A1	DLAT	NADK2	ETHE1	
SLC25A3	DLD	PC	HIBCH	
SLC25A4	FH	PDHA1	L2HGDH	
SLC25A12	HAAO	PDHB	NAXE	
SLC25A19	IDH3A	PDHX	TXN2	
SLC25A24	IDH3B	PDK3	機序不明	
SLC25A26	KYNU	PDP1	APOPT1	OPA3
SLC25A32	MDH1	PPA2	CEP89	RTN4IP1
SLC25A42			C19orf12	SFXN4
SLC39A8			C1QBP	TMEM65
アポトーシス / オートファジー			FBXL4	IARS
MICU1		HTRA2	SQOR	SOD2
MICU2		VPS13C		
MPC1				

網掛けはわれわれが初めて報告したもの．文献2を参考にして作成．

1 ミトコンドリア病診断の現状

ミトコンドリア病の診断は，まずは病歴，診察所見，代謝スクリーニング検査結果などから疑うことが出発点となる．続いて，ミトコンドリア機能異常を証明するための特殊検査（呼吸鎖複合体酵素の活性やタンパク質の評価，酸素消費量，ATP産生能，生検試料を用いた病理検査など）を行う．しかしながら，病因に応じた治療や予後予測，正確な診断に基づいた遺伝カウンセリングのためには遺伝学的検査が必要となる．次世代シークエンサーの普及以降，生化学検査単独では二次的なミトコンドリア機能障害を否定することができない場合があり，genetics-firstな診断アルゴリズムに見直される傾向にあるが[3]，新規病因遺伝子やバリアントの病原性を証明するためには，生化学検査が必要不可欠である．

そのため，ミトコンドリア病の早期確定診断には，侵襲性を考慮しながら適切な組織検体を採取し，遺伝学的検査も含めた，包括的な検査を行うことが重要である．ミトコンドリア病の特徴として組織特異性があるため，検体は罹患臓器を用いるのが理想である．しかし，患者の侵襲を考慮して皮膚生検由来の線維芽細

※1　呼吸鎖複合体
好気的呼吸のエネルギー産生の場であるミトコンドリア内膜に存在し，酸化還元反応によるATP産生を行う酵素群のこと．呼吸鎖複合体Ⅰ，Ⅱ，Ⅲ，Ⅳまで存在し，ATP合成酵素を呼吸鎖複合体Ⅴとすることもある．

表2　ミトコンドリア病の原因遺伝子に合わせた特異的治療法

疾患名	原因遺伝子	治療	治療効果
Brown-Vialetto-Van Laere症候群/Fazio-Londe症候群（難聴など）	*SLC52A2, SLC52A3, SLC52A1*	リボフラビン（経口：10～50 mg/kg/day）	良好
ビオチン反応性基底核症（Leigh）	*SLC19A3*	チアミン（経口：10～20 mg/kg/day），ビオチン（経口：10～15 mg/kg/day）	良好
ビオチニダーゼ欠損症（脳筋症）	*BTD*	ビオチン（経口：5～10 mg/kg/day）	良好
ホロカルボキシラーゼ合成酵素欠損症（新生児Mito）	*HLCS*	ビオチン（経口：10～20 mg/kg/day）	不安定だが良好
チアミンピロホスホキナーゼ欠損症（脳症）	*TPK1*	チアミン（経口：20 mg/kg/day）	不安定（これまで10名以上に投与）
ACAD9欠損症（脳筋症）	*ACAD9*	リボフラビン（経口：10～20 mg/kg/day）	不安定
マルチプルアシルCoA脱水素酵素欠損症（乳児Mito）	*ETFA, ETFB, ETFDH, SLC25A32, FLAD1*	リボフラビン（経口：10 mg/kg/day）	良好
チアミン反応性PDHC欠損症（Leigh）	*PDHA1*	リボフラビン（経口：30～40 mg/kg/day）	不安定
コエンザイムQ10欠損症（腎症，脳筋症）	*PDSS1, PDSS2, COQ2, COQ4, COQ6, COQ7, ADCK3, ADCK4, COQ9*	コエンザイムQ10（経口：10～30 mg/kg/day）	とても不安定（異常がなにかに依る）
シトクロムc酸化酵素欠損症（Leigh他）	*SCO2, COA6*	ヒスチジン銅（投与量不明；500 mgの皮下注射が提案されている）	不明，SCO2異常症一名のみに投与
モリブデン補酵素欠損症（新生児Mito）	*MOCS1, MOCS2, GPHN*	環状ピラノプテリンモノホスファート（静脈注射：80～320 mg/kg/day）	タイプAのモリブデン補酵素欠損症に対して良好
3-ヒドロキシイソ酪酸-CoA加水分解酵素欠損症（Leigh）	*HIBCH*	バリン制限食	不明，数名にのみ投与
エノイルCoAヒドラターゼ欠損症（Leigh）	*ECHS1*	バリン制限食	不明，数名にのみ投与
チオレドキシン2欠損症（脳症）	*TXN2*	抗酸化療法（例：イデベノン20 mg/kg/day）	明らかに良好（患者は一名のみ）
エチルマロン酸脳症（新生児Mito）	*ETHE1*	メトロニダゾール，*N*-アセチル-システイン（グルタチオン前駆体），肝臓移植	不安定

赤字はわれわれの遺伝子解析でも見つかっている遺伝子異常．文献4より引用（ただし赤字への変更は著者らによる）．

胞を使用することも多い．呼吸鎖酵素活性の評価では，各呼吸鎖複合体の酵素欠損症や，複数の酵素の活性が同時に低下する疾患を見出すことができる．ウエスタンブロット法は呼吸鎖酵素の構成タンパク質の量的低下の評価において，Blue Native電気泳動（BN-PAGE解析）は呼吸鎖複合体の量的・質的評価においてそれぞれ有用である．皮膚線維芽細胞を用いた酸素消費量解析では，生きた細胞を用いてリアルタイムに測定を行え，酵素活性よりも鋭敏にミトコンドリア障害を判別できる．

近年，遺伝子診断によって病態が解明され，治療可能なミトコンドリア病があり（表2）[4]，補酵素代謝異常を伴うミトコンドリア病は，この種の治療可能な疾患の大部分を占めている．したがってできるだけ早期に遺伝子診断を行うことがますます重要になってきている．

核DNA・mtDNAも含めた遺伝子の種類を分類すると，以下のようになる[2) 5)]．

① 各呼吸鎖酵素複合体のサブユニットの異常やアセンブリー因子の異常
② mtDNAおよびそれに関係するRNAやタンパク質合成の異常
③ 呼吸鎖の上流反応にあたる，基質産生の異常（TCA回路や脂肪酸酸化など）
④ 呼吸鎖に関連する補因子（cofactor）の異常
⑤ ミトコンドリアのホメオスタシスの異常（ミトコンドリアの分裂・融合など）
⑥ 呼吸鎖に対する阻害物質の産生

乳児・小児ミトコンドリア病の遺伝子検査に関しては，mtDNAおよび核DNAを含む包括的遺伝子解析※2が必要な場合が多い．本邦でも2016年に神田らが日本人ミトコンドリア病140超例の包括的遺伝子解析の報告をしている[6]．さらにLeigh脳症やミトコンドリア肝症など比較的候補遺伝子がある程度絞られる場合は遺伝子パネルを用いることがある．一部のミトコンドリア病に関して，その病態を踏まえた特異的な治療法が行われており，核遺伝子も含めた包括的遺伝子検査の重要性が，年々重要になってきている．

2 世界での遺伝子診断やミトコンドリア病バイオバンクレジストリの動向

オーストラリアではultra-rapid exome sequencingとよばれる，単一遺伝子の異常が疑われる重症な小児に対して迅速に遺伝学的な診断に迫る研究が公的な医療システムで行われた[7]．このシステムでは，サンプル受領から結果報告までの平均時間は3.3日（95％ CI, 3.2～3.5日）であった．また診断のついた症例の76％，診断のつかなかった症例の11％で臨床上での管理方針に影響を与えたと考えられた．

また，ドイツでは2009年からGerman Network for Mitochondrial Diseases（mitoNET）が，ドイツ連邦教育研究省の資金援助で運用されている．この団体は，特に患者登録とバイオバンクを運営し，ミトコンドリア病の自然史に関する研究を行っており，1,700人以上の患者さんのデータが登録されている[8]．

さらにEUが資金提供するプロジェクトGENOMITでは，国際的なデータ収集のためのグローバルミトコンドリア病レジストリが開設されている．現在GENOMITにはドイツ，オーストリア，フランス，イタリア，英国，米国そして日本がグローバルパートナーとして参画している[9]．

ミトコンドリア病は，日本や欧米諸国では出生5,000人に1人の割合で発生するといわれている[10) 11)]．しかし，ある特定の遺伝子に関連した症例は，日本全国で1人か数人であり，超希少疾患といえる．したがって，ミトコンドリア病研究において，遺伝子探索，病態解明，創薬，レジストリなどさまざまな面で国際協力がきわめて重要である．この種のレジストリ登録により，多数の患者を対象としたミトコンドリア病の表現型および遺伝子型スペクトルに関する新たな洞察を得ることができ，臨床試験への参加に関して適切な患者に迅速に連絡することが可能になる．さらに，定期的なフォローアップによって疾患の自然史をモニターすることは，緊急に必要とされる無作為化治療試験の計画にとって非常に重要である．また，前述のような国際連携を進めるとともに，国内でのミトコンドリア病の各種病態の認知を上げ，診断体制を整え，診断の質を向上させ，幅を広げていくことが同時に重要である．われわれはミトコンドリア病診療マニュアルの改訂を行うとともに，国内で新生児や小児のミトコンドリア病の症例登録システムを構築している（J-MO Bank）[12]．臨床・生化学・遺伝学的データを共有し，原因遺伝子の特定や創薬につなげるため，これらのシステムを発展させ，欧米の研究者もアクセス可能なグローバルなミトコンドリア病症例登録の構築を計画している．さらに，国立精神・神経医療研究センターにおいて，成人のミトコンドリア病レジストリを構築する予定である．

> **※2　包括的遺伝子解析**
> 従来の遺伝子解析であるmtDNA全周解析，ミトコンドリア病遺伝子パネル検査に加え，RNAシーケシング，全エクソーム解析/全ゲノム解析，プロテオーム解析などの多階層オミクス技術を用い，病因遺伝子を探っていく手法．詳細についてはわれわれの実施した研究課題（https://kaken.nii.ac.jp/ja/grant/KAKENHI-PROJECT-19H03624/）も参照してほしい．

3 ミトコンドリア病の遺伝子診断

本項ではわれわれの研究グループ（千葉県こども病院・埼玉医科大学・順天堂大学）において実際に行っているミトコンドリア病の遺伝子診断を紹介する．

ミトコンドリア病研究の長年にわたる成果として国内最大規模のミトコンドリア病患者コホートを有し，全国の病院施設から紹介されるミトコンドリア病疑い症例は年々増加傾向にある．各症例の臨床情報・検体受付状況・DNA/RNAサンプルの情報・生化学診断や遺伝子診断の結果等が一覧できる研究用匿名化データベースが完成しており，3施設間でスムーズな情報連携を図っている．

年間200件ほどのミトコンドリア病疑い症例の診断依頼を受け入れ，これまでの解析件数はWGS＝228症例，WES＝707症例，ミトコンドリア病遺伝子パネルシークエンス＝954症例にものぼる．また，新規原因遺伝子の報告は通算13遺伝子を数え，近年はマルチオミクス解析（WGS＋RNA-seq＋Proteome）においても着実に成果を出している．

ミトコンドリアゲノムは母親から遺伝することから，“ミトコンドリア病＝母系遺伝”と誤解されることがあるが，ミトコンドリア病の発症にはミトコンドリア内に存在するミトコンドリアゲノム（mtDNA）と核にコードされたミトコンドリア病原因遺伝子との両方がかかわっている．つまり，ミトコンドリア病の遺伝子診断を行うにはmtDNAと核遺伝子の両方を調べる必要がある．また，発症時期による差異も明らかになってきており，新生児期/小児期発症のミトコンドリア病では核遺伝子に変異を認める常染色体潜性遺伝の症例が多い[13]．われわれの研究グループはミトコンドリア病のなかでも特に新生児期/小児期発症のミトコンドリア病に焦点をあてて研究を進めてきたことから多数の核遺伝子異常を明らかにしており，そのことが新規原因遺伝子の報告にもつながっている．

4 ミトコンドリア病遺伝子パネルシークエンス

ミトコンドリア病疑い症例の遺伝子解析をはじめるにあたり，まず最初にミトコンドリア病遺伝子パネルシークエンスを行っている．順天堂大学難病の診断と治療研究センターでは，核ゲノムにコードされた既知のミトコンドリア病原因遺伝子（合計367遺伝子）とmtDNA全周の両方を1回の実験で調べることができる解析システムを開発し，運用してきた．本解析システムはターゲットキャプチャー方式を採用しているため（アンプリコン方式では検出が難しい）mtDNAの数kb単位の単一欠失を正確なブレイクポイントとともに検出することが可能である．本解析システムを稼働した2020年1月から現在までの解析結果を集計し，図に示した．

1）解析対象

ミトコンドリア病の疑いがある0～64歳の合計449症例（499サンプル）について解析を行った．他の遺伝学的検査と同様，主に血液由来DNA（72.9％）が使用されるが，mtDNA変異を疑う症例においては罹患臓器のDNAの他に尿沈渣DNA（11.2％）の使用も非常に有用である（図右下）．尿沈渣DNAの有用性については別資料に詳しく記載してあるので参考にしていただきたい[14]．

2）解析結果

449症例に対してミトコンドリア病遺伝子パネルシークエンスを行い，98症例の遺伝子診断が確定した．その内訳は核遺伝子に病的バリアントを認めた症例が合計38（8％），mtDNAにMitomap-Cfrmバリアント（MITOMAP[15]に検証済と登録されている疾患関連バリアント）を認めた症例が合計60（13％），mtDNAに単一欠失を認めた症例が合計7（2％）であった（図左上・右上）．また，年齢別に集計すると核遺伝子に病的バリアントを認めた症例は0～1カ月齢が合計16症例と最も多く，次いで1カ月齢～1歳が合計13症例であった（図左下）．この集計結果から核遺伝子に異常をもつ常染色体潜性遺伝形式のミトコンドリア病は新生児期/小児期発症のより重篤なタイプのミトコンドリア病であることが読みとれる．

5 マルチオミクス解析

前述のミトコンドリア病遺伝子パネルシークエンスやWESで解決しなかった症例に対しては，WGS・RNA-seq・Proteome等を行って横断的にデータを精査するマルチオミクス※3解析へと入っていく．ただし，これらの追加解析は全例に対して行われるわけではない．その年度の獲得研究費に応じた実施計画が立てられるため自ずと解析数には上限が発生する．①臨床症状および生化学診断からミトコンドリア病である可能性が高く，②解析に堪え得る高品質サンプルが準備可能である（例えば皮膚線維芽細胞樹立済），等を判断材料として進めていくことになる．

われわれはマルチオミクス解析によって遺伝子異常が明らかになり，遺伝子診断確定に至った症例を多数経験しているが[16]～[19]，ここでは2021年にHuman Mutation誌に発表した*NDUFV2*遺伝子異常をもつ症例[18]を紹介する．当該症例は生化学的にミトコンドリア呼吸鎖Ⅰ活性低下の診断が付され，臨床的にもミトコンドリア病に特徴的な中枢神経症状と先天性高乳酸血症を呈していた．WESでミトコンドリア呼吸鎖Ⅰ複合体のサブユニットである*NDUFV2*にヘテロ接合型のアミノ酸置換バリアントが1つ検出されたため，常染色体潜性遺伝を想定し，対立アレルの遺伝子異常を明らかにする目的でマルチオミクス解析が施行された．その結果，ミトコンドリア病の原因としては世界初の報告となる，Alu因子（レトロトランスポゾンの1種）を介した非常に珍しい遺伝子欠失が同定され，本症例の遺伝子診断が確定するとともにミトコンドリア病の遺伝子診断におけるマルチオミクス解析の重要性が示された．この症例を契機にわれわれのミトコンドリア病コホートのなかから，その後4例のAlu因子を介した挿入や欠失による異常が見つかっている．

※3 マルチオミクス解析
Multi（多数の）とOmics（オミクス）を組合わせた造語であり，人体の機能を司るさまざまな生体物質（DNA，RNA，タンパク質，代謝物など）を包括的に分析する手法を指している．

A. 核遺伝子	症例数
PDHA1	8
COQ4, ECHS1	3
FBXL4, NDUFA4, QRSL1	2
ACAD9, AGK, AIFM1, DNM1L, EARS2, HSD17B10, IARS2, LARS, NAXE, NDUFAF6, OPA1, POLG, SCO2, SLC25A13 SUCLG1, SURF1, TARS2, TOP3A	1
合計	38

B. Mitomap-Cfrm		症例数
3,243	A＞G	28
13,513	G＞A	6
8,993	T＞G	4
14,487	T＞C	3
8,344	A＞G	3
1,555	A＞G	2
1,644	G＞A	2
8,851	T＞C	2
11,778	G＞A	2
14,453	G＞A	2
14,459	G＞A	2
4,300	A＞G	1
9,176	T＞C	1
9,185	T＞C	1
14,674	T＞C	1
合計		60

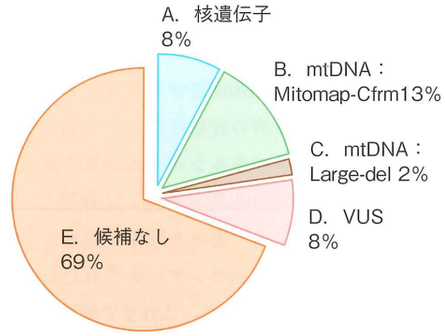

	解析数	%
血液	364	72.9
尿沈渣	56	11.2
皮膚線維芽細胞	23	4.6
心筋	19	3.8
筋肉	18	3.6
肝臓	13	2.6
腎臓	4	0.8
唾液	2	0.4
合計	499	

Age	0-1m	＞1m	＞1y	＞6y	＞20y	N/A
Nuclear gene（38）	16	13	7	2	0	0
mtDNA：Mitomap-Cfrm（60）	12	11	10	6	15	6
mtDNA：Large-del（7）	2	1	0	4	0	0
VUS（173）	16	5	7	3	4	0

図 ミトコンドリア病遺伝子パネルシーケンス
2020.01～2022.11集計，449症例（499サンプル）．

おわりに―今後の展望

令和4年度診療報酬改定でミトコンドリア病の遺伝学的検査が保険診療の対象となった．順天堂大学では4で述べた遺伝子パネルシークエンスを順天堂医院の臨床検査部（ISO15189認定取得）に移管し，保険診療としてスタートすべく着々と準備を進めている．他の病院施設や各臨床検査センターもそれぞれ対応を検討していると聞き及んでいる．これまで研究の範疇で行ってきた遺伝子パネルシークエンスが保険診療に切り替わるとともにミトコンドリア病の遺伝子解析を行う基礎・医学研究者にはより高度で複雑な解析への貢献が期待される．マルチオミクス解析までもが社会実装される将来をめざして日々の研究に精進したいと思う．

文献

1）「ミトコンドリア病診療マニュアル2017」（日本ミトコンドリア学会編集），診断と治療社，2017
2）Murayama K, et al：J Hum Genet, 64：113-125, 2019
3）Gusic M & Prokisch H：FEBS Lett, 595：1132-1158, 2021
4）Distelmaier F, et al：Brain, 140：e11, 2017
5）Mayr JA, et al：J Inherit Metab Dis, 38：629-640, 2015
6）Kohda M, et al：PLoS Genet, 12：e1005679, 2016
7）Lunke S, et al：JAMA, 323：2503-2511, 2020
8）mitoNET https://www.mitonet.org/（2022年12月閲覧）
9）GENOMIT https://genomit.eu/index.html（2022年12月閲覧）
10）Skladal D, et al：Brain, 126：1905-1912, 2003
11）Yamazaki T, et al：Pediatr Int, 56：180-187, 2014
12）J-MO Bank ホームページ http://mo-bank.com/index.html（2022年12月閲覧）
13）Goldstein AC, et al：Neurotherapeutics, 10：212-226, 2013
14）八塚由紀子：ミトコンドリアDNA変異と遺伝子診断の実際，小児内科，54：559-562，2022
15）MITOMAP https://www.mitomap.org/MITOMAP（2022年12月閲覧）
16）Borna NN, et al：Neurogenetics, 20：9-25, 2019
17）Frazier AE, et al：Med (N Y), 2：49-73, 2021
18）Kishita Y, et al：Hum Mutat, 42：1422-1428, 2021
19）Yépez VA, et al：Genome Med, 14：38, 2022

＜著者プロフィール＞

村山　圭：千葉県こども病院遺伝診療センターセンター長，同病院代謝科部長．1997年秋田大学医学部卒業，'97年千葉大学医学部小児科入局，その後小児科代謝グループ所属，2005年千葉県こども病院代謝科医長，'06年千葉大学大学院医学研究院小児病態学博士課程修了，'06年Melbourne Royal Children's Hospital, Murdoc Childrens Research Institute短期留学，'13年千葉県こども病院代謝科および千葉県がんセンター研究所主任医長，'14年千葉県こども病院代謝科部長，'14年Helmholtz Zentrum in Munich, Human Genetics短期研修，'18年千葉県こども病院遺伝診療センターセンター長（代謝科と兼任）．私たちはミトコンドリア病の診療全般から，分子遺伝学的診断，病態解明，治療薬開発まで包括的にとり組んでいます．

岡崎康司：順天堂大学大学院医学研究科教授．同大学難病の診断と治療研究センター長．1986年，岡山大学医学部卒業．大阪大学大学院医学研究科博士課程修了後，理化学研究所へ．2003年，埼玉医科大学教授，その後同大学ゲノム医学研究センター所長．'16年，理化学研究所ライフサイエンス技術基盤研究センターゲノムネットワーク解析支援施設長兼任．'17年，順天堂大学大学院医学研究科教授．同大学難病の診断と治療研究センター長．'19年，理化学研究所応用ゲノム解析技術研究チームチームリーダー兼任．

生体の科学　74(5)：410-411，2023

特集　代謝　Ⅰ．代謝と臓器・疾患

ミトコンドリア病の病態解明と治療法の開発

八塚　由紀子　　岡崎　康司

Yatsuka Yukiko, Okazaki Yasushi：順天堂大学大学院医学研究科難治性疾患診断・治療学講座

Key words：ミトコンドリア病，呼吸鎖複合体，マルチオミクス解析，5-アミノレブリン酸(5-ALA)，ピロールイミダゾールポリアミド(PIポリアミド)

ミトコンドリア病とはミトコンドリアの機能低下によって発症する疾患の総称である。発症時期が新生児期～成人期と広く，臨床症状や遺伝形式も多岐にわたる。そして，ミトコンドリアDNAと核DNAのいずれに存在する遺伝子変異も発症の原因となり得る[1]。このように，臨床的にも遺伝的にも診断が非常に難しい疾患ではあるが，筆者らは，生化学診断とゲノム解析を組合せることによる体系的な病態解明と有効な治療法の開発に取り組んでいる。

ミトコンドリアは細胞が必要とするエネルギー(アデノシン三リン酸；ATP)の95%を産生しており，ミトコンドリアの機能低下はエネルギー不足に直結する。ゆえにミトコンドリア病では，エネルギー需要の高い組織(脳，神経，心筋，骨格筋など)に異常を来すことが多い。ミトコンドリア病を疑った際には，ミトコンドリアの機能異常を証明するための生化学的な特殊検査および遺伝学的検査を行う。次世代シークエンサーの普及以降，遺伝学的検査を先行する“genetic-first”な診断フローが選択される場面が増えたが，病態解明のためには生化学的検査と遺伝学的検査の両方が必要不可欠である。

ミトコンドリア病の診断と病態

先天代謝異常症(ミトコンドリア病を含む)を疑った際には一般生化学検査，アミノ酸分析，尿中有機酸分析，アシルカルニチン分析などのスクリーニング検査から開始し，次いでミトコンドリア病を明らかにするための生化学的検査として，ミトコンドリアの呼吸鎖酵素活性の評価，Blue Native PAGE/ウェスタンブロット法による呼吸鎖複合体構成タンパク質の量的・質的低下の評価，患者由来皮膚線維芽細胞を用いた酸素消費量測定の評価などが行われる。一方でミトコンドリア病の遺伝学的検査としては，まず遺伝子パネルシークエンス[筆者らは核DNAのミトコンドリア病原因遺伝子367個とミトコンドリアDNA(mtDNA)全周16.6 kbを一括で解析している]を行い，遺伝子診断が不十分である場合には全ゲノムシークエンス，RNAシークエンス，プロテオームなどによるマルチオミクス解析に入っていく。

ミトコンドリア病の病態を遺伝子異常から大別すると，①呼吸鎖複合体の異常，②mtDNAおよびそれに関連するRNAやタンパク質合成の異常，③TCAサイクルや脂肪酸β酸化などの基質産生異常，④ミトコンドリアの分裂・融合異常，⑤呼吸鎖に対する阻害物質の産生，となり，各遺伝子異常に対応した治療法の開発が期待されるが，現時点では有効な根治療法がなく対症療法にとどまる。

ミトコンドリア病の治療薬

ミトコンドリア病の治療薬として承認されている薬剤は欧州ではイデベノン(レーベル遺伝性視神経症)，わが国ではタウリン(MELAS症候群)のみである。現在開発中の治療薬としては，5-アミノレブリン酸(5-ALA)とクエン酸第一鉄ナトリウム(SFC)の組合せ使用，mtDNAを標的とするピロールイミダゾールポリアミド(PIポリアミド)，既存薬とは異なる作用機序が期待される新規化合物mitochonic acid-5(MA-5)，パーキンソン病の治療薬であるアポモルフィンのミトコンドリア病への適応拡大，などがある。治験に関する公開情報がわかりやすくまとめられたページがある(https://genex.co.jp/clinical_trial_mitochondrial_disease/)。

0370-9531/10/¥500/ 論文/JCOPY

以下，5-ALA＋SFCとPIポリアミドの開発状況について紹介する。

5-ALA：体内に存在するアミノ酸の一種で，ミトコンドリア内ではヘムとして呼吸鎖複合体Ⅱ，Ⅲ，ⅣおよびシトクロムCを構成するエネルギー代謝に必須の物質である。経口投与後は上部消化管でほぼすべて吸収され全身に分布し，血液脳関門をも通過するという優れた体内動態をとる。培養細胞に対する5-ALA＋SFC投与実験において，ヒト正常皮膚線維芽細胞では呼吸鎖複合体Ⅰ，Ⅱ，Ⅲ，Ⅳの代表的サブユニットの遺伝子発現量に用量依存的な増加，更にLeigh脳症患者由来の複数症例の皮膚線維芽細胞では，最大酸素消費量およびATP産生量の有意な上昇が確認された[2]。脳神経症状を中心とするミトコンドリア病患者に対する医師主導型治験においては，残念ながら主要評価項目に有意差を認めなかったものの，少なくとも一部の症例に格段のQOL改善を認めていた。引き続き開発を進めるべく，ブラッシュアップした臨床治験を計画中である。

PIポリアミド：mtDNAの変異は，ミトコンドリア病だけでなく糖尿病などの成人生活習慣病やがん，更には痴呆や老化にも関与する。変異したmtDNA配列を直接標的とし，ミトコンドリア品質管理機構(MQC)に認識させて除去する，という理想的な治療法を目指して開発された化合物がPIポリアミドである。mtDNAが存在するミトコンドリアへと送達させることを目的として，脂溶性カチオンであるトリフェニルホスホニウムカチオン(TPP)とPIポリアミドの複合体(PIP-TPP)を合成・精製する[3]。わが国で最も症例数が多いmtDNA変異m.3243A>Gに対して設計したPIP-TPPは，変異特異的にミトコンドリアの活性酸素種の産生，マイトファジー，およびアポトーシスを誘導した[4]。現在，AMED難治性疾患実用化研究事業(リン班)として臨床応用を目指して進めているところである。

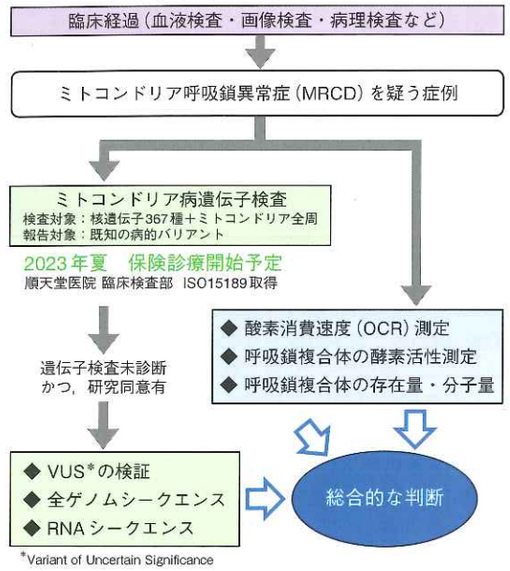

図　ミトコンドリア病の診断フローチャート

おわりに

筆者らは長年にわたり疾患ゲノム解析に携わってきたが，本格的にミトコンドリア病研究というものに焦点を置いたのは文部科学省セルイノベーションプログラム「神経細胞機能に着目した，ミトコンドリア呼吸鎖異常を起こす遺伝子変異の系統的な探索」に採択された平成22年以降である。当時100個程度とされていたミトコンドリア病の原因遺伝子数は今では400個を超え，そのなかには筆者らの研究グループが世界に先駆けて発表した新規原因遺伝子が13個含まれる。ミトコンドリアの正常な機能を維持するのに必要な遺伝子は1,500個とも言われ[5]，今後も新規原因遺伝子の報告が予想されるが，重要なことは各遺伝子異常の関与を明らかにすることでいかに病態解析を推進し，有効な治療薬の開発に結びつけるかという点である。

文献

1) Stenton SL, Prokisch H：*Essays Biochem.* **62**：399-408, 2018
2) Shimura M, Nozawa N, Ogawa-Tominaga M et al：*Sci Rep.* **9**：10549, 2019
3) Smith RA, Porteous CM, Gane AM, Murphy MP：*Proc Natl Acad Sci U S A.* **100**：5407-5412, 2003
4) Koshikawa N, Kida Y, Yasui N et al：*Biochem Biophys Res Commun.* **576**：93-99, 2021
5) Rahman J, Rahman S：*Lancet.* **391**：2560-2574, 2018

〔連絡先：ya-okazaki@juntendo.ac.jp(岡崎康司)〕

Molecular Genetics and Metabolism Reports 34 (2023) 100951

Contents lists available at ScienceDirect

Molecular Genetics and Metabolism Reports

journal homepage: www.elsevier.com/locate/ymgmr

Total and reduced/oxidized forms of coenzyme Q_{10} in fibroblasts of patients with mitochondrial disease

Chika Watanabe [a], Hitoshi Osaka [a,*], Miyuki Watanabe [a], Akihiko Miyauchi [a], Eriko F. Jimbo [a], Takeshi Tokuyama [b], Hideki Uosaki [b], Yoshihito Kishita [c,d], Yasushi Okazaki [c,e], Takanori Onuki [f], Tomohiro Ebihara [f], Kenichi Aizawa [g], Kei Murayama [f], Akira Ohtake [h], Takanori Yamagata [a]

[a] Department of Pediatrics, Jichi Medical University, Tochigi, Japan
[b] Division of Regenerative Medicine, Center for Molecular Medicine, Jichi Medical University, Tochigi, Japan
[c] Diagnostics and Therapeutic of Intractable Diseases, Intractable Disease Research Center, Graduate School of Medicine, Juntendo University, Tokyo, Japan
[d] Department of Life Science, Faculty of Science and Engineering, Kindai University, Osaka, Japan
[e] Laboratory for Comprehensive Genomic Analysis, RIKEN Center for Integrative Medical Sciences, Kanagawa, Japan
[f] Center for Medical Genetics and Department of Metabolism, Chiba Children's Hospital, Chiba, Japan
[g] Division of Clinical Pharmacology, Department of Pharmacology, Jichi Medical University, Tochigi, Japan
[h] Department of Clinical Genomics & Pediatrics, Faculty of Medicine, Saitama Medical University, Saitama, Japan

ARTICLE INFO

Keywords:
Mitochondrial disease
Primary coenzyme Q_{10} deficiency
Coenzyme Q_{10}
Reduced/total CoQ_{10}
Forward electron transport
Reverse electron transport

ABSTRACT

Coenzyme Q_{10} (CoQ_{10}) is involved in ATP production through electron transfer in the mitochondrial respiratory chain complex. CoQ_{10} receives electrons from respiratory chain complex I and II to become the reduced form, and then transfers electrons at complex III to become the oxidized form. The redox state of CoQ_{10} has been reported to be a marker of the mitochondrial metabolic state, but to our knowledge, no reports have focused on the individual quantification of reduced and oxidized CoQ_{10} or the ratio of reduced to total CoQ_{10} (reduced/total CoQ_{10}) in patients with mitochondrial diseases.

We measured reduced and oxidized CoQ_{10} in skin fibroblasts from 24 mitochondrial disease patients, including 5 primary CoQ_{10} deficiency patients and 10 respiratory chain complex deficiency patients, and determined the reduced/total CoQ_{10} ratio.

In primary CoQ_{10} deficiency patients, total CoQ_{10} levels were significantly decreased, however, the reduced/total CoQ_{10} ratio was not changed. On the other hand, in mitochondrial disease patients other than primary CoQ_{10} deficiency patients, total CoQ_{10} levels did not decrease. However, the reduced/total CoQ_{10} ratio in patients with respiratory chain complex IV and V deficiency was higher in comparison to those with respiratory chain complex I deficiency.

Measurement of CoQ_{10} in fibroblasts proved useful for the diagnosis of primary CoQ_{10} deficiency. In addition, the reduced/total CoQ_{10} ratio may reflect the metabolic status of mitochondrial disease.

1. Introduction

CoenzymeQ$_{10}$ (CoQ_{10}), also known as ubiquinone, is a lipophilic molecule composed of a redox-active benzoquinone head group and species-specific isoprenoid side chain (10 subunits in humans) [1,2]. CoQ_{10} takes three forms depending on the redox state of the benzoquinone ring; oxidized (CoQ_{10}, Ubiquinone), fully-reduced ($CoQ_{10}H_2$, Ubiquinol), and semi-reduced (CoQ^{+}_{10}, Semiubiquinone) forms [2]. It presents ubiquitously in all cellular membranes and cells [3]. The amount of CoQ_{10} and the proportion of reduced CoQ_{10} differ between organs and cells; CoQ_{10} is distributed in high amounts in the heart, kidneys, liver, and muscles, and the proportion of reduced CoQ_{10} is lower in the brain and lungs [3]. In cells, it is mostly localized in the mitochondria [3].

CoQ_{10} has multiple functions. One of the main roles of CoQ_{10} is as a component of the mitochondrial respiratory chain. As a mobile electron

* Corresponding author at: Department of Pediatrics, Jichi Medical University, 3311-1 Yakushiji, Shimotsuke-shi, Tochigi 329-0498, Japan.
E-mail address: hosaka@jichi.ac.jp (H. Osaka).

https://doi.org/10.1016/j.ymgmr.2022.100951
Received 25 October 2022; Received in revised form 22 December 2022; Accepted 22 December 2022
Available online 3 January 2023

carrier, CoQ_{10} accepts electrons from complex I and II and transfers them to complex III [2]. In the mitochondrial inner membrane, CoQ_{10} is proposed to exist as two independent pools: a CoQ_{NADH} pool in the super-complex (CI, CIII, CIV) involved in the oxidation of NADH; and a CoQ_{FADH} pool involved in the oxidation of CII and other enzymes that use CoQ as a cofactor [4]; CoQ_{NADH} receives electrons from NADH, and CoQ_{FADH} receives electrons from $FADH_2$ and other enzymes, such as glycerol phosphate dehydrogenase (GPDH), choline dehydrogenase (CHDH), sulphide:quinone oxidoreductase (SQOR), dihydroorote dehydrogenase (DHODH), and electron transfer flavoprotein dehydrogenase (ETFDH), and is reduced [5]. In respiratory chain complex III, electrons are transferred from reduced CoQ_{10} to cytochrome *c* in a process called the Q cycle. The Q cycle results in the oxidation of two molecules of reduced CoQ_{10}, the reduction of two molecules of cytochrome *c*, and the formation of one additional molecule of reduced CoQ_{10} [2]. This normal forward electron transfer results in the creation of an electrical gradient and a pH gradient (proton gradient) between the mitochondrial matrix and intermembrane space. The energy generated by this proton motive force enables complex V(ATP synthase) to synthesize ATP. On the other hand, reverse electron transfer (RET) of CoQ_{10} is also known to occur; in RET, electrons from reduced CoQ_{10} are returned to complex I, reducing NAD+ to NADH, and generating ROS [6] (Supplemental Fig. 1).

Another important role of CoQ_{10} is as an antioxidant. CoQ_{10} is the sole lipid-soluble antioxidant that is endogenously synthesized. Reduced CoQ_{10} inhibits both the initiation and the propagation of lipid peroxidation [7]. NADH-quinone oxidoreductase 1 and cytochrome *b*5 reductase, have been known to be the major oxidoreductases in the plasma membrane [8]. In addition, ferroptosis suppressor protein 1 (FSP1) was also found to be an important oxidoreductase. FSP1 reduces extra-mitochondrial CoQ_{10} and acts as a lipophilic radical-trapping antioxidant to suppress lipid peroxides, resulting in the inhibition of cell death, called ferroptosis [9,10]. Moreover, reduced CoQ_{10} also regenerates the other antioxidants—α-tocopherol and ascorbate—into an active reduced form [7]. CoQ_{10} is also involved in the β-oxidation of fatty acids [11], de novo pyrimidine biosynthesis [12], sulfide oxidation [13], an essential cofactor for uncoupling proteins (UCPs) [14], and modulation of the mitochondrial permeability transition pore [15]. Thus, the importance of the distinct state of CoQ_{10} is gaining growing attention [5].

Primary CoenzymeQ_{10} (CoQ_{10}) deficiency is an autosomal recessive mitochondrial disease caused by a decrease in CoQ_{10} due to mutations in genes involved in CoQ_{10} biosynthesis (*COQ* genes) [16]. To date, defects in at least 10 *COQ* genes (*COQ2, COQ4, COQ5, COQ6, COQ7, COQ8A, COQ8B, COQ9, PDSS1, PDSS2*) have been found to cause this disease [17]. Primary CoQ_{10} deficiency was first reported in 1989 as familial mitochondrial encephalomyopathy [18]. Currently, over 280 patients from 180 families have been reported [17]. Secondary CoQ_{10} deficiencies occur in a wider variety of pathologies, including mitochondrial disease [19,20]. Measuring the CoQ levels is known to be useful for diagnosing CoQ_{10} deficiency [21]. As described above, the ratio of reduction varies among organs and cells. As a result, in addition to the total amount of CoQ_{10}, evaluating the reduced/oxidized CoQ_{10} ratio may also be useful for further elucidating various pathophysiological states in cells.

Methods to measure CoQ_{10} in fibroblast and the reduced/oxidized state of CoQ_{10} have been reported [22,23]. However, to our knowledge, there are no reports on the measurement of the reduced/oxidized CoQ_{10} ratio in primary CoQ_{10} deficiency or mitochondrial diseases. Therefore, we decided to measure the total CoQ_{10} levels as well as the levels of reduced and oxidized CoQ_{10} in skin fibroblasts from patients affected by various mitochondrial diseases.

2. Material, methods, and patients

2.1. Subjects

We studied fibroblasts from 24 patients with mitochondrial disease, including primary CoQ_{10} deficiency (Table 1). The inclusion criterion for patients with primary CoQ_{10} deficiency was childhood onset with biallelic pathogenic variants in the *COQ* gene encoding proteins for the biosynthesis of CoQ_{10} [16]. Fibroblasts were obtained from patients at Kanagawa Children's Medical Center, Chiba Children's Medical Center, and Jichi Medical University under the approval of the Ethics Committee of Jichi Medical University. Written informed consent was obtained from the parents of each patient.

We obtained fibroblasts from five patients with primary CoQ_{10} deficiency. One patient carries biallelic *COQ2* variants with the c.[349G > C];[912 + 1G > del] (Case 1). Four patients had biallelic *COQ4* mutations: one with compound heterozygous biallelic variants c.[718C > T];[421C > T] (Case 2) [24], one with c.[431C > A];[718C > T] (Case 3) [25], and two with c.[190C > T];[479G > A] (Cases 4, 5).

Ten patients had disorders of mitochondrial respiratory chain subunits. Seven patients had mutations related to complex I: one with a c.[55C > T] mutation in *NDUFA1* (Case 6) [26], one with an m.10158 T>C mutation in *MT-ND3* (Case 7) [26], Three with an m.13513G > A mutation in *MT-ND5* (Case 8) [27], (Case 9), (Case 10) [28], one with a c.[811 T > G];[1766-2A > G] mutation in *ACAD9* (Case 11), and one with a c.[1150G > A];[1817 T > A] mutation in *ACAD9* (Case 12) [28]. NDUFA1, MT-ND3, and MT-ND5 are subunits of complex I, and ACAD9 is the assembly factor of complex I. Two patients had mutations related to complex IV: one with a c.[743C>A] mutation in *SURF1* (Case 13) [29], and one with a c.[367_368delAG]; [572delC] mutation in *SURF1* (Case 14) [25]. SURF1 is the assembly factor of complex IV. One patient had an m.8993 T > G mutation in *MT-ATP6* (Case 15) [25]. MT-ATP6 is a subunit of complex V.

Three patients had mitochondrial DNA (mtDNA) depletion syndrome: one with a c.[143-307_170del335];[143-307_170del335] mutation in *DGUOK* (Case 16) [30], one with a c.[451dupC];[308_310del] mutation (Case 17) [30] and one with a c.[148C > T];[149G > A] mutation in *MPV17* (Case 18) [30]. Both DGUOK and MPV17 are involved in the maintenance of mtDNA. One patient had Kearns-Sayre syndrome with a single mtDNA deletion (5513 bp del; m.8290–13,802) (Case 19). Two patients had MELAS: one with an m.3243 A > G mutation of tRNA-Leu (Case 20) [26] and one with an m.5541C > T, mutation of tRNA-Trp (Case 21) [26]. One patient had short-chain enoyl-CoA hydratase (ECHS1) deficiency with heterozygous mutations in maternal c.[832G > A] in *ECHS1* (Case 22) [31]. ECHS1 plays a role in valine and fatty acid catabolism in mitochondria. Two patients had c.[287A > G]; [287A > G] mutation in *BOLA3* (Cases 23) [28],(Case 24). BOLA3 is related to iron-sulfur cluster production and is involved in the assembly of the mitochondrial respiratory chain complex.

Five fibroblasts from healthy individuals were purchased: two fibroblasts from the PromoCell Company (#C-12300, GmbH, Heidelberg, Germany), two fibroblasts from Japanese Collection of Research Bioresources Cell Bank (#TIG-120, #HT-2020, Japan), and fibroblasts from Lonza Japan (#CC-2509, Tokyo, Japan). Another five fibroblasts from patients without mitochondrial disease were used as controls. Cells from passages 4–29 were used for assays.

2.2. Cell culture and growth conditions

The fibroblasts were maintained in 1.0 g/L low glucose Dulbecco's Modified Eagle's Medium (DMEM) (Life Technologies, Carlsbad, CA, USA) supplemented with 10% fetal bovine serum (FBS), 100 units/mL penicillin, and 100 μg/mL streptomycin. Cells were incubated at 37 °C under 5% CO_2.

Table 1
Fibroblast cell lines from patients with mitochondrial disease, including primary CoQ_{10} deficiency.

Case [ref]	diagnosis	DNA mutation	variants, heteroplasmy rate[a]	function
1	primary CoQ_{10} deficiency	*COQ2*	c.[349G > C];[912 + 1G > del]	CoQ_{10} biosynthesis
2 [24]	primary CoQ10 deficiency	*COQ4*	c.[718C > T];[421C > T]	CoQ_{10} biosynthesis
3 [25]	primary CoQ_{10} deficiency	*COQ4*	c.[431C > A];[718C > T]	CoQ_{10} biosynthesis
4	primary CoQ_{10} deficiency	*COQ4*	c.[190C > T];[479G > A]	CoQ_{10} biosynthesis
5	primary CoQ_{10} deficiency	*COQ4*	c.[190C > T];[479G > A]	CoQ_{10} biosynthesis
6 [26]	Leigh syndrome	*NDUFA1*	c.[55C > T], 100% (X-linked)	Respiratory chain subunits, complex I
7 [26]	Leigh syndrome	*MT-ND3*	m.10158 T>C, heteroplasmic (F; 90%)	Respiratory chain subunits, complex I
8 [27]	neonatal cardiomyopathy	*MT-ND5*	m.13513G > A, heteroplasmic (F; 78.87%)	Respiratory chain subunits, complex I
9	infantile mitochondrial disease	*MT-ND5*	m.13513G > A, heteroplasmic (B; 77%)	Respiratory chain subunits, complex I
10 [28]	Leigh syndrome	*MT-ND5*	m.13513G > A, heteroplasmic (F; 26%)	Respiratory chain subunits, complex I
11	mitochondrial cardiomyopathy	*ACAD9*	c.[811 T > G];[1766-2A > G]	Respiratory chain assembly factor, complex I
12 [28]	non-lethal infantile mitochondrial disease	*ACAD9*	c.[1150G > A];[1817 T > A]	Respiratory chain assembly factor, complex I
13 [29]	Leigh syndrome	*SURF1*	c.[743C>A], homoplasmy	Respiratory chain assembly factor, complex IV
14 [25]	Leigh syndrome	*SURF1*	c.[367_368delAG];[572delC]	Respiratory chain assembly factor, complex IV
15 [25]	Leigh syndrome	*MT-ATP6*	m.8993 T > G, homoplasmy	Respiratory chain subunits, complex V
16 [30]	mtDNA depletion syndrome	*DGUOK*	c.[143-307_170del335];[143-307_170del335]	Deoxynucleotide triphosphate synthesis
17 [30]	mtDNA depletion syndrome	*MPV17*	c.[451dupC];[308_310del]	mitochondrial protein synthesis
18 [30]	mtDNA depletion syndrome	*MPV17*	c.[148C > T];[149G > A]	mitochondrial protein synthesis
19	Kearns-Sayre syndrome		Single mtDNA deletion (5513 bp del; m.8290–13,802)	
20 [26]	MELAS	(tRNA-Leu)	m.3243 A > G, heteroplasmic (F; 21%)	Mitochondrial tRNA
21 [26]	MELAS	(tRNA-Trp)	m.5541C > T, heteroplasmic (F; 49%)	Mitochondrial tRNA
22 [31]	ECHS1 deficiency	*ECHS1*	c.[832G > A]	Metabolism of toxic compounds
23 [28]	cardiomyopathy	*BOLA3*	c.[287A > G];[287A > G]	Iron-sulfur protein assembly
24	cardiomyopathy	*BOLA3*	c.[287A > G];[287A > G]	Iron-sulfur protein assembly

[a] F; fibroblasts, B; blood

2.3. CoQ_{10} measurement in fibroblasts

2.3.1. CoQ extraction

The methods for the extraction CoQ_{10} were based on a previously reported method with slight modifications [32]. To extract CoQ_{10} from fibroblast in 60 mm dishes, cells were washed twice with PBS, and pellets were re-suspended in 500 μL of lysis buffer (0.25 mM Sucrose, 2 mM EDTA, 10 mM Tris, and 100 UI/mL heparin, pH 7.4.), and sonicated twice for 5 s. These homogenates were also used to citrate synthase and protein quantification. To measure CoQ_{10}, nine hundred microliters of ethanol containing internal standard CoQ_{10}-d9 (IsoSciences, Ambler, PA) and 20 μM *tert*-butyl hydroquinone (TBHQ) (FUJIFILM Wako, Osaka, Japan) was added to 100 μL of homogenates. TBHQ was added to prevent oxidation of reduced CoQ_{10}. The cell suspensions were vortexed and centrifuged at 15,700 ×*g* for 10 min (4 °C).

2.3.2. Reduction of ubiquinone

Reduced CoQ_{10} was required for use in the calibration curve measurement. However, since reduced CoQ_{10} is easily oxidized, reduced CoQ_{10} was prepared just before the analysis by reducing oxidized CoQ_{10} following a previously reported method with slight modification [33]. Briefly, 50 μL of CoQ_{10} was diluted in 1.95 mL hexane in a glass tube. Twenty milligrams of $NaBH_4$ was added and followed by the addition of 100 μL methanol, vortexed for 3 min, then placed in the dark for 5 min at room temperature. After reduction, 1 mL of water containing 100 μM EDTA was added to stop the reaction, vortexed for 1 min, and centrifuged 1500 ×*g* for 5 min at 4 °C. The upper layer containing reduced CoQ_{10} was transferred to a glass tube.

2.3.3. Liquid chromatography-tandem mass spectrometry (LC-MS/MS) analysis

The method for measuring reduced and oxidized CoQ_{10} was based on the previously reported method with slight modifications [23]. An LC-MS/MS analysis was performed on an LC-electrospray ionization-MS (LC-ESI-MS) with triple quadrupole (Nexera X2 and LCMS-8060, Shimadzu, Kyoto, Japan). A Kinetex C18 column (100 mm × 2.1 mm, 2.6 μm, Phenomenex) and a guard column filled with the same packing material were used. The column temperature was kept at 40 °C. The mobile phase was isocratic with 2 mM ammonium formate in methanol. The flow rate was 0.8 mL/min, the injection volume was 2 μL, and the run time was 6 min. The interface temperature was 300 °C, the desolvation line temperature was 250 °C, and the heat block temperature was 400 °C. The nebulizing gas flow was 3 L/min, the heating gas flow was 10 L/min, and the drying gas flow was 10 L/min. The samples were kept at 4 °C before injection by the autosampler. The MS/MS conditions for each target were optimized using the automated multiple reaction monitoring (MRM) optimization procedures in LabSolutions (Shimadzu). The MRM used for quantification was m/z 880.5 > 197.1 for oxidized CoQ_{10}, 882.4 > 197.0 for reduced CoQ_{10}, and 890.4 > 206.2 for CoQ_{10}-d9 (internal standard). Standards and samples were quantified using the LabSolutions software program to determine the peak area for oxidized CoQ_{10}, reduced CoQ_{10}, CoQ_{10}-d9, and the standard curves were used to determine the total amount of CoQ present in the samples.

Intra-assay coefficients of validation (CVs) and relative errors (REs), as measurements of precision and accuracy, respectively, were determined in five parallel analyses of the same cell. To evaluate inter-assay precision and accuracy, one cell line was independently evaluated on three different days. Precision was calculated as (standard deviation/mean concentration) × 100 (%), and accuracy was calculated as (quantitative value/theoretical value) × 100 (%). The intra-assay precision (CV) of reduced CoQ_{10} and oxidized CoQ_{10} was 0.58% and 1.39%, respectively. The intra-assay accuracy (RE) of reduced CoQ_{10} and oxidized CoQ_{10} was 4.20% and 2.50%, respectively. The inter-assay precision (CV) of reduced CoQ_{10} and oxidized CoQ_{10} was 1.27% and 1.84%, respectively. The intra-assay accuracy (RE) of reduced CoQ_{10} and oxidized CoQ_{10} was 10.54% and 1.18%, respectively (Supplemental Table 1, QC1).

2.3.4. Citrate synthase and protein quantification

Fibroblast CoQ_{10} levels were expressed as citrate synthase (CS) activity (measured CoQ_{10} values/CS units, nmol/CS units). CS activity was measured spectrophotometrically referring to the method described by Srere (1969), with 0.1 mM DTNB, 0.3 mM Acetyl-CoA, 0.5 mM Oxaloacetate, and 12–20 μg protein in 200 μL total incubation volume. CS units are determined as follows: CS Units (μmol/min/mL) = (ΔA_{412}/min x V (mL) × dil)/ 13.6 × L (cm) × V_{enz} (mL), V (mL); the reaction volume, dil; the dilution factor of the original sample, 13.6(mM^{-1} cm^{-1}); the extinction coefficient of TNB at 412 nm, L (cm); pathlength for

absorbance measurement (0.552 cm), V_{enz}(mL); the volume of the enzyme sample. Protein concentrations were quantified using Qubit™ Protein Assay Kits and a Qubit® 2.0 Fluorometer (Life Technologies, Carlsbad, CA, USA).

2.4. Statistical analyses

Statistical analyses were performed using the GraphPad Prism software program (version 9.01, GraphPad Software Inc., La Jolla, CA). Comparisons between samples were performed using a one-way ANOVA. The results are expressed as the mean (standard deviation). *P* values of <0.05 were considered to indicate statistical significance.

3. Results

3.1. Total CoQ_{10} levels were observed to decrease in all patients with primary CoQ_{10} deficiency

We showed the reduced, oxidized, and total (sum of reduced and oxidized) CoQ_{10} values corrected for the CS unit (nmol/CS unit) (Table 2). In addition, we also measured the CoQ_{10} values corrected for protein levels (nmol/g protein) (Supplemental Table 2). Six patients showed decreased the total CoQ_{10} values (<70% of the control): five with primary CoQ_{10} deficiency (Cases 1–5), and one with Kearns-Sayre syndrome (Case 19) (Table 2). The total CoQ_{10} levels were significantly decreased in primary CoQ_{10} deficiency than in controls (primary CoQ_{10} deficiency($n = 5$)1.00 ± 0.19 nmol / CS unit (mean ± SD), controls ($n = 10$)2.30 ± 0.24 nmol / CS unit, $p < 0.0001$) (Fig. 1). However, total CoQ_{10} levels were the same in mitochondrial disease other than primary CoQ_{10} deficiency as in controls (mitochondrial disease($n = 19$)2.23 ± 0.26 nmol / CS unit, $p = 0.93$).

Table 2
Reduced and oxidized CoQ_{10} values and total CoQ deficiency in fibroblasts.

Case	reduced CoQ_{10}		oxidized CoQ_{10}		total CoQ_{10} (nmol/CS unit)		% CoQ deficiency (%)
	mean	SD	mean	SD	mean	SD	
1	0.37	0.15	0.37	0.02	0.74	0.13	32
2	0.12	0.00	0.16	0.00	0.28	0.00	12
3	0.57	0.45	0.59	0.18	1.16	0.63	50
4	0.64	0.03	0.74	0.20	1.38	0.17	60
5	0.78	0.01	0.64	0.02	1.42	0.01	62
6	0.48	0.01	1.65	0.00	2.13	0.01	
7	1.03	0.04	1.00	0.32	2.03	0.29	
8	1.22	0.04	0.82	0.18	2.04	0.22	
9	1.40	0.54	0.96	0.03	2.36	0.51	
10	0.86	0.16	1.34	0.30	2.20	0.46	
11	1.02	0.08	2.17	0.53	3.19	0.44	
12	1.18	0.56	1.31	0.17	2.49	0.38	
13	1.33	0.03	0.57	0.02	1.90	0.00	
14	1.77	0.31	0.58	0.10	2.35	0.21	
15	1.54	0.09	0.71	0.00	2.25	0.09	
16	0.86	0.02	1.46	0.01	2.32	0.01	
17	1.37	0.40	1.28	0.14	2.65	0.25	
18	1.01	0.20	1.52	0.08	2.53	0.29	
19	0.57	0.01	0.72	0.02	1.29	0.02	56
20	1.41	0.40	0.51	0.11	1.92	0.51	
21	1.24	0.28	0.65	0.28	1.89	0.56	
22	1.19	0.11	0.87	0.23	2.06	0.34	
23	0.81	0.19	1.84	0.46	2.65	0.27	
24	0.92	0.01	1.23	0.00	2.15	0.01	
Reference (n = 10)	1.19	0.15	1.11	0.10	2.30	0.24	

% CoQ deficiency: <70% of control CoQ_{10} value.

3.2. The reduced/total CoQ_{10} ratio was unchanged in primary CoQ_{10} deficiency, but was higher in complex IV or V deficiency

We showed the ratio of reduced CoQ_{10} to total CoQ_{10} (reduced/total CoQ_{10}) of fibroblasts (Table 3). The ratio of reduced and oxidized CoQ_{10} to total CoQ_{10} in control fibroblasts was 52% and 48%, respectively (Table 3). In primary CoQ_{10} deficiency, the reduced/total CoQ_{10} ratio did not change compared to the control (reduced/total CoQ_{10} ratio of primary CoQ_{10} deficiency ($n = 5$) 49 ± 7% (mean ± SD), controls ($n = 10$) 52 ± 1%, $p = 0.92$) (Fig. 2). Regarding the cases with respiratory chain complex deficiency, there was no difference between control and complex I deficiency (reduced/total CoQ_{10} ratio of complex I deficiency ($n = 7$) 44 ± 7%, $p = 0.37$). However, the reduced/total CoQ_{10} ratio in complex IV or V deficiency was increased in comparison to the control (complex IV or V deficiency ($n = 3$) 71 ± 3%, $p = 0.022$). In addition, the reduced/total CoQ_{10} ratio in complex IV or V deficiency was higher in comparison to complex I deficiency and primary CoQ_{10} deficiency (complex IV or V deficiency vs. complex I deficiency: $p = 0.0021$, complex IV or V deficiency vs. primary CoQ_{10} deficiency: $p = 0.015$).

In individual cases, the reduced/total CoQ_{10} ratio decreased (<80% of the reduced/total CoQ_{10} ratio in the control) in six cases; three cases with complex I deficiency (Cases 6, 10, 11), two cases with mtDNA depletion syndrome (Cases 16, 18), one case with *BOLA3* mutation (Case 23)(Table 3). On the other hand, the reduced/total CoQ_{10} ratio increased (>120% of the reduced/total CoQ_{10} ratio in the control) in five cases; two cases with complex IV deficiency (Cases 13, 14), two cases with MELAS(Cases 20, 21), one case with complex V deficiency (Case 15) (Table 3).

4. Discussion

We showed here that the total CoQ_{10} values of fibroblasts were significantly lower in patients with primary CoQ_{10} deficiency. In this syndrome, early recognition and therapy can stop progression and improve the prognosis; however, established severe symptoms cannot be reversed [16,34]. Biochemical measurements of low CoQ_{10} levels in muscle biopsy have been utilized for the diagnosis of this syndrome

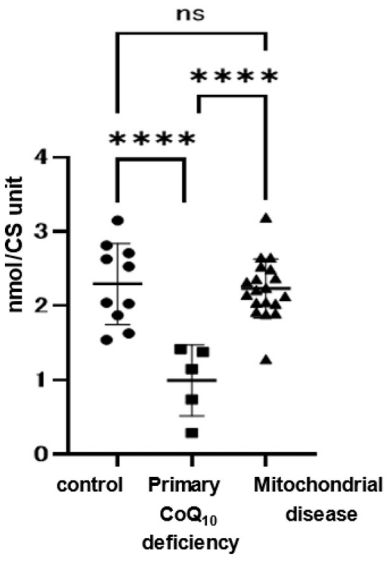

Fig. 1. Total CoQ_{10} values.
Total (sum of reduced and oxidized) CoQ_{10} values of mitochondrial patient fibroblasts. CoQ_{10} deficiency (CoQ_{10} levels <70% of control CoQ_{10}) was found in six cases. All cases of primary CoQ_{10} deficiency showed decreased CoQ_{10} levels. In mitochondrial disease, CoQ_{10} values were not decreased, with the exception of Case 19 (Kearns-Sayre syndrome). Data are expressed as **** $P <$ 0.0001, and n.s. indicates no significance.

Table 3
Ratio of reduced / total CoQ_{10}.

Case	reduced/total CoQ_{10} (%)		Reduced/total CoQ_{10} in cases versus reduced/total CoQ_{10} in controls (%)
	mean	SD	
1	50	11	96
2	43	1	83
3	49	14	95
4	47	8	90
5	55	1	106
6	23	0	44
7	51	9	97
8	60	4	115
9	59	10	114
10	39	1	75
11	32	7	61
12	47	15	91
13	70	1	135
14	75	7	145
15	68	1	131
16	37	1	71
17	52	10	100
18	40	3	77
19	44	0	85
20	74	1	142
21	66	5	127
22	58	4	111
23	30	10	59
24	43	0	83
Reference (n = 10)	52	1	

The reduced/total CoQ_{10} ratio decreased (< 80% of control value); cases 6, 10, 11, 16, 18, 23.
The reduced/total CoQ_{10} ratio increased (120% < of control value); cases 13, 14, 15, 20, 21.

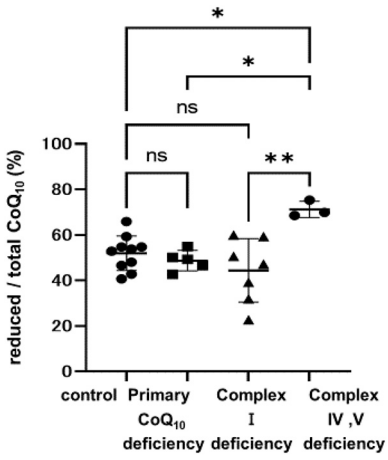

Fig. 2. Comparison of the reduced/total CoQ_{10} ratio.
Comparison of the reduced/total CoQ_{10} ratio in cases with primary CoQ_{10} deficiency, complex I deficiency, and complex IV or V deficiency. In primary CoQ_{10} deficiency, the reduced/total CoQ_{10} ratio was the same as that of the controls. In complex I deficiency, 3/7 cases showed a decreased (< 80% of control value) reduced/total CoQ_{10} ratio. In complex IV or V deficiency, 3/3 cases showed an increased (120% < of control value) reduced/total CoQ_{10} ratio. Data are expressed as $^{*}P < 0.05$, $^{**}P < 0.01$, and n.s. indicates no significance.

[16]. Moreover, the identification of biallelic pathogenic variants in the *COQ* genes, which encode proteins involved in coenzyme Q biosynthesis, enables a definitive diagnosis [16]. However, the invasiveness of muscle biopsy hampers this procedure and can delay the diagnosis. CoQ_{10} levels in fibroblasts were examined and implicated in their usefulness [21]. Our data with LC-MS/MS for the measurement of CoQ_{10} from fibroblasts also supported the usefulness for detecting CoQ_{10} deficiency [32,35]. The fibroblasts from Case 2 showed the lowest CoQ_{10} concentration and showed a very severe phenotype. A correlation between CoQ_{10} levels and phenotype has been suggested [24,36,37]. Therefore, the CoQ_{10} value from skin fibroblast may reflect the clinical severity.

In addition to primary CoQ_{10} deficiency, various mitochondrial diseases have also been reported to decrease CoQ_{10} in fibroblasts and muscle, particularly in mtDNA depletion syndrome [20,38]. However, in our analysis, three patients with mtDNA depletion, including *DGUOK* and *MPV17* mutations, showed no decrease in CoQ_{10} (Cases 16–18). Only one patient with large deletions of mtDNA showed markedly decreased CoQ_{10} (Case 19). Therefore, decreased CoQ_{10} was only a constant feature in primary CoQ_{10} deficiency syndrome in our analysis. Our results support the widely accepted idea that early CoQ_{10} therapy should is therefore indicated if decreased levels of CoQ_{10} are found in the fibroblasts of patients with suspected mitochondrial disease.

To our knowledge, this is the first report to describe the reduced/total CoQ_{10} ratios in patients with mitochondrial diseases, including primary CoQ_{10} deficiency. In primary CoQ_{10} deficiency, the reduced/total CoQ_{10} ratio did not change. On the other hand, the reduced/total CoQ_{10} ratio was decreased in 3/7 of cases of complex I deficiency and was increased in 3/3 of cases of complex IV or V deficiency. Primary CoQ_{10} deficiency is caused by impaired CoQ_{10} biosynthesis, which results in a decrease in the absolute value of CoQ_{10}; however, as expected, our data suggest that it does not affect the redox reaction in mitochondria. Since CoQ_{10} changes from the oxidized form to the reduced form by accepting electrons from complex I, complex II and other dehydrogenases, the reduced/total CoQ_{10} ratio is expected to decrease in complex I deficiency. However, only 3 out of 7 complex I patients in our cohort showed disturbed Q reduced/total ratios. In contrast, CoQ_{10} changes from the reduced form to the oxidized form in complex III, and the reduced/total CoQ_{10} ratio is expected to increase in complex III and later complex deficiencies (Supplemental Fig. 1, left panel). In fact, the reduced CoQ_{10} ratio was significantly decreased with complex I inhibitor, whereas the reduced CoQ_{10} ratio was increased with complex IV inhibitor [23]. Some (but not all) of our results support these observations. Among complex I deficiency patients, patients with isolated complex I deficiency tended to have a decreased reduced/total CoQ_{10} ratio (3/4 cases; Cases 6, 10, 11) (Supplemental Table 3). On the other hand, the reduced/total CoQ_{10} ratio was unchanged in a patient who also had a decreased complex III and IV enzyme activity (Case 8), in a patient without a decreased CI enzyme activity in fibroblasts (Case 12), and in a patient with a decreased CI enzyme activity in muscle (Case 7).

In recent years, it has been reported that the reduced/oxidized CoQ_{10} ratio may be a marker of mitochondrial metabolic status [39]. In situations where CoQ_{FADH} can be excessively reduced, RET is induced, and the production of reactive oxygen species (ROS) from complex I is stimulated, which causes complex I destruction [4,6]. On the other hand, oxidizing the CoQ pool by alternative oxidase (AOX) of *Ciona intestinalis* xenotopically expressed in mouse mitochondria induces forward electron transport (FET) from RET [40]. Our system of measuring the reduced/total CoQ_{10} ratio of skin fibroblasts provide the amount and redox states of CoQ_{10}.

As a limitation of our study, CoQ_{10} is mostly localized in the mitochondria in subcellular fractions but it has also been shown to localize in Golgi, lysosomes, and other organelles [3]. In this study, we measured the whole cell CoQ_{10} level without separating the mitochondrial and non-mitochondrial fractions. Moreover, we examined an only limited number of patients affected by only some mitochondrial diseases, which can be caused by >400 gene mutations [41].

In conclusion, we measured the reduced/total CoQ_{10} ratio in fibroblasts from a cohort of patients with mitochondrial disease for the first time. The reduced/total CoQ_{10} ratio tended to show no change in many of the cells that we measured. However, the reduced/total CoQ_{10} ratio was increased in complex IV or V deficiency, while the reduced/total CoQ_{10} ratio tended to decrease in some cases of complex I deficiency.

Supplementary data to this article can be found online at https://doi.org/10.1016/j.ymgmr.2022.100951.

Author contributions

CW, HO contributed to the conceptualization and performance of the statistical analysis of the data and wrote the manuscript; MW, AM, EFJ, TT, HU, OT, ET, and KA performed sampling and data acquisition; YK, YO performed genetic testing; KM, AO recruited patients, provided clinical information, collected samples; TY conducted supervision of the project. All authors read and approved the final manuscript.

Ethics

All procedures followed were by the ethical standards of the responsible committee on human experimentation and with the Helsinki Declaration of the World Medical Organization. This study was approved by the Ethics Committee of Jichi Medical University and written informed consent was obtained from all participants.

Funding

This work was supported in part by the Practical Research Project for Rare/Intractable Diseases from the Japan Agency for Medical Research and Development, AMED to H·O (JP21im0210625, JP21ek0109511), K. M (JP21ek0109468, JP19ek0109273) and Y·O (JP21kk0305015). Health and Labor Sciences Research Grant to H·O (JP21FC1015). The Acceleration Program for Intractable Diseases Research utilizing Disease-specific iPS cells to H·U (JP22bm0804018). JSPS KAKENHI to H. O. (JP20H03648).

CRediT authorship contribution statement

Chika Watanabe: Conceptualization, Writing – original draft. **Hitoshi Osaka:** Conceptualization, Writing – review & editing, Funding acquisition. **Miyuki Watanabe:** Investigation. **Akihiko Miyauchi:** Investigation. **Eriko F. Jimbo:** Investigation. **Takeshi Tokuyama:** Resources. **Hideki Uosaki:** Resources. **Yoshihito Kishita:** Resources. **Yasushi Okazaki:** Resources. **Takanori Onuki:** Resources. **Tomohiro Ebihara:** Resources. **Kenichi Aizawa:** Resources. **Kei Murayama:** Resources. **Akira Ohtake:** Resources. **Takanori Yamagata:** Supervision.

Declaration of Competing Interest

None.

Data availability

No data was used for the research described in the article.

Acknowledgments

We thank the patients and their families. We thank all the staff, especially Natsumi Oishi, Shiho Aoki, and Narumi Omika, in Jichi Children Medical Center Tochigi and Jichi Medical University Hospital.

References

[1] F.L. Crane, Y. Hatefi, R.L. Lester, C. Widmer, Isolation of a quinone from beef heart mitochondria, Biochim. Biophys. Acta 25 (1957) 220–221.
[2] Y. Wang, S. Hekimi, Understand. Ubiquinone, Trends Cell Biol. 26 (2016) 367–378.
[3] M. Turunen, J. Olsson, G. Dallner, Metabolism and function of coenzyme Q, Biochim. Biophys. Acta 1660 (2004) 171–199.
[4] E. Lapuente-Brun, R. Moreno-Loshuertos, R. Acín-Pérez, A. Latorre-Pellicer, C. Colás, E. Balsa, E. Perales-Clemente, P.M. Quirós, E. Calvo, M.A. Rodríguez-Hernández, P. Navas, R. Cruz, Á. Carracedo, C. López-Otín, A. Pérez-Martos, P. Fernández-Silva, E. Fernández-Vizarra, J.A. Enríquez, Supercomplex assembly determines electron flux in the mitochondrial electron transport chain, Science 340 (2013) 1567–1570.
[5] F. Pallotti, C. Bergamini, C. Lamperti, R. Fato, The roles of coenzyme Q in disease: direct and indirect involvement in cellular functions, Int. J. Mol. Sci. 23 (2021).
[6] F. Scialò, D.J. Fernández-Ayala, A. Sanz, Role of Mitochondrial Reverse Electron Transport in ROS Signaling: Potential Roles in Health and Disease, Front. Physiol. 8 (2017) 428.
[7] M. Bentinger, K. Brismar, G. Dallner, The antioxidant role of coenzyme, Q. Mitochondrion. 7 (Suppl) (2007) S41–S50.
[8] D.H. Hyun, Plasma membrane redox enzymes: new therapeutic targets for neurodegenerative diseases, Arch. Pharm. Res. 42 (2019) 436–445.
[9] K. Bersuker, J.M. Hendricks, Z. Li, L. Magtanong, B. Ford, P.H. Tang, M.A. Roberts, B. Tong, T.J. Maimone, R. Zoncu, M.C. Bassik, D.K. Nomura, S.J. Dixon, J. A. Olzmann, The CoQ oxidoreductase FSP1 acts parallel to GPX4 to inhibit ferroptosis, Nature 575 (2019) 688–692.
[10] S. Doll, F.P. Freitas, R. Shah, M. Aldrovandi, M.C. da Silva, I. Ingold, A.G. Grocin, T. N. Xavier da Silva, E. Panzilius, C.H. Scheel, A. Mourão, K. Buday, M. Sato, J. Wanninger, T. Vignane, V. Mohana, M. Rehberg, A. Flatley, A. Schepers, A. Kurz, D. White, M. Sauer, M. Sattler, E.W. Tate, W. Schmitz, A. Schulze, V. O'Donnell, B. Proneth, G.M. Popowicz, D.A. Pratt, J.P.F. Angeli, M. Conrad, FSP1 is a glutathione-independent ferroptosis suppressor, Nature 575 (2019) 693–698.
[11] S.K. Lee, J.O. Lee, J.H. Kim, N. Kim, G.Y. You, J.W. Moon, J. Sha, S.J. Kim, Y. W. Lee, H.J. Kang, S.H. Park, H.S. Kim, Coenzyme Q10 increases the fatty acid oxidation through AMPK-mediated PPARα induction in 3T3-L1 preadipocytes, Cell. Signal. 24 (2012) 2329–2336.
[12] D.R. Evans, H.I. Guy, Mammalian pyrimidine biosynthesis: fresh insights into an ancient pathway, J. Biol. Chem. 279 (2004) 33035–33038.
[13] P. González-García, A. Hidalgo-Gutiérrez, C. Mascaraque, E. Barriocanal-Casado, M. Bakkali, M. Ziosi, U.B. Abdihankyzy, S. Sánchez-Hernández, G. Escames, H. Prokisch, F. Martín, C.M. Quinzii, L.C. López, Coenzyme Q10 modulates sulfide metabolism and links the mitochondrial respiratory chain to pathways associated to one carbon metabolism, Hum. Mol. Genet. 29 (2020) 3296–3311.
[14] K.S. Echtay, E. Winkler, M. Klingenberg, Coenzyme Q is an obligatory cofactor for uncoupling protein function, Nature 408 (2000) 609–613.
[15] E. Fontaine, F. Ichas, P. Bernardi, A ubiquinone-binding site regulates the mitochondrial permeability transition pore, J. Biol. Chem. 273 (1998) 25734–25740.
[16] L. Salviati, E. Trevisson, M. Doimo, P. Navas, Primary coenzyme Q(10) deficiency, in: M.P. Adam, H.H. Ardinger, R.A. Pagon, S.E. Wallace, L.J.H. Bean, K. Stephens, A. Amemiya (Eds.), GeneReviews(®), University of Washington, Seattle Copyright © 1993–2020, University of Washington, Seattle. GeneReviews Is a Registered Trademark of the University of Washington, Seattle. All rights reserved., Seattle (WA), 1993.
[17] M. Alcázar-Fabra, F. Rodríguez-Sánchez, E. Trevisson, G. Brea-Calvo, Primary coenzyme Q deficiencies: a literature review and online platform of clinical features to uncover genotype-phenotype correlations, Free Radic. Biol. Med. 167 (2021) 141–180.
[18] S. Ogasahara, A.G. Engel, D. Frens, D. Mack, Muscle coenzyme Q deficiency in familial mitochondrial encephalomyopathy, Proc. Natl. Acad. Sci. U. S. A. 86 (1989) 2379–2382.
[19] M.A. Desbats, G. Lunardi, M. Doimo, E. Trevisson, L. Salviati, Genetic bases and clinical manifestations of coenzyme Q10 (CoQ 10) deficiency, J. Inherit. Metab. Dis. 38 (2015) 145–156.
[20] D. Yubero, R. Montero, M.A. Martín, J. Montoya, A. Ribes, M. Grazina, E. Trevisson, J.C. Rodriguez-Aguilera, I.P. Hargreaves, L. Salviati, P. Navas, R. Artuch, C. Jou, C. Jimenez-Mallebrera, A. Nascimento, B. Pérez-Dueñas, C. Ortez, F. Ramos, J. Colomer, M. O'Callaghan, M. Pineda, A. García-Cazorla, C. Espinós, A. Ruiz, A. Macaya, A. Marcé-Grau, J. Garcia-Villoria, A. Arias, S. Emperador, E. Ruiz-Pesini, E. Lopez-Gallardo, V. Neergheen, M. Simões, L. Diogo, A. Blázquez, A. González-Quintana, A. Delmiro, C. Domínguez-González, J. Arenas, M.T. García-Silva, E. Martín, P. Quijada, A. Hernández-Laín, M. Morán, E. Rivas Infante, R. Ávila Polo, C. Paradas Lópe, J. Bautista Lorite, E.M. Martínez Fernández, A.B. Cortés, A. Sánchez-Cuesta, M.V. Cascajo, M. Alcázar, G. Brea-Calvo, Secondary coenzyme Q10 deficiencies in oxidative phosphorylation (OXPHOS) and non-OXPHOS disorders, Mitochondrion 30 (2016) 51–58.
[21] R. Montero, J.A. Sánchez-Alcázar, P. Briones, A.R. Hernández, M.D. Cordero, E. Trevisson, L. Salviati, M. Pineda, A. García-Cazorla, P. Navas, R. Artuch, Analysis of coenzyme Q10 in muscle and fibroblasts for the diagnosis of CoQ10 deficiency syndromes, Clin. Biochem. 41 (2008) 697–700.
[22] P.H. Tang, M.V. Miles, Measurement of oxidized and reduced coenzyme Q in biological fluids, cells, and tissues: an HPLC-EC method, Methods Mol. Biol. 837 (2012) 149–168.
[23] N. Burger, A. Logan, T.A. Prime, A. Mottahedin, S.T. Caldwell, T. Krieg, R. C. Hartley, A.M. James, M.P. Murphy, A sensitive mass spectrometric assay for mitochondrial CoQ pool redox state in vivo, Free Radic. Biol. Med. 147 (2020) 37–47.
[24] G. Brea-Calvo, T.B. Haack, D. Karall, A. Ohtake, F. Invernizzi, R. Carrozzo, L. Kremer, S. Dusi, C. Fauth, S. Scholl-Bürgi, E. Graf, U. Ahting, N. Resta, N. Laforgia, D. Verrigni, Y. Okazaki, M. Kohda, D. Martinelli, P. Freisinger, T. M. Strom, T. Meitinger, C. Lamperti, A. Lacson, P. Navas, J.A. Mayr, E. Bertini, K. Murayama, M. Zeviani, H. Prokisch, D. Ghezzi, COQ4 mutations cause a broad spectrum of mitochondrial disorders associated with CoQ10 deficiency, Am. J. Hum. Genet. 96 (2015) 309–317.
[25] E. Ogawa, T. Fushimi, M. Ogawa-Tominaga, M. Shimura, M. Tajika, K. Ichimoto, A. Matsunaga, T. Tsuruoka, M. Ishige, T. Fuchigami, T. Yamazaki, Y. Kishita, M. Kohda, A. Imai-Okazaki, Y. Okazaki, I. Morioka, A. Ohtake, K. Murayama,

Mortality of Japanese patients with Leigh syndrome: effects of age at onset and genetic diagnosis, J. Inherit. Metab. Dis. 43 (2020) 819–826.
[26] A. Miyauchi, T. Kouga, E.F. Jimbo, T. Matsuhashi, T. Abe, T. Yamagata, H. Osaka, Apomorphine rescues reactive oxygen species-induced apoptosis of fibroblasts with mitochondrial disease, Mitochondrion 49 (2019) 111–120.
[27] H. Shimozawa, T. Sato, H. Osaka, A. Takeda, A. Miyauchi, N. Omika, Y. Yada, Y. Kono, K. Murayama, Y. Okazaki, Y. Kishita, T. Yamagata, A Case of Infantile Mitochondrial Cardiomyopathy Treated with a Combination of Low-Dose Propranolol and Cibenzoline for Left Ventricular Outflow Tract Stenosis, Int. Heart J. 63 (2022) 970–977.
[28] A. Imai-Okazaki, Y. Kishita, M. Kohda, Y. Mizuno, T. Fushimi, A. Matsunaga, Y. Yatsuka, T. Hirata, H. Harashima, A. Takeda, A. Nakaya, Y. Sakata, S. Kogaki, A. Ohtake, K. Murayama, Y. Okazaki, Cardiomyopathy in children with mitochondrial disease: prognosis and genetic background, Int. J. Cardiol. 279 (2019) 115–121.
[29] J. Tanigawa, K. Kaneko, M. Honda, H. Harashima, K. Murayama, T. Wada, K. Takano, M. Iai, S. Yamashita, H. Shimbo, N. Aida, A. Ohtake, H. Osaka, Two Japanese patients with Leigh syndrome caused by novel SURF1 mutations, Brain and Development 34 (2012) 861–865.
[30] M. Shimura, N. Kuranobu, M. Ogawa-Tominaga, N. Akiyama, Y. Sugiyama, T. Ebihara, T. Fushimi, K. Ichimoto, A. Matsunaga, T. Tsuruoka, Y. Kishita, S. Umetsu, A. Inui, T. Fujisawa, K. Tanikawa, R. Ito, A. Fukuda, J. Murakami, S. Kaji, M. Kasahara, K. Shiraki, A. Ohtake, Y. Okazaki, K. Murayama, Clinical and molecular basis of hepatocerebral mitochondrial DNA depletion syndrome in Japan: evaluation of outcomes after liver transplantation, Orphanet J. Rare Dis. 15 (2020) 169.
[31] M. Kuwajima, K. Kojima, H. Osaka, Y. Hamada, E. Jimbo, M. Watanabe, S. Aoki, I. Sato-Shirai, K. Ichimoto, T. Fushimi, K. Murayama, A. Ohtake, M. Kohda, Y. Kishita, Y. Yatsuka, S. Uchino, M. Mimaki, N. Miyake, N. Matsumoto, Y. Okazaki, T. Ogata, T. Yamagata, K. Muramatsu, Valine metabolites analysis in ECHS1 deficiency, Mol. Genet. Metab. Rep. 29 (2021), 100809.
[32] N. Buján, A. Arias, R. Montero, J. García-Villoria, W. Lissens, S. Seneca, C. Espinós, P. Navas, L. De Meirleir, R. Artuch, P. Briones, A. Ribes, Characterization of CoQ_{10} biosynthesis in fibroblasts of patients with primary and secondary CoQ_{10} deficiency, J. Inherit. Metab. Dis. 37 (2014) 53–62.
[33] R. Pandey, C.L. Riley, E.M. Mills, S. Tiziani, Highly sensitive and selective determination of redox states of coenzymes Q(9) and Q(10) in mice tissues: Application of orbitrap mass spectrometry, Anal. Chim. Acta 1011 (2018) 68–76.
[34] G. Montini, C. Malaventura, L. Salviati, Early coenzyme Q10 supplementation in primary coenzyme Q10 deficiency, N. Engl. J. Med. 358 (2008) 2849–2850.
[35] Y.T. Liu, J. Hersheson, V. Plagnol, K. Fawcett, K.E. Duberley, E. Preza, I. P. Hargreaves, A. Chalasani, M. Laurá, N.W. Wood, M.M. Reilly, H. Houlden, Autosomal-recessive cerebellar ataxia caused by a novel ADCK3 mutation that elongates the protein: clinical, genetic and biochemical characterisation, J. Neurol. Neurosurg. Psychiatry 85 (2014) 493–498.
[36] M.A. Desbats, V. Morbidoni, M. Silic-Benussi, M. Doimo, V. Ciminale, M. Cassina, S. Sacconi, M. Hirano, G. Basso, F. Pierrel, P. Navas, L. Salviati, E. Trevisson, The COQ2 genotype predicts the severity of coenzyme Q10 deficiency, Hum. Mol. Genet. 25 (2016) 4256–4265.
[37] A.K. Kwong, A.T. Chiu, M.H. Tsang, K.S. Lun, R.J.T. Rodenburg, J. Smeitink, B. H. Chung, C.W. Fung, A fatal case of COQ7-associated primary coenzyme Q(10) deficiency, JIMD Rep. 47 (2019) 23–29.
[38] R. Montero, M. Grazina, E. López-Gallardo, J. Montoya, P. Briones, A. Navarro-Sastre, J.M. Land, I.P. Hargreaves, R. Artuch, Coenzyme Q_{10} deficiency in mitochondrial DNA depletion syndromes, Mitochondrion 13 (2013) 337–341.
[39] A. Guarás, E. Perales-Clemente, E. Calvo, R. Acín-Pérez, M. Loureiro-Lopez, C. Pujol, I. Martínez-Carrascoso, E. Nuñez, F. García-Marqués, M.A. Rodríguez-Hernández, A. Cortés, F. Diaz, A. Pérez-Martos, C.T. Moraes, P. Fernández-Silva, A. Trifunovic, P. Navas, J. Vazquez, J.A. Enríquez, The CoQH2/CoQ Ratio Serves as a Sensor of Respiratory Chain Efficiency, Cell Rep. 15 (2016) 197–209.
[40] M. Szibor, T. Gainutdinov, E. Fernandez-Vizarra, E. Dufour, Z. Gizatullina, G. Debska-Vielhaber, J. Heidler, I. Wittig, C. Viscomi, F. Gellerich, A.L. Moore, Bioenergetic consequences from xenotopic expression of a tunicate AOX in mouse mitochondria: Switch from RET and ROS to FET, Biochim. Biophys. Acta Bioenerg. 1861 (2020), 148137.
[41] M. Gusic, H. Prokisch, Genetic basis of mitochondrial diseases, FEBS Lett. 595 (2021) 1132–1158.

scientific reports

Check for updates

OPEN

Apomorphine is a potent inhibitor of ferroptosis independent of dopaminergic receptors

Akihiko Miyauchi[1]✉, Chika Watanabe[1], Naoya Yamada[2], Eriko F. Jimbo[1], Mizuki Kobayashi[1], Natsumi Ohishi[1], Atsuko Nagayoshi[1], Shiho Aoki[1], Yoshihito Kishita[3,4], Akira Ohtake[5,6], Nobuhiko Ohno[7,8], Masafumi Takahashi[2], Takanori Yamagata[1] & Hitoshi Osaka[1]✉

Originally, apomorphine was a broad-spectrum dopamine agonist with an affinity for all subtypes of the Dopamine D1 receptor to the D5 receptor. We previously identified apomorphine as a potential therapeutic agent for mitochondrial diseases by screening a chemical library of fibroblasts from patients with mitochondrial diseases. In this study, we showed that apomorphine prevented ferroptosis in fibroblasts from various types of mitochondrial diseases as well as in normal controls. Well-known biomarkers of ferroptosis include protein markers such as prostaglandin endoperoxide synthase 2 (PTGS2), a key gene for ferroptosis-related inflammation PTGS2, lipid peroxidation, and reactive oxygen species. Our findings that apomorphine induced significant downregulation of PTSG2 and suppressed lipid peroxide to the same extent as other inhibitors of ferroptosis also indicate that apomorphine suppresses ferroptosis. To our knowledge, this is the first study to report that the anti-ferroptosis effect of apomorphine is not related to dopamine receptor agonist action and that apomorphine is a potent inhibitor of ferroptotic cell death independent of dopaminergic receptors.

Mitochondrial disease is a genetic disorder consisting of various clinical phenotypes, including Leigh syndrome (LS), myopathy encephalopathy lactic acidosis, stroke-like episodes (MELAS), Kearns-Sayre syndrome (KSS), and mitochondrial cardiomyopathy[1,2]. At present, no curative treatment is available and effective treatment options are eagerly awaited. In our previous study, we screened a chemical library based on drugs already approved for central nervous system (CNS) diseases using fibroblasts from two patients with LS and two patients with MELAS using an L-buthionine-S, R-sulfoximine (BSO)-induced cell viability assay. BSO has been used to induce cell death by inhibiting glutathione (GSH) biosynthesis, which leads to the overproduction of reactive oxygen species (ROS)[3]. In addition, BSO has been recently reported to trigger ferroptosis in various cancer cells[4,5].

While searching for potential therapeutic drugs for mitochondrial diseases, we identified apomorphine as a potential therapeutic drug for LS and MELAS[6]. Apomorphine is a known treatment for Parkinson's disease (PD) and erectile dysfunction[7–9]. It is a broad-spectrum dopamine agonist for all subtypes ranging from the dopamine D1 receptor to the D5 receptor. Apomorphine exerts protective effects by inhibiting oxytosis and stress-dependent non-apoptotic cell death via activation of the dopamine D4 receptor (D4R) in a micromolar order[10,11].

Because oxytosis shares some concepts with ferroptosis proposed in recent years, one hypothesis is that the ferroptotic action of apomorphine is related to dopamine receptors. Ferroptosis is a common form of regulated cell death that is distinguished from apoptosis and necroptosis and is a form of lipid- and iron-dependent cell death associated with GSH depletion[12–14]. The mechanism of ferroptosis includes oxidative damage to cellular structures and dysfunction in membrane stability triggered by polyunsaturated fatty acid peroxidation[13,15]. It can be induced by GSH depletion using chemicals such as BSO, cystine-glutamate transporter inhibition, or GPX4 inhibition[12,16]. Among them, RSL3, which can inactivate GPX4, is the most commonly used inducer of ferroptosis, leading to excessive lipid peroxidation, which causes cell death[16]. There are also several biomarkers of ferroptosis,

[1]Department of Pediatrics, Jichi Medical University, Shimotsuke, Japan. [2]Division of Inflammation Research, Center for Molecular Medicine, Jichi Medical University, Shimotsuke, Japan. [3]Diagnostics and Therapeutics of Intractable Diseases, Intractable Disease Research Center, Graduate School of Medicine, Juntendo University, Tokyo, Japan. [4]Department of Life Science, Faculty of Science and Engineering, Kindai University, Osaka, Japan. [5]Department of Clinical Genomics & Pediatrics (Faculty of Medicine), Saitama Medical University, Saitama, Japan. [6]Center for Intractable Diseases, Saitama Medical University Hospital, Saitama, Japan. [7]Department of Anatomy, Division of Histology and Cell Biology, School of Medicine, Jichi Medical University, Shimotsuke, Japan. [8]Division of Ultrastructural Research, National Institute for Physiological Sciences, Okazaki, Japan. ✉email: r0750am@jichi.ac.jp; hosaka@jichi.ac.jp

including protein markers, such as PTGS2 (which encodes COX-2), lipid peroxidation, and ROS[17–20]. In recent years, ferroptosis has been widely investigated for its involvement in various diseases, including mitochondrial diseases, neurodegenerative diseases, liver toxicity, liver fibrosis, hemochromatosis, and cardiomyopathy[13,21–24]. Also ferroptosis is regulated by various cellular metabolic pathways, including redox homeostasis, mitochondrial activity, and iron metabolism[13,15].

In the present study, we found that apomorphine inhibited ferroptosis in fibroblasts from patients with mitochondrial disease as well as in normal controls, and the cell-protective effect was not related to the agonistic action of the dopamine receptor.

Results

Induction of ferroptosis by GSH depletion by BSO and prevention of BSO-induced ferroptosis by apomorphine in LS patient fibroblasts

BSO reduced GSH production in a concentration-dependent manner[25]. Under these conditions, fibroblasts from LS patients showed enhanced cell death and were more vulnerable to BSO-induced cell stress than control fibroblasts, as previously described (Fig. 1A,B)[6]. We subsequently performed BSO-induced cell survival assays to investigate whether or not they were suppressed by adding ferrostatin-1 (Fer-1), one of the most common ferroptosis inhibitors[13,16], to LS patient-derived fibroblasts. Fer-1 showed dramatic cell-protective effects under BSO-induced stress, and apomorphine showed similar effects (Fig. 1C).

Protective effect of apomorphine against ferroptosis induced by BSO and RSL3

To evaluate the effects of apomorphine against ferroptosis, we examined the survival of LS fibroblasts in the presence of RSL3 as a common assay for ferroptosis screening, in addition to a BSO assay[16,26]. Prior to that, we examined the cell survival rate of control and patient fibroblasts under RSL3-induced stress, an inducer of ferroptosis. Fibroblasts obtained from LS, MELAS, mitochondrial cardiomyopathy, and KSS patients showed enhanced cell death in response to RSL3-induced stress, but this effect was less pronounced than the response to BSO-induced stress (Supplementary Fig. 1A–F).

Subsequently, we compared the cell protective effect of apomorphine with that of Fer-1 and Liproxstatin-1 (Lip-1), well-known specific ferroptosis inhibitors[16,27,28]. Apomorphine in LS fibroblasts under ferroptosis induced by BSO showed cell-protective effects, but we could not investigate the effects of apomorphine in response to BSO-induced stress in control fibroblasts because BSO did not induce cell death in control fibroblasts (Fig. 2A). In the case of RSL3-induced stress, the difference in the survival between control and LS fibroblasts was less than that in response to RSL3-induced stress; apomorphine showed cell-protective effects in both control and LS fibroblasts. The effects of apomorphine were similar to those of Fer-1 and Lip-1 (Fig. 2B). We also examined other fibroblasts from different subtypes of mitochondrial diseases in the presence of RSL3 and obtained similar results (Fig. 2C).

We next examined the effects of various inhibitors of cell death pathways other than ferroptosis to rule out the possibility that apomorphine protects cells via other cell death pathways using GSK-872 (necroptosis inhibitor) or Z-VAD-FMK (apoptosis inhibitor). Although we could not examine the effects of these inhibitors in response to BSO-induced stress in control fibroblasts, BSO did not induce cell death in control fibroblasts, and neither GSK-872 nor Z-VAD-FMK showed any cell-protective effects against cell death induced by BSO and RSL3 (Fig. 3A,B).

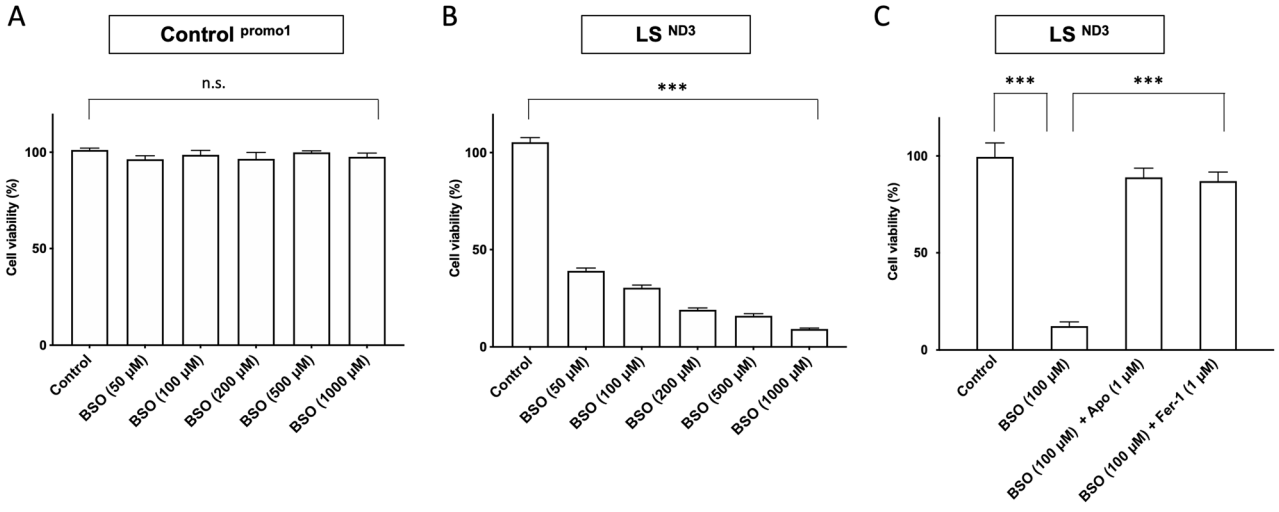

Figure 1. The cell viability assay for fibroblast cells from LS patients (LS^{ND3}) under BSO-induced stress. While the fibroblasts of control subjects were able to maintain almost full viability (**A**), those from patients with LS showed enhanced BSO dose-dependent cell death (**B**). Under the conditions of 100 μM BSO treatment, we evaluated the effects of Fer-1 (1 μM), which is one of the most common ferroptosis inhibitors and Apo (1 μM). Fer-1 showed dramatic cell-protective effects, similar to those of Apo (**C**). *Apo* apomorphine, *Fer-1* Ferrostatin-1. Data (n = 6) are expressed as the mean ± SD ***P < 0.001. *n.s.* no statistical significance.

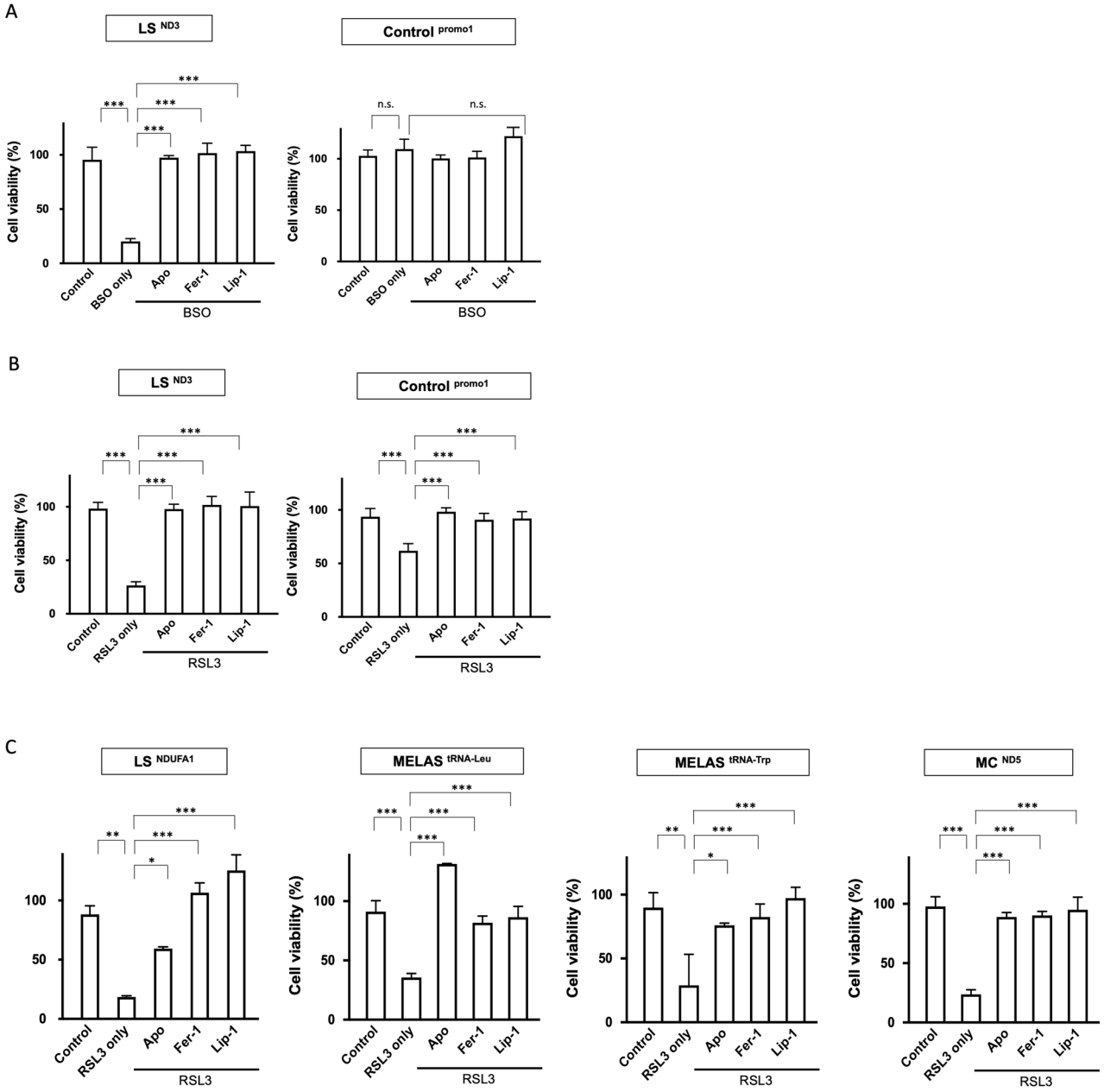

Figure 2. The anti-ferroptosis effect of apomorphine. (**A,B**) The cell viability assay of fibroblasts from LS patients (LS^{ND3}) (left panel) and control (right panel) in the presence of 100 μM BSO and RSL3. (**C**) The cell viability assay of fibroblasts from patients with LS (LS^{NDUFA1}), MELAS ($MELAS^{tRNA\text{-}Leu}$, $MELAS^{tRNA\text{-}Trp}$), mitochondrial cardiomyopathy (MC^{ND5}), and KSS ($KSS^{large\ deletion}$). The cell-protective effects of apomorphine were also shown in comparison to Fer-1, and Lip-1 in the presence of RSL3. *Apo* apomorphine, *Fer-1* Ferrostatin-1. Data (n = 6) are expressed as the mean ± SD *P < 0.05, **P < 0.01, ***P < 0.001. n.s. indicates no significance.

These findings suggest that apomorphine protects against cell death by ferroptosis, but not by necroptosis or apoptosis, in control fibroblasts and fibroblasts derived from patients with mitochondrial disease.

Measurement of intracellular ferroptotic metabolites in our cell lines by a BSO cell lipid oxidation assay

Because the accumulation of lipid ROS is a hallmark of ferroptosis, we monitored the lipid ROS accumulation using C11 BODIPY 581/591 by confocal imaging (Fig. 4). The C11 BODIPY 581/591 changes the fluorescence from red to green upon oxidation[29]. Even in the absence of BSO, LS patient-derived fibroblasts showed the oxidized form of C11 BODIPY, which is indicative of lipid ROS (Fig. 4A_b). Upon BSO treatment, fibroblasts showed an increased lipid ROS accumulation (Fig. 4A_c). Furthermore, Fer-1, one of the most common inhibitors of ferroptosis, recovered the lipid ROS accumulation. When we examined the effect of apomorphine on the

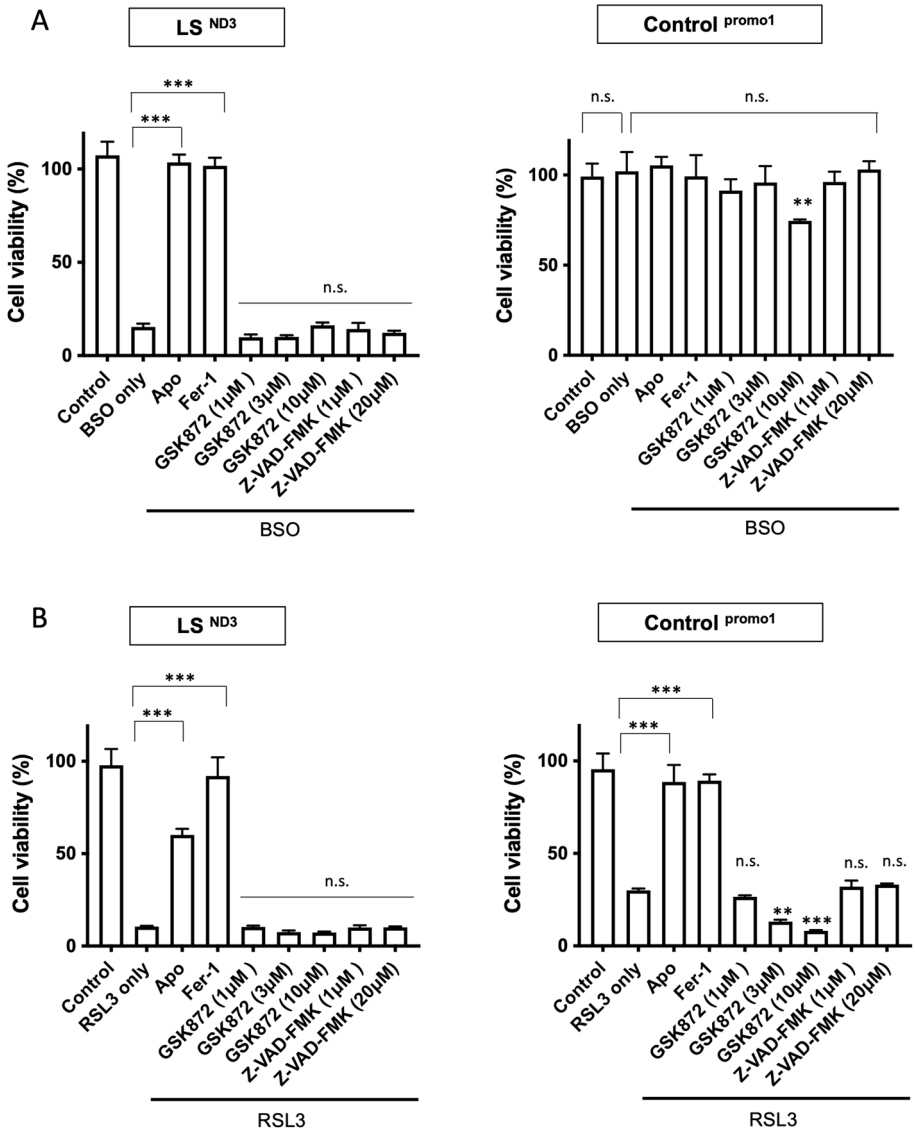

Figure 3. Cell viabilities by apoptosis and necroptosis inhibitors. The effects of an apoptosis inhibitor (GSK872) and a necroptosis inhibitor (Z-VAD-FMK) under conditions of 100 μM BSO- (**A**), and RSL3- (**B**) induced stress for fibroblast cells from LS patients (LS^{ND3}) (left) and controls (right). *Apo* apomorphine, *Fer-1* Ferrostatin-1. Data (n = 3) are expressed as the mean ± SD *P < 0.05, ** P < 0.01, ***P < 0.001. n.s. indicates no significance.

accumulation of lipid ROS in LS patient-derived fibroblasts treated with BSO, apomorphine decreased the lipid ROS accumulation and showed a similar effect to Fer-1 (Fig. 4A_d,e)[16]. In contrast, control fibroblasts showed almost no change in the degree of the lipid ROS accumulation (Fig. 4B_a–o).

The assessment of the expression of genes related to ferroptosis in apomorphine-treated vs. untreated LS fibroblasts by real-time reverse transcription polymerase chain reaction (RT-PCR) and Western blotting

We assessed the expression of *prostaglandin endoperoxide synthase 2 (PTGS2)*, a biomarker of ferroptosis that encodes cyclooxygenase-2 (COX-2)[13,17–19] in LS fibroblasts (LS^{ND3}). Real-time RT-PCR showed that RSL3 upregulated *PTGS2* expression in LS fibroblasts and that this *PTGS2* upregulation was inhibited by apomorphine and Fer-1 treatment (Fig. 5A). Western blotting for PTGS2 showed that apomorphine significantly decreased the protein levels of PTGS2 in LS fibroblasts, and Fer-1 had a similar effect (Fig. 5B). We therefore demonstrated that apomorphine suppressed PTGS2, a key factor linking ferroptosis and inflammation, in LS fibroblasts.

The analysis of the expression of genes related to ferroptosis in apomorphine-treated vs. untreated LS fibroblasts by real-time RT-PCR

To examine how apomorphine inhibits ferroptosis, we assessed the following key genes related to ferroptosis: *AIFM2* (encoding FSP1), *GPX4, ACSL4*, and *SLC7A11* (cystine/glutamate transporter)[13,17–19]. Real-time RT-PCR

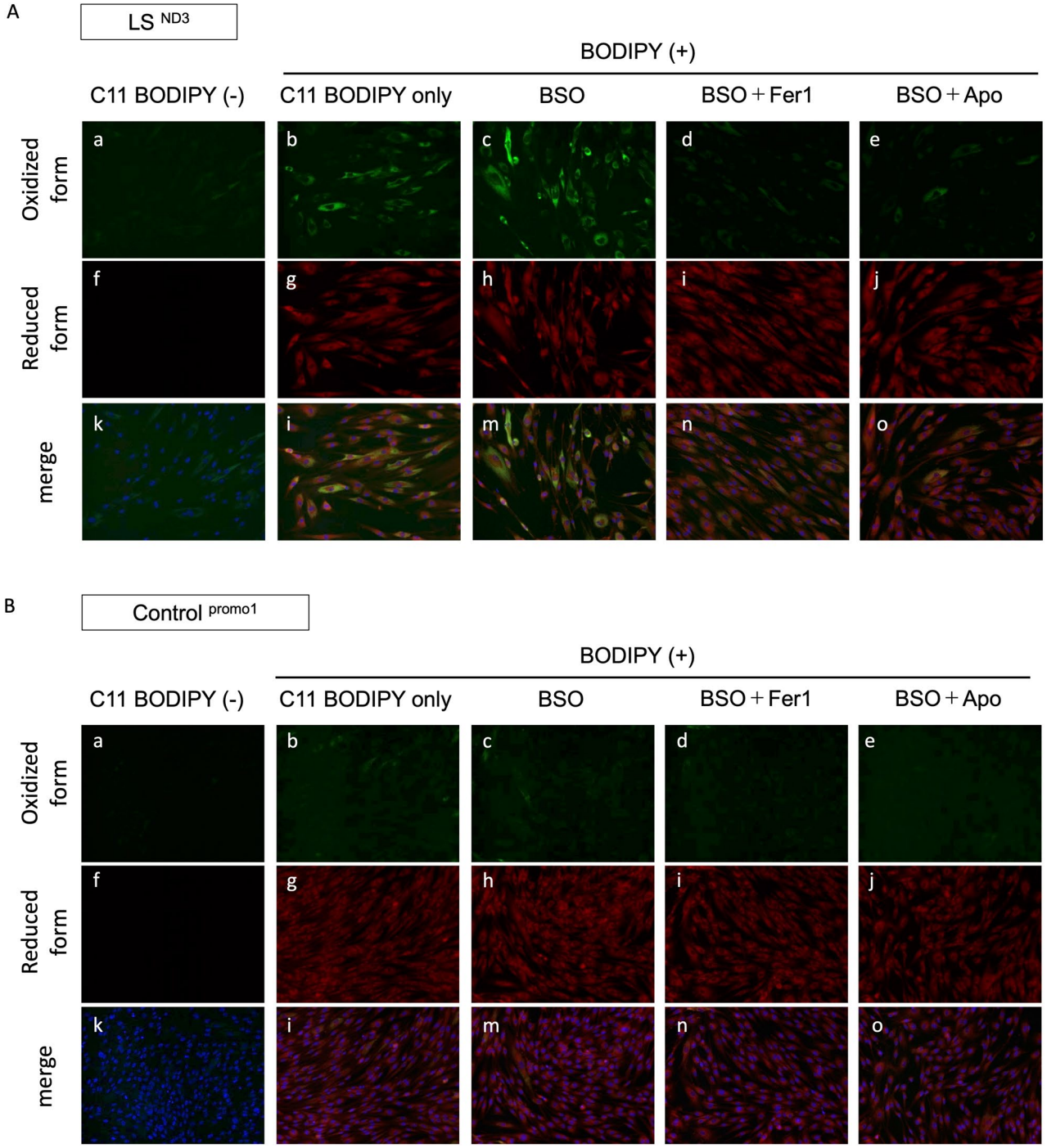

Figure 4. Results of a C11 BODIPY581/591 assay in fibroblasts from patients and controls. Measurement of intracellular ferroptotic metabolites by the BSO cell lipid oxidation assay. (**A**) Fibroblasts from LS patients (LS^{ND3}) were treated with BSO (100 μM) for 24 h in the presence or absence of Apo (1 μM) and Fer-1 (1 μM). (**B**) Control fibroblasts were treated with BSO (100 μM) for 24 h in the presence or absence of Apo (1 μM) and Fer-1 (1 μM). Lipid peroxidation was assessed by C11 BODIPY581/591 staining. Representative images of C11 BODIPY581/591 staining in LS^{ND3} cells and control cells; Oxidized form (**a–e**), Reduced form (**f–j**), and merge (**k–o**). *Apo* apomorphine, *Fer-1* Ferrostatin-1.

showed that apomorphine slightly suppressed the upregulation of *SLC7A11*; however, the differences were not statistically significant. Apomorphine also did not affect the mRNA expression of *AIFM2, GPX4,* or *ACSL4* (Fig. 6A–D).

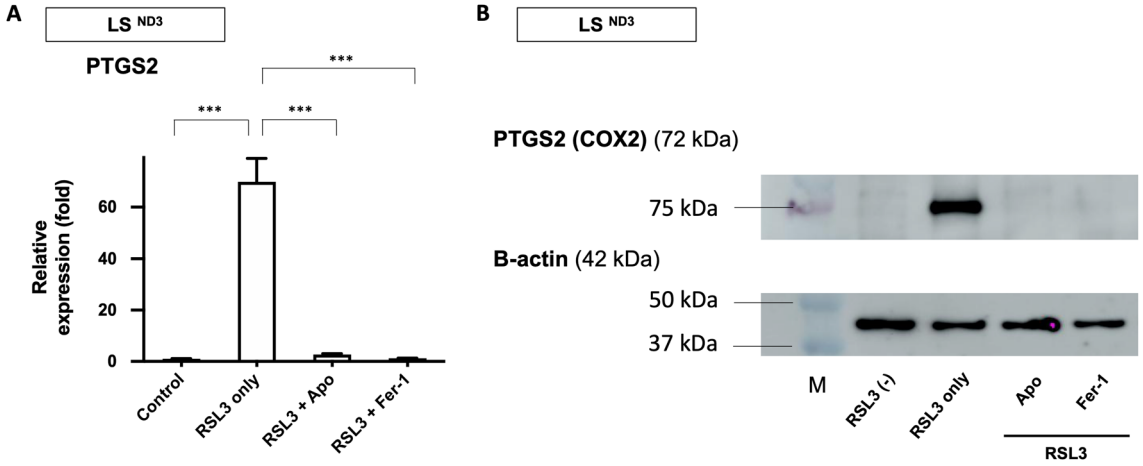

Figure 5. An expression analysis of prostaglandin-endoperoxide synthase 2 (PTGS2). (**A**) *PTGS2* mRNA levels in LS^{ND3} cells treated with RSL3 (100 nM) for 24 h in the presence or absence of Apo (1 μM) and Fer-1 (1 μM) were assessed using real-time RT-PCR. (**B**) PTGS2 protein levels in LS^{ND3} cells treated with RSL3 (100 nM) for 24 h in the presence or absence of Apo (1 μM) and Fer-1 (1 μM) were assessed by Western blotting. Full-length gels and blots are included in a Supplementary (Supplemental Fig. 3) as full-length dot blots. *Apo* apomorphine, *Fer-* Ferrostatin-1. Data are expressed as the mean ± SD; ***P < 0.001.

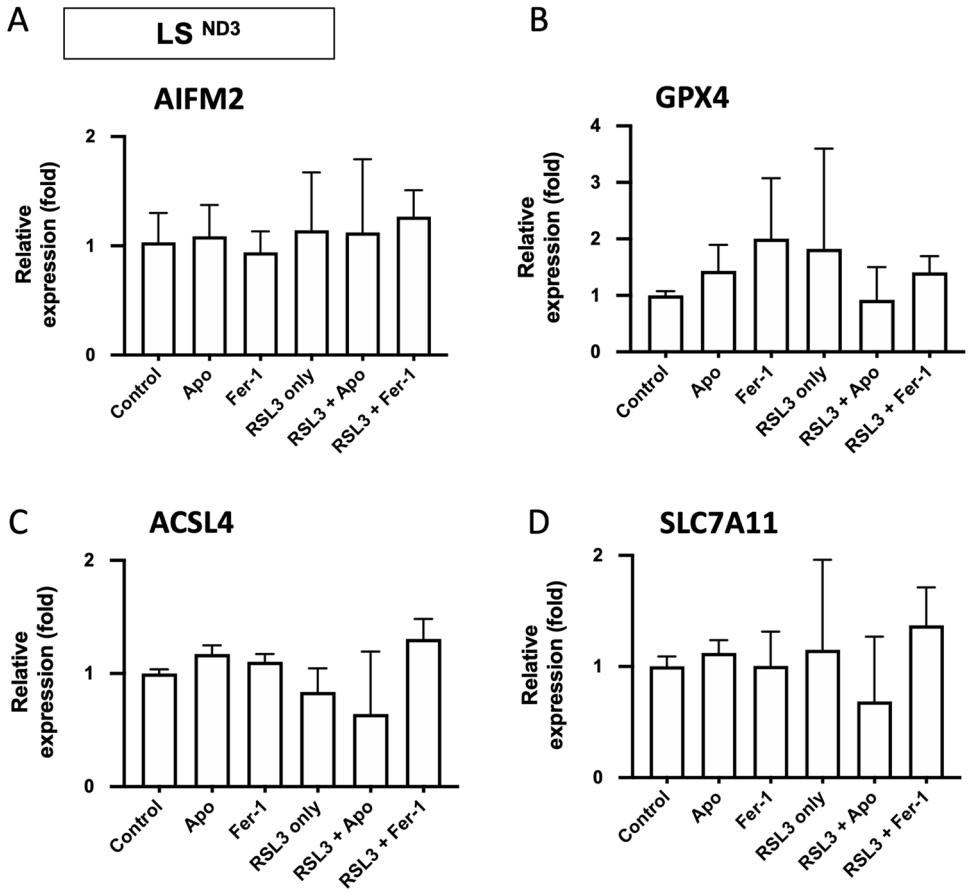

Figure 6. The mRNA levels of various ferroptosis marker genes. (**A**) *AIFM2* (encoding FSP1), (**B**) *GPX4,* (**C**) *ACSL4*, and (**D**) *SCL7A11* (Cystine/glutamate transporter) mRNA levels in LS^{ND3} cells treated with RSL3 (100 nM) for 24 h in the presence or absence of Apo (1 μM) and Fer-1 (1 μM) were assessed by real-time RT-PCR. *Apo* apomorphine, *Fer-1* Ferrostatin-1. Data are expressed as the mean ± SD *P < 0.05, ** P < 0.01, ***P < 0.001. n.s. indicates no significance.

The anti-ferroptosis effect of apomorphine is not related to the dopamine receptor agonist action of apomorphine

Our previous screening did not show the cell protective effects of other dopamine agonists (Ropinirole hydrochloride and Pramipexole dihydrochloride; both specific to D2 receptors) (Supplemental Fig. 2). Therefore, to evaluate whether or not the agonistic action of apomorphine was related to its cell-protective effect, we examined the effect of the addition of agonists and/or antagonists of each dopamine receptor on the cell-protective effect of apomorphine.

Prior to this, the expression of each dopamine receptor in the cells was examined by RT-PCR. The expression of four types of dopamine receptors—D1R, D2R, D4R, and D5R—was confirmed in LS and control fibroblasts, but the expression of D3R was not detected in our fibroblasts (Fig. 7A). Therefore, we examined the action of each dopamine receptor on the protection of apomorphine, except for D3R.

First, we examined the contribution of D4R to the effects of apomorphine using agonists and antagonists of D4R, based on a previous report[10]. As shown in Fig. 7B, the D4R agonists did not enhance the effect of apomorphine, and the antagonists did not inhibit this effect. Similarly, antagonists of D1R and D2R did not affect the effect of apomorphine (Fig. 7C,D). Regarding D5R, as there was no commercially available antagonist for D5R, only the D5R agonist was used, but it did not provide any cell-protective effect (Fig. 7E).

Discussion

We previously showed that apomorphine protects against BSO-induced stress with an EC50 of approximately 50 nM and improves the mitochondrial respiratory activity of fibroblasts from patients with LS and MELAS[6]. In the present study, we showed that fibroblasts from mitochondrial diseases including LS and MELAS were vulnerable to ferroptosis, and apomorphine markedly protected fibroblasts from ferroptosis induced by RSL3 in addition to BSO in various types of mitochondrial diseases as well as in normal fibroblasts. The effect of ferroptosis on cell protection was comparable to that of the specific ferroptosis inhibitors Fer-1 and Lip-1. We observed that BSO- or RSL3-induced ferroptosis was not inhibited by inhibitors of apoptosis (Z-VAD-FMK) or necroptosis (GSK-872), and *PTGS2,* which is known to be a marker of ferroptosis, was decreased by the addition of apomorphine. In addition, we confirmed that the effects of apomorphine were not related to its agonistic dopamine action.

Ferroptosis is an iron-dependent form of cell death caused by the accumulation of lipid hydroperoxides and is distinguished from other forms of cell death, such as apoptosis and necroptosis[14,16]. Ferroptosis occurs when GPX4 is directly or indirectly inhibited by GSH depletion, which leads to the accumulation of membrane lipid peroxidation and results in cell death[13,15,16]. RSL3 is commonly used as a specific inducer of ferroptosis and inactivates GPX4, leading to excessive lipid peroxidation, which causes cell death[16]. In contrast, ferroptosis can be suppressed by lipophilic antioxidants, inhibitors of lipid peroxidation, iron chelators, and polyunsaturated fatty acids[16]. Currently, several biomarkers of ferroptosis exist, including protein markers such as PTGS2, lipid peroxidation, and ROS[17–20].

Apomorphine has been administered to patients with advanced PD as a rescue drug for "off" symptoms because of its short half-life. However, the continuous subcutaneous administration of apomorphine reportedly improves both motor symptoms as well as brain glucose metabolism and non-motor symptoms, such as the cognitive function, the executive function, and apathy in PD patients[30,31]. PD is known for the characteristic pathology of progressive dopaminergic neuronal death associated with iron accumulation, and it is suggested to be driven in part by ferroptosis[32,33]. The anti-ferroptosis effects of apomorphine shown in this study may explain these neuroprotective effects. To test this hypothesis, we need to study the effects in cells derived from patients with PD and animal models.

We have already shown that apomorphine suppresses the production of ROS[6]. In the present study, we showed that apomorphine prevented lipid peroxidation and upregulation of the mRNA expression of *PTGS2* (Fig. 5), which are key features of ferroptosis. Studies on cancer cells have indicated that ferroptosis can directly increase the expression of *PTGS2* and cause inflammation by accelerating AA metabolism and promoting the secretion of pro-inflammatory molecules[34,35]. The downregulation of *PTGS2* may be related to the inhibition of various cytokines and chemokines by apomorphine[6]. Recently, ferroptosis has been suggested to be involved in epilepsy with mitochondrial disease[12]. Our study also supports the hypothesis that fibroblasts from various mitochondrial diseases are vulnerable to ferroptosis.

Apomorphine reportedly protects against glutamate-induced oxidative cell death via dopamine receptors, especially D4, in the HT22 cell line[10]. In this assay system, the protective effect was reversed by D4 antagonists but not by D1 or D2 antagonists. A selective D4 agonist also protects neurons from glutamate-induced cell death. However, in our assay system using fibroblasts, the D4 agonist did not exert cell protective effects, and the D4 antagonist did not prevent the cell-protective effect of apomorphine. Furthermore, our data do not support the involvement of subtypes D1, D2, and D5. Therefore, we conclude that the cell-protective effect of apomorphine is not related to dopamine receptors in our system. Dopamine agonistic action causes several common side effects, especially digestive symptoms, such as nausea, vomiting, loss of appetite, and constipation[36]. Our research presents a promising avenue for the potential development of apomorphine derivatives without dopamine agonist activity, which offer cellular protection without the undesirable effects associated with dopamine agonists.

The limitation of the present study was that we were unable to identify the mechanism underlying the protection from ferroptosis, as we only performed an RT-PCR assay of key inhibitory genes for ferroptosis. Elucidation of the binding proteins that explain anti-ferroptosis and their downstream signaling cascades is the next research question that should be explored.

In conclusion, we found that fibroblasts from patients with mitochondrial diseases were vulnerable to ferroptosis, which is inhibited by apomorphine in this study. The cell-protective effect of apomorphine has long been

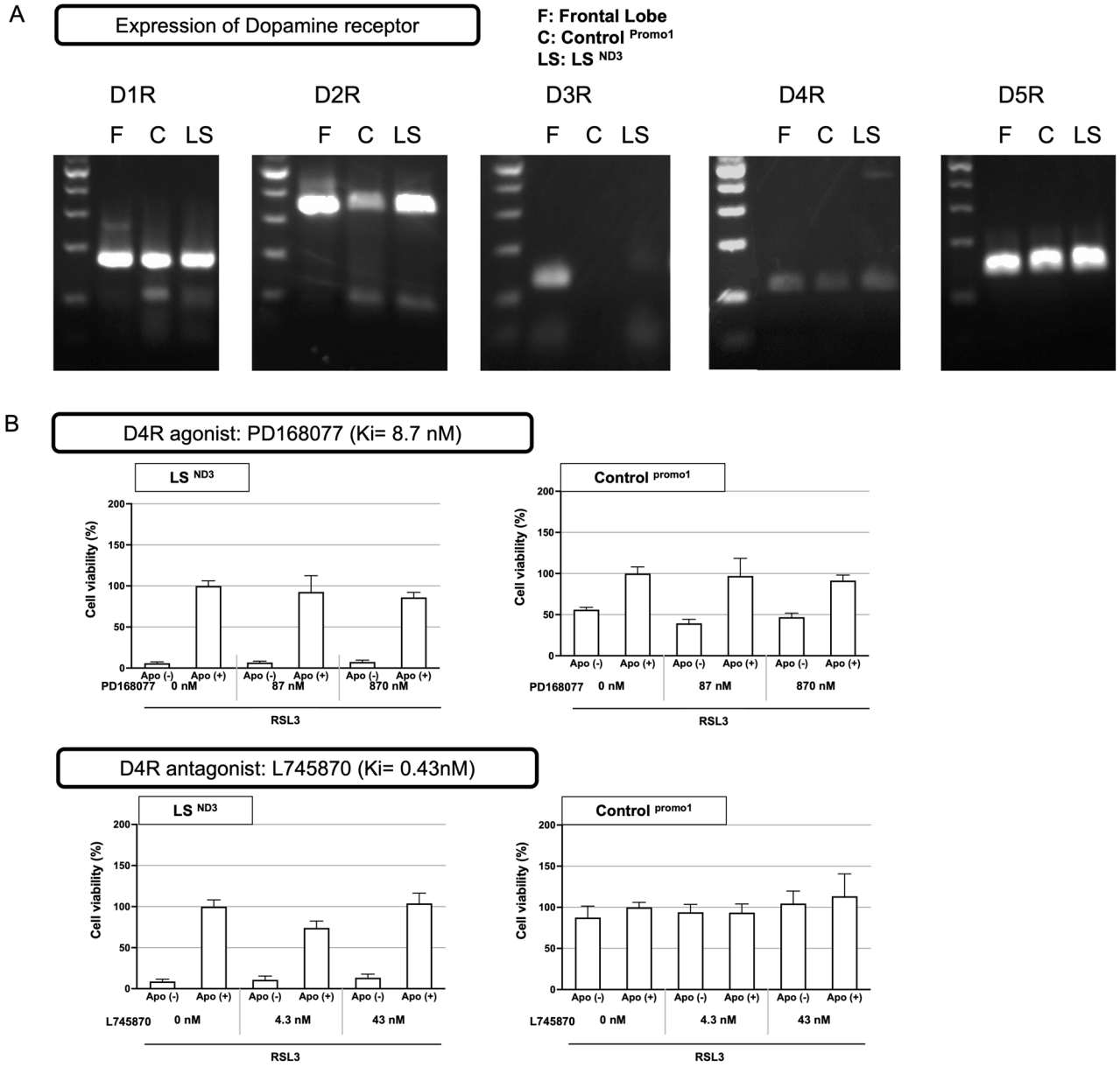

Figure 7. The expression of dopamine receptors (D1R-D5R) and interactions between apomorphine and dopamine receptor agonists or antagonists. (**A**) Agarose gel electrophoresis of the RT-PCR product of dopamine receptors. Results are shown from left to right in the order of D11R(size 184 bp), D2R (size 353 bp), D3R (size 137 bp), D4R (size 115 bp), and D5R (size 149 bp). In each column, the left lane shows the band of the frontal lobe as a positive control, the middle shows the band of control cells, and the right shows the band of LS cells. Original gels are presented in Supplementary Fig. 4. (**B–E**) The results of an RSL3-induced stressed cell viability assay to determine the influence of each dopamine receptor agonist or antagonist on the effects of apomorphine. The cell viability of the Apomorphine-treated group without RSL3 was used as 100% to compare other group's cell viabilities (n = 3). (**B**) D4R agonist: PD168077 (Ki = 8.7 nM) and D4R antagonist: L745870 (Ki = 0.43 nM), (**C**) D1R antagonist: SKF683566 (Ki = 0.56 nM), (**D**) D2R antagonist: Sulpiride (Ki = 0.015 μM), (**E**) D5R agonist: SKF38393 (Ki = 0.5 nM).

believed to be a result of D4R agonistic action, but we first revealed that at least part of its anti-ferroptosis effect is not related to the dopamine receptor agonist action. Our study suggests that ferroptosis may be a potential therapeutic target for mitochondrial disease and also provides hope for the creation of new drugs that maintain their cell-protective effect without the dopamine agonist effect, to avoid the adverse effects of dopamine.

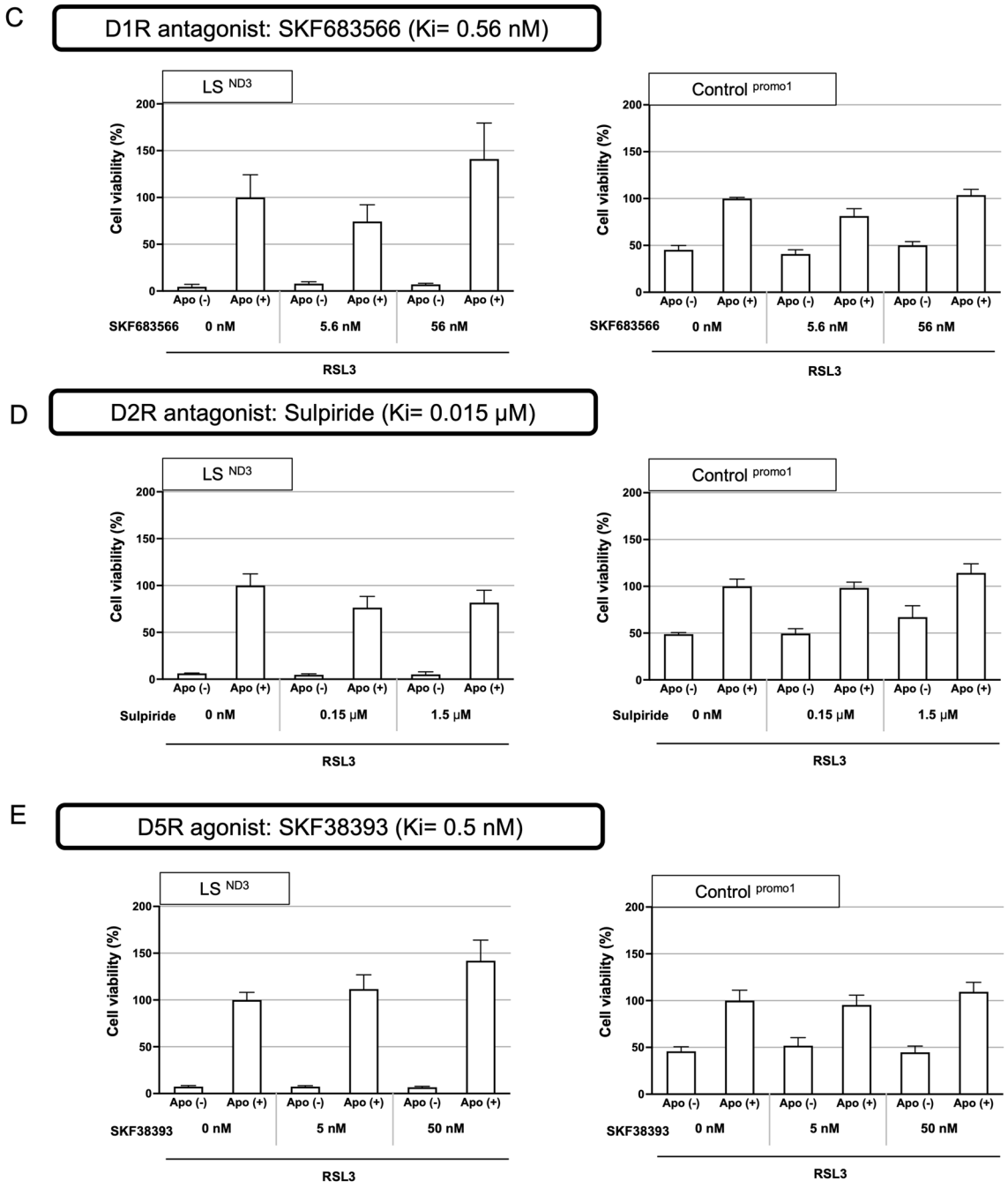

Figure 7. (continued)

Materials and methods

Subjects

This study was approved by the Jichi Medical University Clinical Research Ethics Committee (Approval Number: J21-014) and all methods of this study were performed in accordance with the relevant guidelines and regulations. Fibroblasts were obtained from six patients at Jichi Medical University, Kanagawa Children's Medical Center, and Saitama Medical University. The collection was conducted under the approval of the Jichi Medical University Clinical Research Ethics Committee, the Kanagawa Children's Medical Center Review Board and Ethics Committee, and the Ethics Committee of Saitama Medical Center, Saitama Medical University, with approval numbers J21-014, H2021-094, and 11303-06, respectively. Written informed consent was obtained from the parents of each patient. And we used fibroblasts from healthy individuals as controls (normal human dermal fibroblasts purchased from PromoCell Company [#C-12300; Heidelberg, Germany]). Our four patients were diagnosed with LS and MELAS, as previously described[6]. Two of the patients had genetically identified cases of LS, including one with an m.10158 T>C, p(S34P) mutation in *MT-ND3* (Case 1; LS^{ND3}) and one with a c.55 C>T, p(P19S) mutation in *NDUFA1* (Case 2; LS^{NDUFA1})[37,38]. Both ND3 and NDUFA1 are subunits of Complex I in the mitochondrial respiratory chain. Fibroblasts were also obtained from two patients with MELAS, including one

with an m.3243 A > G mutation in tRNA-Leu (Case 3; MELAS$^{tRNA\text{-}Leu}$) and one with an m.5541 C > T mutation in tRNA-Trp (Case 4; MELAS$^{tRNA\text{-}Trp}$)[39]. We additionally obtained fibroblasts from patients with two other types of mitochondrial diseases: mitochondrial cardiomyopathy (Case 5; MC^{ND5}) and Kearns-Sayer syndrome (KSS) (Case 6; KSS$^{large\ deletion}$). The patient with mitochondrial cardiomyopathy who presented with HCM and died at 4 months old had an m.13513G > A mutation in the ND5 subunit of complex I (*MT-ND5* m.13513G > A), with 78.87% heteroplasmy. The patient with KSS was genetically identified as having a large deletion (m.8290-13802) of mitochondrial DNA (Table 1). Fibroblasts with fewer than 20 passages from patients and controls were used in the experiments. The heteroplasmic rate was analyzed by deep sequencing of mutated regions.

Cell culture and growth conditions

Fibroblasts from patients were cultured in 1.0 g/L low-glucose Dulbecco's Modified Eagle's medium (DMEM) supplemented with 10% fetal bovine serum (FBS), 100 units/mL penicillin, and 100 µg/mL streptomycin. Cells were incubated at 37 °C in 5% CO_2.

Reagents

L-Butionine (S, R)-sulfoximine (BSO, No. B690270), a glutathione synthesis inhibitor, was purchased from Wako Pure Chemical Industries (Tokyo, Japan). RSL3 (No. S8155) was purchased from Selleck Chemicals (Houston, TX, USA). Fer-1 (No. SML0583) and Lip-1 (No. SML1414) were obtained from Sigma-Aldrich (St. Louis, MO, USA). Z-VAD-FMK (No. 3188-v) and GSK-872 (No. HY-101872) were purchased from Peptide Institute Inc. (Osaka, Japan) and MedChemExpress (Shanghai, China), respectively. All reagents were dissolved in dimethyl sulfoxide (DMSO).

Cell viability assays

The BSO assay was performed as previously described[6]. We performed several cell viability assays to investigate ferroptosis. Ferroptotic cell death was induced in fibroblasts by ferroptosis inducers (RSL3 at 50–100 nM). In these cell viability experiments, fibroblasts were cultured to semi-confluence and plated at 5,000 cells per well in a 96-well culture plate in normal medium. After incubation for 24 h, apomorphine and several compounds were added as positive controls (Fer-1, or Lip-1) and cultured in the assay medium. All compounds were applied at a concentration of 1 µM unless otherwise indicated. After incubating the cell plates for 24 h at 37 °C (95% humidity and 5% CO_2), a cell viability assay was performed using Cell Count Reagent SF (Nacalai Tesque, Kyoto, Japan). Fluorescence intensity was measured using a Benchmark Plus microplate reader (Bio-Rad, Hercules, CA, USA) according to the manufacturer's instructions.

The assessment of lipid peroxidation

Lipid peroxidation was examined using the fluorescent dye C11-BODIPY581/591 (No. D3861; Thermo Fisher Scientific, Waltham, MA, USA)[29]. Fibroblasts were cultured to semi-confluence and then plated at 5,000 cells per well in a 96-well culture plate in normal medium. After incubation for 24 h, BSO and several other compounds (e.g. apomorphine and Fer-1) were added to each well. After incubation for 24 h, the cells were labeled with 5 µM C11-BODIPY581/591 for 30 min in the assay medium. The nuclei were stained with Hoechst 33,342. Representative images were obtained using a Keyence All-in-One Fluorescence BZ-X810 microscope (Keyence Co., Itasca, IL, USA).

RNA extraction and real-time RT-PCR

Total RNA was extracted from fibroblasts using an RNeasy® Mini Kit (QIAGEN, Valencia, CA, USA) according to the manufacturer's instructions[40]. Total RNA was reverse transcribed to cDNA, followed by amplification by PCR with a Superscript® VILO cDNA synthesis kit at 60 °C (Invitrogen; Thermo Fisher Scientific). Real-time RT-PCR was performed using the SYBR Green system with a primer set that amplified a fragment of the target genes to measure the mRNA expression. The following primers were used: *PTGS2* (Forward primer 5′-GCCTGAATGTGC

Case	Cell ID	Disease	Age (years)	Gene mutation	Protein	Mutation rate (%)
1	LS^{ND3}	Leigh	0	m.10158 T > C, p.(S34P)	ND3	90
2	LS^{NDUFA1}	Leigh	5	c.55 C > T, p.(P19S)	NDUFA1	Nuclear gene
3	MELAS$^{tRNA\text{-}Leu}$	MELAS	14	m.3243 A > G	(tRNA-Leu)	21
4	MELAS$^{tRNA\text{-}Trp}$	MELAS	23	m.5541 C > T	(tRNA-Trp)	49
5	MC^{ND5}	mitochondrial cardiomyopathy	0	m.13513 G > A p.(D393N)	ND5	79
6	KSS$^{large\ deletion}$	KSS	1	m.8290-13802del	–	–
	Promo1	Control	0	–	–	–

Table 1. Fibroblast cell lines from patients with mitochondrial disease. Respiratory chain activities from fibroblasts: LS^{ND3}—Complex I 9.8%, II 93.9%, III 94.5%, IV 47.6%, and CS 100.9%. LS^{NDUFA1}—Complex I 27.6%, II 104.3%, III 70.1%, IV 77.7%, CS 77.4%. MELAS$^{tRNA\text{-}Leu}$—Not available. MELAS$^{tRNA\text{-}Trp}$—Complex I 48%, II 103%, III 65%, IV 18%, MC^{ND5}—not available. KSS$^{large\ deletion}$—not available. *LS* Leigh syndrome, *MELAS* myopathy encephalopathy, lactic acidosis, and stroke-like episodes, *MC* mitochondrial cardiomyopathy, *KSS* Kearns-Sayer syndrome.

CATAA-GACTGAC-3′, Reverse primer 5′-AAACCCACAGTG-CTTGACACACA-3′), *AIFM2* (Forward primer 5′-ATGGTTCGGCTGACCAAGAG-3′, Reverse primer 5′-GCCACCACATCATTGGCATC-3′), *GPX4* (Forward primer 5′-GCCTTCCCGTGTAACCAGT-3′, Reverse primer 5′-GCGAACTCTTTGATCT-CTTCG-3′), *ACSL4* (Forward primer 5′-CCCTGAAGGATTTGAGATTCACA-3′, Reverse primer 5′-CCTTAGGT-CGGCCAGTA GAAC-3′), *SLC7A11* (Forward primer 5′-ATGCAGTGGCAGTGA-CCTTT-3′, Reverse primer 5′-GGCAAC AAAGATCG-GAACTG-3′), and *GAPDH* (Forward primer 5′-CTTTGTCAAGCTCATTTCCTGG-3′, Reverse primer 5′-TCTTC-CTCTTGTGCTCTTGC-3′). The reactions were performed in triplicate. Gene expression was normalized to that of *GAPDH*, and the data were analyzed in the Excel software program, version 16.75 (Microsoft, Redmond, WA, USA) using the ΔΔCt method.

Western blotting

For whole-cell extracts, cells were lysed in TNE buffer (20 mM Tris–HCL at pH 7.4, 150 mM NaCl, 1 mM EDTA at pH7.4). Protein concentrations were determined using the Qubit® Protein Assay Kit (Invitrogen; Thermo Fisher Scientific). Whole-cell lysates were mixed with an equal volume of 2 × sodium dodecyl sulfate (SDS) sample buffer and boiled. Western blotting was performed using 20 µg of total protein, and immunoprecipitation was performed using XV PANTERA GEL (NXV-361HP; DRC Co., Ltd, Tokyo, Japan). Total cell proteins were separated by 10% SDS–polyacrylamide gel electrophoresis (PAGE) and transferred to a PVDF membrane by electrotransfer. The membrane was blocked for 1 h at room temperature (RT) using 5% skimmed milk/phosphate-buffered saline with Tween (PBST) and then incubated with the following primary antibodies: rabbit monoclonal anti-PTGS2 (Cox2(D5H5)XP #12282; Cell Signaling, Danvers, MA, USA) at 1:1000 and mouse monoclonal anti-beta-actin (A1978; Sigma-Aldrich) at 1:5000 in PBST overnight at 4 °C. After washing with PBST 3 times for 10 min each, the membrane was incubated with the following secondary antibodies: anti-rabbit IgG horseradish peroxidase (HRP; Cell Signaling) at 1:3000 and anti-mouse IgG HRP (Santa Cruz Biotechnology, Santa Cruz, CA, USA) at 1:2000 for 1 h at RT. After washing with PBST 3 times for 15 min each, the membrane was incubated with Hyper HRP Substrate (TAKARA BIO INC., Ohtsu, Japan) for 2 min. Finally, chemiluminescence from the membrane was imaged using Amersham Imager 680 (GE Healthcare UK Ltd., Little Chalfont, UK). Protein intensities were measured using the ImageJ software program (https://imagej.net/ij/) Relative protein levels or protein abundances were normalized to those in the control group.

Detection of dopamine gene receptor (DRD1-DRD5) expression on control and patient-derived fibroblasts by RT-PCR

RNA was extracted from isolated control and LS patient fibroblasts (LS^{ND3}) using an RNeasy Mini Kit (QIAGEN) according to the manufacturer's protocol. Commercial human Adult Normal Tissue: Brain: Frontal Lobe (BioChain, Newark, CA, USA) was used as the Positive Control. Total RNA (1500–2000 ng) was reverse-transcribed into first-strand cDNA using the Superscript VILO cDNA Synthesis kit (Invitrogen; Thermo Fisher Scientific). RT-PCR was performed using intron-spanning primers (Supplemental Table 1). The D1R/D2R/D5R cycle conditions were as follows: 94 °C for 2 min for polymerase activation, followed by 45 cycles at 98 °C for 10 s, 62 °C for 30 s, 68 °C for 1 min. The D3R cycle conditions were as follows: 94 °C for 2 min for polymerase activation, followed by 45 cycles of 98 °C for 10 s, 62 °C for 15 s, 72 °C for 1 min. The D4R cycle conditions were as follows: 94 °C for 2 min for polymerase activation, followed by 5 cycles of 98 °C for 10 s, 68 °C for 1 min, followed by 5 cycles of 98 °C for 10 s, 66 °C for 1 min, followed by 5 cycles of 98 °C for 10 s, 64 °C for 1 min, followed by 25 cycles of 98 °C for 10 s, 62 °C for 1 min, 68 °C for 7 min. The products were resolved on a 2% agarose gel containing ethidium bromide and photographed.

Interactions between apomorphine and dopamine receptor agonists or antagonists: Effects on cell viability

Cell viability assays to examine the influence of dopamine receptor agonists or antagonists on the effects of apomorphine were performed under RSL-induced oxidative stress. SKF 83566 cells (no. HY-103430A; MedChemExpress) was used as the D1R antagonist[41], sulpiride (No. S4655; Selleck Chemicals) as the D2R antagonist[42], PD168077 (No. HY-21098A; MedChemExpress) as the D4R agonist[43]; L745870 (No. HY-14325; MedChemExpress) as the D4R antagonist[44], and SKF38393 (No. S7993; Selleck Chemicals) as the D5R agonist[45]. The concentrations used were determined based on the EC50 and Ki values[41–45].

A cell viability assay was performed as previously described[6]. In brief, fibroblasts were cultured in 1.0 g/L low-glucose DMEM with 10% FBS at 37 °C in 5% CO_2 until they reached semi-confluence. Fibroblasts were seeded at 5,000 cells per well in a 96-well plate. After 24 h of incubation, we divided the cells into 3 groups: a DR agonist- or antagonist-treated group, a DR agonist- or antagonist-treated group at a concentration 10 times the EC50 or Ki values, and a DR agonist- or antagonist-treated group at a concentration 100 times the EC50 or Ki values. Apomorphine was added at a final concentration of 1 µM. After 24 h of incubation, the cell survival rate was checked using Cell Count Reagent SF (Nacalai Tesque). The cell viability of Apomorphin-treated group without RSL3 was used as 100% to compare other group's cell viabilities.

Statistical analyses

The results are expressed as the mean ± standard deviation. Comparisons between multiple-group means were performed using a one-way analysis of variance with Bonferroni's post-hoc test. Statistical significance was set at $P < 0.05$. Statistical analyses were performed using the GraphPad Prism software program version 9.3.1 (GraphPad Software Inc., La Jolla, CA, USA).

Data availability

The datasets and raw data used and/or analyzed during the current study are available from the corresponding author on reasonable request.

Received: 16 September 2023; Accepted: 22 February 2024
Published online: 27 February 2024

References

1. Chi, C. S. Diagnostic approach in infants and children with mitochondrial diseases. *Pediatr. Neonatol.* **56**, 7–18. https://doi.org/10.1016/j.pedneo.2014.03.009 (2015).
2. Vafai, S. B. & Mootha, V. K. Mitochondrial disorders as windows into an ancient organelle. *Nature* **491**, 374–383. https://doi.org/10.1038/nature11707 (2012).
3. Marengo, B. *et al.* Mechanisms of BSO (L-buthionine-S, R-sulfoximine)-induced cytotoxic effects in neuroblastoma. *Free Radic. Biol. Med.* **44**, 474–482. https://doi.org/10.1016/j.freeradbiomed.2007.10.031 (2008).
4. Nishizawa, S. *et al.* Low tumor glutathione level as a sensitivity marker for glutamate-cysteine ligase inhibitors. *Oncol. Lett.* **15**, 8735–8743. https://doi.org/10.3892/ol.2018.8447 (2018).
5. Dai, C. *et al.* Transcription factors in ferroptotic cell death. *Cancer Gene Ther.* **27**, 645–656. https://doi.org/10.1038/s41417-020-0170-2 (2020).
6. Miyauchi, A. *et al.* Apomorphine rescues reactive oxygen species-induced apoptosis of fibroblasts with mitochondrial disease. *Mitochondrion* **49**, 111–120. https://doi.org/10.1016/j.mito.2019.07.006 (2019).
7. Hsieh, G. C. *et al.* Central mechanisms regulating penile erection in conscious rats: The dopaminergic systems related to the proerectile effect of apomorphine. *J. Pharmacol. Exp. Ther.* **308**, 330–338. https://doi.org/10.1124/jpet.103.057455 (2004).
8. Millan, M. J. *et al.* Differential actions of antiparkinson agents at multiple classes of monoaminergic receptor I A multivariate analysis of the binding profiles of 14 drugs at 21 native and cloned human receptor subtypes. *J. Pharmacol. Exp. Ther.* **303**, 791–804. https://doi.org/10.1124/jpet.102.039867 (2002).
9. Stacy, M. & Silver, D. Apomorphine for the acute treatment of "off" episodes in Parkinson's disease. *Parkinsonism Relat. Disord.* **14**, 85–92. https://doi.org/10.1016/j.parkreldis.2007.07.016 (2008).
10. Ishige, K., Chen, Q., Sagara, Y. & Schubert, D. The activation of dopamine D4 receptors inhibits oxidative stress-induced nerve cell death. *J. Neurosci.* **21**, 6069–6076. https://doi.org/10.1523/JNEUROSCI.21-16-06069.2001 (2001).
11. Himeno, E. *et al.* Apomorphine treatment in Alzheimer mice promoting amyloid-beta degradation. *Ann. Neurol.* **69**, 248–256. https://doi.org/10.1002/ana.22319 (2011).
12. Kahn-Kirby, A. H. *et al.* Targeting ferroptosis: A novel therapeutic strategy for the treatment of mitochondrial disease-related epilepsy. *PLoS ONE* **14**, e0214250. https://doi.org/10.1371/journal.pone.0214250 (2019).
13. Jiang, X., Stockwell, B. R. & Conrad, M. Ferroptosis: Mechanisms, biology and role in disease. *Nat. Rev. Mol. Cell Biol.* **22**, 266–282. https://doi.org/10.1038/s41580-020-00324-8 (2021).
14. Dixon, S. J. *et al.* Ferroptosis: An iron-dependent form of nonapoptotic cell death. *Cell* **149**, 1060–1072. https://doi.org/10.1016/j.cell.2012.03.042 (2012).
15. Dixon, S. J. & Pratt, D. A. Ferroptosis: A flexible constellation of related biochemical mechanisms. *Mol. Cell* **83**, 1030–1042. https://doi.org/10.1016/j.molcel.2023.03.005 (2023).
16. Stockwell, B. R. *et al.* Ferroptosis: A regulated cell death nexus linking metabolism, redox biology, and disease. *Cell* **171**, 273–285. https://doi.org/10.1016/j.cell.2017.09.021 (2017).
17. Yang, W. S. *et al.* Regulation of ferroptotic cancer cell death by GPX4. *Cell* **156**, 317–331. https://doi.org/10.1016/j.cell.2013.12.010 (2014).
18. Sampilvanjil, A. *et al.* Cigarette smoke extract induces ferroptosis in vascular smooth muscle cells. *Am. J. Physiol. Heart Circ. Physiol.* **318**, H508–H518. https://doi.org/10.1152/ajpheart.00559.2019 (2020).
19. Chen, X., Comish, P. B., Tang, D. & Kang, R. Characteristics and biomarkers of ferroptosis. *Front. Cell Dev. Biol.* **9**, 637162. https://doi.org/10.3389/fcell.2021.637162 (2021).
20. Li, Q. *et al.* Inhibition of neuronal ferroptosis protects hemorrhagic brain. *JCI Insight* **2**, e90777. https://doi.org/10.1172/jci.insight.90777 (2017).
21. Yamada, N. *et al.* Ferroptosis driven by radical oxidation of n-6 polyunsaturated fatty acids mediates acetaminophen-induced acute liver failure. *Cell Death Dis.* **11**, 144. https://doi.org/10.1038/s41419-020-2334-2 (2020).
22. Yamada, N. *et al.* Iron overload as a risk factor for hepatic ischemia-reperfusion injury in liver transplantation: Potential role of ferroptosis. *Am. J. Transplant.* **20**, 1606–1618. https://doi.org/10.1111/ajt.15773 (2020).
23. Wang, L. *et al.* P53-dependent induction of ferroptosis is required for artemether to alleviate carbon tetrachloride-induced liver fibrosis and hepatic stellate cell activation. *IUBMB Life* **71**, 45–56. https://doi.org/10.1002/iub.1895 (2019).
24. Gao, M. *et al.* Role of Mitochondria in ferroptosis. *Mol. Cell* **73**, 354–363. https://doi.org/10.1016/j.molcel.2018.10.042 (2019).
25. Kim, Y. A., Kim, M. Y. & Jung, Y. S. Glutathione depletion by L-buthionine-S, R-sulfoximine induces apoptosis of cardiomyocytes through activation of PKC-δ. *Biomol. Ther. (Seoul)* **21**, 358–363. https://doi.org/10.4062/biomolther.2013.065 (2013).
26. Shimada, K. *et al.* Global survey of cell death mechanisms reveals metabolic regulation of ferroptosis. *Nat. Chem. Biol.* **12**, 497–503. https://doi.org/10.1038/nchembio.2079 (2016).
27. Yang, W. S. & Stockwell, B. R. Ferroptosis: Death by lipid peroxidation. *Trends Cell Biol.* **26**, 165–176. https://doi.org/10.1016/j.tcb.2015.10.014 (2016).
28. Wei, S. *et al.* Arsenic induces pancreatic dysfunction and ferroptosis via mitochondrial ROS-autophagy-lysosomal pathway. *J. Hazard Mater.* **384**, 121390. https://doi.org/10.1016/j.jhazmat.2019.121390 (2020).
29. Martinez, A. M., Kim, A. & Yang, W. S. Detection of Ferroptosis by BODIPY™ 581/591 C11. *Methods Mol. Biol.* **2108**, 125–130. https://doi.org/10.1007/978-1-0716-0247-8_11 (2020).
30. Auffret, M. *et al.* Apomorphine pump in advanced Parkinson's disease: Effects on motor and nonmotor symptoms with brain metabolism correlations. *J. Neurol. Sci.* **372**, 279–287. https://doi.org/10.1016/j.jns.2016.11.080 (2017).
31. Fernández-Pajarín, G., Sesar, Á., Jiménez Martín, I., Ares, B. & Castro, A. Continuous subcutaneous apomorphine infusion in the early phase of advanced Parkinson's disease: A prospective study of 22 patients. *Clin. Parkinson Relat. Disord.* **6**, 100129. https://doi.org/10.1016/j.prdoa.2021.100129 (2022).
32. Angelova, P. R. *et al.* Alpha synuclein aggregation drives ferroptosis: An interplay of iron, calcium and lipid peroxidation. *Cell Death Differ.* **27**, 2781–2796. https://doi.org/10.1038/s41418-020-0542-z (2020).
33. Lin, K. J. *et al.* Iron brain menace: The involvement of ferroptosis in parkinson disease. *Cells* **11**, 3829. https://doi.org/10.3390/cells11233829 (2022).
34. Keuters, M. H. *et al.* An arylthiazyne derivative is a potent inhibitor of lipid peroxidation and ferroptosis providing neuroprotection in vitro and in vivo. *Sci. Rep.* **11**, 3518. https://doi.org/10.1038/s41598-021-81741-3 (2021).
35. Sun, Y. *et al.* The emerging role of ferroptosis in inflammation. *Biomed. Pharmacother.* **127**, 110108. https://doi.org/10.1016/j.biopha.2020.110108 (2020).

36. Khanam, S. & Siddique, Y. H. Dopamine: Agonists and neurodegenerative disorders. *Curr. Drug Targets* **19**, 1599–1611. https://doi.org/10.2174/1389450118666171117124340 (2018).
37. Kouga, T. *et al.* Japanese Leigh syndrome case treated with EPI-743. *Brain Dev.* **40**, 145–149. https://doi.org/10.1016/j.braindev.2017.08.005 (2018).
38. Miyauchi, A. *et al.* Leigh syndrome with spinal cord involvement due to a hemizygous NDUFA1 mutation. *Brain Dev.* **40**, 498–502. https://doi.org/10.1016/j.braindev.2018.02.007 (2018).
39. Hatakeyama, H., Katayama, A., Komaki, H., Nishino, I. & Goto, Y. Molecular pathomechanisms and cell-type-specific disease phenotypes of MELAS caused by mutant mitochondrial tRNA(Trp). *Acta Neuropathol. Commun.* **3**, 52. https://doi.org/10.1186/s40478-015-0227-x (2015).
40. Novoradovskaya, N. *et al.* Universal reference RNA as a standard for microarray experiments. *BMC Genom.* **5**, 20. https://doi.org/10.1186/1471-2164-5-20 (2004).
41. Stouffer, M. A. *et al.* SKF-83566, a D1-dopamine receptor antagonist, inhibits the dopamine transporter. *J. Neurochem.* **118**, 714–720. https://doi.org/10.1111/j.1471-4159.2011.07357.x (2011).
42. Huang, F. *et al.* Retinal dopamine D2 receptors participate in the development of myopia in mice. *Invest. Ophthalmol. Vis. Sci.* **63**, 24. https://doi.org/10.1167/iovs.63.1.24 (2022).
43. Glase, S. A. *et al.* Substituted [(4-phenylpiperazinyl)-methyl]benzamides: Selective dopamine D4 agonists. *J. Med. Chem.* **40**, 1771–1772. https://doi.org/10.1021/jm970021c (1997).
44. Patel, S. *et al.* Biological profile of L-745,870, a selective antagonist with high affinity for the dopamine D4 receptor. *J. Pharmacol. Exp. Ther.* **283**, 636–647 (1997).
45. Seeman, P. & Van Tol, H. H. Dopamine receptor pharmacology. *Trends Pharmacol. Sci.* **15**, 264–270. https://doi.org/10.1016/0165-6147(94)90323-9 (1994).

Author contributions

A.M., T.Y., and H.O. developed the strategy for the research; methodology, C.W., E.F.J., and N.Y.; performed the research, A.M., A.N., M.K., and N.O.; analyzed the data, A.M. and S.A.; resources, N.Y., Y.K., A.O., M.T.; writing—original draft preparation, A.M.; writing—review and editing, N.O. and H.O..

Funding

Funding was funded by Japan Agency for Medical Research and Development (Grant no. 17ek0109270s0301), Project for Health Research on Infants, Children, Adolescents, and Young Adults from the Agency of Medical Research and Development, Japan, (Grant no: im0210625h0001), Japan Society for the Promotion of Science (Grant no. JP21H03648).

Competing interests

The authors declare no competing interests.

Additional information

Supplementary Information The online version contains supplementary material available at https://doi.org/10.1038/s41598-024-55293-1.

Correspondence and requests for materials should be addressed to A.M. or H.O.

Reprints and permissions information is available at www.nature.com/reprints.

Publisher's note Springer Nature remains neutral with regard to jurisdictional claims in published maps and institutional affiliations.

特集　小児科医が知っておくべき筋疾患診療：遺伝学的理解と治療の最新事情

代表的筋疾患

ミトコンドリア病は多様性の疾患 ―病因，病態，治療の現在

後藤雄一*,**

はじめに

ミトコンドリア病の特徴は「多様性」である。遺伝学的には，核DNA上の遺伝子（300個以上）とミトコンドリアDNA(mtDNA)が原因となる。よって遺伝形式は，メンデル遺伝，母系遺伝，突然変異例など多様である。病態としては，エネルギー産生低下とそれ以外の多様なミトコンドリア機能が障害される。臨床的には，広い発症年齢，ほぼすべての臓器の症状，急性・慢性進行性や症状が改善する臨床経過などがあり，きわめて多様な臨床像を呈する。このようなミトコンドリア病を理解し診療を行うには，遺伝学・病理学・生化学を基盤にした診断方法を知り，眼前の患者で起きている病態をできる限り論理的に洞察し，それら多様な症状に対する対処法を実践することが必要になる。

疾患概念

ミトコンドリア病とは，ミトコンドリア機能の低下を主因とする疾患の総称である。かつてミトコンドリアは細胞のエネルギー産生を担う細胞内小器官と考えられてきたが，現在はそれ以外に，活性酸素排出，アポトーシス，カルシウムイオン貯蔵，感染防御などの機能を有することが明らかになり，単にエネルギー産生低下のみがミトコンドリア病の基盤になっているというわけでない[1,2]。さらに，ミトコンドリア内膜に局在している電子伝達系酵素複合体の働きがもっともミトコンドリアに特徴的であることから，電子伝達系酵素複合体の構造変化や活性低下を伴う疾患群をprimary mitochondrial disease（一次性ミトコンドリア病）とし，それ以外のミトコンドリア機能低下を伴う疾患群をsecondary mitochondrial disease（二次性ミトコンドリア病）と称するようになってきている[3]（図）。

検査と診断

1．臓器症状に応じた検査

ミトコンドリアは成熟赤血球以外の細胞に存在しているので，ほぼすべての細胞が障害を受ける可能性があり，それらの細胞の機能低下や細胞自体の消滅により，組織・臓器の機能が障害され，臓器症状が出現する。表に主な臓器症状を示す。したがって，出現している症状に応じて，臓器特異的な検査を行い，症状の基盤になっている変化を知ることが必要である。ミトコンドリア病で症状が出やすい臓器症状である中枢神経であれば，画像検査，髄液検査，けいれんなどがあれば脳波検査などを行うし，心臓の症状が疑われる場合は心電図や心エコー，各種血液検査を行うことになる。その際，音が聞こえにくい，物が見えにくいなどの症状があるときは，耳鼻科的検査や眼科的検査が必要で，それぞれの専門医にコンサルトすることが必要になることも多い。

2．確定診断に必要な検査

ミトコンドリアの機能変化によって発症していることを証明することがミトコンドリア病の確定

GOTO Yu-ichi
* 国立精神・神経医療研究センターメディカル・ゲノムセンター
〔〒187-8551　東京都小平市小川東町4-1-1〕
** 国立国際医療研究センターNCBN中央バイオバンク
〔〒162-8655　東京都新宿区戸山1-21-1〕

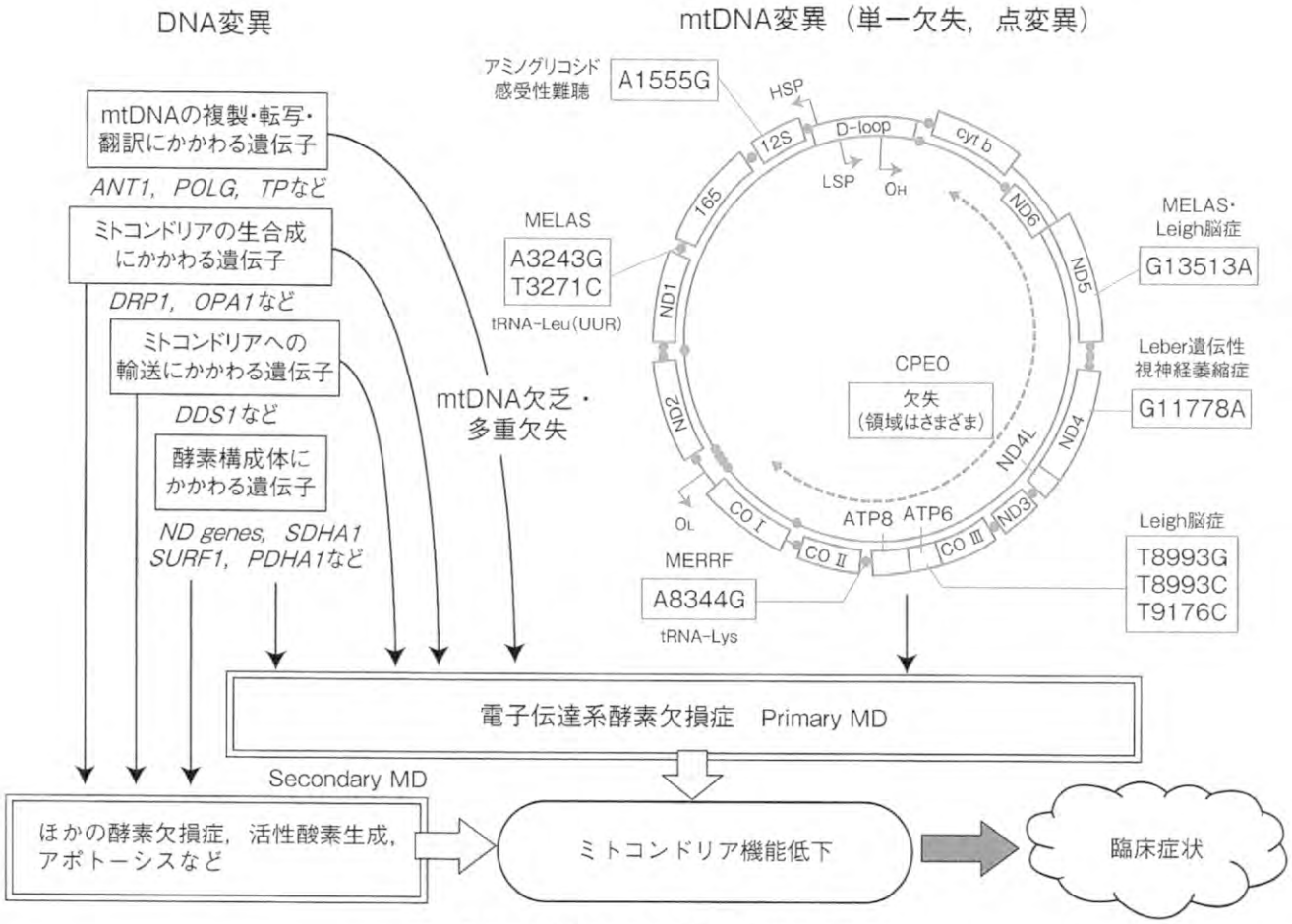

図　ミトコンドリア病の病因の多様性と病態

MD：mitochondrial disease，MELAS：mitochondrial myopathy，encephalopathy，lactic acidosis，and stroke-like episodes，MERRF：myoclonus epilepsy associated with ragged-red fibers，CPEO：chronic progressive external ophthalmoplegia，LSP：L-strand promoter，HSP：H-strand promoter

表　代表的な臨床症状

中枢神経	けいれん，ミオクローヌス，失調，脳卒中様症状，知能低下，片頭痛，精神症状，ジストニア，ミエロパチー
骨格筋	筋力低下，易疲労性，高 CK 血症，ミオパチー
心臓	伝導障害，Wolff-Parkinson-White（WPW）症候群，心筋症，肺高血圧症
眼	視神経萎縮，外眼筋麻痺，網膜色素変性
肝	肝機能障害，肝不全
腎	Fanconi 症候群，尿細管機能障害，糸球体病変，ミオグロビン尿
膵	糖尿病，外分泌不全
血液	鉄芽球性貧血，汎血球減少症
内耳	感音性難聴
大腸・小腸	下痢，便秘
皮膚	発汗低下，多毛
内分泌腺	低身長，低カルシウム血症，甲状腺機能低下症

（難病情報センター[6]）

診断である。

1）遺伝学的検査

すでに300以上の核DNA上の原因遺伝子が同定されている[3]。図には代表的な遺伝子のみを示している。これだけ多くの原因遺伝子があると，パネル検査やNGS（next generation sequencing）を用いた検査が必要になってきた。しかし，このような網羅的検査を最初から行うよりは，頻度の高い原因遺伝子に絞って検査を行い，その後に網羅的検査を行うのが一般的である[4,5]。日本においては，網羅的遺伝学的検査を行えるところが限られており，体制整備が徐々に進んでいるところである。

一方，わずか1.6 kbの小さい環状DNAであるmtDNAは，一細胞内に数千コピーで存在する（マルチコピー性），突然変異の頻度が高い（易変異性），卵からしか遺伝しない（母系遺伝）という特徴をもっている。これらの特徴は，突然変異や母系遺伝という遺伝学的特徴や細胞内に変異型と野生型が混在する状態（ヘテロプラスミー）や変異蓄積などの状態の基盤となっている。変異型が細胞内に存在する場合は，変異率は0～100％まであり得るが，ヘテロプラスミーの状態では，ある一定の比率以上にならないと細胞障害が起きないことが知られている（閾値効果）。

ヘテロプラスミーで起きる病気の代表であるミトコンドリア脳筋症・乳酸アシドーシス・脳卒中様症候群（MELAS）や慢性進行性外眼筋麻痺症候群（CPEO）などでは，全身の細胞毎で変異率が異なっており，変異率の高い細胞が多い組織や臓器ではその障害が現れるものと理解されている。

2）病理学的検査

ミトコンドリア病における筋生検は，遺伝学的検査で確定できないときには必須の検査であることに変わりはない。欠失したmtDNA（図）は，罹患臓器である骨格筋でしか捉えられない場合があり，血液を用いた検査では不十分のこともある。ミトコンドリア病に特徴的な赤色ぼろ線維（ragged-red fiber：RRF），高コハク酸脱水素酵素活性線維（strongly SDH-reactive blood vessel：SSV），シトクローム酸化酵素欠損線維（COX-negative fiber）などを特殊染色で同定する。

3）生化学的検査

血中・髄液中の乳酸・ピルビン酸測定以外に，GDF15（growth differentiation factor 15）値測定（今後は測定キットが販売される予定），尿中有機酸分析，血中アミノ酸分析などの代謝スクリーニング検査が有用である。また，電子伝達系酵素の活性測定は直接的に診断が可能になることもあり有用であるものの，骨格筋で酵素欠損や酵素蛋白量の低下が認められるものの線維芽細胞では同定できないこともあり，生化学検査でも生検筋での測定が決定打になることがある。骨格筋生検の際に筋芽細胞や線維芽細胞を樹立しておくと，病因追求の貴重な材料になるので，専門施設にコンサルトすることをお勧めする。

診断基準

ミトコンドリア病は指定難病になっており，診断基準が公開されている[6]。現在，改定版が完成しており，2024年4月に正式に移行するとされている。改定版は，最近の遺伝学的検査法を取り入れたものとなっている。

治　療

1．対症治療

ミトコンドリア病では多彩な臓器症状が出現する。根本的な治療法がない現況では，対症治療に頼らなくてはならないものの，けいれんには抗けいれん薬，精神症状には精神薬，難聴には補聴器や人工内耳など著効するものがあり，臨床的に重要な対処法である。その際，自分の専門外の臓器症状があれば専門医と相談して治療を行うことが必要であり，また小児科であれば他科の診療内容も含めて全人的に診てゆくことが肝要である。

2．特異的治療と根本治療の可能性

1）薬物治療

ミトコンドリア機能の低下で起きている代謝異常を調整することは全身状態の改善につながる可能性がある。ミトコンドリア内で作用するビタミン類を経口投与するのは理にかなっているように考えられるが，ビタミン剤による厳密な臨床試験は行われていない。効くに違いないと考えて投与

している場合が多く，食事がしっかり摂れている子に大量のビタミン剤を与えて，食事の量が減ってしまう事態は本末転倒であり，バランスの取れた食事ができることがより重要である。

MELASの脳卒中様発作の予防にタウリン大量治療が有効であり，2019年2月に保険収載された。MELASの原因となるmtDNA内のm.3243A>G変異があると，ミトコンドリア内のロイシン転移RNAにタウリン修飾障害が起こり成熟型にならないことが知られており[7]，それを経口タウリンの大量投与で修飾障害を改善させ脳卒中様発作を減らすことができるとされている[8]。そのほか，いくつかの薬剤の臨床試験が行われたり，行っていたりしているが，ここでは触れない。

2）生殖補助医療

① 出生前遺伝学的診断，着床前遺伝学的診断

通常，核DNA上の病因遺伝子変異で起きる乳幼児に発症する重篤なミトコンドリア病は，その病的変異が同定されていれば次子の出生前遺伝学的検査は可能である。しかし，mtDNAの場合は，ヘテロプラスミーで起きる病態か，ホモプラスミー（すべてがほとんど同じバリアントをもつ）の病態かでその適用は異なる。ヘテロプラスミーの場合は，診断に用いる羊水細胞や絨毛細胞の変異率が胎児個体の細胞の変異率をきちんと反映しているのか，または発生の過程で胎児の細胞内の変異率が変化してゆく可能性があり，検査結果で将来の発症を予測するのが困難である。そのため，mtDNAの変化で起きる病気の出生前検査は，ホモプラスミーで起きる病気（たとえば，m.8993T>GやM8993T>Cで起きるLeigh脳症）に限定される。

② ミトコンドリア・ドネーション

ミトコンドリア・ドネーションとは，ミトコンドリア置換法ともよばれ，母親の核DNAを維持しながら，ミトコンドリアのみを女性ドナーのミトコンドリアと入れ替えることをいう。具体的には，ドナーの卵子の核を取り出し，① その卵子に母親の核を入れてから（未受精胚核置換）父親の精子と人工授精させるか，② その卵子に母親の受精卵の核を入れること（受精胚核置換）をいう。②は，作成について「ヒトに関するクローン技術等の規制に関する法律（クローン技術規制法）」に触れる特定胚となる。

この操作を受けた胚には，核DNAを提供した父親，母親とミトコンドリアDNAを提供した女性ドナーの3人の親が存在することになり，大きな倫理的問題を含んでいた。また，病気に関係するmtDNAがわずかながらも卵子内に残る問題や，異なるmtDNAが2種類含まれている場合に正常に発生が進むのかどうかなど生物学的，技術的課題が挙げられおり，長期間の議論が行われた。英国では長い検討期間の後，2015年法律を制定して，このミトコンドリア・ドネーションを臨床的に容認した。遅れて2022年3月にオーストラリアが法律を制定してこの方法を法的に認めている[9]。

一方，日本でも臨床応用を含めた議論が総合科学技術・イノベーション会議（CSTI）で行われ，令和元（2019）年6月に，ミトコンドリア病研究を目的にしたヒト受精胚に核置換を用いる研究を認める旨の見解が示され，その後文部科学省において速やかな指針の整備を進めることになり，結果的に令和4（2022）年6月にクローン技術規制法が改正され，研究での作成に道が開かれたところである。

おわりに

ミトコンドリア病の特徴は多様性である。ミトコンドリア病は，DNA，ミトコンドリア，細胞，組織，臓器レベルで理解することが必要であり，それぞれのレベルに対応する分子遺伝学，病理学，生化学，電気生理学，そして生殖補助医療を取り扱う臨床遺伝学などの種々のアプローチを必要とする。とくに，若い医師が興味をもってこの分野に参入してもらいたいと考えている。

文　献

1) Picard M, Shirihai OS : Mitochondrial signal transduction. Cell Metab **34** : 1620-1653, 2022
2) Pekkurnaz G, Wang X : Mitochondrial heterogeneity and homeostasis through the lens of a neuron. Nat Metab **4** : 802-812, 2022
3) Frazier AN, Thorburn DR, Compton AG : Mitochondrial energy generation disorders : genes,

Key Points

❶ 典型的な症状や複数の臓器症状があるときにミトコンドリア病を疑う。
❷ 診断検査の手始めは，血中乳酸・ピルビン酸値やGDF15値（今後は測定キットが販売される予定）などを測定する。
❸ 確定診断には遺伝学的検査が主体になりつつあるが，罹患臓器（骨格筋など）の病理や生化学検査が必要となることも多い。
❹ 多彩な症状の出現に応じて，各臓器の専門科へのコンサルトと全人的な医療を行うことが重要である（ほかの診療科への丸投げはしない）。

mechanisms, and clues to pathology. J Biol Chem **294**：5386-5396, 2019
4) Mavraki E, Labrum R, Sergeant K, et al：Genetic testing for mitochondrial diseases：The United Kingdom best practice guidelines. Eur J Hum Genet **31**：148-163, 2022
5) Moore M, Yeske P, Parikh S：Navigating life with primary mitochondrial myopathies：The importance of the patient voice and implications for clinical practice. J Primary Care Community Health **14**：21501319231193875, 2023
6) 難病情報センター：ミトコンドリア病（指定難病21），診断・治療指針 https://www.nanbyou.or.jp/wp-content/uploads/upload_files/File/021-201704-kijyun.pdf（2023年10月3日アクセス）
7) Kirino Y, Goto Y, Campos Y, et al：Specific correlation between the wobble modification deficiency in mutant tRNAs and the clinical features of a human mitochondrial disease. Proc Natl Acad Sci U S A **102**：7127-7132, 2005
8) Ohsawa Y, Hagiwara H, Nishimatsu SI, et al：Taurine supplementation for prevention of stroke-like episodes in MELAS：a multicenter, open-label, 52-week phase Ⅲ trial. J Neurol Neurosurg Psychiat **90**：529-536, 2019
9) Australian Government, Department of Health and Aged Care：Mitochondrial donation https://www.health.gov.au/our-work/mitochondrial-donation（2023年10月3日アクセス）

*　　*　　*

Journal of Neurology
https://doi.org/10.1007/s00415-023-11906-9

ORIGINAL COMMUNICATION

Characteristics of the muscle involvement along the disease progression in a large cohort of oculopharyngodistal myopathy compared to oculopharyngeal muscular dystrophy

Nobuyuki Eura[1,2] · Satoru Noguchi[1] · Masashi Ogasawara[1,3] · Theerawat Kumutpongpanich[1] · Shinichiro Hayashi[1] · Ichizo Nishino[1] · the OPDM/OPMD Image Study Group

Received: 18 June 2023 / Revised: 24 July 2023 / Accepted: 25 July 2023

Abstract

Background and objectives Oculopharyngodistal myopathy (OPDM) is an autosomal dominant myopathy clinically characterized by distal muscle weakness. Even though the identification of four causative genes, *LRP12*, *GIPC1*, *NOTCH2NLC* and *RILPL1*, it is unclear whether the myopathy progressed similarly among OPDM subtypes. We aimed to establish diagnostic clues in muscle imaging of OPDM in comparison with clinicopathologically similar oculopharyngeal muscular dystrophy (OPMD).

Methods Axial muscle CT and/or T1-weighted MRI data from 54 genetically confirmed patients with OPDM (OPDM_LRP12; n = 43, OPDM_GIPC1; n = 6, OPDM_NOTCH2NLC; n = 5) and 57 with OPMD were evaluated. We scored the degree of fat infiltration in each muscle by modified Mercuri score and performed hierarchical clustering analyses to classify the patients and infer the pattern of involvement on progression.

Results All OPDM subtypes showed a similar pattern of distribution in the affected muscles; soleus and medial gastrocnemius involved in the early stage, followed by tibialis anterior and extensor digitorum longus. For differentiating OPDM and OPMD, severely affected gluteus medius/minimus and adductor magnus was indicative of OPMD.

Discussion We identified a diagnostic muscle involvement pattern in OPDM reflecting its natural history. The results of this study will help in the appropriate intervention based on the diagnosis of OPDM, including its stage.

Keywords Oculopharyngodistal myopathy · Oculopharyngeal muscular dystrophy · Skeletal muscle imaging

Introduction

Oculopharyngodistal myopathy (OPDM) is an autosomal dominant myopathy that is characterized, clinically, by slowly progressive ptosis, ophthalmoplegia, dysphagia, and predominantly distal limb muscle weakness; and, pathologically, by the presence of rimmed vacuoles and small angular fibers. To date, the cause of OPDM has been identified as CGG repeat expansion in the 5'UTR of *LRP12*, *GIPC1*, *NOTCH2NLC,* and *RILPL1* genes [1–5]. However, it is curious that the clinicopathological phenotype is believed to be similar despite the different causative genes [6].

Oculopharyngeal muscular dystrophy (OPMD), on the other hand, is caused by the expansion of the alanine stretch in N-terminal of a protein encoded by *PABPN1* gene, and is clinicopathologically similar to OPDM in terms of oculopharyngeal muscle involvement; however, showing predominantly proximal limb weakness [7]. Interestingly, it has been

The list of "the OPDM/OPMD Image Study Group" members were listed in Acknowledgements section.

✉ Ichizo Nishino
nishino@ncnp.go.jp

[1] Department of Neuromuscular Research, National Institute of Neuroscience, National Center of Neurology and Psychiatry (NCNP), 4-1-1 Ogawahigashi, Kodaira, Tokyo 187-8502, Japan

[2] Department of Neurology, Nara Medical University School of Medicine, Kashihara, Nara, Japan

[3] Department of Pediatrics, Showa General Hospital, Kodaira, Tokyo, Japan

Published online: 27 August 2023

reported that some OPDM patients can show predominantly proximal muscle weakness, mimicking OPMD [8]. These situations naturally raise the following three questions: (1) Is OPDM a heterogeneous disease? (2) Do the subtypes of OPDM with different causative genes represent different clinical phenotypes? (3) Is the distribution of affected muscles different between OPDM and OPMD?

Skeletal muscle computed tomography (CT) and magnetic resonance imaging (MRI) have been widely used in the diagnosis of neuromuscular diseases. The selective fatty replacement patterns on muscle imaging sometimes show disease-specificity and have been used for diagnosis [9, 10]. Therefore, it may be possible to answer the three questions by using skeletal muscle imaging data, which show the specific patterns of affected muscles in OPDM and OPMD. However, there have been only a few studies of muscle imaging on OPDM [11–16], and in particular, no studies have discussed the differences in skeletal muscle imaging for each OPDM harboring different causative genes. In this study, using imaging data from a large cohort of genetically confirmed patients with OPDM, we aimed to identify the characteristic distribution of muscle involvement reflecting its natural history and to provide helpful information that can be translated into clinical practice.

Methods

Subjects

Among the patients with muscles and/or blood samples sent for diagnostic purposes to the National Center of Neurology and Psychiatry (NCNP), a nationwide referral center for neuromuscular diseases in Japan, from January 1, 1978 to December 31, 2021, we searched for the patients with muscle images who were genetically diagnosed to have CGG repeat expansion in *LRP12, GIPC1, NOTCH2NLC,* and GCN repeat expansion or reported missense mutation in *PABPN1* [17–19]. Images taken at multiple time points in the same patient were treated as independent image series.

Clinical data

The demographic data of the patients with OPDM and OPMD was obtained from the records maintained in the NCNP muscle repository. The clinical information collected on the patients included the gender, age at muscle imaging, disease duration, genetic information, initial symptoms, and symptoms at examination such as ptosis, ophthalmoplegia, dysphagia, and weakness of limb and neck muscles. We determined the distribution of muscle weakness by comparing between the sum of the Medical Research Council scale in the proximal (shoulder abduction, elbow flexion and extension, hip flexion and extension, knee flexion and extension) and that of the distal (wrist flexion and extension, finger flexion and extension, ankle flexion and extension) limb.

Muscle imaging

We reviewed axial muscle imaging data of CT or T1-weighted MRI in OPDM and OPMD patients, including the muscles of the trunk (cervical paraspinal; C-PS, sternocleidomastoid; SCM, levator scapulae; LS, splenius capitis; SC, pectoralis major; PM, deltoid; DEL, infraspinatus; InfS, subscapularis; SubS, trapezius; TPZ, rhomboid; RH, serratus anterior; SeA, thoracic paraspinal; Th-PS, iliocostalis lumborum; ICL, longissimus: LO, multifidus; MF, rectus abdominis; RA), pelvis (gluteus maximus/medius/minimus; GMA/GME/GMI), thigh (rectus femoris; RF, sartorius; SA, gracilis; GR, vastus lateralis/medialis/intermedius; VL/VM/VIM, adductor longus/magnus; AL/AM, semimembranosus; SM, semitendinosus; ST, the short/long head of biceps femoris; SBF/LBF) and calf (tibialis anterior/posterior; TA/TP, extensor digitorum longus; EDL, fibularis longus/brevis; FL/FB, soleus; SOL, medial/lateral gastrocnemius; MGC/LGC). Each muscle was evaluated on both sides and scored at the level of the maximum area. The degree of fat infiltration was determined according to the modified Mercuri score (mMS); stage 0: normal appearance; stage 1: mildly decreased signal density (CT) or increased signal intensity (T1-weighted MRI); stage 2: moderately decreased signal density (CT) or increased signal intensity (MRI) with the confluence in less than 50% of the muscle; stage 3: severely decreased signal density (CT) or increased signal intensity (MRI) in more than 50% of the muscle; and stage 4: the whole muscle is replaced by lower density (CT) or high signal intensity (MRI) [10, 20]. Asymmetry was defined as mMS differing by two or more points on the left and right sides [21]. The MRI and CT images were scored independently by two neurologists who were blinded for the clinical information of the patients.

Statistical analysis

We used Student's *t* test to compare the quantitative variables in two groups and one-way ANOVA with Tukey's multiple comparisons test for more than two groups. To investigate the correlation between the clinical and muscle imaging findings, Spearman's rank correlation was used. The data was shown as mean ± SD and considered statistically significant at $p < 0.05$. Statistical analyses, including principal component (PC) analysis, were performed by using GraphPad Prism version 9.4.1 for Windows (GraphPad Software, San Diego, California, USA). The hierarchical analysis with graphical representation as a heatmap was performed using R software version 4.2.1.

Standard protocol approvals, registrations, and patient consents

This study was approved by the ethical committees of the NCNP (A2022-045).

All of the participants provided a written informed consent for using their data for research.

Data availability

The data supporting the findings in this study are available from the corresponding author upon request.

Results

Clinical findings

A total of 111 patients composed of 43 OPDM_LRP12, 6 OPDM_GIPC1, 5 OPDM_NOTCH2NLC, and 57 OPMD patients were enrolled. The clinical features were shown in Table 1. In OPDM, the average age at onset of symptoms in OPDM_NOTCH2NLC was significantly younger than that of OPDM_GIPC1 ($p = 0.02$). Regarding the initial symptoms, ptosis and muscle weakness were common in OPDM_LRP12 and OPDM_GIPC1. In contrast, OPDM_NOTCH2NLC had no ptosis but had neuropsychiatric symptoms as an initial symptom. In all of the OPDM subtypes, most of the patients showed predominantly distal muscle weakness, while a proportion of patients also showed weakness in the proximal muscles equally, and some showed mainly proximal muscle weakness. In OPMD, on the other hand, the average age at symptom onset was significantly older than those in the OPDM subtype ($p < 0.0001$). Ptosis was the most common symptom at onset, which was followed by muscle weakness and dysphagia. It is important to note that 9.1% of the patients showed non-proximal muscle weakness. Neck muscle weakness was observed in all of the subtypes of OPDM and OPMD, but was particularly frequent in OPDM_NOTCH2NLC.

Muscle imaging

We evaluated 39 muscles among all the enrolled patients. One OPDM_NOTCH2NLC patient, along with 3 OPDM_LRP12 and 2 OPDM_GIPC1 patients, had multiple image series at different time points (7, 5, 2, 2, 3, 2 series, respectively). As a result, we reviewed a total of 4914 muscle images of 126 series in 111 patients (Supplemental Table). To analyze the CT and MRI data together in same platform, we evaluated the data from these imaging modalities in the same individuals. Among the enrolled patients, both CT and MRI data were obtained in 178 muscles from 15 patients. The mMS by CT and MRI in these muscles correlated well ($mMS_{MRI} = 0.9 \times mMS_{CT} + 0.3$, $r^2 = 0.84$) as shown in the Supplemental Figure. Using this formula, CT scores were

Table 1 Clinical demographics of OPDM and OPMD

	OPDM_LRP12 (n = 43)	OPDM_GIPC1 (n = 6)	OPDM_NOTCH2NLC (n = 5)	OPMD_PABPN1 (n = 57)
Age at onset (y, mean ± SD)	41 ± 9.4	46 ± 10	30 ± 11*	55.4 ± 10.0****
Male (%)	58	33	40	56
Initial symptom (%)				
Ptosis	37	50	0	58
Dysphagia	14	0	0	21
Muscle weakness	40	33	40	26
Neuropsychiatric	0	0	60	0
Symptoms at diagnosis (%)				
Ptosis	100	100	60	96
Dysphagia	95	100	60	96
Muscle weakness	95	100	100	91
Proximal > distal	0	17	0	80
Proximal = distal	14	33	40	5.5
Proximal < distal	77	50	60	3.6
Neck	51	40	80	38
CK (IU/L, mean ± SD)	484 ± 339	279 ± 276	474 ± 514	423 ± 459

OPDM oculopharyngodistal myopathy, *OPMD* oculopharyngeal muscular dystrophy, *CK* creatine kinase

****$p < 0.0001$ (vs OPDM_LRP12, OPDM_GIPC1, OPDM_NOTCH2NLC),

*$p < 0.05$ (vs OPDM_GIPC1)

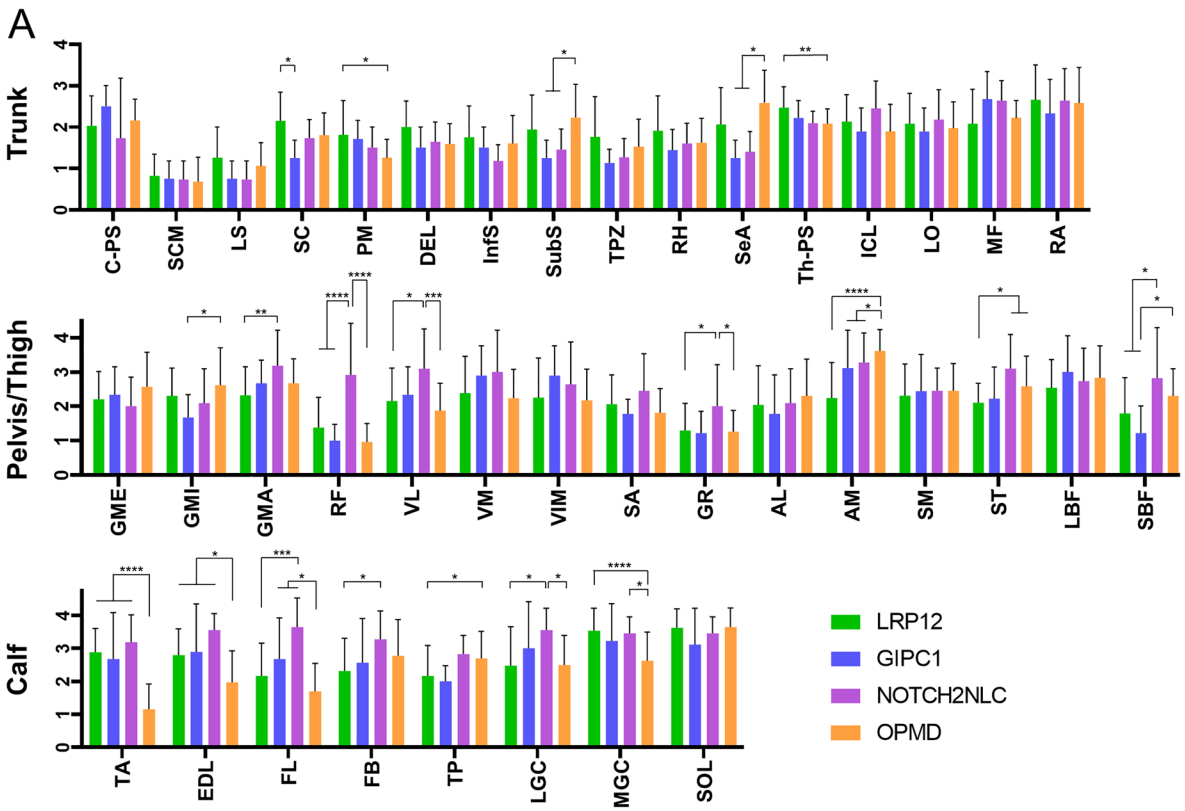
A
Trunk
C-PS
SCM
LS
SC
PM
DEL
InfS
SubS
TPZ
RH
SeA
Th-PS
ICL
LO
MF
RA
Pelvis/Thigh
GME
GMI
GMA
RF
VL
VM
VIM
SA
GR
AL
AM
SM
ST
LBF
SBF
Calf
TA
EDL
FL
FB
TP
LGC
MGC
SOL
LRP12
GIPC1
NOTCH2NLC
OPMD

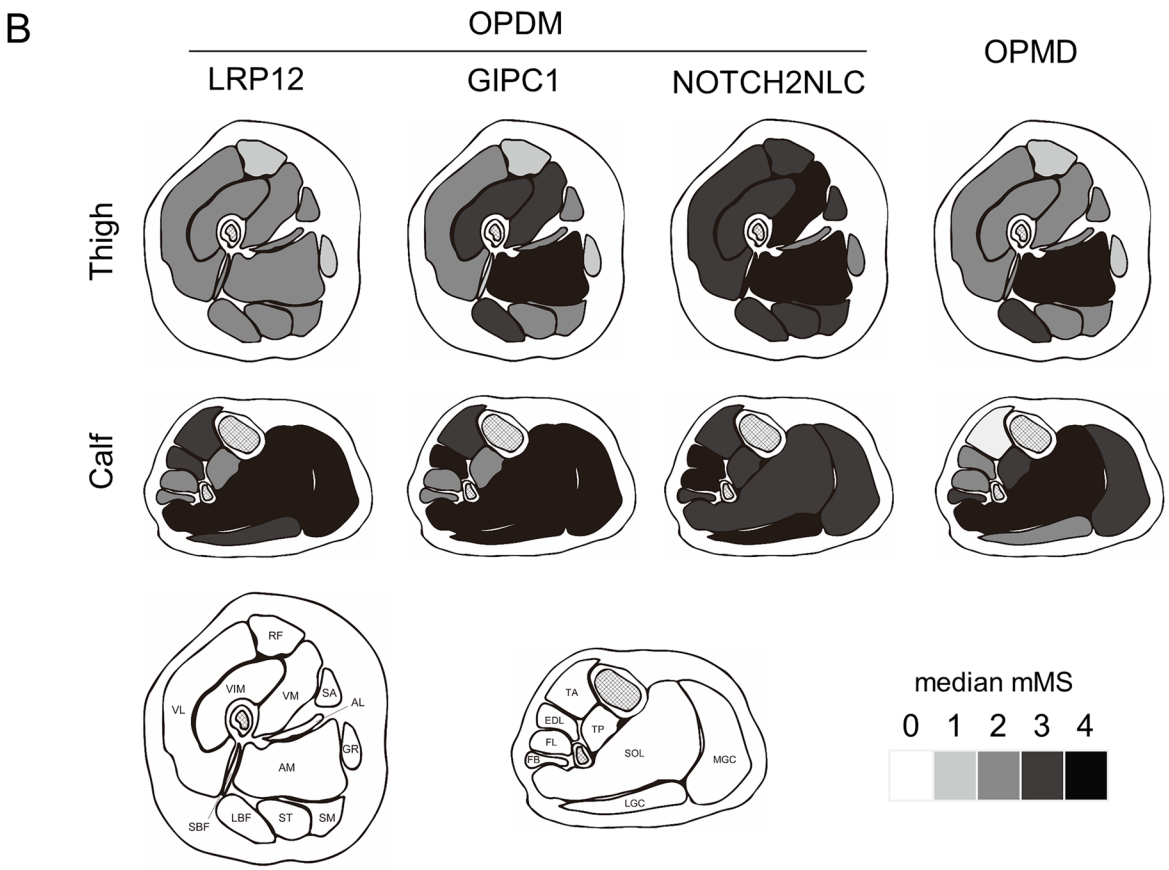
B
OPDM
OPMD
LRP12
GIPC1
NOTCH2NLC
Thigh
Calf
RF
VIM
VM
SA
AL
VL
GR
AM
SBF
LBF
ST
SM
TA
EDL
TP
FL
FB
SOL
MGC
LGC
median mMS
0 1 2 3 4

◂**Fig. 1** The mMSs of trunk and limb muscles in OPDM and OPMD. (**A**) The average mMSs of each muscle for three subtypes of OPDM and OPMD are shown in bar plots. *p < 0.05; **p < 0.01; ***p < 0.001; ****p < 0.0001. (**B**) A graphical summary of the degree of fat replacement in the thigh and calf muscles. *OPDM* oculopharyngodistal myopathy, *OPMD* oculopharyngeal muscular dystrophy, *mMS* modified Mercuri score, *C-PS* cervical paraspinal, *SCM* sternocleidomastoid, *LS* levator scapulae, *SC* splenius capitis, *PM* pectoralis major, *DEL* deltoid, *InfS* infraspinatus, *SubS* subscapularis, *TPZ* trapezius, *RH* rhomboid, *SeA* serratus anterior, *Th-PS* thoracic paraspinal, *ICL* iliocostalis lumborum, *LO* longissimus, *MF* multifidus, *RA* rectus abdominis, *GMA* gluteus maximus, *GME* gluteus medius, *GMI* gluteus minimus, *RF* rectus femoris, *SA* sartorius, *GR* gracilis, *VL* vastus lateralis, *VM* vastus medialis, *VIM* vastus intermedius, *AL* adductor longus, *AM* adductor magnus, *SM* semimembranosus, *ST* semitendinosus, *SBF* the short head of biceps femoris, *LBF* the long head of biceps femoris, *TA* tibialis anterior, *EDL* extensor digitorum longus, *FL* fibularis longus, *FB* fibularis brevis, *TP* tibialis posterior, *LGC* lateral head of gastrocnemius, *MGC* medial head of gastrocnemius, *SOL* soleus

converted to MRI scores and the converted MRI scores were used for analyses after being rounded off. The two scores were equal in all data. The average mMS of each muscle was shown in Fig. 1A and a graphical summary of the thigh and calf muscles using the median mMS was shown in Fig. 1B.

In OPDM, calf muscles were more extensively replaced by fat compared with the thigh muscles (mMS = 2.89 ± 0.41 vs 2.20 ± 0.38, p = 0.002). In particular, TA, EDL, MGC, and SOL were severely affected in all subtypes of OPDM. Among the subtypes of OPDM, OPDM_NOTCH2NLC had more severely affected muscles in comparison with the other subtypes (GMA, RF, VL, GR, AM, SBF, FL, FB, LGC). As for OPMD, there was no significant difference in the degree of fat replacement between thigh and calf muscles (mMS = 2.16 ± 0.66 vs 2.36 ± 0.71, p = 0.55). AM and SOL were the most severely affected, while TA, RF, and GR were relatively spared. Comparing OPDM and OPMD, TA and EDL were significantly more severely affected in OPDM than in OPMD, while AM was more severely affected in OPMD. These results suggest that these muscles would be informative in differentiating between the two diseases. In the truncal muscles, SeA and SubS were more severely affected in OPMD than OPDM_GIPC1 or OPDM_NOTCH2NLC. Additionally, asymmetric muscle involvement was observed in 15 of 43 OPDM_LRP12 (25.6%), 1 of 9 OPDM_GIPC1 (11.1%), 2 of 11 OPDM_NOTCH2NLC (22.2%), and 6 of 57 OPMD (10.5%) image series.

To visualize the pattern of muscle involvement, we performed a hierarchical analysis and drew the heatmap for the patients with all 28 muscles available in the pelvis, thigh, calf, and thoracic/lumbar paraspinal (OPDM_LRP12: 32 patients [38 image series], OPDM_GIPC1: 6 patients [9 image series], OPDM_NOTCH2NLC: 5 patients [11 image series], OPMD: 36 patients [36 image series]). In the heatmap of OPDM (Fig. 2A), 58 image series were classified into two large groups, the right group with a significantly longer disease duration than the left (17.9 ± 9.5 vs 10.0 ± 8.8 years, p = 0.002). Also, the dendrogram showed that 28 muscles were classified into four clusters according to the pattern of muscle involvement. Together with disease duration, these clusters may indicate the following implications; MGC, SOL: severely affected from the earliest stage of the disease; FL, FB, LGC, TA, EDL: severely affected in the later stage and can be in early stage; AL, VIM, VM, VL, GMA, AM, SM, LBF, MF, Th-PS, GMI, GME, RA, TP, ST, SA, LO, ICL: affected in the later stage; GR, RF, SBF: relatively spared in the later stage. On the other hand, hierarchical analysis did not clearly divide the patients into each OPDM subtype. Similarly, a PC analysis using each mMS of 28 muscles also did not reveal differences between the OPDM subtypes (Fig. 2B). This may indicate that it is difficult to differentiate OPDM subtypes based on the image findings of these 28 muscles.

We also performed a hierarchical analysis on OPMD (n = 36) and the heatmap was shown in Fig. 3. The patients were classified into two large clusters, the right had an older age at muscle imaging than the left (70.3 ± 6.5 vs 65.3 ± 10.0 years, p = 0.104). Muscles were classified into four large clusters, indicating that; AM, SOL: affected in the earliest stage of the disease; FB, GME, GMI, SBF, RA, TP, MGC, LBF, LGC, GMA, ST: severely affected in the later stage; AL, VL, SA, VM, VIM, FL, EDL, ICL, LO, SM, Th-PS, MF: affected in the later stage; GR, RF, TA: spared even in the advanced stage. The patients were not divided by the GCN repeat size.

Next, we investigated the correlation between mMS and clinical information, such as age at muscle imaging (Age) and disease duration (Duration). Based on the heatmap, we selected only the muscles whose severity correlated with disease progression; excluding GR, RF, SBF, MGC, and SOL for OPDM and GR, RF, TA, AM, and SOL for OPMD, and summed the mMS of these muscles. The scores were set as "sum_OPDM" and "sum_OPMD", respectively. In OPDM, we observed a significant positive correlation between Age and sum_OPDM only in OPDM_NOTCH2NLC (p < 0.0001) (Fig. 4, left) while the Duration and mMS sum_OPDM were significantly correlated in OPDM_LRP12 and OPDM_NOTCH2NLC (p < 0.05) (Fig. 4, right). Similarly, in OPMD, sum_OPMD were significantly correlated with both Age and Duration.

Then, to examine the image-based separation of OPDM and OPMD patients, we performed a hierarchical analysis on the combined OPDM and OPMD images (79 patients, 94 image series) (Fig. 5A). The patients were classified into subclusters according to each disease. Interestingly, even the patients with atypical muscle weakness, i.e., equal weakness in proximal and distal muscles, or distal muscle

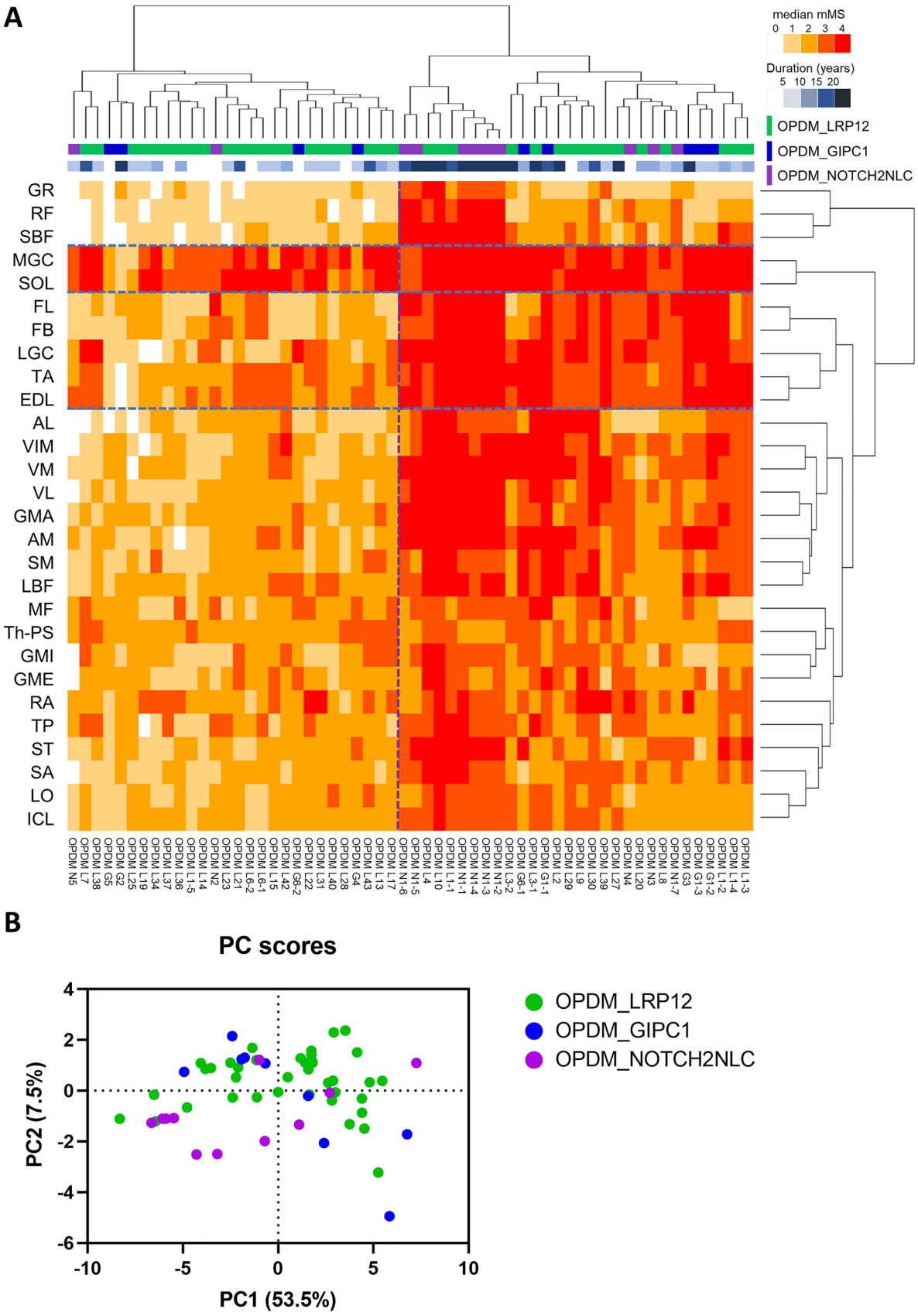
A
median mMS
0 1 2 3 4
Duration (years)
5 10 15 20
OPDM_LRP12
OPDM_GIPC1
OPDM_NOTCH2NLC
GR
RF
SBF
MGC
SOL
FL
FB
LGC
TA
EDL
AL
VIM
VM
VL
GMA
AM
SM
LBF
MF
Th-PS
GMI
GME
RA
TP
ST
SA
LO
ICL
B
PC scores
PC2 (7.5%)
PC1 (53.5%)
OPDM_LRP12
OPDM_GIPC1
OPDM_NOTCH2NLC

◂**Fig. 2** Hierarchical and PC analysis of OPDM. (**A**) The heatmap shows the fat replacement in the thigh, calf, lumbar paraspinal, and thoracic paraspinal muscles (row) in each patient (column). The muscles and patients are clustered based on the degree of fat infiltration, OPDM subtype, duration of the disease, and age. The degree of fat infiltration is indicated by the red scale color as shown in the right upper corner. At the top of the heatmap, the duration of the disease is shown in grayscale and the OPDM subtype of each patient is color-coded. (**B**) PC analysis did not show a distinct separation between OPDM subtypes

predominance in OPMD or proximal muscle predominance in OPDM, were correctly included in the disease subclusters.

Lastly, to identify the informative muscles differentiating OPDM and OPMD, we performed PC analysis on the data of mMS of 28 muscles from combined OPMD and OPDM patients. The plot showed that OPDM and OPMD are clearly separated and with a relative difference in distribution (Fig. 5B). The loading plot showed that AM, GME, GMI, and TP have a strongly negative influence on PC2 (more likely to be affected in OPMD), while TA, EDL, MGC, Th-PS, and FL have a strongly positive influence (preferentially affected in OPDM), indicating that these muscles are important for distinguishing between OPDM and OPMD (Fig. 5C). In our study, patients whose mMS for TA score was greater than or equal to that for AM would correspond to the diagnosis of OPDM with a sensitivity of 86.4% and a specificity of 100%.

Discussion

Our large cohort study of the muscle imaging findings of genetically confirmed patients with OPDM and OPMD illustrated the pattern of characteristic muscle involvement that can differentiate the two diseases. By hierarchical clustering and PC analysis, we obtained three major results: (1) In OPDM, SOL and MGC were the most severely affected from the earliest stage, followed by FL, FB, LGC, TA, and EDL, while GR, RF, SBF were spared even in the advanced stage; (2) Imaging findings could not significantly differentiate the three subtypes of OPDM; (3) For differentiation between OPDM and OPMD, severe involvement in TA, EDL, and MGC suggests OPDM, whereas if in AM, GMI, GME indicates OPMD.

For all subtypes of OPDM and OPMD except for OPDM_GIPC1, disease duration correlated with the severity of fat infiltration. However, the age at muscle imaging did not correlate with mMS in OPDM_LRP12 and OPDM_GIPC1. This may reflect the possibility that age by itself does not necessarily correlate with disease progression, since disease onset depends on the repeat length in these subtypes of OPDM [6, 11, 22].

To date, only limited case series have reported the imaging features of OPDM with selective involvement in the posterior calf muscles, such as SOL and MGC/LGC, regardless of the causative gene, in addition to AM and LBF in OPDM_NOTCH2NLC [2–5, 11, 20, 22, 23]. And one report by Yu et al. described that the pattern of muscle involvement with disease progression is similar among OPDM subtypes caused by *LRP12*, *GIPC1*, and *NOTCH2NLC* mutation [4]. In our study, we found that OPDM_NOTCH2NLC tended to exhibit a more extensive and severely affected muscle distribution at thigh level than the other subtypes; however, hierarchical and PC analysis did not differentiate the muscle involvement pattern among OPDM subtypes. This may be due to the small number of cases in OPDM_GIPC1 and OPDM_NOTCH2NLC. Therefore, further accumulation of the cases and investigation on image analysis is needed. In OPMD, on the other hand, the early involvement in AM and SOL has been reported [12–14], which was consistent with our findings. In the truncal muscles, selective fat replacement of the serratus anterior and subscapularis muscles has been reported [12], but in our study, there was no significant difference between OPDM_LRP12 and OPMD in these muscles. In addition, GNE myopathy and Miyoshi type myopathy are also important differentials of OPDM as distal myopathy. In the former, the quadriceps femoris muscles are relatively spared, while TA, thigh flexors, and adductor muscles are selectively affected [24]. Miyoshi myopathy has recently been reported to have equal degree of fat replacement in distal and proximal muscles regardless of the stage of the disease, as is thought to be the same disease as limb girdle muscular dystrophy R2 [25, 26]. Although these findings appear to be similar in part to those of OPDM, we may clarify the differences in the pattern of muscle involvement in these "distal myopathies" by using hierarchical and principal component analysis which we used in this study and will contribute to make the differential diagnosis of these myopathies by imaging findings in future.

The strength of our study is that we identified affected muscles with natural disease courses as a group rather than a single one using a hierarchical analysis. Interestingly, even cases with a distribution of atypical muscle weakness were classified exactly as OPDM or OPMD. This provides more robust clues for diagnosis and clarifies where we should focus our attention on physical examinations. For example, observing how the patient walks and measuring the strength of the GME and GMI may help us get closer to a diagnosis even without the skeletal muscle imaging. Furthermore, our findings would provide insight into the patient's stage of disease and prognosis of muscle symptoms. This could serve as indices when clinical trials are conducted in the future and be useful in guiding patients in their daily lives, rehabilitation, and orthotic adjustments.

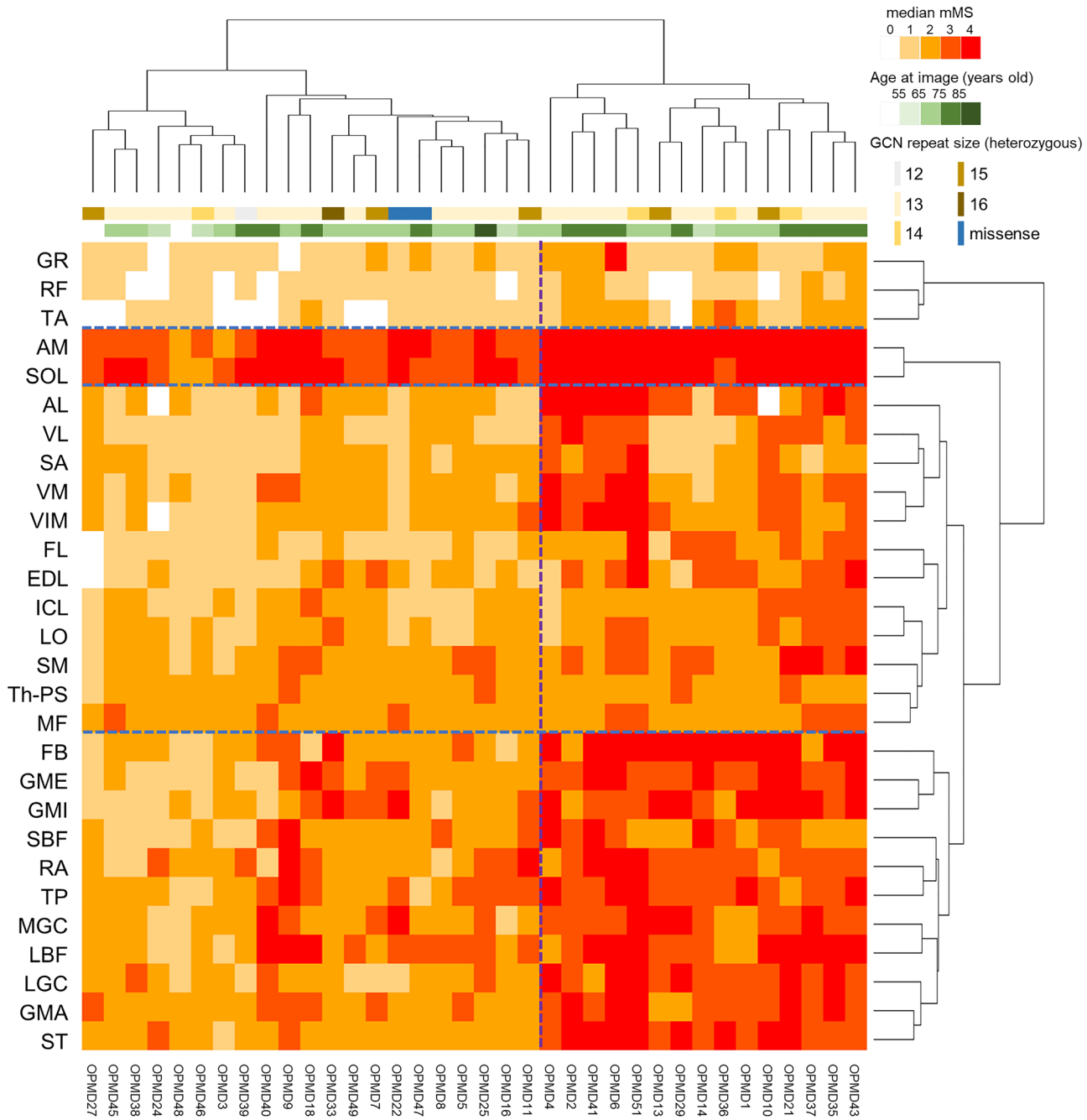

Fig. 3 Hierarchical analysis of OPMD. The involved muscles in the thigh, calf, lumbar paraspinal, and thoracic paraspinal muscle on each patient are shown. The muscles and patients are clustered based on the degree of fat infiltration and age. The degree of fat infiltration is indicated by the red scale color. The age at muscle imaging is shown in green scale, and genotype is shown in yellow scale

This study has several limitations. First, the number of patients harboring CGG repeat expansion in *GIPC1* or *NOTCH2NLC* was small compared to patients with *LRP12*. In addition, patients with *RILPL1* mutation were reported only from China and not included in our cohort [27]. Second, we regarded the repeated scans of patients as individual imaging series for analysis. This can lead to biases in which individual characteristics influence group ones. For example, we used 7 image series of the same patient in the OPDM_NOCTH2NLC group (n = 11), and it is possible that the pattern of muscle involvement of this patient affected that of this group. However, we did not detect any statistical difference in the distribution of affected muscles in OPDM_NOCTH2NLC from OPDM due to other causative genes, therefore, this type of bias may not be significant in our study. Third, this study was retrospective and we

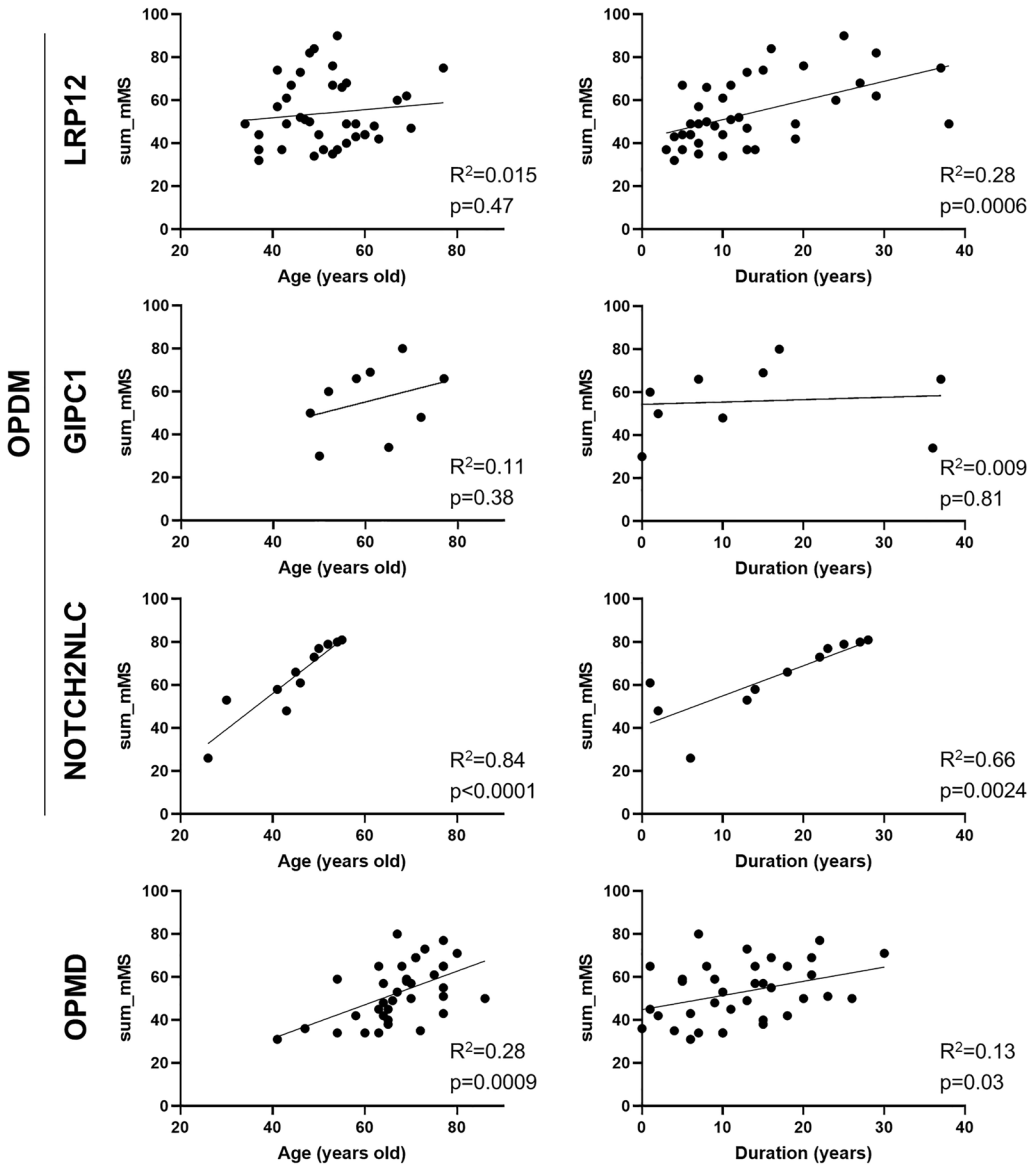

Fig. 4 Correlation of total mMS with clinical features. On linear regression analyses, a significant positive correlation between age at muscle imaging (Age) and sum of mMS was seen in OPDM_NOTCH2NLC ($p < 0.0001$), while the disease duration (Duration) and sum of mMS were significantly correlated in all subtypes of OPDM ($p < 0.05$). In OPMD, sum of mMS was significantly correlated with both Age and Duration

only analyzed 28 muscles due to incomplete data. To better characterize skeletal muscle imaging in OPDM, and to confirm the results from our study, a prospective cohort with whole-body muscle imaging data will be needed. However, we demonstrated that these 28 muscles could explicitly characterize the distribution of affected muscles in OPDM and were at least adequate in differentiating OPDM from OPMD.

This study provided the following answers to the questions raised in Introduction: (1) Is OPDM a heterogeneous disease?—Yes, OPDM is genetically and clinically heterogeneous. (2) Do the subtypes of OPDM with different causative genes represent different clinical phenotypes?—No, the subtypes of OPDM with different causative genes represent similar clinical patterns of affected muscles on disease progression. (3) Is the distribution of affected muscles different between OPDM and OPMD?—Yes, the distribution is different between OPDM and OPMD. This large cohort study has statistically defined the disease stage-dependent muscle involvement pattern in OPDM caused by CGG repeat expansion in *LRP12, GIPC1,* and *NOTCH2NLC*. This is not only useful for the diagnosis of OPDM including its disease stage, but also for more efficient genetic testing by highlighting the differences from OPMD, which is often difficult to differentiate.

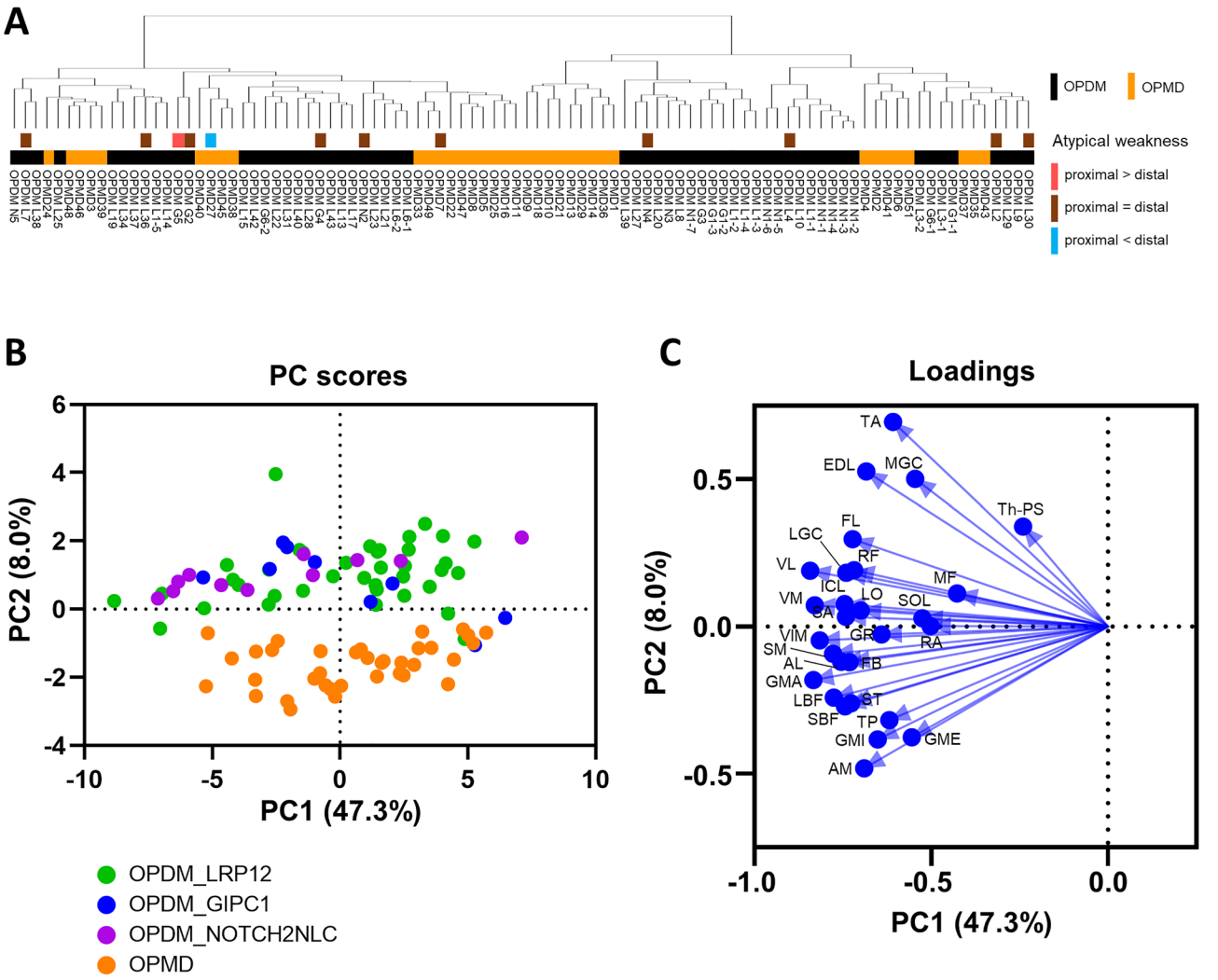

Fig. 5 Hierarchical and PC analysis of OPDM and OPMD. (**A**) The patients were classified based on the hierarchical clustering indicated by the subclusters according to each disease. The patients with atypical muscle weakness were also correctly included in the disease subclusters. (**B**) PC analysis showed that OPDM and OPMD are clearly separated. (**C**) The loadings on the PC analysis revealed muscles with positive/negative influence on PC2, indicating which is more likely to be affected in OPDM/OPMD, respectively

Supplementary Information The online version contains supplementary material available at https://doi.org/10.1007/s00415-023-11906-9.

Acknowledgements We would like to thank the attending physicians and patients for sending muscle imaging data to us and Dr. Francia Victoria De Los Reyes, NCNP, for her critical reading. The list of the OPDM/OPMD Image Study Group members: Takahiko Mukaino: Department of Neurology, Neurological Institute, Graduate School of Medical Sciences, Kyushu University, Fukuoka, Japan; Madoka, Mori-Yoshimura: Department of Neurology, National Center Hospital, National Center of Neurology and Psychiatry, Kodaira, Japan; Makiko Nagai: Department of Neurology, Kitasato University School of Medicine, Sagamihara, Japan; Masayuki Ochi: Department of Neurology and Geriatric Medicine, Ehime University Graduate School of Medicine, Ehime, Japan; Makoto Shibata: Department of Neurology, Gunma University Graduate School of Medicine, Maebashi, Japan; Kazutaka Shiomi: Division of Respirology, Rheumatology, Infectious Diseases, and Neurology, Department of Internal Medicine, Faculty of Medicine, University of Miyazaki, Miyazaki, Japan; Satoshi Yamashita: Department of Neurology, Graduate School of Medical Sciences, Kumamoto University, Kumamoto, Japan and Department of Neurology, International University of Health and Welfare Narita Hospital, Narita, Japan; Toru Yamashita: Department of Neurology, Graduate School of Medicine, Dentistry and Pharmaceutical Sciences, Okayama University, Okayama, Japan.

Author's contributions NE and IN designed the study; NE, SN, M-Og, TK, SH, IN, TM, MMY, MN, M-Oc, MS, KS, SY and TY acquired and analyzed the data; NE, SN, SH and IN wrote and edited the manuscript; and IN supervised the project. All authors read and approved the final manuscript.

Funding This study was supported partly by Intramural Research Grant (2-5 and 29-4 to IN) for Neurological and Psychiatric Disorders of NCNP and by AMED under Grant Numbers 20ek0109490h0001, JP19ek0109285h0003 and JP21ek0109490h0002 (to IN).

Declarations

Conflicts of interest The authors report no competing interests.

References

1. Ishiura H, Shibata S, Yoshimura J et al (2019) Noncoding CGG repeat expansions in neuronal intranuclear inclusion disease, oculopharyngodistal myopathy and an overlapping disease. Nat Genet 51:1222–1232
2. Deng J, Yu J, Li P et al (2020) Expansion of GGC repeat in GIPC1 is associated with oculopharyngodistal myopathy. Am J Hum Genet 106:793–804
3. Ogasawara M, Iida A, Kumutpongpanich T et al (2020) CGG expansion in NOTCH2NLC is associated with oculopharyngodistal myopathy with neurological manifestations. Acta Neuropathol Commun 8:204
4. Yu J, Deng J, Guo X et al (2021) The GGC repeat expansion in NOTCH2NLC is associated with oculopharyngodistal myopathy type 3. Brain 144:1819–1832
5. Yu J, Shan J, Yu M et al (2022) The CGG repeat expansion in RILPL1 is associated with oculopharyngodistal myopathy type 4. Am J Hum Genet 109:533–541
6. Eura N, Ogasawara M, Nishino I (2022) Recent topics of oculopharyngodistal myopathy. Neurol Clin Neurosci 00:1–6
7. Brais B, Bouchard JP, Xie YG et al (1998) Short GCG expansions in the PABP2 gene cause oculopharyngeal muscular dystrophy. Nat Genet 18:164–167
8. Minami N, Ikezoe K, Kuroda H, Nakabayashi H, Satoyoshi E, Nonaka I (2001) Oculopharyngodistal myopathy is genetically heterogeneous and most cases are distinct from oculopharyngeal muscular dystrophy. Neuromuscul Disord 11:699–702
9. Straub V, Carlier PG, Mercuri E (2012) TREAT-NMD workshop: pattern recognition in genetic muscle diseases using muscle MRI: 25–26 February 2011, Rome, Italy. Neuromuscul Disord 22(Suppl 2):S42-53
10. Fischer D, Kley RA, Strach K et al (2008) Distinct muscle imaging patterns in myofibrillar myopathies. Neurology 71:758–765
11. Kumutpongpanich T, Ogasawara M, Ozaki A et al (2021) Clinicopathologic features of oculopharyngodistal myopathy with LRP12 CGG repeat expansions compared with other oculopharyngodistal myopathy subtypes. JAMA Neurol 78:853–863
12. Alonso-Jimenez A, Kroon R, Alejaldre-Monforte A et al (2019) Muscle MRI in a large cohort of patients with oculopharyngeal muscular dystrophy. J Neurol Neurosurg Psychiatry 90:576–585
13. Gloor M, Fasler S, Fischmann A et al (2011) Quantification of fat infiltration in oculopharyngeal muscular dystrophy: comparison of three MR imaging methods. J Magn Reson Imaging 33:203–210
14. Fischmann A, Gloor M, Fasler S et al (2011) Muscular involvement assessed by MRI correlates to motor function measurement values in oculopharyngeal muscular dystrophy. J Neurol 258:1333–1340
15. van der Sluijs BM, Lassche S, Knuiman GJ et al (2017) Involvement of pelvic girdle and proximal leg muscles in early oculopharyngeal muscular dystrophy. Neuromuscul Disord 27:1099–1105
16. King MK, Lee RR, Davis LE (2005) Magnetic resonance imaging and computed tomography of skeletal muscles in oculopharyngeal muscular dystrophy. J Clin Neuromuscul Dis 6:103–108
17. Robinson DO, Hilton-Jones D, Mansfield D et al (2011) Two cases of oculopharyngeal muscular dystrophy (OPMD) with the rare PABPN1 c.35G>C; p.Gly12Ala point mutation. Neuromuscul Disord 21:809–811
18. Nishii YS, Noto YI, Yasuda R et al (2021) A Japanese case of oculopharyngeal muscular dystrophy (OPMD) with PABPN1 c.35G > C; p.Gly12Ala point mutation. BMC Neurol 21:265
19. Takahashi Y, Morimoto N, Nada T et al (2023) A case of oculopharyngeal muscular dystrophy caused by a novel PABPN1 c.34G > T (p.Gly12Trp) point mutation without polyalanine expansion. J Neuromuscul Dis 10:459–463
20. Zhao J, Liu J, Xiao J et al (2015) Clinical and muscle imaging findings in 14 mainland chinese patients with oculopharyngodistal myopathy. PLoS ONE 10:e0128629
21. Tasca G, Monforte M, Ottaviani P et al (2016) Magnetic resonance imaging in a large cohort of facioscapulohumeral muscular dystrophy patients: pattern refinement and implications for clinical trials. Ann Neurol 79:854–864
22. Xi J, Wang X, Yue D et al (2021) 5' UTR CGG repeat expansion in GIPC1 is associated with oculopharyngodistal myopathy. Brain 144:601–614
23. Zeng YH, Yang K, Du GQ et al (2022) GGC repeat expansion of RILPL1 is associated with oculopharyngodistal myopathy. Ann Neurol 92:512–526
24. Fatehi F, Advani S, Okhovat AA, Ziaadini B, Shamshiri H, Nafissi S (2021) Thigh and leg muscle MRI findings in GNE myopathy. J Neuromuscul Dis 8:735–742
25. Paradas C, Llauger J, Diaz-Manera J et al (2010) Redefining dysferlinopathy phenotypes based on clinical findings and muscle imaging studies. Neurology 75:316–323
26. Moore U, Gordish H, Diaz-Manera J et al (2021) Miyoshi myopathy and limb girdle muscular dystrophy R2 are the same disease. Neuromuscul Disord 31:265–280
27. Eura N, Iida A, Ogasawara M, Hayashi S, Noguchi S, Nishino I (2022) RILPL1-related OPDM is absent in a Japanese cohort. Am J Hum Genet 109:2088–2089

ESC European Society of Cardiology
European Heart Journal - Case Reports (2023) **7**, 1
https://doi.org/10.1093/ehjcr/ytad348

Anti-mitochondrial antibody–mediated myopathy with cardiac involvement: reply

Online publish-ahead-of-print 25 July 2023

We would like to thank Finsterer[1] for his interest in our article.[2] In his letter,[1] the importance of differential diagnosis including the other muscular disorders was emphasized.

In our case, presence of myopathy was evidenced by pathological changes in muscle biopsy samples.[1] Of note, we routinely perform a full battery of histochemistry for all muscle biopsy samples, including succinate dehydrogenase (SDH), cytochrome c oxidase (COX), SDH/COX double stain, as well as more than 20 different antigens for immunohistochemistry, including a variety of proteins deficient in muscular dystrophies. In our case, there were no findings suggestive of mitochondrial abnormalities, such as ragged red fibres, COX-negative fibres, and strongly SDH-reactive blood vessels, and all muscular dystrophy-associated proteins were normally expressed. Further, there were no findings of fatty replacement on muscle imagining analysis, which is one of the features suggesting hereditary myopathy.[3] Blood test showed positive anti-mitochondrial M2 antibody (AMA) and normal lactate level (0.9 mmol/L). There were no findings indicating dysfunction of the other organs based on physical examination, blood tests, and imaging studies. The information on detailed family history showed no histories of muscular or cardiac disorders, pacemaker implantation, or sudden death, except for atrial fibrillation in her mother. These findings ensured an adequate diagnosis of AMA-associated myopathy, and there was no clear indication for genetic testing.

We are afraid that his suggestion that mitochondrial myopathy should be ruled out seems to be irrelevant for the reasons as follows. First, as mentioned above, there were no clinicopathological features suggesting mitochondrial disease. Second, AMA has never been associated with mitochondrial myopathy.[4] Although he showed recent meta-analysis,[5] it merely evaluated the diagnostic value of AMA for cardiac involvement in idiopathic inflammatory myopathies (IIMs), not its pathogenicity.

Among a variety of myositis-specific antibodies (MSAs) reported in IIMs, anti-nuclear antibody was positive (×80), but ribonucleoprotein, Sjö gren's syndrome - A, Sjö gren's syndrome - B, and Jo-1 antibodies were all negative in our case. Remarkably, MSAs have the particularity of being mutually exclusive, the co-existence of two or more in the same patient being exceedingly rare (reportedly 0.18%).[6]

We are sure that the other cardiac diseases were adequately ruled out. There were no findings indicating arrhythmogenic right ventricular (RV) cardiomyopathy including electrocardiogram changes, regional RV wall motion abnormalities, or pathological changes in endomyocardial biopsy samples. Amyloidosis was ruled out since Congo red staining was negative both in skeletal muscle and myocardial tissues. Fluor-deoxy-glucose (FDG)-positron emission tomography was performed for suspected sarcoidosis. Although that showed diffuse uptake of FDG in cardiac muscles indicating false positive finding, there were no other lesions (i.e. lymph nodes) with FDG uptake. Biomarkers and gallium scintigraphy demonstrated negative findings. There was no evidence of epithelioid cell granulomas in endomyocardial biopsy samples. From these findings, sarcoidosis was deemed highly unlikely.[1]

In summary, in our case, the diagnosis of AMA-related myopathy was made, and the other cardiac and muscular disorders were ruled out with certainty. The pathogenicity of AMA and mitochondrial derangement in AMA-associated myopathy remain to be elucidated and need further investigation.

Conflict of interest: None declared.

Funding: None declared.

Data availability

Data that are referenced are publicly available.

References

1. Finsterer J. Anti-mitochondrial antibody mediated myopathy with cardiac involvement. *Eur Heart J Case Rep* 2023:ytad292.
2. Ishiguro M, Nagatomo Y, Inoue K, Yoshikawa T, Yoshizawa S, Oya Y, *et al.* Sick sinus syndrome concomitant with myopathy associated with anti-mitochondrial antibodies: a case report. *Eur Heart J Case Rep* 2023;**7**:ytac158.
3. Marago I, Roberts M, Roncaroli F, DuPlessis D, Sewry C, Nagaraju S, *et al.* Limb girdle muscular dystrophy R12 (LGMD 2L, anoctaminopathy) mimicking idiopathic inflammatory myopathy: key points to prevent misdiagnosis. *Rheumatology (Oxford)* 2022;**61**: 1645–1650.
4. Gonzalez-Chapa JA, Macêdo MB, Lood C. The emerging role of mitochondrial dysfunction in the pathogenesis of idiopathic inflammatory myopathies. *Rambam Maimonides Med J* 2023;**14**:e0006.
5. Wang H, Zhu Y, Hu J, Jin J, Lu J, Shen C, *et al.* Associations between anti-mitochondrial antibodies and cardiac involvement in idiopathic inflammatory myopathy patients: a systematic review and meta-analysis. *Z Rheumatol* 2022. [in press]
6. Betteridge Z, Tansley S, Shaddick G, Chinoy H, Cooper RG, New RP, *et al.* Frequency, mutual exclusivity and clinical associations of myositis autoantibodies in a combined European cohort of idiopathic inflammatory myopathy patients. *J Autoimmun* 2019; **101**:48–55.

Yuji Nagatomo[1,2]*, Saeko Yoshizawa[3], Yasushi Oya[4], and Ichizo Nishino[5]
[1]Department of Cardiology, Sakakibara Heart Institute, 3-16-1 Asahi-cho, Fuchu, Tokyo 183-0003, Japan; [2]Department of Cardiology, National Defense Medical College, 3-2 Namiki, Tokorozawa 359-8513, Japan; [3]Department of Surgical Pathology, Tokyo Women's Medical University, 8-1 Kawada-cho, Shinjuku-ku, Tokyo 162-8666, Japan; [4]Department of Neurology, National Center Hospital, National Center of Neurology and Psychiatry, 4-1-1 Ogawa-Higashi, Kodaira, Tokyo 187-8551, Japan; [5]Department of Neuromuscular Research, National Institute of Neuroscience, National Center of Neurology and Psychiatry, 4-1-1 Ogawa-Higashi, Kodaira, Tokyo 187-8502, Japan

* Corresponding author. Tel: +81 4 2995 1597, Email: con401@ndmc.ac.jp

Handling Editor: David Duncker

RESEARCH ARTICLE OPEN ACCESS

Clinical Classification of Variants in the Valosin-Containing Protein Gene Associated With Multisystem Proteinopathy

Marianela Schiava, MD, Chiseko Ikenaga, MD, Ana Topf, PhD, Marta Caballero-Ávila, MD, Tsui-Fen Chou, PhD, Shan Li, PhD, Feng Wang, PhD, Jil Daw, MD, Tanya Stojkovic, MD, Rocio Villar-Quiles, MD, Ichizo Nishino, MD, PhD, Michio Inoue, MD, Yukako Nishimori, MD, Yoshihiko Saito, MD, PhD, Masahisa Katsuno, MD, PhD, Seiya Noda, MD, Chihiro Ito, MD, Mieko Otsuka, MD, Sruthi Nahir, MD, Georgios Manousakis, MD, David Walk, MD, Colin Quinn, MD, Lindsay Alfano, PhD, Zarife Sahenk, MD, Giorgio Tasca, MD, PhD, Mauro Monforte, MD, PhD, Mario Sabatelli, MD, Giulia Bisogni, MD, PhD, Anders Oldfors, MD, PhD, Anna Rydeliu, MD, Endre Pal, MD, Carmen Paradas, MD, Beatriz Velez, MD, Jan L. De Bleecker, MD, PhD, Maria Elena Farugia, MD, Cheryl Longman, MD, Matthew B. Harms, MD, Stuart Ralston, MD, Edmar Zanoteli, MD, Andre Macedo Serafim da Silva, MD, Javier Sotoca, MD, Raul Juntas-Morales, PhD, Jorge Bevilacqua, MD, PhD, Mireya Balart, MD, Stuart Talbot, MD, Volker Straub, MD, PhD, Michela Guglieri, MD, Chiara Marini-Bettolo, PhD, Jordi Diaz-Manera, PhD,* and Conrad Chris Weihl, MD, PhD*

Correspondence
Dr. Diaz-Manera
jordi.diaz-manera@newcastle.ac.uk

Neurol Genet 2023;9:e200093. doi:10.1212/NXG.0000000000200093

Abstract

Background and Objectives

Pathogenic variants in the valosin-containing protein (*VCP*) gene cause a phenotypically heterogeneous disorder that includes myopathy, motor neuron disease, Paget disease of the bone, frontotemporal dementia, and parkinsonism termed multisystem proteinopathy. This hallmark pleiotropy makes the classification of novel *VCP* variants challenging. This retrospective study describes and assesses the effect of 19 novel or nonpreviously clinically characterized *VCP* variants identified in 28 patients (26 unrelated families) in the retrospective VCP International Multicenter Study.

Methods

A 6-item clinical score was developed to evaluate the phenotypic level of evidence to support the pathogenicity of the novel variants. Each item is allocated a value, a score ranging from 0.5 to 5.5 points. A receiver-operating characteristic curve was used to identify a cutoff value of 3 to consider a variant as high likelihood disease associated. The scoring system results were confronted with results of in vitro ATPase activity assays and with in silico analysis.

*These authors contributed equally to this work.

From the John Walton Muscular Dystrophy Research Centre (M. Schiava, A.T., V.S., M.G., C.M.-B., J.D.-M.), Institute of Genetic Medicine, Centre for Life, Newcastle University and Newcastle Hospitals NHS Foundation Trusts, Newcastle Upon Tyne, United Kingdom; Johns Hopkins University School of Medicine (C. Ikenaga), Baltimore, MD; Unidad de Enfermedades Neuromusculares (M.C.-Á.), Servicio de Neurología, Hospital de la Santa Creu i Sant Pau, Barcelona, Spain; Division of Biology and Biological Engineering (T.-F.C., S.L., F.W.), California Institute of Technology, Pasadena; Department of Neurology (J.D.), Washington University School of Medicine, St. Louis, MO; APHP Centre de référence des maladies neuromusculaires Institut de Myologie Sorbonne Université APHP Hôpital Pitié-Salpêtrière Paris (T.S., R.V.-Q.), France; Department of Neuromuscular Research (I.N., M.I., Y.N., Y.S.), National Institute of Neuroscience, National Center of Neurology and Psychiatry (NCNP); Departments of Neurology (M.K., S. Noda) and Clinical Research Education (M.K., S. Noda), Nagoya University Graduate School of Medicine; Department of Neurology (M.K., S. Noda), National Hospital Organization Suzuka Hospital; Department of Neurology (C. Ito), Aichi Medical University School of Medicine; Department of Neurology (M.O.), International University of Health and Welfare Hospital, Japan; Department of Neurology Sree Chitra Tirunal Institute for Medical Sciences and Technology (S. Nahir), Thiruvananthapuram, Kerala, India; Department of Neurology (G.M., D.W.), University of Minnesota, Minneapolis; Department of Neurology (C.Q.), University of Pennsylvania, Perelman School of Medicine, Philadelphia; Center for Gene Therapy (L.A., Z.S.), The Abigail Wexner Research Institute at Nationwide Children's Hospital; Department of Pediatrics (L.A., Z.S.), The Ohio State University College of Medicine, Columbus; Unità Operativa Complessa di Neurologia Fondazione Policlinico Universitario A Gemelli IRCCS (G.T., M.M.); Centro clinico NEMO- Fondazione policlinico universitario A. Gemelli IRCCS (M. Sabatelli, G.B.), Rome, Italy; Department of Laboratory Medicine, Institute of Biomedicine, University of Gothenburg (A.O.); Department of Neurology (A.R.), Clinical Sciences Lund, Lund University, Sweden; Departments of Neurology and Neuropathology (E.P.), University of Pécs, Hungary; Neurology Department, Neuromuscular Disorders Unit, Hospital Universitario Virgen del Rocío (C.P., B.V.); Instituto de Biomedicina de Sevilla (C.P.); Centre for Biomedical Network Research on Neurodegenerative Disorders (CIBERNED) Instituto de Salud Carlos III (C.P., B.V.), Madrid, Spain; Neurology Department and Neuromuscular Reference Centre (J.L.D.B.), Gent, Blegium, part of the ERN NMD; Institute of Neurological Sciences (M.E.F.); West Scotland Regional Genetics Service (C.L.), Queen Elizabeth University Hospital, Glasgow, United Kingdom; Columbia University Irving Medical Centre (M.B.H.), New York; Centre for Genomic and Experimental Medicine (S.R.), Institute of Genetics and Cancer, University of Edinburgh, Western General Hospital Edinburgh, United Kingdom; Department of Neurology (E.Z., A.M.S.S.), School of Medicine, Universidade de São Paulo (FMUSP), Brazil; Neurology Service (J.S., R.J.-M.), Neuromuscular Disorders Unit, Hospital Universitari Vall d'Hebron, Barcelona, Spain; Departamento de Neurología y Neurocirugía (J.B.), HCUCH, Departamento de Anatomía y Medicina Legal, Facultad de Medicina, Universidad de Chile; Departamento de Neurología y Neurocirugía Clínica (M.B.), Clínica Dávila, Santiago Chile; Newcastle University (S.T.), Newcastle Upon Tyne, United Kingdom; and Department of Neurology (C.C.W.), Washington University School of Medicine, Saint Louis, MO.

Go to Neurology.org/NG for full disclosures. Funding information is provided at the end of the article.

The Article Processing Charge was funded by the authors.

Glossary

ALA = age at last assessment; **ALS** = amyotrophic lateral sclerosis; **ACMG** = American College of Medical and Genomic Genetics; **AOO** = age of onset; **CADD score** = combined annotation dependent depletion; **CM** = cardiomyopathy; **D** = dementia; **Dys** = dysautonomia; **ED** = extrapyramidal disorder; **FTD** = fronto temporal dementia; **IBMPFD** = Hereditary Inclusion-Body Myopathy with Paget's Disease of the Bone and Frontotemporal Dementia; **LL** = lower limbs; **LMN** = lower motor neuron signs; **LP** = likely pathogenic; **MND** = motor neuron disease; **MSP** = multisystem proteinopathy; **Myo** = myopathic pattern; **Neu** = neurogenic pattern; **NGS** = next generation sequencing; **PDB** = Paget disease of the bone; **RA** = regional atrophy; **RV** = rimmed vacuoles; **SIFT** = sorting intolerant from tolerant; **SW** = scapular winging; **UL** = upper limbs; **UMN** = upper motor neuron signs; **VCP** = Valosin-containing protein; **VUS** = variant of unknown significance.

Results

All variants were missense, except for one small deletion-insertion, 18 led to amino acid changes within the N and D1 domains, and 13 increased the enzymatic activity. The clinical score coincided with the functional studies in 17 of 19 variants and with the in silico analysis in 12 of 19. For 12 variants, the 3 predictive tools agreed, and for 7 variants, the predictive tools disagreed. The pooled data supported the pathogenicity of 13 of 19 novel VCP variants identified in the study.

Discussion

This study provides data to support pathogenicity of 14 of 19 novel *VCP* variants and provides guidance for clinicians in the evaluation of novel variants in the *VCP* gene.

Introduction

Valosin-containing protein (VCP), or p97, is an hexameric protein from the AAA+ (ATPases Associated with diverse cellular Activities) family involved in the remodeling of molecules using the energy of ATP hydrolysis.[1] VCP is encoded by the *VCP* gene, a 17-exon gene on chromosome 9.[2] Variants in the *VCP* gene were initially described in patients with inclusion body myopathy, Paget disease of the bone, and frontotemporal dementia (IBMPFD).[2] However, this acronym is insufficient to capture the expanding phenotypic spectrum of VCP patients, and currently, this disease is more accurately considered a member of a group of conditions known as multisystem proteinopathy (MSP).[3,4] In fact, only 3–12% of patients with VCP-MSP show the typical triad of IBMPFD[5]; there is heterogeneous phenotypes within families[6-8]; and variants in *VCP* can lead to a plethora of clinical presentations making the diagnosis a complicated task.[6,9-19]

To date, only missense variants have been described in patients with VCP-MSP.[3,7,20] In all cases, the pattern of inheritance is dominant. The mechanism of VCP dysfunction is likely context-dependent because assays studying VCP mutant function in vitro and in vivo support a gain and loss of function mechanism. In vitro, most pathogenic variants have an increase in ATPase activity, what reflects an induced structural change allowing for an increase in ATP accessibility and ADP release. By contrast, cells and animals expressing VCP-MSP variants behave similarly to VCP chemical or genetic inhibition suggesting that VCP pathogenic variants are dysfunctional.[21] How the apparent increase in ATPase activity in vitro correlates with a loss of VCP function in vivo remains to be explored but is likely due to the complex interactions of adaptor proteins mediated by the ATPase cycle.

Challenges in asserting the pathogenicity to novel *VCP* variants are due to the diverse phenotypic presentations, the possible varied gene penetrance, and the fact that ancillary tests may support the diagnosis but do not show pathognomonic features. In addition, patients could be seen by clinicians with different backgrounds; neurologists specialized in dementia, movement disorders, or muscle diseases; endocrinologists; or rheumatologists, which could lead to fragmented and siloed care making difficult the recognition that there is a monogenic disease segregating in the family.

Current strategies to evaluate the pathogenicity of novel variants often rest solely on genetic evidence such as variant rarity in population databases or segregation of the variant with phenotype in families. This approach does not consider that in multisystem diseases, such as in VCP-MSP, sometimes only limited phenotypic information is available for the ordering clinician. In addition, there is no clear consensus on functional assays that may help define pathogenic function of VCP variants.

In this study, we report 19 novel variants in the *VCP* gene identified in the collaborative VCP International Multicenter Study.[8] We have developed a scoring system to help in the assessment of the potential pathogenicity of novel *VCP* variants and have confronted the results of our score with results of functional testing.

Methods

Patients

Patients included in this report are part of the descriptive retrospective VCP International Multicenter Study that collected

Table 1 Scoring System

Item	Description	Points allocated
Item 1	Presence of a VCP-MSP core phenotype in the patient: myopathy, dementia,[a] PDB, motor neuron disease, and/or extrapyramidal disorder	1
Item 2	Positive family segregation following an autosomal dominant pattern of inheritance	1
Item 3	First-degree relative showing any of the VCP-MSP core phenotypes (even without genetic confirmation)	1
Item 4	Novel variant reported in an unrelated individual (from an unrelated family) with a VCP-MSP core phenotype[b]	1
Item 5	Muscle biopsy of the patient showing rimmed vacuoles or protein inclusions/aggregates	1
Item 6	Presence of "fat pockets" on axial T1-w MRI of the tight and/or legs.	0.5

Abbreviations: MSP = multisystem proteinopathy; PDB = Paget disease of the bone.
The scoring system aids in evaluating the phenotypic level of evidence supporting the pathogenicity of a novel and/or nonpreviously clinically characterized variant in the VCP gene using clinical, family history, and ancillary test data available on clinical practice. For each variant, the points of the items present are added, and based on the total score, the variant is classified as follows:
•High likelihood disease associated variant: >3 points.
•Probable disease associated variant: 2–3 points.
•Variant with undetermined association: 0.5–1.5 points.
This scoring system is suggested to be applied after a novel/VUS variant in the VCP gene was identified and other genetic diagnosis are less likely to explain the clinical phenotype of the patient.
This scoring should be reapplied on each regular patient's clinical follow-up to build up the phenotypic level of evidence longitudinally. This may require collecting additional data on sign/symptoms, family history, ancillary test results, and published literature evidence.
[a] Preferably, but not exclusively, frontotemporal dementia.
[b] This is the case for variant p.Ile216Met, p.Ile369Thr, p.Ile241Ser, or p.Met158Thr in this study.

clinical, genetic, and ancillary test data from 255 patients seen in 52 centers from 24 countries.[8] "To standardize variant interpretation, which was performed differently within individual countries, all genetic variants were centrally reviewed by an experienced geneticist from the John Walton Muscular Dystrophy Centre using the criteria suggested by the American College of Medical and Genomic Genetics (ACMG) as a guide.[22] All variants were analyzed using larger databases including 1,000 genomes, dbSNP, ExAC and Exome Variant Server. Variant nomenclature was based on transcript reference NM_007216.3. Inclusion criteria for the present report were adapted from the one used in the VCP International Multicenter Study and included: (1) patients ≥18 years old heterozygous for a novel or a previously reported but not thoroughly clinically characterized as pathogenic (P) or Likely Pathogenic (LP) variant in the *VCP* gene and (2) enough data available in the clinical notes to answer questions about age of disease onset, symptoms and clinical signs at onset and/or during disease's progression, family segregation analysis, and ancillary test results.[8]" Two additional patients with novel pathogenic variants who were not part of the VCP International Multicenter Study were also included in this study.

Standard Protocol Approvals, Registrations, and Patient Consents

The VCP International Multicenter Study obtained Caldicott approval from The Newcastle upon Tyne Hospitals Register Audit (project number 10833, Caldicott Approval: 7918) and institutional review board approvals from the LMU Klinikum at Ludwig-Maximilians University in Munich (project 21-0071); Washington University School of Medicine Institutional Review Board, USA (no 201103416); and the Johns Hopkins Hospital Institutional Review Board, Baltimore, USA (no 00288171). The novel variants in the VCP gene associated with the VCP-MSP article was approved by the human studies review committee at Washington University School of Medicine in St. Louis (201903027). These ethics committees cataloged this study as an audit because it collected deidentified retrospective data of patients with VCP. This study has been performed in accordance with the ethical standards laid down in the 1964 Declaration of Helsinki and its later amendments.

Development of a Pathogenicity Score

To evaluate the phenotypic level of evidence to support the pathogenicity of the novel and/or nonpreviously clinically characterized variants, a score was developed (Table 1). The score consists of 6 items assessing information that can be obtained on daily clinical practice. These items were chosen based on the authors' clinical experience and because they are commonly used to support a diagnosis of VCP-MSP in the literature. Item 6, which refers to muscle MRI, requires the presence of the so-called fat pockets in the skeletal muscle of the patients. This is a feature that can be found in patients with VCP-MSP as previously reported[23] and as shown in the muscle MRI images in eAppendix 1 (links.lww.com/NXG/A625). Each item is allocated a value to support their contribution to the variant association with the clinical phenotype. The sum of all the items leads to a total score, with a minimum of 0.5 and maximum of 5.5 points. We considered a variant to be high likelihood disease associated if its total score was greater than 3 points, probably associated if the total score was between 2 and 3 points, and undetermined association if the score was less than 2 points.

Table 2 Classification of the Novel Variants Based on the Scoring System

DNA m (Protein m)	Highest score in the variant
Scoring system applied to the 4 most frequent variants identified in the VCP International Multicenter Study	
c.464G>A, (p.Arg155His)	5.5
c.463C>T (p.Arg155Cys)	5.5
c.476G>A (p.Arg159His)	5.5
c.277C>T (p.Arg93Cys)	5.5
High likelihood disease associated variant	
c.648A>G (p.Ile216Met)	5.5
c.722T>G (p.Ile241Ser)	5
c.1105A>T (p.Ile369Phe)	4.5
c.431_432delGAinsAC (p.Arg144His)	4.5
c.473T>C (p.Met158Thr)	4.5
c.1106T>C (p.Ile369Thr)	4.5
Probable disease associated variant	
c.268A>G (p.Asn90Asp)	3
c.367G>A (p.Val123Met)	3
c.196G>A (p.Glu66Lys)	2.5
c.463C>G (p.Arg155Gly)	2
c.490A>C (p.Lys164Gln)	2
c.286C>G (p.Leu96Val)	2
c.625T>G (p.Cys209Gly)	2
Variant with undetermined association	
c.80T>C (p.Ile27Thr)	1.5
c.1988A>G (p.Lys663Arg)	1.5
c.265 C>G (p.Arg89Gly)	1
c.1057A>G (p.Ile353Val)	1
c.697A>G (p.Ile233Val)	1
c.335A>G (p.Lys112Arg)	1

For a detailed description of the clinical scoring system applied to each novel variants, please refer to eAppendix 2 (links.lww.com/NXG/A626).

To assess the validity of the scoring system, we first tested the score using several patients harboring the 4 most frequent pathogenic variants included in the VCP International Multicenter Study: p.Arg155His, p.Arg155Cys, p.Arg159His, and p.Arg93Cys, and then, we scored the novel nonpreviously clinically characterized variants and all the variants included in the VCP International Multicenter Study (eAppendix 2, links.lww.com/NXG/A626, 58 variants in total).

In Silico Analysis

The deleteriousness of the novel variants was predicted by 3 independent in silico tools commonly used in daily routine: Mutation Taster (mutationtaster.org/),[24] SIFT (sorting intolerant from tolerant, sift.bii.a-star.edu.sg/),[25] and CADD (combined annotation-dependent depletion, cadd.gs.washington.edu/).[26] These tools use predictive algorithms, based on different variables such as sequence homology, physical properties of amino acids, or evolutionary conservation of the protein sequence to establish whether an amino acidic change could affect protein function and, therefore, its potential pathogenicity.

In vitro ATPase Assay

Human VCP plasmid (TCB197) was subjected to site-directed mutagenesis with primers containing mutations to create each of the indicated variants. Proteins were purified as described.[27] Purified VCP (12.5 μL of 50 μM; final concentration in the reaction was 25 nM) was diluted in 20 mL of assay buffer [5 mL of 5× assay buffer A (1× = 50 mM Tris pH 7.4, 20 mM MgCl2, 1 mM EDTA) mixed with 15 mL of water and 25 μL 0.5M TCEP, 25 μL 10% Triton] to make the enzyme solution. 40 μL of the enzyme solution was dispensed into each well of a 96-well plate. The ATPase assay was prepared by adding 10 μL of 1,000 μM ATP (Roche, pH 7.5) to each well and by incubating the reaction at room temperature for 25 minutes. Reactions were stopped by adding 50 μL of BIOMOL Green reagent (Enzo Life Sciences). Absorbance at 635 nm was measured after 4 minutes on the Synergy Neo Microplate Reader (Bio-Tek). All assays were performed in triplicate, and the activity was averaged from independent experiments.

Statistical Analysis

Data were expressed as number and percentage for categorical variables and as mean ± SD for quantitative ones. For VCP ATPase assays, statistical significance was defined using a 2-way analysis of variance across all samples compared with the wild-type control.

Mean difference in the 6-item score between pathogenic/likely pathogenic variants and variants of unknown significance, of the 58 variants included in the VCP International Study, was explored using independent sample T tests. To identify which score predicted with the highest sensitivity and specificity whether a variant was pathogenic/likely pathogenic based on the ACGM criteria, a receiver-operating characteristic curve was performed (eAppendix 3, links.lww.com/NXG/A627) and its area under the curve and the optimal cutoff point (Youden index) were calculated.

A level of significance of 0.05 was used for hypothesis testing. Statistical analysis was performed using the program IBM SPSS statistics, version 28.

Data Availability

The clinical, genetic, and enzymatic test data reported in this study are available on reasonable request to the corresponding authors.

Figure 1 Location of the Novel Mutations in the VCP Gene and Protein

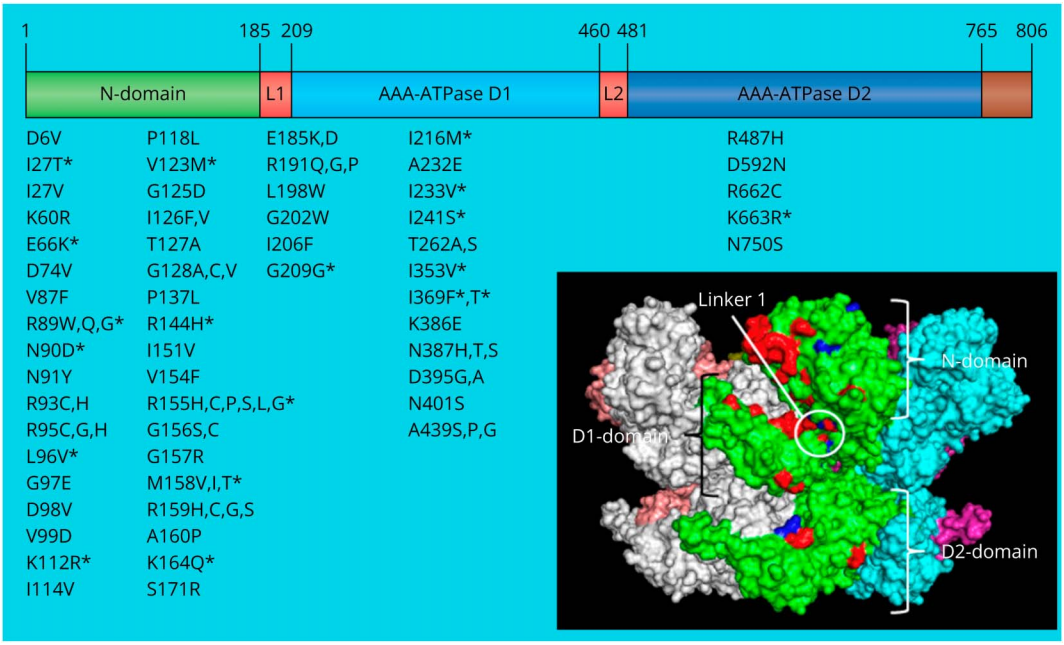

Scheme of the location of all the variants described in the VCP gene and protein structure. The VCP protein contains 806 amino acids and is constituted by an N-terminal domain involved in the cofactor and ubiquitin-binding function, a D1 domain involved in the assembly of VCP homohexamer, a D2 domain responsible for the major ATPase activity, and the C-terminal domain involved in nuclear localization by interacting with other proteins. The N-domain and D1 domain are connected by N-D1 linker (L1), and the D1and D2 domains are connected by flexible D1-D2 linker (L2). All variants are listed underneath the domain affected; those with an asterisk are considered novel. The black square contains a 3D render of a VCP hexamer. Each subunit is independently colored. The positions of previously reported pathogenic residues are denoted in red and the novel reported variant residues in blue within a single green monomer. VCP = valosin-containing protein.

Results

We identified 19 previously uncharacterized variants in the *VCP* gene from 28 patients with presumed VCP-MSP from 26 unrelated families (Table 2, eAppendix 2, links.lww.com/NXG/A626, and eAppendix 4, links.lww.com/NXG/A628). Eighteen of the 19 variants had not been previously reported in GNOMAD. One variant, p.Ile233Val, had been reported twice, and GNOMAD provided with a minor allele frequency of 7.95E-06. Six of the 19 variants had been reported in ClinVar, and one of these 6 were additionally reported in LOVD. These 7 previously reported variants were not thoroughly clinically characterized in the literature though. Figure 1 shows the localization of the novel variants in the *VCP* gene.

Phenotypic Scoring

As shown in eAppendix 2 (links.lww.com/NXG/A626), at least one patient carrying the novel variants on the *VCP* gene manifested with one or more of the VCP-MSP core phenotypes (e.g., myopathy, PDB, FTD, ALS or parkinsonism), except for one patient (Family 26 III-1), harboring the c.335A>G (p.Lys112Arg) variant, who presented with signs of upper motor neuron involvement without muscle weakness. In all cases, pathogenic variants in other genes were excluded by exome or panel-based sequencing. Notably, muscle weakness was reported in 85.7% (24/28) of the cases, FTD in 21.4% (6/28), and PDB in 18.0% (5/28). No patient showed the classical IBMPFD triad. Fifteen of the 28 patients had a first-degree relative with an VCP-MSP core phenotype, dementia being the most common symptom in the relatives (10/28).

All patients were heterozygous for their *VCP* variant, compatible with a dominant inheritance. All variants were missense, except for one small deletion-insertion that created the missense variant p.Arg144His. Eighteen of the 19 variants led to amino acid changes within the N and D1 domains, where 64 of the 68 previously reported VCP-MSP variants were located (Figure 1).

To establish the validity of our scoring system, we first evaluated the score obtained by the 4 most common *VCP* variants—p.Arg155His, p.Arg155Cys, p.Arg159His, and p.Arg93Cys. These 4 variants achieved the highest score possible of 5.5 points. Then, we applied the scoring system to the 28 patients with the 19 novel variants described here, obtaining a range of scores from 0.5 to 5.5 (Table 2). Examples of the classical clinical and ancillary test findings seen in patients with VCP-MSP found in our cohort are described in eAppendix 1 (links.lww.com/NXG/A625).

In Silico Analysis

The in silico predictions on the 4 most common pathogenic mutations predicted them to be probably deleterious. Table 3

Table 3 In Silico Analysis

DNA change	Protein change	CADD score	Mutation taster	POLYPHEN-2
More prevalent pathogenic variants				
c.464G>A	p.Arg155His	24.5	DC	PrD 0.989
c.463C>T	p.Arg155Cys	33	DC	PrD 1
c.476G>A	p.Arg159His	24.1	DC	PsD 0.517
c.277C>T	p.Arg93Cys	31	DC	PrD 0.998
Novel variants				
c.648A>G	p.Ile216Met	23.6	DC	PrD 1
c.722T>G	p.Ile241Ser	29.9	DC	PrD 1
c.1105A>T	p.Ile369Phe	27.2	DC	PrD 1
c.431_432delGAinsAC	p.Arg144His	n/a	DC	PrD 1
c.473T>C	p.Met158Thr	24.2	DC	PB 0.988
c.1106T>C	p.Ile369Thr	26.7	DC	PrD 1
c.268A>G	p.Asn90Asp	23.1	DC	PsD 0.602
c.367G>A	p.Val123Met	26.9	DC	PsD 0.696
c.196G>A	p.Glu66Lys	23.9	DC	B 0.002
c.463C>G	p.Arg155Gly	25.8	DC	PrD 1
c.490A>C	p.Lys164Gln	25.2	DC	PrD 1
c.286C>G	p.Leu96Val	23.2	DC	B 0.028
c.625T>G	p.Cys209Gly	24.1	DC	PsD 0.704
c.80T>C	p.Ile27Thr	23	DC	PrD 0.968
c.1988A>G	p.Lys663Arg	23.7	DC	B 0.005
c.335A>G	p.Lys112Arg	22.9	DC	B 0.066
c.265C>G	p.Arg89Gly	23.2	DC	PrD 1
c.1057A>G	p.Ile353Val	20.3	DC	B 0.008
c.697A>G	p.Ile233Val	22.6	DC	PsD 0.810

Abbreviations: B = benign; DC = disease-causing; PB = possible benign; PrD = probable deleterious; PrD = probable deleterious; PsD possible deleterious.
In silico scores for the 4 prevalent variants identified in the VCP International Multicenter Study and the 19 variants described in this study.
CADD scores >20: top 1% deleterious variants in the genome.

shows the results of the predictive algorithms for each of the 19 novel variants that ranged from benign to probably deleterious.

In Vitro ATPase Assays

To further understand whether the variants identified lead to a functional change in the VCP protein, we purified a recombinant wild-type VCP, the 4 most common pathogenic VCP mutants (VCP-Arg155His, VCP-Arg155Cys, VCP-Arg159His, and VCP-Arg93Cys), a previously reported benign variant (VCP-Ile27Val), and the new 19 VCP variants. VCP hydrolyzes ATP, and the rate of hydrolysis is enhanced by most of the previously described VCP pathogenic variants. VCP-WT ATPase activity was arbitrarily set to 100%. The common 4 pathogenic variants demonstrated a 4 to 5-fold increase in ATPase activity consistent with previous studies, whereas the VCP- p.Ile27Val benign variant had only a 1.6-fold increase in ATPase activity. Using these data points, we selected a 3-fold increase as being consistent with a dysfunctional variant. Thirteen of the novel variants met this threshold (Figure 2).

A summary of the evidence obtained for each variant using the scoring system, in silico analysis, and enzymatic activity is provided in Table 4. For 12 variants, there was agreement between the 3 predictive tools, including 9 variants predicted to be deleterious and 3 variants predicted to be nondeleterious.

For 7 variants, the predictive tools disagreed. For 3 of them (p.Met158Thr, p.Glu66Lys and p.Leu96Val), clinical score and enzymatic activity supported pathogenicity while in silico studies did not. Conversely, in other 2 variants (p.Ile27Thr and p.Ile233Val), clinical score and enzymatic activity supported nonpathogenicity while in silico studies did.

For the variant p.Arg144His, both the scoring system and the in silico algorithms predicted pathogenicity, but the enzymatic activity did not. This variant was found in a patient with isolated muscle disease with a muscle biopsy showing rimmed vacuoles and a MRI showing patchy fat replacement in the quadriceps and who had several relatives with dementia, ALS, and muscle disease. The variant obtained 4.5 of 5.5 points in the scoring system, but the enzymatic activity was normal.

For the variant p.Arg89Gly, the in silico studies and enzymatic activity suggested pathogenicity, but the clinical score was very low (1 point). This variant was found in a patient with isolated muscle weakness, with no relevant family history, who had just fiber atrophy in the muscle biopsy but not rimmed vacuoles or protein aggregates and who did not have an MRI.

Discussion

The increasing availability of next-generation sequencing panels and whole-exome/genome sequencing is leading to the identification of new variants in the *VCP* gene.[28] The evaluation of these novel variants is challenging because of the intrafamilial and interfamilial phenotype variability[7] and because of the progressive nature of the condition, implying that patients might not show the whole clinical spectrum when the results of the genetic tests are obtained. As a result, VCP-MSP diagnosis can be missed in early stages of the disease or clinical features could be attributed to other diagnosis.[20] This situation can be even more complex if thorough family history or segregation studies are not obtained. Moreover, patients present with a variety of clinical, ancillary tests or family history findings and allocating them a hierarchical weight in

Figure 2 Enzymatic in Vitro Test

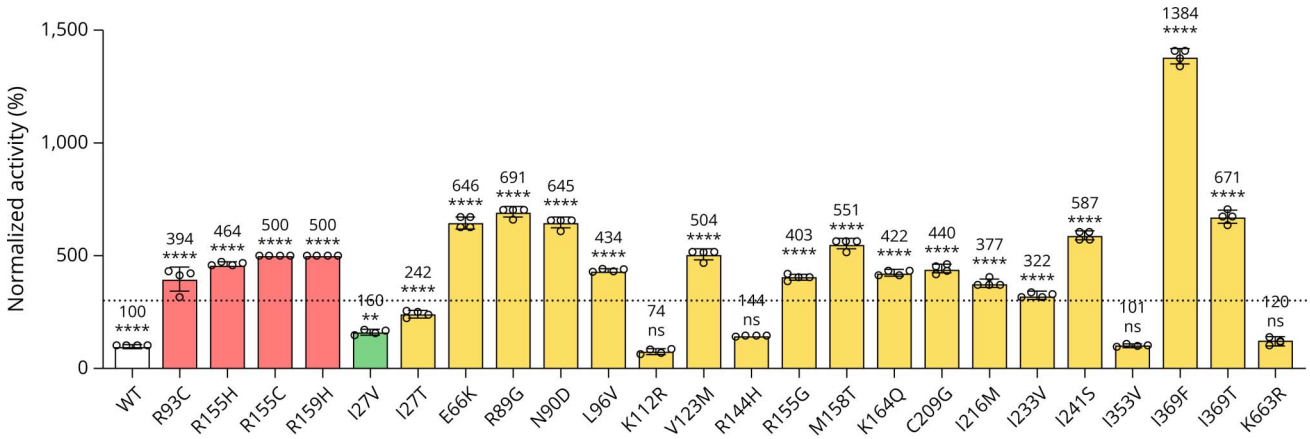

Basal ATPase activity was determined from purified recombinant VCP protein. Values are normalized to VCP-wild type activity and presented as percent change from VCP-wild type. Red bars represent known pathogenic variants. Green bars represent known benign variants. Yellow bars represent the novel variants investigated. The dotted line represents the 3-fold increase threshold in ATPase activity consistent with a dysfunctional variant. ns: nonsignificant difference. $^{**}p < 0.05$; $^{****}p < 0.0001$. VCP = valosin-containing protein.

the analysis of the potential pathogenicity of a new variant is challenging. It is crucial to estimate adequately the pathogenicity of new variants to avoid overestimating variants that could lead to a wrong diagnosis and stop the surveillance of other etiologies behind the patients' phenotype. In addition, when it comes to interpreting novel variants, information about its rarity based on their frequency in population databases is not enough to confirm pathogenicity. Even if a variant is labelled as VUS following the ACGM criteria, clinicians should consider other information such as patient phenotype, family history, segregation in the family, and ancillary test results to support the potential pathogenicity of the variant.

The scoring system proposed here intends to be a tool to support clinicians when facing a novel variant in the VCP gene in clinical practice. The current standard of care in VCP suggests that symptomatic patients should be assessed every 6–12 months or more frequently if required.[29] The evolving nature of this disease implies that a novel variant that scored low early in disease progression can end up having a higher score. This could be the case of the p.Arg89Gly variant, for which the in silico and enzymatic studies suggested pathogenicity, but it was found in a young patient with isolated weakness, therefore, leading to a low clinical score. Updating the scoring system on each clinical visit is encouraged in these cases because new symptoms can appear later in disease progression further supporting the diagnosis of the disease. The clinical score coincided with the functional studies in 17 of 19 new variants and with the in silico prediction in 12 of 19 new variants, suggesting that functional studies, which assess enzymatic function, may provide a more reliable prediction of the potential pathogenicity of variants.

VCP has 2 ATPase domains, D1 and D2, which are organized as 2 stacked rings with a central channel, whereas its regulatory N domain is situated at the periphery of the D1 ring.[30] Reported pathogenic variants do not seem to alter VCP oligomerization but increase basal ATP hydrolysis activity, which is mediated through the D2 domain.[30] Pathogenic variant residues are commonly found in the interface between the N and D1 domains, suggesting that communication between these 2 regions is important for disease pathogenesis.[1] Other variants might affect the association of VCP with cofactors.[31] All the novel mutations identified in this study change an amino acid in the N terminal or D1 domain, except for the variant p.Lys663Arg located in the D2 domain. Being an ATPase enzyme, VCP hydrolyzes ATP releasing an inorganic phosphate. We have performed an enzymatic test comparing the intrinsic ATPase activity of VCP-wild type with several previously reported MSP mutations and the novel mutations, as reported in other studies.[13] Most of the novel variants reported here increased ATP activity compared with VCP-wild type. For those variants in which the ATPase activity did not differ from the VCP-wild type, clinical score and/or in silico analysis suggested nonpathogenicity. The only exception to this is the p.Arg144His variant that was suggested as pathogenic by the in silico studies and found in a patient with clinical data highly suggestive of the disease, but with a normal enzymatic activity. An elevation in basal ATPase activity has been described for most VCP variants, with the exception of 2 previously reported variants. Specifically, the p.Glu185Lys variant described in a large family with axonal CMT and p.Asp395Gly in 2 families with a pathologically distinct dementia (vacuolar tauopathy) had unchanged and reduced ATPase activity, respectively.[32,33] These variants suggest that VCP mutations could alter VCP functionality by an ATPase-independent manner. Thus, a reliance exclusively on in vitro ATPase assays of VCP function may be misleading.

Table 4 Summary of the Study Results

Variant	Scoring system	In silico analysis	Enzymatic analysis	Interpretation
c.648A>G; p.Ile216Met	5.5	Deleterious	+	Agreement in the 3 tools, deleterious
c.722T>G; p.Ile241Ser	5	Deleterious	+	Agreement in the 3 tools, deleterious
c.1105A>T; p.Ile369Phe	4.5	Deleterious	+	Agreement in the 3 tools, deleterious
c.431_432delGAinsAC; p.Arg144His	4.5	Deleterious	−	Enzymatic analysis disagrees
c.473T>C; p.Met158Thr	4.5	Inconclusive	+	In silico analysis disagrees, Polyphen-2 PB
c.1106T>C; p.Ile369Thr	4.5	Deleterious	+	Agreement in the 3 tools, deleterious
c.268A>G; p.Asn90Asp	3	Deleterious	+	Agreement in the 3 tools, deleterious
c.367G>A; p.Val123Met	3	Deleterious	+	Agreement in the 3 tools, deleterious
c.196G>A; p.Glu66Lys	2.5	Inconclusive	+	In silico analysis disagrees, Polyphen-2 B
c.463C>G; p.Arg155Gly	2	Deleterious	+	Agreement in the 3 tools, deleterious
c.490A>C; p.Lys164Gln	2	Deleterious	+	Agreement in the 3 tools, deleterious
c.286C>G; p.Leu96Val	2	Inconclusive	+	In silico analysis disagrees, Polyphen-2 B
c.625T>G; p.Cys209Gly	2	Deleterious	+	Agreement in the 3 tools, deleterious
c.80T>C; p.Ile27Thr	1.5	Deleterious	−	In silico analysis disagrees, Polyphen-2 PrD
c.1988A>G; p.Lys663Arg	1.5	Inconclusive	−	Agreement in the 3 tools, nondeleterious
c.335A>G; p.Lys112Arg	1	Inconclusive	−	Agreement in the 3 tools, nondeleterious
c.265 C>G; p.Arg89Gly	1	Deleterious	+	Scoring system disagrees
c.1057A>G; p.Ile353Val	1	Inconclusive	−	Agreement in the 3 tools, nondeleterious
c.697A>G; p.Ile233Val	1	Deleterious	−	In silico analysis disagrees, Polyphen-2 PrD

The table shows the evidence obtained for each variant using the scoring system, the in silico analysis, and the in vitro ATPase assay (enzymatic activity) and the variant effect interpretation based on the agreement of the 3 tools.

The results of muscle biopsy and MRI in patients with VCP-MSP are not specific[34] and can overlap with conditions such as myofibrillar myopathies, other multisystem proteinopathies, or myopathies with rimmed vacuoles.[4] In this context, an enzymatic test that measures the effect of a variant in the ATPase activity can aid in diagnosis.[13,35] However, assessing the intrinsic ATPase enzymatic activity in VCP requires purified recombinant protein. Moreover, there is not an easier assay that uses blood, muscle, or even cerebrospinal fluid samples. Other blood biomarkers, such as tumor necrosis factor alpha and epidermal growth factor, have been suggested to differentiate patients with VCP-MSP from healthy controls,[36] but these biomarkers are not disease-specific and can be found in other inflammatory conditions.[37,38]

Three of the variants described here affected amino acidic residues that have been previously identified in patients with VCP-MSP. One variant affected the hot spot amino acid position Arginine 155 codified by exon 5, creating the p.Arg155Gly variant. A second variant was identified at amino acid residue Arginine at position 89, creating a p.Arg89Gly missense variant. Notably, p.Arg89Gln and p.Arg89Trp variants have been reported in a patient with sporadic ALS and distal myopathy with cognitive impairment without family history, respectively.[39,40] Another variant created a p.Ile27Thr missense change which affected the same amino acid that the already reported p.Ile27Val variant. Although this later variant has been found in cohorts of sporadic inclusion body myositis and Parkinson disease, it has a MAF of 0.005 to 0.0006 depending on population ethnicity and was equally represented in healthy controls, suggesting that it may be benign.[29,41]

Limitations of this study include the retrospective nature of the VCP International study, from which the novel variants were obtained. Missing data could affect the score system result leading to underestimation of the variant pathogenicity. The sensitivity of the clinical scoring system to label the variants can progress over time because the clinical, muscle MRI and biopsy results can be modified along disease progression, reinforcing the idea that the scoring system should be applied on a regular basis. A greater than 3-fold increase in VCP-variant ATPase activity is helpful to support MSP-VCP mutant pathogenicity but could miss potential pathogenic variants because VCP mutation dysfunction may occur

independent of ATPase activity. Other assays of VCP function may need to be used. These could include assays of cellular autophagic or proteosomal activity.

In conclusion, we have developed a clinical score able to predict pathogenicity of new variants in the *VCP* gene with high accuracy that highly correlates with the results of in silico and enzymatic activity studies. This score could be of great help in the diagnostic process of patients with novel variants in daily clinics. This study provides data to support pathogenicity of 13 of 19 new *VCP* variants based on the fact that (1) patients affected had clinical and family history data highly suggestive of the VCP-MSP; (2) most of the new variants reported resulted in an increase in enzymatic activity in the in vitro assays; (3) novel variants are not present in public databases of controls (dbSNP); (4) these variants affected highly conserved residues across species in the N-terminal and D1 domain, in which most pathogenic VCP pathogenic variants have been reported; (5) no variants were found in other genes which were reported in the patients with MSP, FTD, or ALS previously; and (6) these variants were predicted to be deleterious by 3 prediction in silico assays.

Acknowledgment

The authors are grateful to all families, site investigators, clinical evaluators, research nurses, geneticist, pathologists, and physiotherapists who actively collaborated in the collecting data process. All the authors of this manuscript comply with the ethical guidelines for authorship and publishing of the Neurology journal.

Study Funding

Two grants from the National Institute of Health (R01AG031867 and K24R073317 to C.W.) and a grant from Academy of Medical Sciences (APR04/007 to J.D.-M.).

Disclosure

The authors report no relevant disclosures. Go to Neurology.org/NG for full disclosure.

Publication History

Received by *Neurology: Genetics* March 1, 2023. Accepted in final form June 14, 2023. Submitted and externally peer reviewed. The handling editor was Raymond P. Roos, MD, FAAN.

Appendix Authors

Name	Location	Contribution
Marianela Schiava, MD	John Walton Muscular Dystrophy Research Centre, Newcastle University and Newcastle Hospitals NHS Foundation Trusts, United Kingdom	Conceptualized the study, acquisition of data, analyzed the data, drafted the manuscript for intellectual content
Chiseko Ikenaga, MD	Johns Hopkins University School of Medicine, Baltimore	Conceptualized the study, acquisition of data, drafted the manuscript for intellectual content
Ana Topf, PhD	John Walton Muscular Dystrophy Research Centre, Newcastle University and Newcastle Hospitals NHS Foundation Trusts, United Kingdom	Conceptualized the study, acquisition of data, analyzed the data, drafted the manuscript for intellectual content
Marta Caballero-Ávila, MD	Unidad de Enfermedades Neuromusculares Servicio de Neurología Hospital de la Santa Creu i Sant Pau de Barcelona España	Conceptualized the study, acquisition of data, reviewed the manuscript for intellectual content
Tsui-Fen Chou, PhD	Division of Biology and Biological Engineering, California Institute of Technology Pasadena	Conceptualized the study, acquisition of data, analyzed the data, reviewed the manuscript for intellectual content
Shan Li, PhD	Division of Biology and Biological Engineering, California Institute of Technology, Pasadena	Conceptualized the study, acquisition of data, analyzed the data, reviewed the manuscript for intellectual content
Feng Wang, PhD	Division of Biology and Biological Engineering, California Institute of Technology, Pasadena	Conceptualized the study, acquisition of data, analyzed the data, reviewed the manuscript for intellectual content
Jil Daw, MD	Department of Neurology, Washington University School of Medicine, St Louis, MO	Conceptualized the study, acquisition of data, analyzed the data, reviewed the manuscript for intellectual content
Tanya Stojkovic, MD	APHP Centre de référence des maladies neuromusculaires Institut de Myologie Sorbonne Université APHP Hôpital Pitié-Salpêtrière Paris, France	Conceptualized the study, acquisition of data, reviewed the manuscript for intellectual content
Rocio Villar-Quiles, MD	APHP, Centre de référence des maladies neuromusculaires, Institut de Myologie, Sorbonne Université, APHP, Hôpital Pitié-Salpêtrière Paris, France	Conceptualized the study, acquisition of data, reviewed the manuscript for intellectual content
Ichizo Nishino, MD, PhD	Department of Neuromuscular Research, National Institute of Neuroscience, National Center of Neurology and Psychiatry (NCNP), Japan	Acquisition of data, reviewed the manuscript for intellectual content
Michio Inoue, MD	Department of Neuromuscular Research, National Institute of Neuroscience, National Center of Neurology and Psychiatry (NCNP), Japan	Acquisition of data, reviewed the manuscript for intellectual content
Yukako Nishimori, MD	Department of Neuromuscular Research, National Institute of Neuroscience, National Center of Neurology and Psychiatry (NCNP), Japan	Acquisition of data, reviewed the manuscript for intellectual content

Continued

Appendix *(continued)*

Name	Location	Contribution
Yoshihiko Saito, MD, PhD	Department of Neuromuscular Research, National Institute of Neuroscience, National Center of Neurology and Psychiatry (NCNP), Japan	Acquisition of data, reviewed the manuscript for intellectual content
Masahisa Katsuno, MD, PhD	Departments of Neurology and Clinical Research Education, Nagoya University Graduate School of Medicine, Japan	Acquisition of data, reviewed the manuscript for intellectual content
Seiya Noda, MD	Department of Neurology, Nagoya University Graduate School of Medicine; Department of Neurology, National Hospital Organization Suzuka Hospital, Japan	Acquisition of data, reviewed the manuscript for intellectual content
Chihiro Ito, MD	Department of Neurology, Aichi Medical University School of Medicine, Japan	Acquisition of data, reviewed the manuscript for intellectual content
Mieko Otsuka, MD	Department of Neurology, International University of Health and Welfare Hospital, Japan	Acquisition of data, reviewed the manuscript for intellectual content
Sruthi Nahir, MD	Department of Neurology Sree Chitra Tirunal Institute for Medical Sciences and Technology, Thiruvananthapuram, Kerala, India	Acquisition of data, reviewed the manuscript for intellectual content
Georgios Manousakis, MD	Departments of Neurology, University of Minnesota, Minneapolis	Acquisition of data, reviewed the manuscript for intellectual content
David Walk, MD	Departments of Neurology, University of Minnesota, Minneapolis	Acquisition of data, reviewed the manuscript for intellectual content
Colin Quinn, MD	Department of Neurology, University of Pennsylvania, Perelman School of Medicine, Philadelphia, PA, USA	Acquisition of data, reviewed the manuscript for intellectual content
Lindsay Alfano, PhD	Center for Gene Therapy, The Abigail Wexner Research Institute at Nationwide Children's Hospital; Department of Pediatrics, The Ohio State University College of Medicine, Columbus	Acquisition of data, reviewed the manuscript for intellectual content
Zarife Sahenk, MD	Center for Gene Therapy, The Abigail Wexner Research Institute at Nationwide Children's Hospital; Department of Pediatrics, The Ohio State University College of Medicine, Columbus	Acquisition of data, reviewed the manuscript for intellectual content
Giorgio Tasca, MD, PhD	Unità Operativa Complessa di Neurologia Fondazione Policlinico Universitario A Gemelli IRCCS, Rome, Italy	Acquisition of data, reviewed the manuscript for intellectual content

Appendix *(continued)*

Name	Location	Contribution
Mauro Monforte, MD, PhD	Unità Operativa Complessa di Neurologia Fondazione Policlinico Universitario A Gemelli IRCCS, Rome, Italy	Acquisition of data, reviewed the manuscript for intellectual content
Mario Sabatelli, MD	Centro clinico NEMO-Fondazione policlinico universitario A Gemelli IRCCS, Rome, Italy	Acquisition of data, reviewed the manuscript for intellectual content
Giulia Bisogni, MD, PhD	Centro clinico NEMO-Fondazione policlinico universitario A Gemelli IRCCS, Rome, Italy	Acquisition of data, reviewed the manuscript for intellectual content
Anders Oldfors, MD, PhD	Department of Laboratory Medicine, Institute of Biomedicine, University of Gothenburg, Sweden	Acquisition of data, reviewed the manuscript for intellectual content
Anna Rydelius, MD	Department of Neurology, Clinical Sciences Lund, Lund University, Sweden	Acquisition of data, reviewed the manuscript for intellectual content
Endre Pal, MD	Departments of Neurology and Neuropathology, University of Pécs, Hungary	Acquisition of data, reviewed the manuscript for intellectual content
Carmen Paradas, MD	Neurology Department, Neuromuscular Disorders Unit, Hospital Universitario Virgen del Rocío; Instituto de Biomedicina de Sevilla; Centre for Biomedical Network Research on Neurodegenerative Disorders (CIBERNED) Instituto de Salud Carlos III, Madrid, Spain	Acquisition of data, reviewed the manuscript for intellectual content
Beatriz Velez, MD	Neurology Department, Neuromuscular Disorders Unit, Hospital Universitario Virgen del Rocío; Centre for Biomedical Network Research on Neurodegenerative Disorders (CIBERNED) Instituto de Salud Carlos III, Madrid, Spain	Acquisition of data, reviewed the manuscript for intellectual content
Jan L. De Bleecker, MD, PhD	Neurology Department and Neuromuscular Reference Centre, Gent, Blegium, part of the ERN NMD	Acquisition of data, reviewed the manuscript for intellectual content
Maria Elena Farrugia, MD	Institute of Neurological Sciences, Queen Elizabeth University Hospital, Glasgow, United Kingdom	Acquisition of data, reviewed the manuscript for intellectual content
Cheryl Longman, MD	West Scotland Regional Genetics Service, Queen Elizabeth University Hospital, Glasgow, United Kingdom	Acquisition of data, reviewed the manuscript for intellectual content
Matthew B. Harms, MD	Columbia University Irving Medical Centre, Columbia	Acquisition of data, reviewed the manuscript for intellectual content
Stuart Ralston, MD	Centre for Genomic and Experimental Medicine, Institute of Genetics and Cancer, University of Edinburgh, Western General Hospital Edinburgh, United Kingdom	Acquisition of data, reviewed the manuscript for intellectual content

Appendix *(continued)*

Name	Location	Contribution
Edmar Zanoteli, MD	Department of Neurology, School of Medicine, Universidade de São Paulo (FMUSP), Brazil	Acquisition of data, reviewed the manuscript for intellectual content
Andre Macedo Serafim da Silva, MD	Department of Neurology, School of Medicine, Universidade de São Paulo (FMUSP), Brazil	Acquisition of data, reviewed the manuscript for intellectual content
Javier Sotoca, MD	Neurology Service, Neuromuscular Disorders Unit, Hospital Universitari Vall d'Hebron, Barcelona, Spain	Acquisition of data, reviewed the manuscript for intellectual content
Raul Juntas-Morales, PhD	Neurology Service, Neuromuscular Disorders Unit, Hospital Universitari Vall d'Hebron, Barcelona, Spain	Acquisition of data, reviewed the manuscript for intellectual content
Jorge Bevilacqua, MD, PhD	Departamento de Neurología y Neurocirugía, HCUCH, Departamento de Anatomía y Medicina Legal, Facultad de Medicina, Universidad de Chile	Acquisition of data, reviewed the manuscript for intellectual content
Mireya Balart, MD	Departamento de Neurología y Neurocirugía Clínica, Clínica Dávila, Santiago Chile	Acquisition of data, reviewed the manuscript for intellectual content
Stuart Talbot, MD	Newcastle University, Newcastle Upon Tyne, United Kingdom	Acquisition of data, reviewed the manuscript for intellectual content
Volker Straub, MD, PhD	John Walton Muscular Dystrophy Research Centre, Newcastle University and Newcastle Hospitals NHS Foundation Trusts, United Kingdom	Acquisition of data, reviewed the manuscript for intellectual content
Michela Guglieri, MD	John Walton Muscular Dystrophy Research Centre, Newcastle University and Newcastle Hospitals NHS Foundation Trusts, United Kingdom	Acquisition of data, reviewed the manuscript for intellectual content
Chiara Marini-Bettolo, PhD	John Walton Muscular Dystrophy Research Centre, Newcastle University and Newcastle Hospitals NHS Foundation Trusts, United Kingdom	Acquisition of data, reviewed the manuscript for intellectual content
Jordi Diaz-Manera, PhD	John Walton Muscular Dystrophy Research Centre, Newcastle University and Newcastle Hospitals NHS Foundation Trusts, United Kingdom	Conceptualized the study, acquisition of data, analyzed the data, drafted the manuscript for intellectual content
Conrad Chris Weihl, MD, PhD	Department of Neurology, Washington University School of Medicine, Saint Louis MO	Conceptualized the study, acquisition of data, drafted the manuscript for intellectual content

References

1. Meyer H, Weihl CC. The VCP/p97 system at a glance: connecting cellular function to disease pathogenesis. *J Cell Sci.* 2014;127(18):3877-3883. doi:10.1242/jcs.093831
2. Kovach MJ, Waggoner B, Leal SM, et al. Clinical delineation and localization to chromosome 9p13.3-p12 of a unique dominant disorder in four families: hereditary inclusion body myopathy, Paget disease of bone, and frontotemporal dementia. *Mol Genet Metab.* 2001;74(4):458-475. doi:10.1006/mgme.2001.3256
3. Evangelista T, Weihl CC, Kimonis V, et al. 215th ENMC International Workshop VCP-related multi-system proteinopathy (IBMPFD) 13-15 November 2015, Heemskerk, The Netherlands. *Neuromuscul Disord.* 2016;26(8):535-547. doi:10.1016/j.nmd.2016.05.017
4. Korb MK, Kimonis VE, Mozaffar T. Multisystem proteinopathy: where myopathy and motor neuron disease converge. *Muscle Nerve.* 2021;63(4):442-454. doi:10.1002/mus.27097
5. Ikenaga C, Findlay AR, Seiffert M, et al. Phenotypic diversity in an international cure VCP disease registry. *Orphanet J Rare Dis.* 2020;15(1):267. doi:10.1186/s13023-020-01551-0
6. Spinaa S, Van Laarb AD, Murrella JR, et al. Phenotypic variability in three families with valosin-containing protein mutation. *Eur J Neuro.* 2013;20(2):251-258. doi:10.1111/j.1468-1331.2012.03831.x
7. Abrahao A, Abath Neto O, Kok F, et al. One family, one gene and three phenotypes: a novel VCP (valosin-containing protein) mutation associated with myopathy with rimmed vacuoles, amyotrophic lateral sclerosis and frontotemporal dementia. *J Neurol Sci.* 2016;368:352-358. doi:10.1016/j.jns.2016.07.048
8. Schiava M, Ikenaga C, Villar-Quiles RN, et al. Genotype – phenotype correlations in valosin containing protein disease: a retrospective muticentre study. *Neurol Neurosurg Psychiatry.* 2022;jnnp-2022-328921. doi:10.1136/jnnp-2022-328921
9. Sacconi S, Camaño P, de Greef JC, et al. Patients with a phenotype consistent with facioscapulohumeral muscular dystrophy display genetic and epigenetic heterogeneity. *J Med Genet.* 2012;49(1):41-46. doi:10.1136/jmedgenet-2011-100101
10. Palmio J, Sandell S, Suominen T, et al. Distinct distal myopathy phenotype caused by VCP gene mutation in a Finnish family. *Neuromuscul Disord.* 2011;21(8):551-555. doi:10.1016/j.nmd.2011.05.008
11. González-Pérez P, Cirulli ET, Drory VE, et al. Novel mutation in VCP gene causes atypical amyotrophic lateral sclerosis. *Neurology.* 2012;79(22):2201-2208. doi:10.1212/WNL.0b013e318275963b
12. De Bot ST, Schelhaas HJ, Kamsteeg EJ, Van De Warrenburg BPC. Hereditary spastic paraplegia caused by a mutation in the VCP gene. *Brain.* 2012;135(12):e223. doi:10.1093/brain/aws201
13. Gonzalez MA, Feely SM, Speziani F, et al. A novel mutation in VCP causes Charcot-Marie-Tooth Type 2 disease. *Brain.* 2014;137(11):2897-2902. doi:10.1093/brain/awu224
14. Gite J, Milko E, Brady L, Baker SK. Phenotypic convergence in Charcot-Marie-Tooth 2Y with novel VCP mutation. *Neuromuscul Disord.* 2020;30(3):232-235. doi:10.1016/j.nmd.2020.02.002
15. Mariani LL, Tesson C, Charles P, et al. Expanding the spectrum of genes involved in Huntington disease using a combined clinical and genetic approach. *JAMA Neurol.* 2016;73(9):1105-1114. doi:10.1001/jamaneurol.2016.2215
16. Schröder R, Watts GDJ, Mehta SG, et al. Mutant valosin-containing protein causes a novel type of frontotemporal dementia. *Ann Neurol.* 2005;57(3):457-461. doi:10.1002/ana.20407
17. Weihl CC, Pestronk A, Kimonis VE. Valosin-containing protein disease: inclusion body myopathy with Paget's disease of the bone and fronto-temporal dementia. *Neuromuscul Disord.* 2009;19(5):308-315. doi:10.1016/j.nmd.2009.01.009
18. Wang SC, Smith CD, Lombardo DM, Kimonis V. Characteristics of VCP mutation-associated cardiomyopathy. *Neuromuscul Disord.* 2021;31(8):701-705. doi:10.1016/j.nmd.2021.06.005
19. Columbres RCA, Chin Y, Pratti S, et al. Novel variants in the VCP gene causing multisystem proteinopathy 1. *Genes (Basel).* 2023;14(3):676. doi:10.3390/genes14030676
20. Al-Tahan S, Al-Obeidi E, Yoshioka H, et al. Novel valosin-containing protein mutations associated with multisystem proteinopathy. *Neuromuscul Disord.* 2018;28(6):491-501. doi:10.1016/j.nmd.2018.04.007
21. Weihl CC, Dalal S, Pestronk A, Hanson PI. Inclusion body myopathy-associated mutations in p97/VCP impair endoplasmic reticulum-associated degradation. *Hum Mol Genet.* 2006;15(2):189-199. doi:10.1093/hmg/ddi426
22. Richards S, Aziz N, Bale S, et al. Standards and guidelines for the interpretation of sequence variants: a joint consensus recommendation of the American College of Medical Genetics and Genomics and the Association for Molecular Pathology. *Genet Med.* 2015;17(5):405-424. doi:10.1038/gim.2015.30
23. Díaz-Manera J, Llauger J, Gallardo E, Illa I. Muscle MRI in muscular dystrophies. *Acta Myol.* 2015;34(2-3):95-108.
24. Schwarz JM, Cooper DN, Schuelke M, Seelow D. Mutation Taster 2: mutation prediction for the deep-sequencing age. *Nat Methods.* 2014;11(4):361-362. doi:10.1038/nmeth.2890
25. Ng PC, Henikoff S. SIFT: predicting amino acid changes that affect protein function. *Nucleic Acids Res.* 2003;31(13):3812-3814. doi:10.1093/nar/gkg509
26. Kircher M, Witten DM, Jain P, Roak BJO, Cooper GM, Shendure J. A general framework for estimating the relative pathogenicity of human genetic variants. *Nat Genet.* 2014;46(3):310-315. doi:10.1038/ng.2892
27. Chou T, Bulfer SL, Weihl CC, et al. Specific inhibition of p97/VCP ATPase and kinetic analysis demonstrate interaction between D1 and D2 ATPase domains. *J Mol Biol.* 2015;426(15):2886-2899. doi:10.1016/j.jmb.2014.05.022
28. Johnson JO, Mandrioli J, Benatar M, et al. Exome sequencing reveals VCP mutations as a cause of familial ALS. *Neuron.* 2010;68(5):857-864. doi:10.1016/j.neuron.2010.11.036

29. Rohrer JD, Warren JD, Reiman D, et al. A novel exon 2 I27V VCP variant is associated with dissimilar clinical syndromes. *J Neurol.* 2011;258(8):1494-1496. doi:10.1007/s00415-011-5966-4
30. Niwa H, Ewens CA, Tsang C, Yeung HO, Zhang X, Freemont PS. The role of the N-domain in the atpase activity of the mammalian AAA ATPase p97/VCP. *J Biol Chem.* 2012;287(11):8561-8570. doi:10.1074/jbc.M111.302778
31. Sun X, Qiu H. Valosin-containing protein, a calcium-associated ATPase protein, in endoplasmic reticulum and mitochondrial function and its implications for diseases. *Int J Mol Sci.* 2020;21(11):3482. doi:10.3390/ijms21113842
32. Darwich NF, Phan JM, Kim B, et al. Autosomal dominant VCP hypomorph mutation impairs disaggregation of PHF-tau. *Science*. 2020;370(6519):eaay8826. doi:10.1126/science.aay8826
33. Gonzalez MA, Feely SM, Speziani F, et al. Novel mutation inVCP causes Charcot-Marie-Tooth type 2 disease. *Brain*. 2014;137(Pt 11):2897-2902. doi:10.1093/brain/awu224
34. Mehta SG, Khare M, Ramani R, et al. Genotype-phenotype studies of VCP-associated inclusion body myopathy with Paget disease of bone and/or frontotemporal dementia. *Clin Genet.* 2013;83(5):422-431. doi:10.1111/cge.12000
35. Jerath NU, Crockett CD, Moore SA, et al. Rare manifestation of a c.290 C>T, p.Gly97Glu VCP mutation. *Case Rep Genet.* 2015;2015:239167. doi:10.1155/2015/239167
36. Dec E, Rana P, Katheria V, et al. Cytokine profiling in patients with VCP-associated disease. *Clin Transl Sci.* 2014;7(1):29-32. doi:10.1111/cts.12117
37. Jung YJ, Tweedie D, Scerba MT, Greig NH. Neuroinflammation as a factor of neurodegenerative disease: thalidomide analogs as treatments. *Front Cell Dev Biol.* 2019;7:313. doi:10.3389/fcell.2019.00313
38. Rauf A, Badoni H, Abu-Izneid T, et al. Neuroinflammatory markers: key indicators in the pathology of neurodegenerative diseases. *Molecules*. 2022;27(10):3194. doi:10.3390/molecules27103194
39. Falcão de Campos C, de Carvalho M. Distal myopathy and rapidly progressive dementia associated with a novel mutation in the VCP gene: expanding inclusion body myopathy with early-onset Paget disease and frontotemporal dementia spectrum. *J Clin Neurosci*. 2019;64:8-10. doi:10.1016/j.jocn.2019.03.063
40. Deng J, Wu W, Xie Z, et al. Novel and Recurrent mutations in a cohort of Chinese patients with young-onset amyotrophic lateral sclerosis. *Front Neurosci.* 2019;13:1289. doi:10.3389/fnins.2019.01289
41. Weihl CC, Baloh RH, Lee Y, et al. Targeted sequencing and identification of genetic variants in sporadic inclusion body myositis. *Neuromuscul Disord.* 2015;25(4):289-296. doi:10.1016/j.nmd.2014.12.009

Introduction

CHRONIC KIDNEY DISEASE (CKD) is a global public health concern.[1] In Japan, the number of CKD in the adult population increased to 14.8 million in 2015, which was 14.6% of the adult population.[2] CKD potentially progresses to end-stage kidney disease (ESKD), requiring renal replacement therapy (RRT) and is a recognized risk factor for cardiovascular disease (CVD) and premature death.[3,4]

The Frontier of Renal Outcome Modifications in Japan (FROM-J) is a prospective, stratified, cluster-randomized trial that evaluates the effectiveness of a practice facilitation program involving multidisciplinary care for CKD management by primary care physicians (PCPs). Since April 1, 2008, to October 19, 2008, 2,379 patients with CKD aged between 40 and 74 years have enrolled from 49 local medical associations in 15 different prefectures and were followed up in the FROM-J study. Participants were assigned to two intervention groups as follows: standard intervention, standard treatment according to the CKD clinical guideline[5]; and advanced intervention based on a practice facilitation program. The practice facilitation program comprised patient education by dieticians at PCPs' clinics, newsletters to patients, patient encouragement to visit PCPs during interruptions, alerts to PCPs to inform the timing of referral to nephrologists, and support for PCPs to control patient data.[6] Recently, additional data collection and analyses, including patient-reported outcome measures, were conducted to investigate the long-term outcomes of the intervention in the 10th-year after the start of the FROM-J study (FROM-J 10 study). A total of 1,473 participants had continued clinical visits to PCPs, who became older people aged ≥70 years, while there were dropouts, withdrawals, and deaths. Among 2,379 patients with CKD, 7.5% initiated RRT, 8.5% developed CVD, 12.4% had a 50% decline in estimated glomerular filtration (eGFR), and 8.9% died, as shown in Figure 1. A certain percentage of long-term CKD survivors lived with serious complications, including ESKD and CVD.[7]

An increasing number of clinical studies on CKD have used patient-reported outcome measures, including questionnaires measuring health-related quality of life (HRQOL).[8–13] EuroQol 5 Dimension 5 Level (EQ-5D-5L) is one of the most frequently used generic preference-based HRQOL measures for CKD.[14] The quality of life (QOL) score is known to decrease in patients with advanced CKD.[8–11] CKD survivors have lived with the disease and its complications, such as anemia, malnutrition, ESKD, and CVD,[7,15,16] which might affect their QOL scores. However, there are few studies on QOL scores in long-term survivors of CKD.[10] Therefore, we aimed to measure QOL scores in 10 years long-term survivors with CKD using EQ-5D-5L and examine the predictors and determinants of the clinical indices for the measured QOL scores.

Methods

Instrument for HRQOL

EQ-5D-5L, a generic preference-based measure of HRQOL that is standardized and validated for use in Japan, was used in this study.[17,18] It is administered to patients who are asked to grade five dimensions (mobility, self-care, usual activities, pain/discomfort, and anxiety/depression) of their health state at one of five levels ("no problem," "slight problems," "moderate problems," "severe problems," and "extreme problems"). The QOL score, with ranges of 1 for perfect health (no problem in any dimension), 0 for death, and −0.025 for severe problems in all dimensions, is determined by the five-dimension health state profile according to a tariff reflecting the preference of the population. Moreover, it is a scalar quantity and is easy to use for statistical analysis compared with multidimensional QOL measurements. A higher score indicates better HRQOL, whereas a smaller or negative score indicates worse HRQOL.

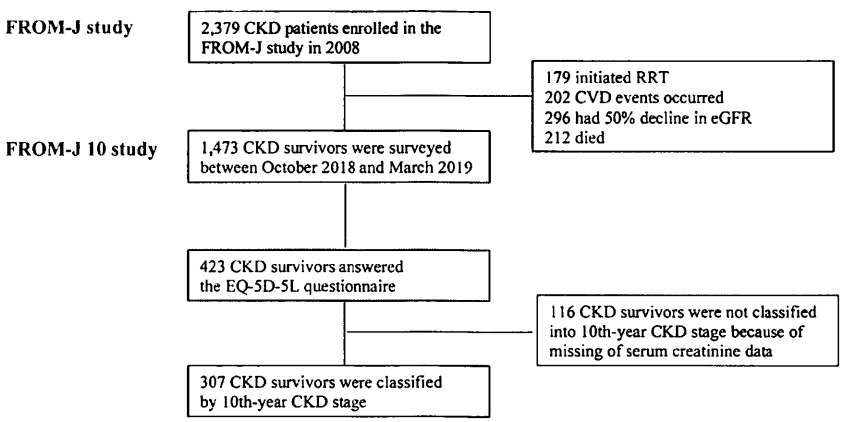

Figure 1. Flow diagram of the study. Among 1,473 CKD survivors enrolled in the FROM-J study, 423 CKD survivors (38.2%) responded to the EQ-5D-5L. A total of 307 CKD survivors were classified into 10th-year CKD stages. A total of 116 participants were not classified into the 10th-year CKD stage because of missing serum creatinine data.

Table 1. Patients' Characteristics (n = 423)

Variables	Baseline data (2008) n	Baseline data (2008) % or mean (SD)	10th-year data (2018) n	10th-year data (2018) % or mean (SD)
Male	299	70.7%	299	70.7%
Mean age (years)	423	61.6 (7.9)	423	71.6 (7.9)
Body mass index	367	25.9 (3.9)	401	24.4 (4.0)
Systolic blood pressure (mmHg)	419	135 (13)	399	130 (13)
Diastolic blood pressure (mmHg)	419	78 (9)	398	74 (10)
Mean albumin (g/dL)	315	4.3 (0.3)	144	4.1 (0.3)
Mean hemoglobin (g/dL)	357	13.9 (1.6)	267	13.5 (2.0)
Comorbidities				
Hypertension	376	89.1%	376	89.1%
Diabetes	219	51.8%	219	51.8%
Hyperlipidemia	292	69.2%	292	69.2%
Hyperuricemia	171	40.5%	171	40.5%
Renal function				
Mean serum creatine(mg/dL)*	387	1.04 (0.45)	275	1.55 (1.28)
Mean eGFR (mL/min/1.73 m^2)*	387	60.3 (20.0)	275	45.2 (20.5)
CKD stages†				
G1	35	8.3%	4	0.9%
G2	163	38.5%	57	13.5%
G3a	148	35.0%	79	18.7%
G3b	47	11.1%	70	16.6%
G4	28	6.6%	45	10.6%
G5	2	0.5%	20	4.7%
G5D	–	–	32	7.6%
stage unknown	–	–	116	27.4%
Clinical events				
Initiation of RRT	–	–	32	7.6%
Occurrence of CVD	–	–	23	5.4%
50% decline in eGFR‡	–	–	47	11.1%
Intervention groups				
Standard intervention	206	48.7%	206	48.7%
Advanced intervention	217	51.3%	217	51.3%

CKD, chronic kidney disease; CVD, cardiovascular disease; eGFR, estimated glomerular filtration rate; RRT, renal replacement therapy; SD, standard deviation.

*Participants with RRT were not included.

†The baseline CKD stage (2008) was estimated from serum creatine values either at the enrollment or in October 2008.

‡50% decrease in eGFR was defined as a 50% or greater decrease in eGFR at 10th-year from October 2008 or April 2009.

Study Design and Participants

We conducted a patient questionnaire survey on CKD survivors enrolled in the FROM-J study. The 10th-year data collection was performed by either PCPs or participants who filled out questionnaires, including EQ-5D-5L questionnaires, from October 2018 to March 31, 2019. The detailed designs and main results of the FROM-J and FROM-J 10 studies have already been reported.[6,7] This study was conducted in accordance with the Declaration of Helsinki and approved by the Ethics Committee of Clinical Research at the University of Tsukuba (No.80 and No.1311).

Study Variables

The baseline and 10th-year demographic and clinical characteristics, laboratory data (serum albumin, hemoglobin, and serum creatinine), and the presence of comorbidities were based on the FROM-J and FROM-J 10 studies, respectively. The prevalence of comorbidities remained the same over the 10th-year follow-up. The eGFR was calculated from serum creatine, age, and sex using the Japanese equation as follows: eGFR (mL/min/1.73 m^2) = 194 × serum creatinine$^{-1.094}$ × age$^{-0.287}$ × 0.739 (for female). The baseline and 10th-year CKD stages were determined in the FROM-J and FROM-J 10 studies, respectively, according to the modified classification for the Japanese people based on the CKD clinical guidelines.[5] RRT was defined as chronic maintenance dialysis (hemodialysis and peritoneal dialysis) and renal transplantation, and the initiation of these therapies was assessed. CVD events were defined as cardiovascular death; and nonfatal myocardial infarction, nonfatal stroke, and heart failure (requiring hospitalization).[6,7] A 50% decline in eGFR was defined as a 50% or greater decrease in eGFR at 10th-year from October 2008 or April 2009.

Statistical Analysis

Data are summarized using proportions, means, or median values, as appropriate. The differences in QOL scores between the sex and intervention groups were tested using the Mann–Whitney U test. The QOL score differences among age groups and CKD stages were tested using the Jonckheere–Terpstra test for trend and illustrated utilizing box and whisker plots. The Tobit model was applied to identify the clinical indices predicting and determining 10th-year QOL scores, considering that its distribution was censored at 1. All analyses were performed using the Stata SE software version 17 (StataCorp LLC, College Station, TX, USA). Statistical significance was set at $P < .05$.

Results

We collected 423 responses from 1,473 CKD survivors, as shown in Figure 1. The overall response rate was 38.2%. A total of 116 participants could not be classified into the 10th-year CKD stages because of the lack of serum creatinine data. Table 1 shows the baseline and 10th-year characteristics of patients. The respondents included 299 males (70.7%) and 124 females (29.3%). Regarding the 10th-year data, the mean age was 71.6 year old, serum creatinine was 1.55 mg/dL, and eGFR was 45.2 mL/min/1.73 m^2. Proportions of 10th-year CKD stages were 0.9% for G1, 13.5% for G2, 18.7% for G3a, 16.6% for G3b, 10.6% for G4, 4.7% for G5, 7.6% for G5D, and

Table 2. 10th-year QOL Scores by EQ-5D-5L (n = 423)

Characteristics	*n*	Mean	Median	95% confidence interval	Interquartile range	*P* value
All	423	0.893	1.000	0.880–0.906	0.826–1.000	
Sex						
Male	299	0.894	1.000	0.877–0.911	0.826–1.000	.370
Female	124	0.891	0.895	0.868–0.914	0.823–1.000	
Age at the 10th-year survey						
<60	31	0.944	1.000	0.906–0.982	0.895–1.000	<.001
60–69	132	0.924	1.000	0.906–0.943	0.871–1.000	
70–79	185	0.895	1.000	0.875–0.915	0.831–1.000	
≧80	75	0.811	0.826	0.770–0.852	0.707–1.000	
Comorbidities						
Hypertension						
presence	376	0.892	1.000	0.878–0.906	0.826–1.000	.448
absence	46	0.902	1.000	0.857–0.946	0.867–1.000	
Diabetes						
presence	219	0.900	0.895	0.858–0.899	0.825–1.000	.077
absence	204	0.908	1.000	0.891–0.926	0.831–1.000	
Hyperlipidemia						
presence	292	0.894	0.948	0.878–0.909	0.825–1.000	.832
absence	130	0.892	1.000	0.866–0.917	0.826–1.000	
Hyperuricemia						
presence	171	0.873	0.895	0.850–0.896	0.825–1.000	.021
absence	251	0.906	1.000	0.890–0.923	0.831–1.000	
CKD stages at the 10th-year survey						
G1+G2	61	0.892	1.000	0.856–0.928	0.825–1.000	.125
G3a	79	0.900	1.000	0.866–0.933	0.831–1.000	
G3b	70	0.948	1.000	0.928–0.969	0.895–1.000	
G4	45	0.851	0.867	0.802–0.900	0.780–1.000	
G5	20	0.909	0.892	0.867–0.951	0.828–1.000	
G5D	32	0.824	0.828	0.767–0.881	0.755–1.000	
Stage unknown	116	0.888	0.948	0.861–0.914	0.825–1.000	
Clinical events						
Initiation of RRT						
presence	32	0.824	0.828	0.767–0.881	0.755–1.000	.002
absence	391	0.899	1.000	0.885–0.912	0.831–1.000	
Occurrence of CVD						
presence	23	0.877	1.000	0.811–0.943	0.753–1.000	.647
absence	400	0.894	1.000	0.880–0.908	0.826–1.000	
50% decline in eGFR*						
presence	47	0.893	0.889	0.860–0.926	0.825–1.000	.118
absence	223	0.906	1.000	0.888–0.925	0.844–1.000	
Intervention groups						
Standard intervention	206	0.890	1.000	0.870–0.911	0.825–1.000	.988
Advanced intervention	217	0.895	1.000	0.878–0.913	0.826–1.000	

CKD, chronic kidney disease; CVD, cardiovascular disease; eGFR, estimated glomerular filtration rate; QOL, quality of life; RRT, renal replacement therapy.

The differences in QOL scores between the sex, comorbidities, clinical events, and intervention groups were tested using the Mann–Whitney U test.

The QOL score differences among age groups and CKD stages were tested using the Jonckheere–Terpstra test for trend.

*Participants receiving RRT were not included.

27.4% for stage unknown. Regarding clinical events, 32 participants initiated RRT, 29 were on hemodialysis, 2 were on peritoneal dialysis, 1 was on kidney transplantation, 23 developed CVD and 47 participants had 50% decline in eGFR during 10 years.

Table S1 shows the health status according to the EQ-5D-5L questionnaire. The proportion of patients who responded "no problem" was 69.7% for mobility, 94.3% for self-care, 78.5% for usual activities, 66.2% for pain/discomfort, and 86.5% for anxiety/depression.

Table 2 presents the mean and median QOL scores. The mean QOL score of all was 0.893 (95% confidence interval (CI), 0.880–0.906), and the median QOL score was 1.000 (interquartile range (IQR), 0.826–1.000). The mean QOL

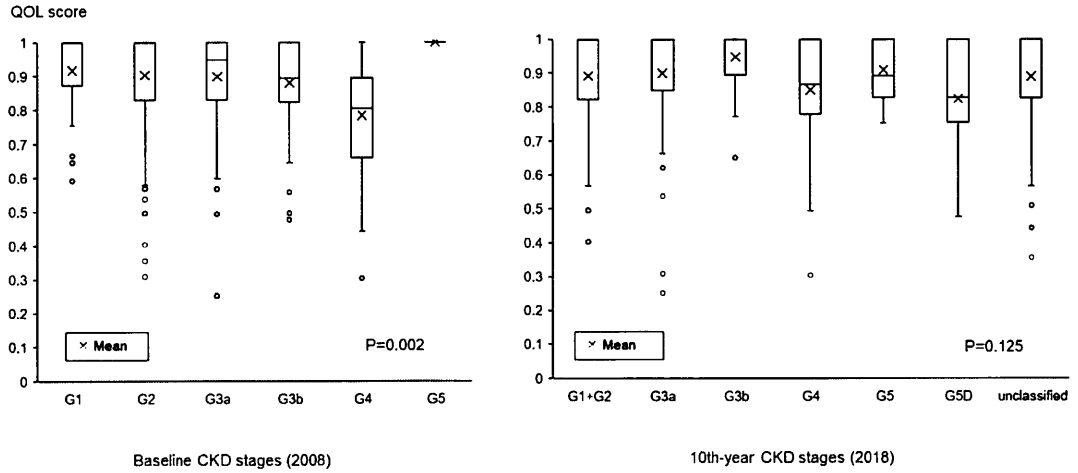

Figure 2. Box and whisker plots of QOL scores based on the baseline and 10th-year CKD stages. The decrease in QOL scores along with baseline CKD stages was significant according to the Jonckheere–Terpstra test for trend ($P = .002$). The measured QOL scores were not significantly associated with the 10th-year CKD stages according to the Jonckheere–Terpstra test for trend ($P = .125$).

score in participants with RRT was 0.824 (95% CI, 0.767–0.881), and the median was 0.828 (IQR, 0.755–1.000). Limited to hemodialysis patients, the mean QOL score was 0.822 (95% CI, 0.760–0.884), and the median was 0.831 (IQR, 0.757–1.000). The mean QOL score in participants with CVD was 0.877 (95% CI, 0.811–0.943), and the median was 1.000 (IQR, 0.723–1.000). The mean QOL score in participants with 50% decline in eGFR was 0.893 (95% CI, 0.860–0.926), and the median was 0.889 (IQR, 0.825–1.000). Figure 2 illustrates the measured QOL scores based on the baseline and 10th-year CKD stages in a box plot with a mark showing the mean. The decrease in QOL scores along with baseline CKD stages was significant according to the Jonckheere–Terpstra test for trend ($P = .002$).

Table 3 shows the results of the Tobit regression analysis aimed at identifying the clinical predictors of 10th-year QOL scores among the baseline data. We performed three models of regression analysis, selecting hemoglobin (model 1), serum creatine (model 2), and eGFR (model 3) considering the multicollinearity based on results of simple regression analysis. The analysis revealed that baseline age, systolic blood pressure, and history of hyperuricemia were significant predictors. The intervention groups (standard or advanced intervention) were not associated with the 10th-year QOL scores.

Table 4 shows the results of the Tobit regression analysis aimed at identifying the clinical determinants of 10th-year QOL scores among the 10th-year data. Sex, age, and 10-year diabetes and hyperuricemia were significant factors.

Discussion

We measured QOL scores using the EQ-5D-5L in 10 years long-term survivors with CKD based on the FROM-J study. Our results demonstrated the QOL scores of patients surviving CKD under the clinical practices of PCPs. The measured mean QOL scores decreased with age, with values of 0.944 (<60 years), 0.924 (60–69), 0.895 (70–79), and 0.811 (≥80 years). Although all our participants had CKD, some had more serious comorbidities than others, and the age-related decline in QOL scores was similar to previous general population norm studies in Japan and overseas.[17–22] The measured mean QOL score in males was slightly higher than that in females, which is also commonly observed in many countries; however, the underlying reason is unclear.[18–22]

Advanced intervention by a practice facilitation program in the FROM-J study has been shown to have long-term effects on patients with CKD by preventing CVD events.[7] The mean QOL score of participants in the advanced intervention was 0.895 (95% CI, 0.878–0.913), which was slightly higher than 0.890 (95% CI, 0.870–0.911) in the standard intervention. However, there was no significant difference, and the practice groups were not predictors of the QOL scores. In our study, the QOL score of participants with CVD events was lower than that of those without CVD events. We considered that the practice facilitation program might indirectly have positive effects on QOL scores in patients with CKD through the reduction of CVD events.

Similar to previous studies, this study showed a significant trend of a decline in QOL scores along with the baseline CKD stage.[8–11] The renal function was found to be neither a clinical predictor nor determinant of 10th-year QOL scores. Some studies have reported that renal function estimated from serum creatinine may not adequately reflect the renal function of older people because serum creatine levels are affected by muscle mass, sex, and age.[23,24] We considered that 10th-year renal function in our participants might be affected by their older ages and serious complications.

Table 3. Tobit Regression Analysis for Clinical Predictors of 10th-year QOL Scores Among Baseline Data (2008)

	Simple regression analysis		Multiple regression analysis					
			Model 1 (hemoglobin)		Model 2 (creatinine)		Model 3 (eGFR)	
Variables	Coefficients	*P* value	Coefficients	*P* value	Coefficients	*P* value	Coefficients	*P* value
Sex (male = 0, female = 1)	−0.0175	.549	−0.0262	.482	−0.0562	.084	−0.0551	.085
Age	−0.0096	<.001	−0.0085	<.001	−0.0093	<.001	−0.0097	<.001
Body mass index	−0.0034	.345	−0.0036	.342	−0.0035	.341	−0.0030	.412
Systolic blood pressure (mmHg)	−0.0022	.029	−0.0023	.051	−0.0024	.037	−0.0024	.036
Diastolic blood pressure (mmHg)	0.0018	.024						
Mean albumin (g/dL)	0.0796	.096						
Mean hemoglobin (g/dL)	0.0225	.009	0.0108	.300				
Comorbidities								
Hypertension	−0.0275	.531						
Diabetes	−0.0551	.040	−0.0393	.195	−0.0559	.069	−0.0470	.124
Hyperlipidemia	−0.0048	.870	−0.0005	.988	0.0054	.862	0.0066	.833
Hyperuricemia	−0.0703	.010	−0.0867	.005	−0.0840	.008	−0.0977	.003
Renal function								
Serum creatine (mg/dL)	−0.0511	.081			−0.0173	.623		
eGFR (mL/min/1.73 m^2)	0.0012	.068					−0.0005	.555
CKD stage*								
G2	−0.0312	.545						
G3a	−0.0480	.355						
G3b	−0.0779	.199						
G4	−0.2286	.001						
G5	1.1614	.985						
Intervention groups (standard intervention = 0, advanced intervention = 1)	0.0056	.835	−0.0013	.964	0.0103	.717	0.0073	.797
Constant			1.8590	<.001	2.1138	<.001	2.1402	<.001
Number of observations			316		337		337	
Pseudo R-squared			0.1591		0.1747		0.1752	

CKD, chronic kidney disease; QOL, quality of life; eGFR, estimated glomerular filtration rate.
We performed three models of regression analysis by considering the multicollinearity.
*Compared with CKD stage G1

The mean QOL scores in participants receiving RRT and hemodialysis were 0.824 and 0.822, respectively. These scores were lower than 0.899 for non-RRT patients with CKD. This result is consistent with previous studies showing that the QOL scores of hemodialysis patients were lower than those of nondialysis patients with CKD.[8,25] There is one report about QOL scores measured by EQ-5D-5L for 717 Japanese older patients aged 72.9 ± 6.5 years who received maintenance hemodialysis for more than 5 years. Their QOL score was 0.738 (95% CI, 0.723–0.754),[26] which was lower than that of our study. They reported that hemodialysis duration was a determinant of lower QOL scores. We also consider that difference in QOL scores might be due to the duration of hemodialysis, which was 15.4 ± 8.8 years compared with our 4.4 ± 0.5 years.

The significance of a history of hyperuricemia as both a predictor and determinant of QOL scores is a new finding of this study. A previous study reported that gout reduces physical HRQOL, regardless of serum uric acid levels or urate-lowering therapy.[27] We considered that there might be some participants with gouts in the presence of hyperuricemia because hyperuricemia is the most important risk factor for the development of gout.[28] The baseline systolic blood pressure was negatively associated with the QOL scores. This result is consistent with a previous study[9] and a Chinese study on QOL scores measured using the

Table 4. Tobit Regression Analysis for Clinical Determinants of 10th-year QOL Scores Among 10th-year Data (2018)

	Simple regression analysis		Multiple regression analysis					
			Model 1 (hemoglobin)		Model 2 (creatinine)		Model 3 (eGFR)	
Variables	Coefficients	*P* value	Coefficients	*P* value	Coefficients	*P* value	Coefficients	*P* value
Sex (male = 0, female = 1)	−0.0175	.549	−0.0769	.058	−0.0888	.006	−0.0938	.040
Age	−0.0096	<.001	−0.0108	<.001	−0.0110	<.001	−0.0113	<.001
Body mass index	0.0015	.653	−0.0004	.926	−0.0036	.378	−0.0034	.399
Systolic blood pressure (mmHg)	−0.0023	.028	−0.0012	.346	−0.0010	.360	−0.0011	.295
Diastolic blood pressure (mmHg)	0.0003	.814						
Mean albumin (g/dL)	0.1529	.029						
Mean hemoglobin (g/dL)	0.0170	.054	−0.0009	.928				
Comorbidities								
10-year hypertension	−0.0275	.531						
10-year diabetes	−0.0551	.040	−0.0712	.053	−0.0992	.001	−0.0939	.002
10-year hyperlipidemia	−0.0048	.870	−0.0131	.729	−0.0018	.953	−0.0017	.956
10-year hyperuricemia	−0.0703	.010	−0.0885	.016	−0.0931	.002	−0.1043	.001
Renal function								
Serum creatine(mg/dL)	−0.0016	.901			0.0043	.713		
eGFR (mL/min/1.73 m^2)	−0.0002	.771					−0.0012	.131
CKD stage*								
G3a	0.0145	.749						
G3b	0.1194	.015						
G4	−0.0702	.170						
G5	0.0074	.913						
G5D	−0.1157	.039						
stage unknown	−0.0071	.866						
Clinical events								
Initiation of RRT	−1.2874	.007	−0.0582	.521	−0.1365	.203	−0.1495	.010
Occurrence of CVD	−0.0169	.775	−0.0608	.374	0.0398	.552	0.0285	.670
50% decline in eGFR†	−0.0443	.319						
Intervention groups (standard intervention = 0, advanced intervention = 1)	0.0056	.835	0.0203	.552	0.0131	.651	0.0125	.665
Constant			2.1441	<.001	2.1988	<.001	2.307	<.001
Number of observations			249		292		292	
Pseudo R-squared			0.1720		0.2897		0.2999	

CKD, chronic kidney disease; CVD, cardiovascular disease; eGFR, estimated glomerular filtration rate; QOL, quality of life.
We performed three models of regression analysis by considering the multicollinearity.
*Compared with CKD stage G1+G2.
†Participants receiving RRT were not included.

EQ-5D-3L in patients with hypertension.[29] The management of hypertension, diabetes and hyperuricemia, shown as significant predictors or determinants of 10th-year QOL scores, is recommended in the CKD guidelines.[5] We suggest the importance of CKD guideline-based practices from the perspective of HRQOL improvement.

This study had some limitations. First, the sample size was small owing to excessive missing 10-year values. Moreover, 27.4% of participants with CKD were not categorized based on their 10-year CKD stages, which might affect the association between QOL scores and renal function. These missing values also affected the selection of

the variables in the multiple regression analysis. Second, because of the self-reported questionnaire surveys by mailing, participants who responded to the questionnaires tended to be healthier than those who could not. Sicker patients, especially those with CKD stage G5, may have already initiated RRT or were lost to death before the survey. Third, we could not evaluate clinical events other than the initiation of RRT, CVD or 50% decline in eGFR and could not examine changes in the clinical indices or drug treatments. These unevaluated factors that might contribute to QOL scores in patients with CKD should be examined in further studies.

In conclusion, our results suggest that baseline age, a history of hyperuricemia and systolic blood pressure are important clinical predictors of QOL scores in long-term CKD survivors. CKD guideline-based practices,[5] prevention of ESKD/CVD and management of hypertension, diabetes and hyperuricemia, might contribute to future HRQOL in patients with CKD.

Practical Application

This study shows that CKD complications, such as ESKD and CVD, negatively affect the QOL scores in 10 years long-term survivors with CKD. The baseline age, a history of hyperuricemia and systolic blood pressure are important clinical predictors of the 10th-year QOL scores in older survivors aged ≥70 years with CKD. Therefore, our study suggests that CKD guideline-based practice is important for patients with CKD from the perspective of improving HRQOL.

Credit Authorship Contribution Statement

Reiko Okubo: Conceptualization, Methodology, Formal analysis, Data curation, Writing – original daft, Visualization. **Masahide Kondo:** Conceptualization, Methodology, Formal analysis, Data curation, Writing – review & editing, Supervision. **Toshiyuki Imasawa:** Project administration, Conceptualization, Writing - review & editing. **Chie Saito:** Resources, Project administration. **Hirayasu Kai:** Resources, Project administration. **Ryoya Tsunoda:** Project administration, Resources. **Junichi Hoshino:** Conceptualization. Writing – review & editing. **Tsuyoshi Watanabe:** Resources, Writing – review & editing. **Ichiei Narita:** Resources, Writing – review & editing. **Seiichi Matsuo:** Resources, Writing – review & editing. **Hirofumi Makino:** Resources, Writing – review & editing. **Akira Hishida:** Resources, Writing – review & editing. **Kunihiro Yamagata:** Conceptualization, Writing – review & editing, Supervision, Project administration.

Acknowledgments

We would like to express our sincere gratitude to the doctors at the centers, members of the protocol review committee, members of the event determination committee, and 49 medical associations that participated in this study for their support. We also acknowledge Ms. Yukiko Ito (Tsukuba Clinical Research & Development Organization [T-CReDO]) for her help with the data management.

Supplementary Data

Supplementary data associated with this article can be found in the online version at https://doi.org/10.1053/j.jrn.2023.10.001.

References

1. Nelson RG, Grams ME, Ballew SH, et al. Development of risk prediction equations for incident chronic kidney disease. *JAMA*. 2019;322:2104-2114.

2. Nagai K, Asahi K, Iseki K, Yamagata K. Estimating the prevalence of definitive chronic kidney disease in the Japanese general population. *Clin Exp Nephrol*. 2021;25:885-892.

3. Go AS, Chertow GM, Fan D, McCulloch CE, Hsu CY. Chronic kidney disease and the risks of death, cardiovascular events, and hospitalization. *N Engl J Med*. 2004;351:1296-1305.

4. Jha V, Garcia-Garcia G, Iseki K, et al. Chronic kidney disease: global dimension and perspectives. *Lancet*. 2013;382:260-272.

5. Japanese Society of Nephrology. *Clinical practice guidebook for diagnosis and treatment of chronic kidney disease 2012*. Tokyo: Tokyo Igakusha; 2012.

6. Yamagata K, Makino H, Iseki K, et al. Effect of behavior modification on outcome in early- to moderate-stage chronic kidney disease: a cluster-randomized trial. *PLoS One*. 2016;11:e0151422.

7. Imasawa T, Saito C, Kai H, et al. Long-term effectiveness of a primary care practice facilitation program for chronic kidney disease management: an extended follow-up of a cluster-randomized FROM-J study. *Nephrol Dial Transplant*. 2022;38:158-166.

8. Gorodetskaya I, Zenios S, McCulloch CE, et al. Health-related quality of life and estimates of utility in chronic kidney disease. *Kidney Int*. 2005;68:2801-2808.

9. Tajima R, Kondo M, Kai H, et al. Measurement of health-related quality of life in patients with chronic kidney disease in Japan with EuroQol (EQ-5D). *Clin Exp Nephrol*. 2010;14:340-348.

10. Jesky MD, Dutton M, Dasgupta I, et al. Health-related quality of life impacts mortality but not progression to end-stage renal disease in pre-dialysis chronic kidney disease: a prospective observational study. *PLoS One*. 2016;11:e0165675.

11. Thancharoen O, Waleekhachonloet O, Limwattananon C, Anutrakulchai S. Cognitive impairment, quality of life and healthcare utilization in patients with chronic kidney disease stages 3 to 5. *Nephrology*. 2020;25:625-633.

12. Tabata A, Yabe H, Katogi T, et al. Factors affecting health-related quality of life in older patients with chronic kidney disease: a single-center cross-sectional study. *Int Urol Nephrol*. 2022;54:2637-2643.

13. Busa I, Ordóñez-Mena JM, Yang Y, et al. Quality of life in older adults with chronic kidney disease and transient changes in renal function: Findings from the oxford renal cohort. *PLoS One*. 2022;17:e0275572.

14. Drummond MF, Sculpher MJ, Claxton K, Stoddart GL, Torrance GW. In: *Methods for the economic evaluation of health care programmes*. 4th ed Oxford: Oxford University Press; 2015.

15. Fraser SDS, Roderick PJ, May CR, et al. The burden of comorbidity in people with chronic kidney disease stage 3: a cohort study. *BMC Nephrol*. 2015;16:193.

16. Tonelli M, Wiebe N, Guthrie B, et al. Comorbidity as a driver of adverse outcomes in people with chronic kidney disease. *Kidney Int*. 2015;88:859-866.

17. Shiroiwa T, Ikeda S, Noto S, et al. Comparison of value set based on DCE and/or TTO data: scoring for EQ-5D-5L health states in Japan. *Value Health*. 2016;19:648-654.

18. Shiroiwa T, Noto S, Fukuda T. Japanese population norms of EQ-5D-5L and health utilities index mark 3: disutility catalog by disease and symptom in community settings. *Value Health.* 2021;24:1193-1202.

19. Feng Y, Devlin N, Herdman M. Assessing the health of the general population in England: how do the three- and five-level versions of EQ-5D compare? *Health Qual Life Outcomes.* 2015;13:171-178.

20. McCaffrey N, Kaambwa B, Currow DC, Ratcliffe J. Health-related quality of life measured using the EQ-5D-5L: South Australian population norms. *Health Qual Life Outcomes.* 2016;14:133.

21. Mangen MJ, Bolkenbaas M, Huijts SM, van Werkhoven CH, Bonten MJM, de Wit GA. Quality of life in community-dwelling Dutch elderly measured by EQ-5D-3L. *Health Qual Life Outcomes.* 2017;15:3-5.

22. Marten O, Greiner W. EQ-5D-5L reference values for the German general elderly population. *Health Qual Life Outcomes.* 2021;19:76.

23. Baxmann AC, Ahmed MS, Marques NC, et al. Influence of muscle mass and physical activity on serum and urinary creatinine and serum cystatin C. *Clin J Am Soc Nephrol.* 2008;3:348-354.

24. Ferguson MA, Waikar SS. Established and emerging markers of kidney function. *Clin Chem.* 2012;58:680-689.

25. Legrand K, Speyer E, Stengel B, et al. Perceived health and quality of life in patients with CKD, including those with kidney failure: Findings from national surveys in France. *Am J Kidney Dis.* 2020;75:868-878.

26. Shimizu U, Aoki H, Sakagami M, Akazawa K. Walking ability, anxiety and depression, significantly decrease EuroQol 5-dimension 5-level scores in older hemodialysis patients in Japan. *Arch Gerontol Geriatr.* 2018;78:96-100.

27. Roddy E, Zhang W, Doherty M. Is gout associated with reduced quality of life? A case-control study. *Rheumatology.* 2007;46:1441-1444.

28. Dalbeth N, Gosling AL, Gaffo A, Abhishek A. Gout. *Lancet.* 2021;397:1843-1855.

29. Yan R, Gu H, Wang W, Ma L, Li W, CHIEF Research Group. Health-related quality of life in blood pressure control and blood lipid-lowering therapies: results from the CHIEF randomized controlled trial. *Hypertens Res.* 2019;42:1561-1571.

Heliyon 9 (2023) e14923

Contents lists available at ScienceDirect

Heliyon

journal homepage: www.cell.com/heliyon

Case report

Changes in histopathology and heteroplasmy rates over 8 years and effectiveness of taurine supplementation in a patient with mitochondrial nephropathy caused by *MT-TL1* mutation: A case report

Toshiyuki Imasawa [a,*], Hiroshi Kitamura [b], Takehiko Kawaguchi [a], Yukiko Yatsuka [c], Yasushi Okazaki [c], Kei Murayama [d]

[a] *Department of Nephrology, National Hospital Organization Chiba-Higashi National Hospital, 673 Nitona-cho, Chuoh-ku, Chiba, 260-8712 Japan*
[b] *Department of Clinical Pathology, National Hospital Organization Chiba-Higashi National Hospital, 673 Nitona-cho, Chuoh-ku, Chiba, 260-8712 Japan*
[c] *Diagnostics and Therapeutic of Intractable Diseases, Intractable Disease Research Center, Graduate School of Medicine, Juntendo University, 2-1-1, Hongo, Bunkyo-ku, Tokyo, 113-8421 Japan*
[d] *Center for Medical Genetics, Department of Metabolism, Chiba Children's Hospital, 579-1 Heta-cho, Midori-ku, Chiba, 266-0007 Japan*

ARTICLE INFO

Keywords:
Case report
Mitochondrial nephropathy
MT-TL1
m.3243A>G mutation
Heteroplasmy
Taurine

ABSTRACT

The m.3243A > G mutation in the *mitochondrially encoded tRNA leucine 1* (*MT-TL1*) gene is known to cause mitochondrial nephropathy. However, its long-term effects of the m.3243A > G mutation on renal histopathology or heteroplasmy rates remain unknown. Here we present the case of a female patient who underwent renal biopsy at 34 years of age to investigate the reason for a low estimated glomerular filtration rate (eGFR) of 47.9 mL/min/1.73 m^2. Light microscopy revealed nephrosclerosis with granular swollen epithelial cells (GSECs) in the renal tubules. Genetic testing revealed the m.3243A > G mutation in the *MT-TL1* gene. Over a follow-up period of 8 years, the eGFR declined at a rate of 1.50 mL/min/1.73 m^2/year. A second renal biopsy was performed at the age of 42 years; the patient's glomerular sclerosis rate had increased from 45.5% to 63.2%, and the frequency of GSECs in the collecting ducts had increased from 5.8% to 20.8%. Furthermore, the heteroplasmy rate in blood cells and urinary sediment cells increased from 9% to 20% and 20% to 53%, respectively. Taurine therapy was initiated just after the second kidney biopsy. To date, after approximately 3 years of taurine administration, the rate of eGFR decline has markedly decreased to 0.26 mL/min/1.73 m^2/year. This experience suggests that an increased heteroplasmy rate may be associated with the progression of mitochondrial nephropathy caused by *MT-TL1* mutation. Furthermore, our case is the first to suggest the effectiveness of taurine for mitochondrial nephropathy caused by the m.3243A > G mutation in the *MT-TL1* gene.

* Corresponding author. Department of Nephrology, National Hospital Organization Chiba-Higashi National Hospital, 673 Nitona-cho, Chuoh-ku, Chiba-city, Chiba 206-8712, Japan.
E-mail address: imasawa.toshiyuki.qh@mail.hosp.go.jp (T. Imasawa).

https://doi.org/10.1016/j.heliyon.2023.e14923
Received 11 February 2023; Received in revised form 14 March 2023; Accepted 22 March 2023
Available online 30 March 2023

1. Introduction

Several reports have shown that focal segmental glomerulosclerosis (FSGS) is a characteristic pathological change in mitochondrial nephropathies caused by mitochondrial DNA (mtDNA) mutations, such as those in the *mitochondrial tRNA leucine 1* (*MT-TL1*) gene [1–3]. In such cases, the mitochondria in glomerular podocytes lose their normal function, and the resulting podocyte damage has been thought to be involved in the etiopathogenesis of FSGS lesions [4]. However, our prior analysis of 63 renal biopsy cases with the m.3243A > G mutation in *MT-TL1* showed that 11.4% of these cases were diagnosed via histopathology as nephrosclerosis without FSGS lesions [3]. Although the lack of FSGS lesions in renal biopsy sections may be due to sampling errors, whether this error alone can explain the lack of FSGS lesions is debatable. The clinical manifestations and pathological changes of mitochondrial disease caused by mtDNA mutations are highly variable and are impacted by the heteroplasmy rate that differs among organs and cells [5].

The long-term effects of the m.3243A > G mutation on renal histopathology or heteroplasmy rates are unknown. In addition, although taurine is reportedly effective at treating mitochondrial diseases with *MT-TL1* mutations that were already proven to cause a taurine modification defect in tRNALeu (UUR), as in m.3243A > G [6], its effect on mitochondrial nephropathy is unclear. In this context, we present a patient with an m.3243A > G mutation who underwent two renal biopsies performed 8 years apart, necessitated by a gradual decrease in estimated glomerular filtration rate (eGFR). We investigated the factors contributing to the progression of nephropathy in this patient by analyzing the changes in histopathology and heteroplasmy rates of mtDNA. Furthermore, this study is the first report verifying the effectiveness of taurine in such patients.

2. Case presentation

Herein, we describe the case of a 45-year-old Japanese woman with no significant medical history prior to the second pregnancy at 32 years of age. The patient was initially found to have proteinuria and a decreased renal function in week 27 of the second pregnancy and gave birth to the second child at 28 weeks of gestation due to an imminent risk of premature birth. One day after delivery, proteinuria was 1.2 g/day and eGFR was 48.3 mL/min/1.73 m^2, as calculated using the serum creatinine value and the Japanese equation (eGFR [mL/min/1.73 m^2] = 194 × $Age^{-0.287}$ x $Cre^{-1.094}$ [x 0.739 if female]) [7]. Although the proteinuria disappeared 3 months after delivery, the eGFR was persistently <50 mL/min/1.73 m^2. At 34 years of age, 15 months after the second delivery, the patient was referred to our hospital by her primary doctor for decreased renal function. At the first visit to our hospital, the serum creatinine level was 1.12 mg/dL (eGFR: 46.0 mL/min/1.73 m^2), without proteinuria. Three months after the first visit to us, the patient was admitted for a kidney biopsy to investigate the reason for persistent renal dysfunction.

Physical examination at admission showed the following: height 160.0 cm, body weight 45.5 kg, body mass index 17.8, blood pressure 116/73 mmHg, and a regular heart rate of 67 bpm. Neurological examination results were normal. The patient had no headaches, edema, or skin lesions. The serum creatinine level was 1.08 mg/dL (eGFR: 47.9 mL/min/1.73 m^2) (Table 1) without proteinuria (0.03 g/day) or hematuria (0–1/HPF). Except for hyperuricemia (uric acid: 6.5 mg/dL), all blood test results were normal

Table 1
Laboratory tests on admission.

	1st biopsy	2nd biopsy
Age	34	42
Blood cell count		
WBC (/μL)	3900	5400
RBC (/μL)	415 × 104	458 × 104
Platelet (/μl)	1,67,000	1,87,000
Blood chemistry		
Albumin (g/dL)	4.9	4.7
Sodium (mEq/L)	139	140
Potassium (mEq/L)	4.1	4.2
Chloride (mEq/L)	101	108
BUN (mg/dL)	15.5	25.1
Cre (mg/dL)	**1.08**	**1.48**
eGFR (ml/min/1.73m2)	**47.9**	**31.9**
Uric acid (mg/dL)	**6.5**	**7.8**
Fasted blood glucose (mg/dL)	88	98
HbA1c (%)	5.7	5.8
Serum lactate (mg/dL)	9.1	12.5
Serum pyruvic acid (mg/dL)	0.46	0.86
Urinarysis		
Glucose (test tape)	(−)	(−)
Protein (g/day)	0.03	0.02
RBC (/HPF)	0–1	0–1
NAG (IU/L)	5.2	4.6
b2-MG (mg/L)	37	75

WBC, white blood cells; RBC, red blood cells; BUN, blood urea nitrogen; Cre, creatinine; eGFR, estimated glomerular filtration rate; UA, uric acid; HbA1c, hemoglobin A1c by NGSP; NAG, N-acetylglutamate; b2-MG, microglobulin; HPF, high-power field. Bold texts indicate abnormal values.

(Table 1), and the serum lactate level was within the normal range (9.1 mg/dL). Blood tests did not suggest the existence of diabetes mellitus, the patient was not a smoker, and was not taking any prescribed medications. Audiometric tests revealed pure tone averages of 25.0 dB in the right and 20.0 dB in the left ears ([500 Hz + 1000 Hz x 2 + 2000 Hz]/4), indicating a normal hearing ability. An echocardiogram revealed a normal heart function. Brain magnetic resonance imaging (MRI) was not performed as neurological symptoms and stroke-like episodes were absent.

The patient reported that her mother had died at 42 years of age due to diabetic nephropathy-induced uremia. Her brother was diagnosed with mitochondrial encephalomyopathy, lactic acidosis, and stroke-like episodes (MELAS) at 7 months of age and died at 37 years of age. The present patient was born after 36 weeks of gestation, with a birth weight of 2720 g. Both of her children are healthy with no symptoms; the first was born prematurely at 29 weeks of gestation, with a birth weight of 1566 g, and the second at 28 weeks of gestation with a birth weight of 1502 g. Neither showed proteinuria or renal dysfunction during health checkups.

The renal pathological findings of the present case are summarized in Table 2. Fig. 1A–C shows the light microscopy images of the first kidney biopsy. Renal pathology showed nephrosclerosis. Five glomeruli among observed eleven glomeruli had global sclerosis (45.5%), and two glomeruli were collapsed (18.2%). All other glomeruli showed almost normal appearance without any sclerotic lesions, tuft adhesions, or endocapillary proliferation. Age-inappropriate disarranged and irregularly sized vascular smooth muscle cells (AiDIVs) were also observed in the intralobular arteries (Fig. 1A) and afferent arterioles (Fig. 1B); arteriolar hyalinosis and intimal thickening were not observed. Furthermore, granular swollen epithelial cells (GSECs) were also apparent in the collecting ducts on Masson Trichrome staining (Fig. 1C). Electron microscopy examination showed an increase in the number of abnormal mitochondria in podocytes and collecting duct cells (Fig. 1D–F).

The presence of GSECs, podocytes with abnormal mitochondria, and a relevant family history prompted us to consider the possibility of mitochondrial nephropathy due to mtDNA mutation. We performed genetic analysis using mtDNA extracted from peripheral blood mononuclear cells and urine sediment cells [8]. The m.3243A > G mtDNA mutation was detected in both blood and urine sediment cells. Heteroplasmy rates of blood and urine sediment cells were 9% and 20%, respectively (Table 2).

After the first kidney biopsy and genetic analysis, the patient was followed up without prescribing any medications as there were no apparent clinical symptoms, and proteinuria was never detected (<0.15 g/g Cre). Urinary N-Acetylglucosamine and β2-microglobulin levels were within the normal range. However, after the first kidney biopsy, the patient became aware that her hearing ability was decreasing. In addition, the eGFR slowly but gradually decreased. Therefore, the patient was later admitted for a second kidney biopsy to investigate the cause of the gradually decreasing renal function.

On the 2nd admission, the patient's body weight was 45.5 kg, and blood pressure was 110/61 mmHg. Physical examination did not reveal any abnormalities; the serum creatinine level had increased to 1.48 mg/dL (eGFR: 31.9 mL/min/1.73 m^2) without proteinuria (0.02 g/day). Although the uric acid level was high (6.5 mg/dL), all blood test results were normal and had not changed from the results at the first admission (Table 1). An audiometric test showed pure tone averages of 45.0 dB in the right and 40.0 dB in the left ears ([500 Hz + 1000 Hz x 2 + 2000 Hz]/4), indicating that the patient had experienced hearing loss. The echocardiogram was normal.

The renal pathological findings are summarized in Table 2. Light microscopy of the second biopsy specimen (containing 19 glomeruli) yielded 12 glomeruli with global sclerosis (63.2%) and one collapsing glomerulus; all other glomeruli appeared normal. There were more GSECs in the collecting ducts in this biopsy compared to the first biopsy (53% and 20%, respectively) (Fig. 2A, Table 2). AiDIVs were observed in the intralobular arteries and afferent arterioles, similar to those at the first biopsy (Fig. 2B and C). An electron microscopical analysis revealed accumulation of abnormal mitochondria in podocytes (Fig. 2D). In addition, vascular smooth muscle cells of arterioles were filled with abnormal mitochondria (Fig. 2E and F).

Next, we analyzed heteroplasmy rates of mtDNA with m.3243A > G. The heteroplasmy rates in the peripheral blood mononuclear cells and urinary sediment cells were 20% and 53%, respectively, showing an increase over the 8 years (Table 2). The heteroplasmy rate of kidney tissue was 75%.

Due to the gradually decreasing eGFR and the confirmed renal tissue damage with progressively increasing global glomeruli sclerosis, we decided to administer taurine (12 g/day in three divided doses after each meal). The least squares regression line of the eGFR trend using all the values from the first visit date showed that the patient's eGFR was declining at a rate of 1.50 mL/min/1.73 m^2/year prior to taurine treatment (Fig. 3). After a period of 1022 days (about 2.8 years) since taurine was first prescribed, the rate of eGFR decline markedly decreased to 0.26 mL/min/1.73 m^2/year, as determined by linear regression using least square method (Fig. 3). The

Table 2
Comparison of histopathological findings and heteroplasmy rates of mtDNA.

	1st biopsy	2nd biopsy
Renal Pathology		
Global sclerosis	5/11 (45.5%)	12/19 (63.2%)
Segmental sclerosis	0/11	0/19
Podocytes with abnormal mitochondria accumulation	+	+
GSECs in collecting ducts	16/274 (5.8%)	38/183 (20.8%)
Rate of m.3243 A > G heteroplasmy		
Blood cells	9%	20%
Cells in urinary sediments	20%	53%
Kidney tissue	n.d.	75%

mtDNA, mitochondrial DNA; GSEC, granular swollen epithelial cell.
n.d., not done.

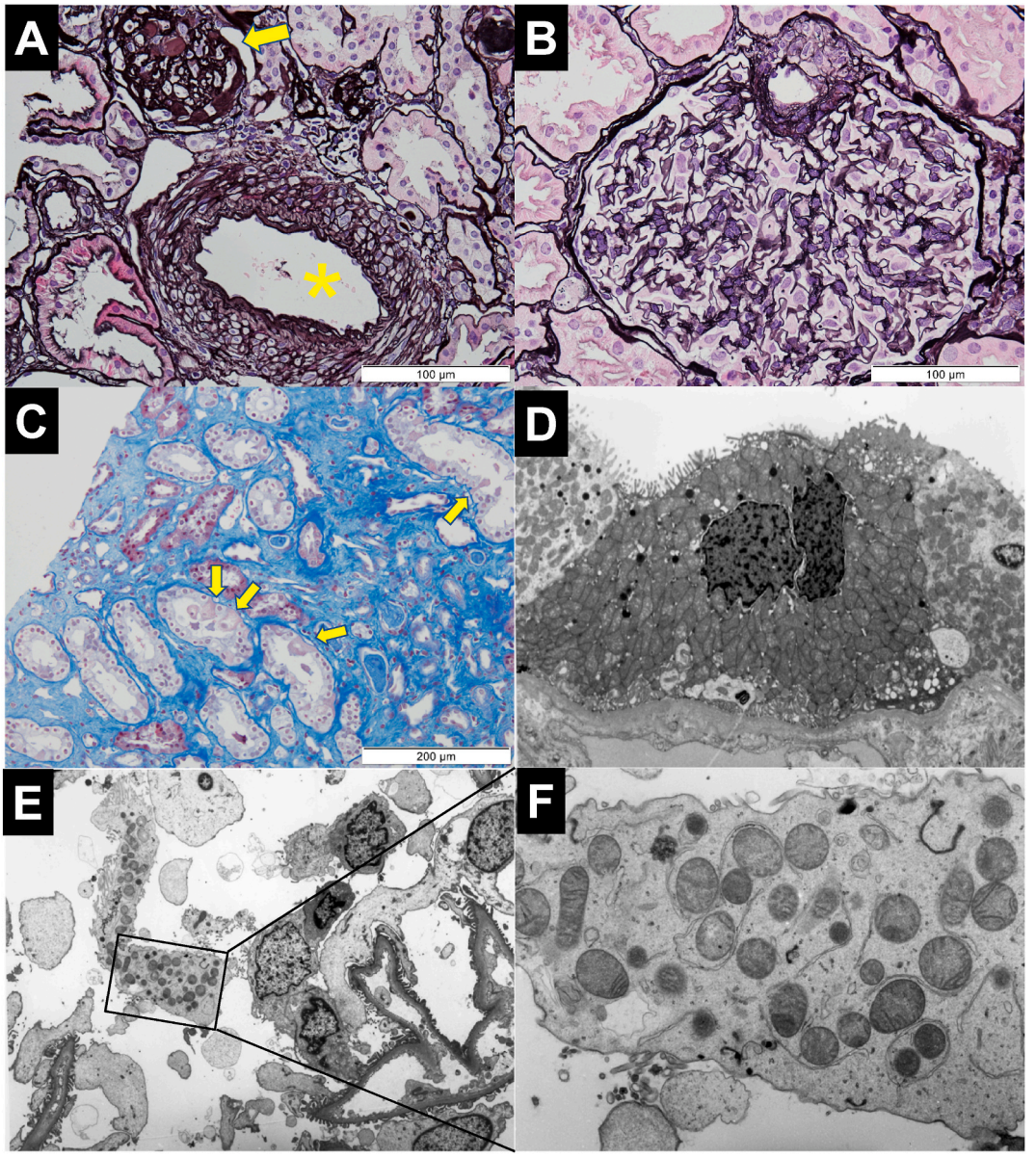

Fig. 1. Microscopic histopathological examination of the first kidney biopsy specimen. (A) One glomerulus is globally sclerosed (arrow). Age-inappropriate disarranged and irregularly sized vascular smooth muscle cells (AiDIVs) can be observed in an interlobular artery (asterisk) on periodic acid-methenamine-silver and hematoxylin eosin (PAM-HE) staining. **(B)** Residual glomeruli show a normal appearance. The afferent arteriole of this glomerulus showed AiDIVs on PAM-HE staining. **(C)** Granular swollen epithelial cells (GSECs) can be observed among the renal tubules and in the collecting duct (arrows) on Masson Trichrome staining. **(D)** Mitochondria with abnormal cristae structures accumulate in a collecting duct cell (electron microscopy; magnification 1500 ×). **(E)** Mitochondria are increased in a podocyte (electron microscopy; magnification 1500 ×). **(F)** High magnification of the area enclosed in the square shown in (E). The mitochondrial cristae structures exhibit ripping and loss, and the mitochondria are enlarged (electron microscopy; magnification 8000 ×).

only drug prescribed to the patient during this 2.8-year period was taurine. The uric acid level normalized after taurine administration. However, there has been no improvement in hearing impairment.

3. Discussion

FSGS cases with the m.3243A > G mutation often show an accumulation of abnormal mitochondria in podocytes upon electron microscopy, which suggests that mitochondrial dysfunction-induced podocytopathy may underline this disease [1,2,4]. However, our prior analysis showed that 11.4% of mitochondrial nephropathy cases with the m.3243A > G mutation were diagnosed as

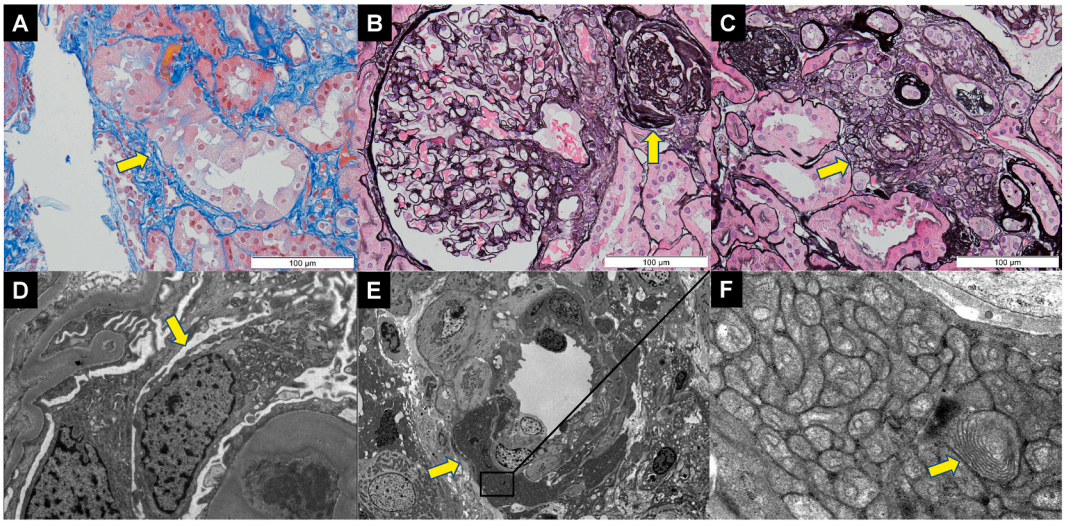

Fig. 2. Microscopic histopathological examination after the second kidney biopsy. (A) Most of the cells in the collecting duct (arrow) were classified as GSECs on Masson Trichrome staining. **(B)** One glomerulus is globally sclerosed (arrow). Another residual glomerulus appears normal while the vascular smooth muscle cells of the afferent arteriole of this glomerulus shows AiDIVs on PAM-HE staining. **(C)** AiDIVs can be observed in an arteriole (arrow) on PAM-HE staining. **(D)** Enlarged mitochondria can be observed in a podocyte (arrow; electron microscopy; magnification 10,000 ×). **(E)** A vascular smooth muscle cell (arrow) of an arteriole is filled with enlarged mitochondria (electron microscopy; magnification 2500 ×). **(F)** High magnification of the area enclosed in square (E). Cristae structures in accumulated mitochondria are disarranged. The crista structure of one mitochondrion exhibits a spiral shape (arrow; electron microscopy; magnification 30,000 ×).

nephrosclerosis without FSGS lesions [3]. The pathogenesis of why nephrosclerotic lesions without FSGS occur in mitochondrial nephropathy remains unclear. Sampling error may mean that FSGS lesions were not included in the limited renal biopsy specimens. However, we believe that sampling error alone cannot explain our data, as renal biopsy was performed twice in our case. As observed upon electron microscopy, abnormal mitochondria accumulated in the vascular smooth muscle cells (Fig. 2E and F). This finding suggests that mitochondrial dysfunction may occur and cause cellular dysfunction in vascular smooth muscle cells. In fact, despite the absence of hypertension and in spite of the patient's age, the mesenteric vascular smooth muscle cells of the interlobular arteries were unequal in size and arrangement (Figs. 1A, 3B and 3C). Thus, these age-inappropriate disarranged and irregularly sized vascular smooth muscle cells (AiDIVs) were assumed to cause abnormal glomerular hemodynamics, resulting in pathological changes similar to hypertension-induced nephrosclerosis.

In our case, two renal biopsies were performed with an intervening period of over 8 years. One weakness of this report was that the specimens from the first renal biopsy were not available for re-examination, and the mtDNA heteroplasmy rate could not be determined in the kidney. However, the rate of heteroplasmy increased markedly in the blood and urine sediment cells during this 8-year period, and the GSECs also increased between the first and second biopsy. This increase suggests that the rise in the heteroplasmy rate and the reduced mitochondrial function in the renal cells contributed to the progression of nephropathy. A previous report showed a relationship between the elevated m.3243A > G heteroplasmy rate in leukocytes and age-related changes [9], which may explain the age-inappropriate pathological changes in the renal lesions observed in our patient based on the increased heteroplasmy rate. Alternatively, other reports have shown that the heteroplasmy rates of the m.3243A > G pathogenic variant of *MT-TL1* in leukocytes decrease over time [10,11], which differs from the results in our case, where the heteroplasmy rates in leukocytes and urine sediment cells increased over time. Although the reason for this cannot be clearly demonstrated, it has been speculated that the decline in quality control of mtDNA decreases with age and the heteroplasmy rate of mtDNA increases, and this impaired quality control of mtDNA may have been the cause in this case as well [12–14]. In the future, it will be necessary to investigate the change in heteroplasmy rate of mtDNA over time in mitochondrial nephropathy cases with this pathological variant in order to resolve this difference.

Prior to treatment, the eGFR in the present patient declined at a rate of 1.50 mL/min/1.73 m^2 per year. As the eGFR was 31.9 mL/min/1.73 m^2 at the time of the second renal biopsy, it was estimated that the patient would reach end-stage kidney disease (ESKD) (under 10 mL/min/1.73 m^2) at approximately 60 years of age. The m.3243A > G mutation reduces the taurine modification of the leucine tRNA anticodon, resulting in the UUG codon not being appropriately recognized, leading to abnormal synthesis of mitochondrial proteins [15,16]. This reduction in tRNA function in cases with the pathogenic variants in *MT-TL1* that were already proven to cause a taurine modification defect in tRNALeu (UUR), as in m.3243A > G, can be improved by taurine supplementation, which restores mitochondrial function [6]. So far, the patient has been taking taurine for approximately three years, during which time the rate of eGFR decline improved markedly to 0.26 mL/min per year (Fig. 3). Assuming that this rate of eGFR decline could be maintained, we calculated that the patient would reach ESKD (under 10 mL/min/1.73 m^2) at approximately 115 years of age, because the current eGFR is about 28 mL/min/1.73 m^2. Although this is a single patient case report, it is the first study to show the long-term effects of taurine treatment on mitochondrial nephropathy caused by impaired taurine modification of mitochondrial tRNAs. It should be

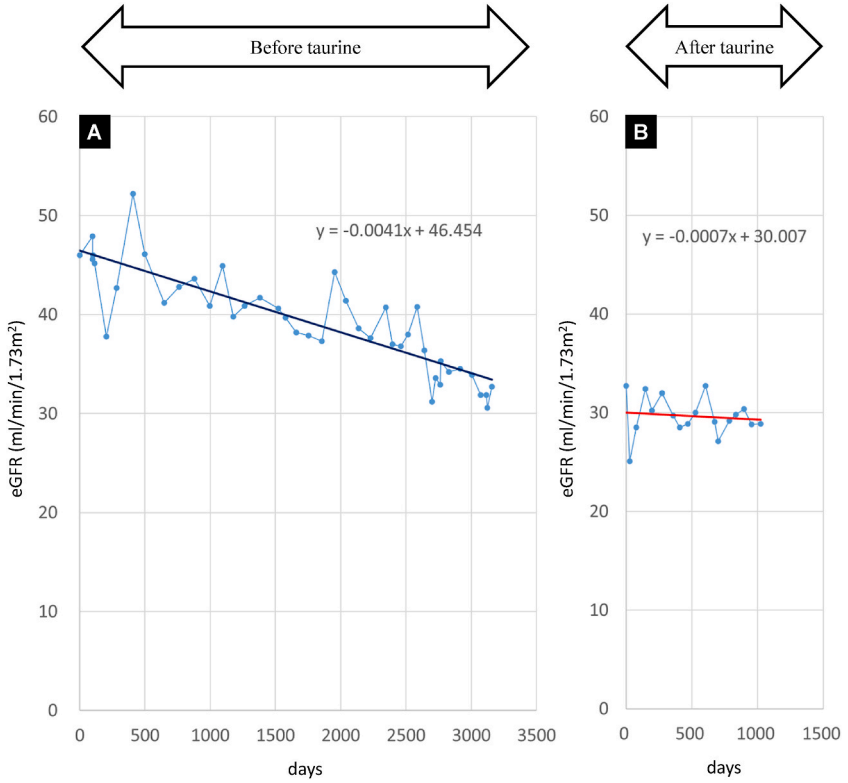

Fig. 3. Estimated glomerular filtration rate (eGFR) before (A) and after (B) taurine treatment. The slope is determined by a linear regression line using least square method. The horizontal axis shows the time in days, and the coefficient was multiplied by 365 to obtain the slope per year. The slope of eGFR prior to taurine administration was calculated using all eGFR measurements taken from the date of the first visit to the date of initiation of taurine administration, including the day of administration. The first renal biopsy was performed on day 99 and the second one was on day 3124. The slope of the post-taurine eGFR uses all measurements from the date of taurine administration to the present.

noted that this is an evaluation based on only one case treated with taurine, and the effect cannot be proven until additional cases are analyzed. Ultimately, randomized clinical trials with taurine supplementation are needed to address this research.

4. Conclusion

In conclusion, we believe that this case report provides three important insights into mitochondrial nephropathy. First, our analysis suggests that the etiopathogenesis of nephrosclerosis in mitochondrial nephropathy may be caused by abnormal mitochondrial function in vascular smooth muscle cells. Second, the heteroplasmy rates of mutated mtDNA increase over time, resulting in progression of nephropathy; these changes may be non-invasively captured by the analysis of urine sediment cells. Third, taurine administration may be effective at ameliorating *MT-TL1* mutation-induced mitochondrial nephropathy, although further studies are needed to independently validate our findings.

Declarations

Author contribution statement

Toshiyuki Imasawa: Conceived and designed the experiments; Wrote the paper.
Hiroshi Kitamura, Yukiko Yatsuka, Yasushi Okazaki: Performed the experiments.
Takehiko Kawaguchi, Kei Murayama: Analyzed and interpreted the data; Contributed reagents, materials, analysis tools or data.

Funding statement

MD, PhD Toshiyuki Imasawa; Yasushi Okazaki; Kei Murayama were supported by The Japan Agency for Medical Research and Development, AMED [19ek0109273, 20ek0109468].

Data availability statement

Data will be made available on request.

Declaration of interest's statement

The authors declare no conflict of interest.

Ethics approval and consent to participate

This study was approved by the Ethics Committee of Chiba Children's Hospital [2014-11-05 (on 18th November 2014), 2017-024 (on 23rd August 2017), and 2020-015 (on 9th June 2020)]. The patient provided informed consent for publication of this case report.

Consent for publication

Written informed consent was obtained from the patient for the publication of this case report and all accompanying images.

Acknowledgements

We would like to thank Editage (www.editage.com) for English language editing.

References

[1] H. Mochizuki, K. Joh, H. Kawame, A. Imadachi, H. Nozaki, T. Ohashi, et al., Mitochondrial encephalomyopathies preceded by de-Toni-Debré-Fanconi syndrome or focal segmental glomerulosclerosis, Clin. Nephrol. 46 (1996) 347–352.
[2] O. Hotta, C.N. Inoue, S. Miyabayashi, T. Furuta, A. Takeuchi, Y. Taguma, Clinical and pathologic features of focal segmental glomerulosclerosis with mitochondrial tRNALeu (UUR) gene mutation, Kidney Int. 59 (2001) 1236–1243, https://doi.org/10.1046/j.1523-1755.2001.0590041236.x.
[3] T. Imasawa, D. Hirano, K. Nozu, H. Kitamura, M. Hattori, H. Sugiyama, et al., Clinicopathologic features of mitochondrial nephropathy, Kidney Int. Rep. 7 (2022) 580–590, https://doi.org/10.1016/j.ekir.2021.12.028.
[4] T. Imasawa, R. Rossignol, Podocyte energy metabolism and glomerular diseases, Int. J. Biochem. Cell Biol. 45 (2013) 2109–2118, https://doi.org/10.1016/j.biocel.2013.06.013.
[5] J.B. Stewart, P.F. Chinnery, The dynamics of mitochondrial DNA heteroplasmy: implications for human health and disease, Nat. Rev. Genet. 16 (2015) 530–542, https://doi.org/10.1038/nrg3966.
[6] Y. Ohsawa, H. Hagiwara, S.I. Nishimatsu, A. Hirakawa, N. Kamimura, H. Ohtsubo, et al., Taurine supplementation for prevention of stroke-like episodes in MELAS: a multicentre, open-label, 52-week phase III trial, J. Neurol. Neurosurg. Psychiatry 90 (2019) 529–536, https://doi.org/10.1136/jnnp-2018-317964.
[7] S. Matsuo, E. Imai, M. Horio, Y. Yasuda, K. Tomita, K. Nitta, et al., Revised equations for estimated GFR from serum creatinine in Japan, Am. J. Kidney Dis. 53 (2009) 982–992, https://doi.org/10.1053/j.ajkd.2008.12.034.
[8] Y. Nishigaki, H. Ueno, J. Coku, Y. Koga, T. Fujii, K. Sahashi, et al., Extensive screening system using suspension array technology to detect mitochondrial DNA point mutations, Mitochondrion 10 (2010) 300–308, https://doi.org/10.1016/j.mito.2010.01.003.
[9] G.J. Tranah, S.M. Katzman, K. Lauterjung, K. Yaffe, T.M. Manini, S. Kritchevsky, et al., Mitochondrial DNA m.3243A > G heteroplasmy affects multiple aging phenotypes and risk of mortality, Sci. Rep. 8 (1) (2018), 11887, https://doi.org/10.1038/s41598-018-30255-6.
[10] L.M. 't Hart, J.J. Jansen, H.H. Lemkes, P. de Knijff, J.A. Maassen, Heteroplasmy levels of a mitochondrial gene mutation associated with diabetes mellitus decrease in leucocyte DNA upon aging, Hum. Mutat. 7 (3) (1996) 193–197, https://doi.org/10.1002/(sici)1098-1004, 1996 7:3%3C193::aid-humu2%3E3.0.co;2-c.
[11] A. Pyle, R.W. Taylor, S.E. Durham, M. Deschauer, A.M. Schaefer, D.C. Samuels, et al., Depletion of mitochondrial DNA in leucocytes harbouring the 3243A->G mtDNA mutation, J. Med. Genet. 44 (1) (2007) 69–74, https://doi.org/10.1136/jmg.2006.043109.
[12] P.I. Tsai, E. Korotkevich, P.H. O'Farrell, Mitigation of age-dependent accumulation of defective mitochondrial genomes, Proc. Natl. Acad. Sci. U. S. A. 119 (31) (2022), e2119009119, https://doi.org/10.1073/pnas.2119009119.
[13] M.A. Sazonova, V.V. Sinyov, V.A. Barinova, A.I. Ryzhkova, Y.V. Bobryshev, A.N. Orekhov, et al., Association of mitochondrial mutations with the age of patients having atherosclerotic lesions, Exp. Mol. Pathol. 99 (3) (2015) 717–719, https://doi.org/10.1016/j.yexmp.2015.11.019.
[14] R. Del Bo, A. Bordoni, F. Martinelli Boneschi, M. Crimi, M. Sciacco, N. Bresolin, et al., Evidence and age-related distribution of mtDNA D-loop point mutations in skeletal muscle from healthy subjects and mitochondrial patients, J. Neurol. Sci. 202 (1–2) (2002) 8–91.
[15] T. Yasukawa, T. Suzuki, T. Ueda, S. Ohta, K. Watanabe, Modification defect at anticodon wobble nucleotide of mitochondrial tRNAsLeu (UUR) with pathogenic mutations of mitochondrial myopathy, encephalopathy, lactic acidosis, and stroke-like episodes, J. Biol. Chem. 275 (2000) 4251–4257, https://doi.org/10.1074/jbc.275.6.4251.
[16] T. Suzuki, T. Suzuki, T. Wada, K. Saigo, K. Watanabe, Taurine as a constituent of mitochondrial tRNAs: new insights into the functions of taurine and human mitochondrial diseases, EMBO J. 21 (2002) 6581–6589, https://doi.org/10.1093/emboj/cdf656.

Molecular Genetics and Metabolism Reports 35 (2023) 100963

Contents lists available at ScienceDirect

Molecular Genetics and Metabolism Reports

journal homepage: www.elsevier.com/locate/ymgmr

Case Report

Focal segmental glomerulosclerosis with a mutation in the *mitochondrially encoded NADH dehydrogenase 5* gene: A case report

Tsukasa Naganuma [a,1], Toshiyuki Imasawa [b,*,1], Ikuo Nukui [a], Masakiyo Wakasugi [a], Hiroshi Kitamura [c], Yukiko Yatsuka [d], Yoshihito Kishita [d,e], Yasushi Okazaki [d], Kei Murayama [f], Yoshimi Jinguji [a]

[a] Division of Nephrology, Department of Internal Medicine, Yamanashi Prefectural Central Hospital, 1-1-1 Fujimi, Kofu, Yamanashi 400-0027, Japan
[b] Department of Nephrology, National Hospital Organization Chiba-Higashi National Hospital, 673 Nitona-cho, Chuoh-ku, Chiba-city, Chiba 206-8712, Japan
[c] Department of Clinical Pathology, National Hospital Organization Chiba-Higashi National Hospital, 673 Nitona-cho, Chuoh-ku, Chiba-city, Chiba 206-8712, Japan
[d] Diagnostics and Therapeutics of Intractable Diseases, Intractable Disease Research Center, Graduate School of Medicine, Juntendo University, 2-1-1, Hongo, Bunkyo-ku, Tokyo 113-8421, Japan
[e] Department of Life Science, Faculty of Science and Engineering, Kindai University, 3-4-1 Kowakae, Higashiosaka, Osaka 577-8502, Japan
[f] Center for Medical Genetics, Department of Metabolism, Chiba Children's Hospital, 579-1, Heta-cho, Midori-ku, Chiba 266-0007, Japan

ARTICLE INFO

Keywords:
Focal segmental glomerulosclerosis
Mitochondrial nephropathy
NADH dehydrogenase 5
Podocyte
Case report

ABSTRACT

NADH dehydrogenase 5 (ND5) is one of 44 subunits composed of Complex I in mitochondrial respiratory chain. Therefore, a *mitochondrially encoded ND5* (*MT-ND5*) gene mutation causes mitochondrial oxidative phosphorylation (OXPHOS) disorder, resulting in the development of mitochondrial diseases. Focal segmental glomerulosclerosis (FSGS) which had podocytes filled with abnormal mitochondria is induced by mitochondrial diseases. An *MT-ND5* mutation also causes FSGS. We herein report a Japanese woman who was found to have proteinuria and renal dysfunction in an annual health check-up at 29 years old. Because her proteinuria and renal dysfunction were persistent, she had a kidney biopsy at 33 years of age. The renal histology showed FSGS with podocytes filled with abnormal mitochondria. The podocytes also had foot process effacement and cytoplasmic vacuolization. In addition, the renal pathological findings showed granular swollen epithelial cells (GSECs) in tubular cells, age-inappropriately disarranged and irregularly sized vascular smooth muscle cells (AiDIVs), and red-coloured podocytes (ReCPos) by acidic dye. A genetic analysis using peripheral mononuclear blood cells and urine sediment cells detected the m.13513 G > A variant in the *MT-ND5* gene. Therefore, this patient was diagnosed with FSGS due to an *MT-ND5* gene mutation. Although this is not the first case report to show that an *MT-ND5* gene mutation causes FSGS, this is the first to demonstrate podocyte injuries accompanied with accumulation of abnormal mitochondria in the cytoplasm.

1. Introduction

Mitochondrial diseases/disorders are rare and occur every 1 in 5000 births [1]. Mitochondria play a key role in the biosynthesis of adenosine triphosphate (ATP), the main energy source of cells, through oxidative phosphorylation (OXPHOS) using the mitochondrial respiratory chain (MRC) complex. Given that the genes related to the MRC complex are encoded in mitochondrial DNA (mtDNA) and nuclear DNA (nDNA), mitochondrial diseases can occur in cases of mtDNA or nDNA mutations [2,3]. As ATP is mandatory for all cells that require energy, the clinical phenotypes of mitochondrial diseases are versatile and are expressed as encephalopathy [4], myopathy [5], cardiomyopathy [6], hepatopathy

Abbreviations: ND5, NADH dehydrogenase 5; *MT-ND5*, mitochondrially encoded ND5; OXPHOS:, oxidative phosphorylation; MELAS, mitochondrial encephalomyopathy, lactic acidosis, and stroke-like episodes; FSGS, focal segmental glomerulosclerosis; GSECs, granular swollen epithelial cells; AiDIVs, age-inappropriately disarranged and irregularly sized vascular smooth muscle cells; ReCPos, red-coloured podocytes; ATP, adenosine triphosphate; MRC, mitochondrial respiratory chain; mtDNA, mitochondrial DNA; nDNA, nuclear DNA; Cr, creatinine; sCr, serum creatinine; eGFR, estimated glomerular filtration rate; COX IV, cytochrome *c* oxidase subunit 4.

* Corresponding author.
E-mail address: imasawa@nifty.com (T. Imasawa).
[1] These authors contributed equally.

https://doi.org/10.1016/j.ymgmr.2023.100963
Received 12 December 2022; Received in revised form 27 February 2023; Accepted 28 February 2023
Available online 9 March 2023

[7], deafness [8], and diabetes mellitus [9]. Mitochondrial nephropathy, which occurs because of a mitochondrial disorder in nephrons, has also been reported [10–12].

Focal segmental glomerulosclerosis (FSGS) is a histological term, rather than a specific disease category and diagnosed by the presence of sclerosis in parts of at least one glomerulus in the kidney biopsy specimen [13]. It can be classified into primary, secondary, genetic, and unknown forms of FSGS [14]. Among causative genes of mitochondrial nephropathy, m.3243A > G pathogenic variant in *MT-TL1* gene on mtDNA, which encodes mitochondrial transfer RNA leucine 1, is majority [12]. The m.3243A > G mutation leads to genetic cause of FSGS with accumulation of abnormal mitochondria in podocytes [11,15]. Because podocyte injury plays a key role in the pathogenesis of FSGS [16–18], impaired mitochondrial function in podocytes should induce FSGS [19–22].

The pathogenic variants in *mitochondrially encoded NADH dehydrogenase 5* (*MT-ND5*) gene cause mitochondrial diseases such as mitochondrial encephalomyopathy with lactic acidosis and stroke-like episodes (MELAS) [23–25]. ND5 is one of the 44 subunits of mitochondria respiratory complex I. The pathogenic variants in *MT-ND5* gene also cause FSGS [26–29]. However, in all cases with FSGS lesions presented in the past reports, abnormal mitochondria or their accumulation were not identified in podocytes. In another recent report of three cases with nephropathy due to *MT-ND5* gene mutation, one of the cases showed FSGS lesion. The authors of this report concluded that FSGS lesion of their case was secondary [28]. The pathogenesis of the secondary FSGS is considered to involve intraglomerular hypertension caused by hypertension or obesity, by adaptation to nephron loss due to progression of glomerulosclerosis or by a low nephron number due to low birth weight [30,31]. Therefore, it has not been evident whether genetic FSGS occurs with a pathogenic variant in *MT-ND5* gene. Here, we report the case with an *MT-ND5* mutation with apparent FSGS lesions. In this case, foot process effacement and cytoplasmic vacuolization in podocytes with accumulation of abnormal mitochondria were observed.

2. Case presentation

This case occurred in a Japanese woman born at 39 weeks of gestation with a birth weight of 3210 g. She had no remarkable medical history. Annual health check-ups showed no proteinuria on urinalysis until age 29. At 29 years of age, the annual health check-up revealed proteinuria (1+) for the first time using a urine dipstick and a high serum creatinine (sCr) level of 1.01 mg/dL. Her estimated glomerular filtration rate (eGFR) using the Japanese Eq. [32] was calculated to be 54.0 mL/min/1.73 m^2. At the same check-up, she was also found to have a slight hearing disturbance. Additionally, she had a headache once a week from 30 years of age and was diagnosed by a neurologist with migraine, uncontrolled with triptan. Her health check-up at 32 years of age again showed proteinuria (1+) and increased sCr (1.06 mg/dL). Hematuria has never been noted before. At 33 years of age, she was referred to the Yamanashi Prefectural Central Hospital by her primary doctor to examine the reason for her proteinuria and decreased eGFR. At the first visit, proteinuria (1.09 g/gCr), elevated sCr (1.28 mg/dL), and elevated uric acid (7.5 mg/dL) were detected. Febuxostat and sodium bicarbonate were prescribed for the treatment of hyperuricemia. Because of the continued presentation of proteinuria and decreased renal function, she was admitted for a kidney biopsy, at 6 months following the initial visit.

Upon admission, her blood pressure was 114/70 mmHg. Physical examination showed a height of 152 cm, body weight of 43.8 kg, and body mass index of 19.0. No crackles or murmurs were detected on chest auscultation. No abnormal neurological findings were observed. Neither skin lesions nor pitting oedema were detected. The laboratory data on admission are summarised in Table 1, which shows decreased eGFR and proteinuria. Hematuria was not observed. In the data we measured, there were no data to suggest the presence of tubular dysfunction such as Fanconi's syndrome or distal tubular acidosis. The long × short axis of the kidneys measured 101 × 38 mm on the left and 104 × 50 mm on the right, indicating no renal atrophy. The electrocardiogram test result was normal, and echocardiography revealed normal cardiac function. The standard pure-tone hearing test showed a right-ear value of 38.8 dB and a left-ear value of 40.0 dB. She was therefore diagnosed with sensorineural hearing loss by an otolaryngologist. No visual field defects were noted. Furthermore, because of hearing loss and headache symptoms, a brain magnetic resolution imaging (MRI) was also performed to examine for brain lesions, but no abnormal findings were found.

Her parents had died because of cancer (mother, breast cancer,

Table 1
Laboratory data on admission.

Blood cell count			Blood chemistry			Immunology			Urinalysis		
WBC	5400	/μL	TP	6.8	g/dL	CH50	54	U/mL	Gravity	1.01	
RBC	373	$\times 10^4$/μL	Alb	3.9	g/dL	C3	76.1	mg/dL	pH	7.0	
Hb	11.5	g/dL	AST	21	IU/L	C4	19.3	mg/dL	RBC	1–4	/HPF
Ht	35.1	%	ALT	11	IU/L	IgG	1340.3	mg/dL	WBC	<1	/HPF
MCV	94.1	fl	LDH	186	IU/L	IgA	225.7	mg/dL	Protein	2.04	g/gCr
MCHC	32.8	%	ALP	149	IU/L	IgM	180.1	mg/dL	Glucose	(−)	
Plt	25.7	$\times 10^4$/μL	Tbil	0.56	mg/dL	ANA	(−)		NAG	8.6	U/L
			BUN	21.8	mg/dL	M protein	(−)				
Coagulation			Cr	1.26	mg/dL	HBs Ag	(−)				
APTT	34.0	*sec*	eGFR	40.8	mL/min/1.73 m^2	HCV Ab	(−)				
PT	99.0	%	K	5.0	mEq/L						
INR	0.97	INR	P	3.1	mg/dL						
Fib	373.0	mg/dL	UA	5.4	mg/dL						
			Tcho	255	mg/dL						
			CRP	0.01	mg/dL						
			FBS	85	mg/dL						
			HbA1c	5.3	%						

Aberrant values are underlined.
WBC, white blood cells; RBC, red blood cells; Hb, haemoglobin; Hct, haematocrit; MCV, mean corpuscular volume; MCHC, mean corpuscular haemoglobin concentration; Plt, platelet; APTT, activated partial thromboplastin time; PT, prothrombin time; INR, international normalized ratio; Fib, fibrinogen; TP, total protein; Alb, albumin; AST, aspartate aminotransferase; ALT, alanine aminotransferase; LDH, lactate dehydrogenase; ALP, alkaline phosphatase; Tbil, total bilirubin; BUN, blood urea nitrogen; Cr, creatinine; eGFR, estimated glomerular filtration rate (by the Japanese equation); K, potassium; P, phosphate; UA, uric acid; Tcho, total cholesterol; CRP, C-reactive protein; FBS, fasting blood sugar; HbA1c, haemoglobin A1c (NGSP); CH50, 50% haemolytic complement activity; C3, complement 3; IgG, immunoglobulin G; ANA, antinuclear antibody; M protein, monoclonal protein; HBs Ag, hepatitis B surface antigen; HCV Ab, hepatitis C virus antibody; NAG, *N*-acetyl glucosaminidase; HPF, high power field.

father, colon cancer) without kidney disease or any hearing difficulty. Neither of her two older brothers had any abnormalities in kidney function, urine, or hearing. She had a 7-year-old daughter and a 5-year-old son. Her daughter's birth weight was 2840 g at 41 weeks and 2 days of gestation, and her son's birth weight was 2632 g at 39 weeks of gestation. Her daughter was born using suction delivery, whereas her son was born through normal delivery. None of her children had any urinary abnormalities or hearing difficulties, as examined during medical check-ups. However, the children sometimes complained of headaches that had not yet been diagnosed by any doctor.

A percutaneous kidney biopsy was performed under ultrasound guidance. Light microscopy photographs of renal biopsy specimens are shown in Fig. 1. Nine glomeruli were observed in the specimens. One glomerulus was globally sclerosed. Furthermore, segmental sclerosis was observed at the perihilar area in two glomeruli, compatible with the perihilar variant in the Columbia classification of FSGS (Fig. 1a) [13,30]. Interestingly, red-coloured podocytes (ReCPos), whose cytoplasm was dyed red, were observed using AZAN trichrome staining (Fig. 1a and b). Neither mesangial proliferation nor hypercellularity were detected. Interstitial fibrosis and tubular atrophy were observed in almost 30% of the interstitium. There were no abnormal findings such as thickening or lamellation of the tubular basement membrane. Characteristically, granular swollen epithelial cells (GSECs), reported to be specific to mitochondrial diseases [33,34], were markedly observed in the distal tubular cells using AZAN trichrome staining (Fig. 1c). Such GSECs were emphasised by staining with anti-cytochrome *c* oxidase subunit 4 (COX IV) antibody [mouse anti-COX IV antibody (20E8C12)] (ab14744; Abcam PLC., Cambridge, UK; Fig. 1d). COX IV staining is recognised as a loading control for mitochondria [34,35]. Furthermore, the sizes of the vascular smooth muscle cells in arterioles were irregular, and their arrangement was disorganized in a manner similar to that seen in older patients, despite the younger age (33 years) of the patient, without any medical history that may have caused arteriosclerosis (Fig. 1e). Such age-inappropriately disarranged and irregularly sized vascular smooth muscle cells (AiDIVs) were also noticeable in the interlobular arteries (Fig. 1f). Immunofluorescence analysis revealed IgM, C3 and C1q deposits in the glomeruli (Fig. 1g-i). IgG and IgA were negative in observed glomeruli. Electron microscopy analyses (Fig. 2a–e) also showed podocytes with increased mitochondria that had lost their normal cristae structure. Foot processes of such podocytes with accumulation of abnormal mitochondria were effaced (Fig. 2b and d). A vacuolization was also observed in the cytoplasm in the podocyte with mitochondrial accumulation (Fig. 2b). We also detected cells with increased abnormal mitochondria in the parietal epithelial cells of the Bowman's capsule (Fig. 2f). Although the glomerular basement membrane was partially thin at the part along with the podocytes with abnormal mitochondria, the membranes at other parts showed normal thickness (> 250 nm) without lamination or reticulation. Electron dense deposits were not observed in mesangium or glomerular basement membranes. These renal pathology findings strongly suggest genetic FSGS due to mitochondrial disease.

The serum lactate and pyruvate levels were slightly elevated at 21.0 mg/dL (normal: 3.0–17.0 mg/dL) and 1.34 mg/dL (normal: 0.30–0.94 mg/dL), respectively. The pathological finding of accumulation of abnormal mitochondria in glomerular epithelial cells and tubules, the presence of sensorineural hearing difficulty, and elevated blood lactate led us to perform a comprehensive genetic analysis of mitochondrial diseases.

After obtaining informed consent from the patient according to protocol and permission from our ethics committees, genomic DNA extracted from the patient's peripheral mononuclear blood cells and urine sediment cells was analysed by targeted resequencing coupled with next-generation sequencing, followed by Sanger sequencing. The DNA was subjected to fragmentation and library preparation using the Lotus DNA Library Prep Kit (#10001074; Integrated Device Technology, Inc., San Jose, CA, USA) according to the manufacturer's instructions. Target enrichment was performed with xGen Human mtDNA Research Panel (#1075705; Integrated Device Technology) targeting the whole mtDNA and with custom xGen® Predesigned Gene Capture Pools (Integrated Device Technology)/xGen Lockdown Probe pool (Integrated Device Technology) targeting the exons of 367 nuclear-encoded genes that cause mitochondrial diseases. The library was then sequenced on the Illumina MiSeq platform using the MiSeq Reagent Kit v2 (MS-102-2002; Illumina, Inc., San Diego, CA, USA). A pathogenic mtDNA variant of m.13513G > A was detected in both the patient's blood cells and urine sediment cells (Fig. 3). The Minor Variant Finder (MVF) software program (Thermo Fisher Scientific, Waltham, MA, USA) revealed that the heteroplasmy rates of the blood cells and urine sediment cells were 10.3% (forward: 11.6%/reverse: 9.0%) and 62.2% (forward: 63.7%/reverse: 60.7%), respectively. Therefore, we diagnosed her with renal dysfunction and proteinuria due to FSGS caused by an *MT-ND5* mutation.

3. Discussion and conclusions

MT-ND5 gene encodes NADH dehydrogenase 5 (ND5), which is a subunit of mitochondria respiratory complex I. Therefore, *MT-ND5* mutations cause mitochondrial diseases such as MELAS [23,36,37], Leigh syndrome [36–39], and Leber hereditary optic neuropathy [37]. Our case with the m.13513G > A variant in the *MT-ND5* gene showed FSGS lesions with injured podocytes that had accumulation of abnormal mitochondria in the cytoplasm. The m.13513G > A has already been confirmed as a pathogenic variant of the mitochondrial disease using MITOMAP, a human mitochondrial genome database (https://www.mitomap.org/MITOMAP).

Mitochondrial diseases cause genetic FSGS [11,12,15]. Its etiology is postulated to be caused by genetically disrupted mitochondrial function in podocytes [19,22]. As an indication of this, cases with FSGS due to m.3243A > G mutation had podocytes filled with mitochondria with abnormal cristae structure [10,11]. In the past, several cases of mitochondrial diseases due to *MT-ND5* mutations have been also reported to show FSGS lesions [26–29]. However, in these cases, pathological findings of podocyte injuries with accumulation of abnormal mitochondria were not confirmed, leaving the possibility of secondary FSGS caused by intraglomerular hypertension [14,28,30,31]. In contrast, our present case showed apparent FSGS lesions, and we detected increased abnormal mitochondria in the glomerular podocytes that also had pathological findings indicating their injuries such as foot process effacement and the cytoplasmic vacuolization. Our patient did not have hypertension, obesity, or a history of low birth weight. Furthermore, the diameters of all glomeruli observed under light microscopy in this patient were < 250 μm (mean ± SD; 149 ± −72 μm). Therefore, we deemed the etiology of FSGS, in this case, to be a disorder of the mitochondrial OXPHOS system due to an *MT-ND5* mutation and not due to 'secondary' by intraglomerular hypertension [14,30,31]. The pathological picture of tubulointerstitial nephropathy with GSECs was also observed in this case. This tubulointerstitial damage may be due to the *MT-ND5* mutation, as has been reported in the past [28].

In general, mitochondrial diseases induced by mtDNA mutations vary markedly based on differences in the rates of heteroplasmy by cell type or organ [40,41]. Therefore, while the reason for the differences between the present and the previous cases with the pathogenic variant in *MT-ND5* gene could not be completely ascertained, the heteroplasmy rate of mtDNA with the pathogenic variant in podocytes might have been higher in our case than that in the previous cases.

In this case, IgM, C3, and C1q were positive in glomeruli (Fig. 1g-i). Since neither hematuria, mesangial cell proliferation, nor electron dense deposits were observed, we considered that it was unlikely that IgM nephropathy or C1q nephropathy was complicated [42,43]. On the other hand, glomerular IgM and C3 deposits frequently accompany FSGS [44]. In addition, IgM and C3 were positive in glomeruli of two out of three cases report by Bakis et al., too [28]. Therefore, IgM and C3

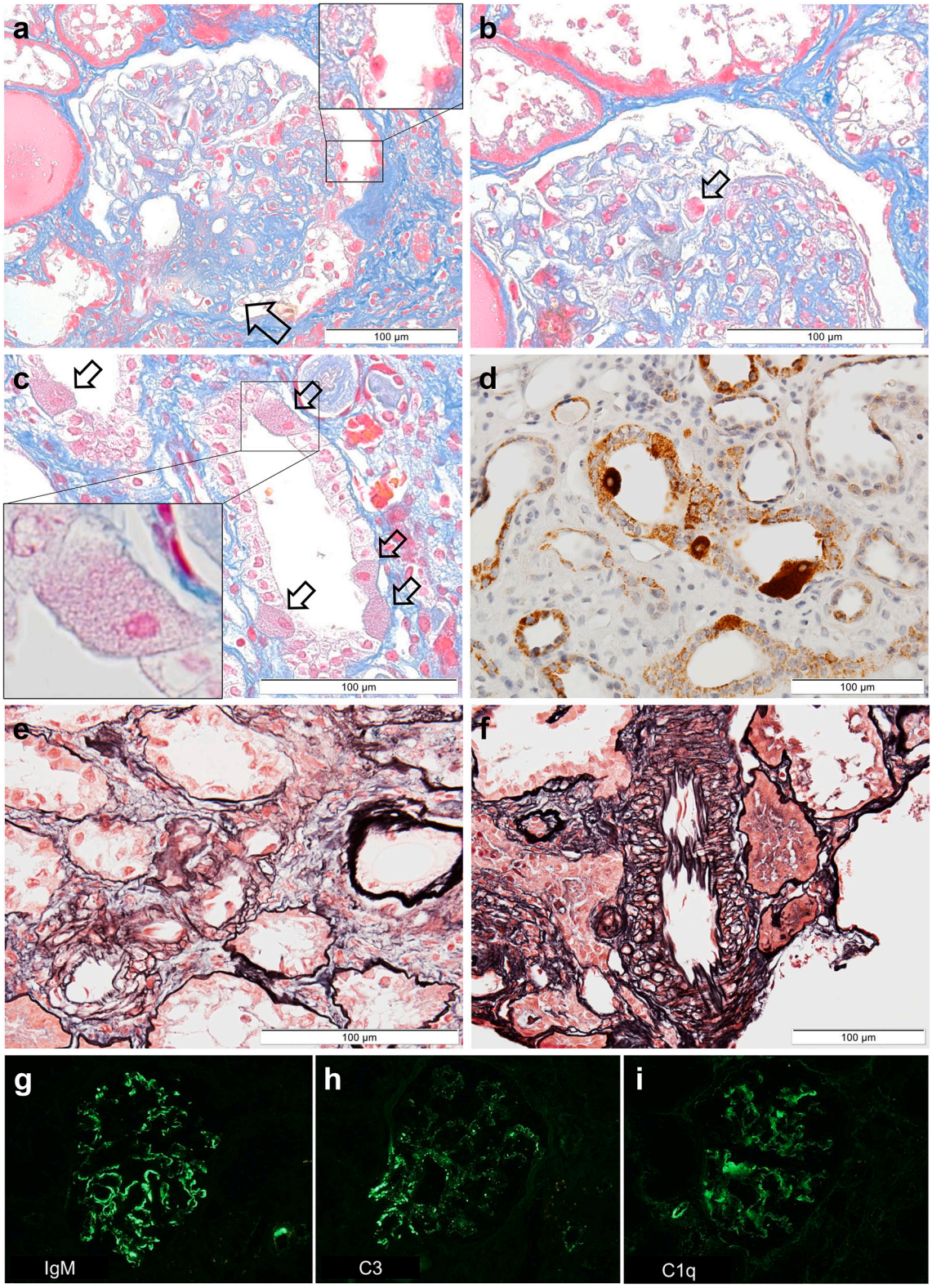

Fig. 1. Light microscopy and immunofluorescence findings (a): The segmental sclerosis lesion at the perihilar area is indicated by an arrow. A red-coloured podocyte (ReCPo) is surrounded by a square, magnified at the top right (AZAN stain). (b): The ReCPo is indicated by an arrow (AZAN stain). (c): GSECs in the distal tubules are indicated by arrows (AZAN stain). One GSEC is magnified at the lower left. (d): Staining of COX IV emphasizes tubular cells, including many mitochondria, which correspond to GSECs. (e): In the afferent arteriole that connects to the glomerulus of (a), the sizes of the vascular smooth muscle cells are irregular, and their arrangement is disorganized, similar to those seen in older patients (PAM-HE stain). (f): Age-inappropriately disarranged and irregularly sized vascular smooth muscle cells (AiDIVs) are observed in an interlobular artery (PAM-HE stain). (g): IgM deposits are detected in glomeruli. (h): IgG deposits are detected in glomeruli. (i): C1q deposits are detected in glomeruli.

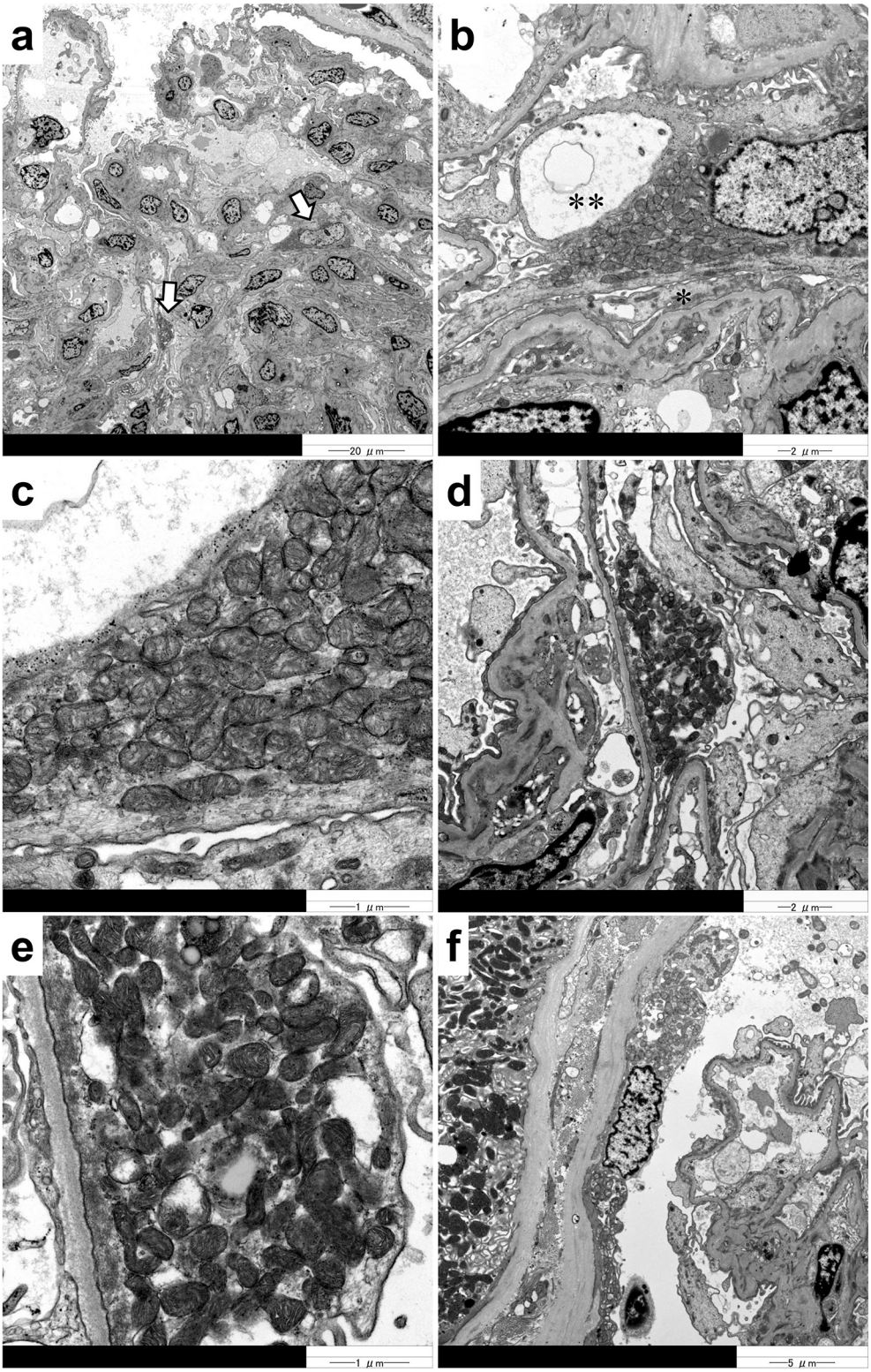

Fig. 2. Electron microscopy findings (a): Arrows indicate podocytes filled with increased mitochondria. (b): In a podocyte, abnormally high numbers of mitochondria are seen in the cytoplasm. Foot process effacement (*) and cytoplasmic vacuolization (**) are observed in this podocyte. (c): Magnification of (b) reveals that the increased mitochondria have lost their organized cristae structure. (d): A podocyte is filled with mitochondria. The foot process of this podocyte is effaced. (e): Magnification of (d) reveals that mitochondria with disorganized cristae increase. (f): The parietal epithelial cells in Bowman's capsule are also filled with abnormal mitochondria.

deposition may be related to a part of the pathogenesis of FSGS caused by *MT-ND5* mutation. Although the reason for C1q deposition in glomeruli is also not clear. Because C1q is reported to bind to mitochondria, it may be associated with the pathogenesis of FSGS by driving oxidative stress [45–47].

This case should be suggestive because it had several characteristic light-microscopical findings of mitochondrial nephropathy. In our case, GSECs with red-coloured cytoplasm were observed with AZAN trichrome staining. As mitochondria are dyed red by acidic dyes such as AZAN, red-coloured GSECs indicate that they abnormally include many mitochondria [33]. In addition, as COX IV is a subunit of complex IV, COX IV staining can be used to stain mitochondria [35] and may help confirm the presence of abnormally increased numbers of mitochondria [34,48]. Furthermore, age-inappropriately disarranged and irregularly sized vascular smooth muscle cells (AiDIVs) were observed in the arterioles and intralobular arteries in this case. Such findings have also been

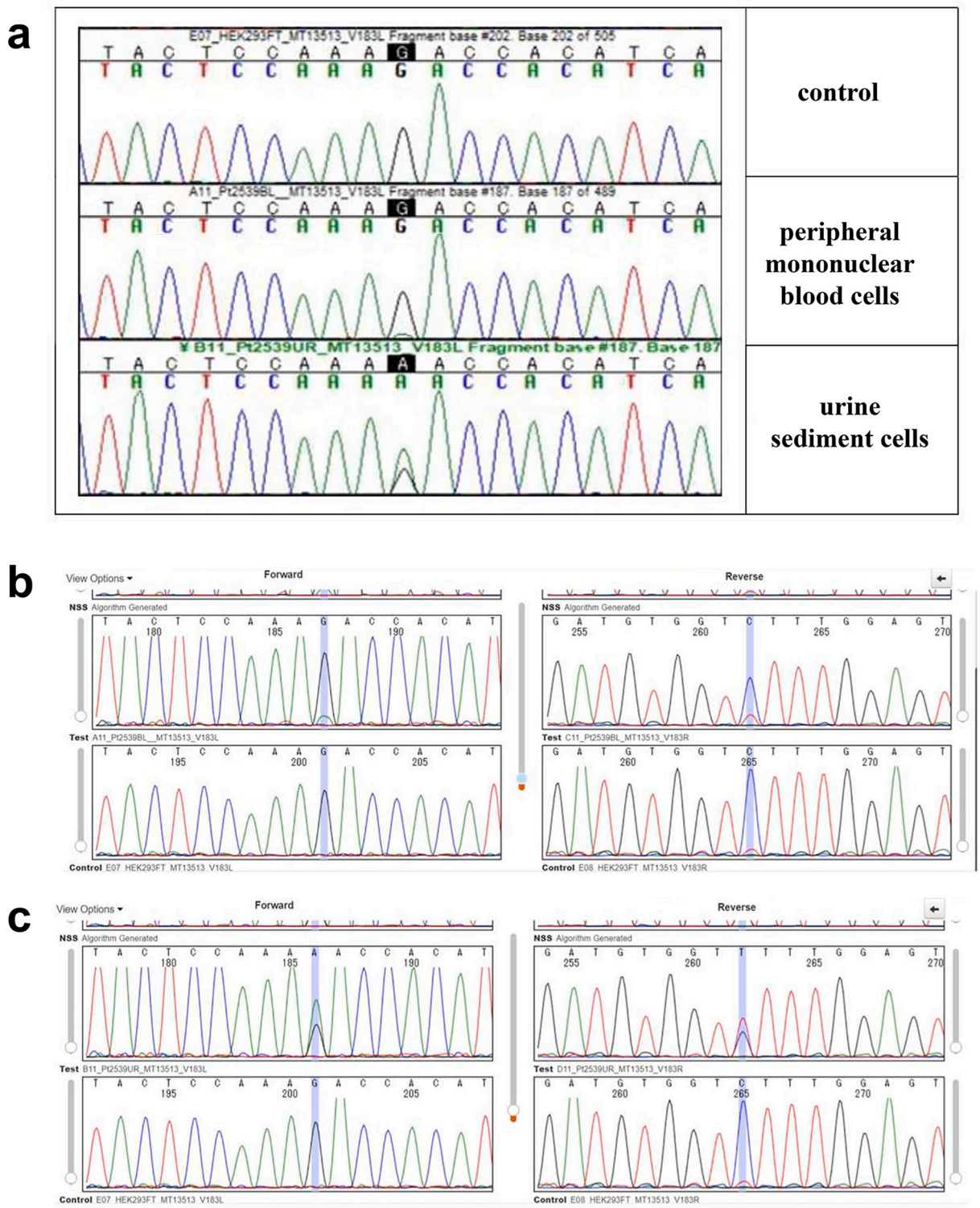

Fig. 3. Genetic analysis (a): The electropherogram from Sanger sequencing indicates that the patient has the m.13513 G > A variant in her peripheral mononuclear blood and urine sediment cells. (b): The rate of heteroplasmy calculated by the MVF software program is 10.3% (forward: 11.6%/reverse: 9.0%) in peripheral mononuclear blood cells (upper panel: patient, lower panel: control). (c): The rate of heteroplasmy is 62.2% (forward: 63.7%/reverse: 60.7%) in urine sediment cells (upper panel: patient, lower panel: control).

reported in other cases of mitochondrial nephropathy [12,34]. Interestingly, red-coloured podocytes (ReCPos) were detected using AZAN trichrome staining, as we recently reported in a case of mitochondrial nephropathy [49]. Like GSECs, ReCPos abnormally include many mitochondria in their cytoplasm [49]. In summary, in cases of FSGS or glomerulosclerosis with unknown aetiologies, the existence of GSECs, AiDIVs, and ReCPos should be carefully evaluated. COX IV staining may aid in the detection of abnormally increased mitochondrial counts.

We describe the weaknesses of our report. In this case, because mitochondrial disease was suspected based on the pathological findings of abnormal mitochondria, the presence of hearing loss, and high blood lactate levels, we comprehensively examined the genes associated with

mitochondrial diseases. Therefore, genetic FSGS due to other gene mutation [50] cannot be completely ruled out. In addition, because genetic testing was performed only on the patient but not on other family members, it could not be investigated whether they carried the heteroplasmic mitochondrial variant. The parents were already deceased and the two healthy brothers did not consent to genetic analysis. The two her children were still under 18 years old and the patient did not wish genetic test. Furthermore, measurement of MRC enzyme activity using kidney biopsy specimens is an effective for confirming mitochondrial dysfunction [51,52]. However, it could not be performed due to the paucity of kidney specimens for this analysis.

In conclusion, this is the first case report which indicates that the pathogenic variant an *MT-ND5* gene causes accumulation of abnormal mitochondria in podocytes, which leads to forming FSGS.

Ethics approval and consent to participate

The original study to perform a genetic analysis for mitochondrial diseases was approved by the Ethics Committee of Chiba Children's Hospital (2014-11-05). In addition, the analysis of this case was also approved by the Ethics Committee of Yamanashi Prefectural Central Hospital (2020–16). The patient provided informed consent and permission to participate in the study.

Consent for publication

Written informed consent was obtained from the patient for the publication of this case report and accompanying images. A copy of the written consent is available for review by the editor of this journal. All authors consented to the publication of the manuscript in *BMC Nephrology*.

Funding

This work was supported in part by the Practical Research Project for Rare/Intractable Diseases from the Japan Agency for Medical Research and Development, AMED (19ek0109273, 20ek0109468) (http://www.amed.go.jp/en/) to TI, YO, and KM.

Authors' contributions

TN drafted the manuscript. TI was involved in the coordination of the study and draft preparation. IN and MW provided clinical information. KH performed the pathological analysis. YY and YK performed molecular genetic studies. YO performed sequence alignment and data curation. KM was involved in the coordination of the study and data curation. YJ was involved in the coordination of the study and clinical information. All authors read and approved the final manuscript.

Declaration of Competing Interest

The authors declare that they have no competing interests.

Data availability

Most of the clinical data used and analysed in this case report are presented in this manuscript. More detailed information is available from the corresponding author upon request.

Acknowledgements

We thank Minako Tominaga and Eri Gomi for their technical assistance. We would like to thank Editage (http://www.editage.com) for English language editing.

References

[1] D. Skladal, J. Halliday, D.R. Thorburn, Minimum birth prevalence of mitochondrial respiratory chain disorders in children, Brain. 126 (Pt 8) (2003) 1905–1912, https://doi.org/10.1093/brain/awg170.
[2] S. Dimauro, G. Davidzon, Mitochondrial DNA and disease, Ann. Med. 37 (3) (2005) 222–232, https://doi.org/10.1080/07853890510007368.
[3] D.M. Kirby, D.R. Thorburn, Approaches to finding the molecular basis of mitochondrial oxidative phosphorylation disorders, Twin Res. Hum. Genet. 11 (4) (2008) 395–411, https://doi.org/10.1375/twin.11.4.395.
[4] D. Leigh, Subacute necrotizing encephalomyelopathy in an infant, J. Neurol. Neurosurg. Psychiatry 14 (3) (1951) 216–221, https://doi.org/10.1136/jnnp.14.3.216.
[5] S. Yatsuga, N. Povalko, J. Nishioka, et al., MELAS: a nationwide prospective cohort study of 96 patients in Japan, Biochim. Biophys. Acta 1820 (5) (2012) 619–624, https://doi.org/10.1016/j.bbagen.2011.03.015.
[6] M.G. Bates, J.P. Bourke, C. Giordano, G. d'Amati, D.M. Turnbull, R.W. Taylor, Cardiac involvement in mitochondrial DNA disease: clinical spectrum, diagnosis, and management, Eur. Heart J. 33 (24) (2012) 3023–3033, https://doi.org/10.1093/eurheartj/ehs275.
[7] W.S. Lee, R.J. Sokol, Mitochondrial hepatopathies: advances in genetics and pathogenesis, Hepatology. 45 (6) (2007) 1555–1565, https://doi.org/10.1002/hep.21710.
[8] P.R. Olmos, G.R. Borzone, J.P. Olmos, et al., Mitochondrial diabetes and deafness: possible dysfunction of strial marginal cells of the inner ear, J. Otolaryngol. Head Neck Surg. 40 (2) (2011) 93–103.
[9] S. Suzuki, Diabetes mellitus with mitochondrial gene mutations in Japan, Ann. N. Y. Acad. Sci. 1011 (2004) 185–192, https://doi.org/10.1007/978-3-662-41088-2_19.
[10] P.S. Thorner, J.W. Balfe, L.E. Becker, R. Baumal, Abnormal mitochondria on a renal biopsy from a case of mitochondrial myopathy, Pediatr. Pathol. 4 (1–2) (1985) 25–35, https://doi.org/10.3109/15513818509025900.
[11] H. Mochizuki, K. Joh, H. Kawame, et al., Mitochondrial encephalomyopathies preceded by de-Toni-Debré-Fanconi syndrome or focal segmental glomerulosclerosis, Clin. Nephrol. 46 (5) (1996) 347–352.
[12] T. Imasawa, D. Hirano, K. Nozu, et al., Clinicopathologic features of mitochondrial nephropathy, Kidney Int. Rep. 7 (3) (2022) 580–590, https://doi.org/10.1016/j.ekir.2021.12.028.
[13] V.D. D'Agati, A.B. Fogo, J.A. Bruijn, J.C. Jennette, Pathologic classification of focal segmental glomerulosclerosis: a working proposal, Am. J. Kidney Dis. 43 (2) (2004) 368–382, https://doi.org/10.1053/j.ajkd.2003.10.024.
[14] K. Sun, Q. Xie, C.M. Hao, Mechanisms of scarring in focal segmental glomerulosclerosis, Kidney Dis. (Basel) 7 (5) (2021 Sep) 350–358, https://doi.org/10.1159/000517108.
[15] O. Hotta, C.N. Inoue, S. Miyabayashi, T. Furuta, A. Takeuchi, Y. Taguma, Clinical and pathologic features of focal segmental glomerulosclerosis with mitochondrial tRNALeu(UUR) gene mutation, Kidney Int. 59 (4) (2001) 1236–1243, https://doi.org/10.1046/j.1523-1755.2001.0590041236.x.
[16] W. Kriz, N. Gretz, K.V. Lemley, Progression of glomerular diseases: is the podocyte the culprit? Kidney Int. 54 (3) (1998) 687–697, https://doi.org/10.1046/j.1523-1755.1998.00044.x.
[17] M. Nagata, Podocyte injury and its consequences, Kidney Int. 89 (6) (2016) 1221–1230, https://doi.org/10.1016/j.kint.2016.01.012.
[18] V.D. D'Agati, Pathobiology of focal segmental glomerulosclerosis: new developments, Curr. Opin. Nephrol. Hypertens. 21 (3) (2012 May) 243–250, https://doi.org/10.1097/MNH.0b013e32835200df.
[19] J. Müller-Deile, M. Schiffer, The podocyte power-plant disaster and its contribution to glomerulopathy, Front. Endocrinol. (Lausanne) 5 (2014 Dec 15) 209, https://doi.org/10.3389/fendo.2014.00209.
[20] S. Güçer, B. Talim, E. Aşan, et al., Focal segmental glomerulosclerosis associated with mitochondrial cytopathy: report of two cases with special emphasis on podocytes, Pediatr. Dev. Pathol. 8 (6) (2005 Nov-Dec), https://doi.org/10.1007/s10024-005-0058-z, 710-7.
[21] M. Hagiwara, K. Yamagata, R.A. Capaldi, A. Koyama, Mitochondrial dysfunction in focal segmental glomerulosclerosis of puromycin aminonucleoside nephrosis, Kidney Int. 69 (7) (2006 Apr) 1146–1152, https://doi.org/10.1038/sj.ki.5000207.
[22] T. Imasawa, R. Rossignol, Podocyte energy metabolism and glomerular diseases, Int. J. Biochem. Cell Biol. 45 (9) (2013 Sep) 2109–2118, https://doi.org/10.1016/j.biocel.2013.06.013.
[23] F.M. Santorelli, K. Tanji, R. Kulikova, et al., Identification of a novel mutation in the mtDNA ND5 gene associated with MELAS, Biochem. Biophys. Res. Commun. 238 (2) (1997) 326–328, https://doi.org/10.1006/bbrc.1997.7167.
[24] M. McKenzie, D. Liolitsa, N. Akinshina, et al., Mitochondrial ND5 gene variation associated with encephalomyopathy and mitochondrial ATP consumption, J. Biol. Chem. 282 (51) (2007 Dec 21) 36845–36852, https://doi.org/10.1074/jbc.M704158200.
[25] S. Shanske, J. Coku, J. Lu, et al., The G13513A mutation in the ND5 gene of mitochondrial DNA as a common cause of MELAS or Leigh syndrome: evidence from 12 cases, Arch. Neurol. 65 (3) (2008 Mar) 368–372, https://doi.org/10.1001/archneurol.2007.67.
[26] A. Motoda, T. Kurashige, T. Sugiura, et al., A case of MELAS with G13513A mutation presenting with chronic kidney disease long before stroke-like episodes, Rinsho Shinkeigaku 53 (6) (2013), https://doi.org/10.5692/clinicalneurol.53.446, 446-51. Japanese.

[27] P.S. Ng, M.V. Pinto, J.L. Neff, et al., Mitochondrial cerebellar ataxia, renal failure, neuropathy, and encephalopathy (MCARNE), Neurol. Genet. 5 (2) (2019 Mar 6), e314, https://doi.org/10.1212/NXG.0000000000000314.
[28] H. Bakis, A. Trimouille, A. Vermorel, et al., Adult onset tubulo-interstitial nephropathy in MT-ND5-related phenotypes, Clin. Genet. 97 (4) (2020) 628–633, https://doi.org/10.1111/cge.13670.
[29] V. Barone, C. La Morgia, L. Caporali, et al., Case report: optic atrophy and nephropathy with m.13513G>a/MT-ND5 mtDNA pathogenic variant, Front. Genet. 13 (2022 Jun 3), 887696, https://doi.org/10.3389/fgene.2022.887696.
[30] A. Tsuchimoto, Y. Matsukuma, K. Ueki, et al., Utility of Columbia classification in focal segmental glomerulosclerosis: renal prognosis and treatment response among the pathological variants, Nephrol. Dial. Transplant. 35 (7) (2020) 1219–1227, https://doi.org/10.1093/ndt/gfy374.
[31] A. Shabaka, A. Tato Ribera, G. Fernández-Juárez, Focal segmental glomerulosclerosis: state-of-the-art and clinical perspective, Nephron. 144 (9) (2020) 413–427, https://doi.org/10.1159/000508099.
[32] S. Matsuo, E. Imai, M. Horio, et al., Revised equations for estimated GFR from serum creatinine in Japan, Am. J. Kidney Dis. 53 (6) (2009) 982–992, https://doi.org/10.1053/j.ajkd.2008.12.034.
[33] A. Kobayashi, Y. Goto, M. Nagata, Y. Yamaguchi, Granular swollen epithelial cells: a histologic and diagnostic marker for mitochondrial nephropathy, Am. J. Surg. Pathol. 34 (2) (2010) 262–270, https://doi.org/10.1097/PAS.0b013e3181cb4ed3.
[34] T. Imasawa, M. Tanaka, Y. Yamaguchi, T. Nakazato, H. Kitamura, M. Nishimura, 7501 T>a mitochondrial DNA variant in a patient with glomerulosclerosis, Ren. Fail. 36 (9) (2014) 1461–1465, https://doi.org/10.3109/0886022X.2014.945181.
[35] D.J. Mahad, I. Ziabreva, G. Campbell, et al., Mitochondrial changes within axons in multiple sclerosis, Brain. 132 (Pt 5) (2009) 1161–1174, https://doi.org/10.1093/brain/awp046.
[36] T. Pulkes, L. Eunson, V. Patterson, et al., The mitochondrial DNA G13513A transition in ND5 is associated with a LHON/MELAS overlap syndrome and may be a frequent cause of MELAS [published correction appears in Ann Neurol 2000 Jun; 47(6):841], Ann. Neurol. 46 (6) (1999) 916–919, https://doi.org/10.1002/1531-8249(199912)46:6<916::aid-ana16>3.0.co;2-r.
[37] M. Chol, S. Lebon, P. Bénit, et al., The mitochondrial DNA G13513A MELAS mutation in the NADH dehydrogenase 5 gene is a frequent cause of Leigh-like syndrome with isolated complex I deficiency, J. Med. Genet. 40 (3) (2003) 188–191, https://doi.org/10.1136/jmg.40.3.188.
[38] V. Carelli, C. La Morgia, M.L. Valentino, P. Barboni, F.N. Ross-Cisneros, A. A. Sadun, Retinal ganglion cell neurodegeneration in mitochondrial inherited disorders, Biochim. Biophys. Acta 1787 (5) (2009) 518–528, https://doi.org/10.1016/j.bbabio.2009.02.024.
[39] E. Ogawa, T. Fushimi, M. Ogawa-Tominaga, et al., Mortality of Japanese patients with Leigh syndrome: effects of age at onset and genetic diagnosis, J. Inherit. Metab. Dis. 43 (4) (2020) 819–826, https://doi.org/10.1002/jimd.12218.
[40] J. van den Ameele, A.Y.Z. Li, H. Ma, P.F. Chinnery, Mitochondrial heteroplasmy beyond the oocyte bottleneck, Semin. Cell Dev. Biol. 97 (2020) 156–166, https://doi.org/10.1016/j.semcdb.2019.10.001.
[41] X. Geng, Y. Zhang, J. Yan, et al., Mitochondrial DNA mutation m.3243A>G is associated with altered mitochondrial function in peripheral blood mononuclear cells, with heteroplasmy levels and with clinical phenotypes, Diabet. Med. 36 (6) (2019) 776–783, https://doi.org/10.1111/dme.13874.
[42] A. Tejani, A.D. Nicastri, Mesangial IgM nephropathy, Nephron. 35 (1) (1983) 1–5, https://doi.org/10.1159/000183035.
[43] J.C. Jennette, C.G. Hipp, C1q nephropathy: a distinct pathologic entity usually causing nephrotic syndrome, Am. J. Kidney Dis. 6 (2) (1985 Aug) 103–110, https://doi.org/10.1016/s0272-6386(85)80150-5.
[44] D. Strassheim, B. Renner, S. Panzer, et al., IgM contributes to glomerular injury in FSGS, J. Am. Soc. Nephrol. 24 (3) (2013 Feb) 393–406, https://doi.org/10.1681/ASN.2012020187.
[45] S.B. Storrs, W.P. Kolb, R.N. Pinckard, M.S. Olson, Characterization of the binding of purified human C1q to heart mitochondrial membranes, J. Biol. Chem. 256 (21) (1981 Nov 10), 10924–9.
[46] A. Comis, S.B. Easterbrook-Smith, C1q binding to mitochondria: a possible artefact? FEBS Lett. 185 (1) (1985 Jun 3) 105–108, https://doi.org/10.1016/0014-5793(85)80749-3.
[47] V.S. Ten, J. Yao, V. Ratner, et al., Complement component c1q mediates mitochondria-driven oxidative stress in neonatal hypoxic-ischemic brain injury, J. Neurosci. 30 (6) (2010 Feb 10) 2077–2087, https://doi.org/10.1523/JNEUROSCI.5249-09.2010.
[48] T. Imasawa, M. Tanaka, N. Maruyama, et al., Pathological similarities between low birth weight-related nephropathy and nephropathy associated with mitochondrial cytopathy, Diagn. Pathol. 9 (2014) 181. Published 2014 Sep 30, https://doi.org/10.1186/s13000-014-0181-0.
[49] Y. Maeoka, T. Doi, M. Aizawa, et al., A case report of adult-onset COQ8B nephropathy presenting focal segmental glomerulosclerosis with granular swollen podocytes, BMC Nephrol. 21 (1) (2020) 376. Published 2020 Aug 28, https://doi.org/10.1186/s12882-020-02040-z.
[50] E.J. Brown, M.R. Pollak, M. Barua, Genetic testing for nephrotic syndrome and FSGS in the era of next-generation sequencing, Kidney Int. 85 (5) (2014 May) 1030–1038, https://doi.org/10.1038/ki.2014.48.
[51] M. Rudnicki, J.A. Mayr, J. Zschocke, et al., MELAS syndrome and kidney disease without Fanconi syndrome or proteinuria: a case report, Am. J. Kidney Dis. 68 (6) (2016) 949–953, https://doi.org/10.1053/j.ajkd.2016.06.027.
[52] A. Ghose, C.M. Taylor, A.J. Howie, A. Chalasani, I. Hargreaves, D.V. Milford, Measurement of respiratory chain enzyme activity in human renal biopsy specimens, J. Clin. Med. 6 (9) (2017 Sep 19) 90, https://doi.org/10.3390/jcm6090090.

ミトコンドリア病の診療水準やQOL向上を目指した調査研究班

区　　分	氏　名	所　　属　　等	職　　名
研　究　代　表　者	三牧 正和	学校法人　帝京大学　医学部小児科学講座	主任教授
研　究　分　担　者	井川 正道	福井大学　学術研究院医学系部門	教　授
	大竹　明	学校法人　埼玉医科大学　ゲノム医療科・小児科	特任教授
	岡崎 康司	順天堂大学　大学院医学研究科	教　授
	小坂　仁	学校法人　自治医科大学　医学部小児科学	教　授
	後藤 雄一	国立研究開発法人国立精神・神経医療研究センター　メディカルゲノムセンター	特任研究部長
	小牧 宏文	国立研究開発法人国立精神・神経医療研究センター　トランスレーショナル・メディカルセンター	センター長
	立花 眞仁	東北大学大学院医学系研究科　周産期医学分野	准教授
	西野 一三	国立精神・神経医療研究センター　神経研究所　疾病研究第一部	部　長
	藤野 善久	産業医科大学　産業生態科学研究所・環境疫学研究室	教　授
	村山　圭	順天堂大学　　難治性疾患診断・治療学	教　授
	八ツ賀 秀一	学校法人　福岡大学　医学部小児科学講座	講　師
	今澤 俊之	国立病院機構千葉東病院診療部	統括診療部長
	武田 充人	北海道大学大学院医学研究院　生殖・発達医学分野　小児科学教室	講　師